ANGELA MARIA GONELLA-DIAZA

Effect of Peri-Ovulatory Endocrine Milieu in the Oviductal Physiology of Beef Cows: Regulation of the Transcriptome, Tissue Morphology, Cell Proliferation, Extracellular Matrix Remodeling, microRNAs Abundance Profile, and Oviductal Fluid Composition.

Pirassununga

2017

ANGELA MARIA GONELLA-DIAZA

Effect of Peri-Ovulatory Endocrine Milieu in the Oviductal Physiology of Beef Cows: Regulation of the Transcriptome, Tissue Morphology, Cell Proliferation, Extracellular Matrix Remodeling, microRNAs Abundance Profile, and Oviductal Fluid Composition.

Thesis presented to the Graduate School in Animal Reproduction of the School of Veterinary Medicine and Animal Sciences of the University of São Paulo, as a requirement for the title of Doctor in Science

Department:

Animal Reproduction

Concentration Area:

Animal Reproduction

Advisor:

Prof. Mario Binelli, PhD.

Approved by:_____

Advisor

Pirassununga

2017

Note: The original version is available at the FMVZ / USP Library

DADOS INTERNACIONAIS DE CATALOGAÇÃO NA PUBLICAÇÃO

(Biblioteca Virginie Buff D'Ápice da Faculdade de Medicina Veterinária e Zootecnia da Universidade de São Paulo)

T. 3499
FMVZ

Gonella Diaza, Angela Maria
Effect of peri-ovulatory endocrine milieu in the oviductal physiology of beef cows: regulation of the transcriptome, tissue morphology, cell proliferation, extracellular matrix remodeling, microRNAs abundance profile, and oviductal fluid composition. / Angela Maria Gonella Diaza. – 2017.
244 p. : il.

Título traduzido: Efeito do ambiente endócrino peri-ovulatório na fisiologia do oviduto de vacas de corte: regulação do transcriptoma, morfologia do tecido, proliferação celular, remodelamento da matriz extracelular, perfil de abundância de microRNAs e composição do fluído oviductal.

Tese (Doutorado) - Universidade de São Paulo, Faculdade de Medicina Veterinária e Zootecnia. Departamento de Reprodução Animal, Pirassununga, 2017.

Programa de Pós-Graduação: Reprodução Animal.

Área de concentração: Reprodução Animal.

Orientador: Prof. Dr. Mario Binelli.

1. Ampulla. 2. Isthmus. 3. Estradiol. 4. Progesterone. 5. Beef Cattle. I. Título.

CERTIFICADO

Certificamos que a proposta intitulada "Diferenças no perfil endócrino peri-ovulatório e sua relação com o ambiente do oviduto em vacas de alta e baixa fertilidade. ", protocolada sob o CEUA nº 4293160916, sob a responsabilidade de **Mario Binelli** *e equipe; Angela Maria Gonella Diaza* - que envolve a produção, manutenção e/ou utilização de animais pertencentes ao filo Chordata, subfilo Vertebrata (exceto o homem), para fins de pesquisa científica ou ensino - está de acordo com os preceitos da Lei 11.794 de 8 de outubro de 2008, com o Decreto 6.899 de 15 de julho de 2009, bem como com as normas editadas pelo Conselho Nacional de Controle da Experimentação Animal (CONCEA), e foi **aprovada** pela Comissão de Ética no Uso de Animais da Faculdade de Medicina Veterinária e Zootecnia da Universidade de São Paulo (CEUA/FMVZ) na reunião de 03/01/2017.

We certify that the proposal "The peri-ovulatory endocrine profile dictates the bovine oviductal morpho-physiology and transcriptome ", utilizing 14 Bovines (14 females), protocol number CEUA 4293160916, under the responsibility of **Mario Binelli** *and team; Angela Maria Gonella Diaza* - which involves the production, maintenance and/or use of animals belonging to the phylum Chordata, subphylum Vertebrata (except human beings), for scientific research purposes or teaching - is in accordance with Law 11.794 of October 8, 2008, Decree 6899 of July 15, 2009, as well as with the rules issued by the National Council for Control of Animal Experimentation (CONCEA), and was **approved** by the Ethic Committee on Animal Use of the School of Veterinary Medicine and Animal Science (University of São Paulo) (CEUA/FMVZ) in the meeting of 01/03/2017.

Finalidade da Proposta: Pesquisa

Vigência da Proposta: de 10/2016 a 05/2017 Área: Reprodução Animal

Origem:	Não aplicável biotério						
Espécie:	Bovinos	sexo:	Fêmeas	idade:	3 a 10 anos	N:	14
Linhagem:	Nelore			Peso:	400 a 600 kg		

Resumo: As tubas uterinas ou ovidutos são estruturas pares que são responsáveis pelo transporte de gametas e embriões, e se estendem das proximidades do ovário até a união com o útero. Desde o descobrimento do oviduto por Gabriele Falloppio em 1561 e até a década de 1900, acreditava-se que este era simplesmente uma via para a passagem do espermatozoide e do embrião, sem funções metabólicas ou fisiológicas. No entanto, atualmente é conhecido que o oviduto desempenha um papel importante na formação de reservatórios de espermatozoides, na capacitação espermática, na fertilização e no desenvolvimento embrionário precoce. Em bovinos, as concentrações circulantes de estradiol (E2) durante o proestro-estro e de progesterona (P4) durante o metaestro-diestro estão associadas positivamente com a probabilidade de sucesso de gestação. Por exemplo, a suplementação de P4 durante os primeiros dias do diestro regula a expressão gênica do endométrio e favorece o maior crescimento do concepto. Em trabalhos recentes do nosso grupo de pesquisa, foi testado um modelo experimental no qual, usando protocolos de sincronização de cio, dois grupos de animais foram obtidos: vacas que ovularam um folículo maior e formaram um corpo lúteo maior (FG-CLG) e, consequente tinham maiores concentrações de E2 no estro e P4 no diestro inicial; e vacas que ovularam um folículo de menor diâmetro formando um CL menor (FP-CLP) com menores concentrações de E2 e de P4. Usando este modelo, foi determinado que as vacas do grupo FG-CLG, têm uma expressão gênica endometrial diferenciada e uma maior taxa de concepção, quando comparadas com as vacas do grupo FP-CLP No presente estudo, objetivamos avaliar se estas mudanças nas concentrações de E2 e P4 nos grupos FG-CLG e FP-CLP expostas acima, modificam o ambiente do oviduto. Para isto, utilizaremos técnicas laboratoriais como sequenciamento de RNA (RNAseq), reação em cadeia da polimerase em tempo real, (qPCR), analise da morfometria do tecido e expressão proteica.

Local do experimento: As analises moleculares (qPCR, western blot, eletrophoreses) serão realizadas no laboratório de Fisiologia e Endocrinologia molecular sob a responsabilidade do Professor Mario Binelli. O sequenciamento de RNA será realizado no laboratório de Biotecnologia Animal da Escola Superior de Agricultura Luiz de Queiroz. As analises de morfometria e imunohistoquimica serão realizadas no Laboratório de Patologia da Faculdade de Zootecnia e engenheira de alimentos.

São Paulo, 18 de janeiro de 2017

Profa. Dra. Denise Tabacchi Fantoni
Presidente da Comissão de Ética no Uso de Animais
Faculdade de Medicina Veterinária e Zootecnia da Universidade de São Paulo

Roseli da Costa Gomes
Secretaria Executiva da Comissão de Ética no Uso de Animais
Faculdade de Medicina Veterinária e Zootecnia da Universidade de São Paulo

EVALUATION FORM

Author: GONELLA-DIAZA, Angela Maria

Títtle: **Effect of Peri-Ovulatory Endocrine Milieu in the Oviductal Physiology of Beef Cows:** Regulation of the Transcriptome, Tissue Morphology, Cell Proliferation, Extracellular Matrix Remodeling, microRNAs Abundance Profile, and Oviductal Fluid Composition.

Thesis presented to the Graduate School in Animal Reproduction of the School of Veterinary Medicine and Animal Sciences of the University of São Paulo, as a requirement for the title of Doctor in Science.

Date: ___/___/_____

Examination Board

Prof. Dr. _____ Institution: _____
Verdict: _____ Signature: _____

Prof. Dr. _____ Institution: _____
Verdict: _____ Signature: _____

Prof. Dr. _____ Institution: _____
Verdict: _____ Signature: _____

Prof. Dr. _____ Institution: _____
Verdict: _____ Signature: _____

Prof. Dr. _____ Institution: _____
Verdict: _____ Signature: _____

I dedicate this doctoral Thesis to my wonderful husband Alejandro Ojeda (Tatuyo). Thank you for supporting me throughout all of this process. You and our daughter Nina are my greatest happiness. I love you both.

ACKNOWLEDGMENTS

I would like to thank the University of São Paulo. It was a great honor to have been here these past four years. I also want to thank the College of Veterinary Medicine, especially the Department of Animal Reproduction. I am very happy to have had the opportunity of being here surrounded by such excellent professionals.

I would like to acknowledge The Department of Animal Reproduction for allowing me to conduct my research and providing all the assistance I requested from them. Special thanks go to the members of Staff Development and Human Resources for their continuous support, particularly Harumi Shiraishi and Clayton Costa.

I wish to thank the FAPESP (The São Paulo Research Foundation) for the economic support given to the project “Assinaturas da Receptividade”.

I want to express my eternal gratitude to the CAPES (Coordination for the Improvement of Higher Education Personnel) foundation and the PEC-PG program for granting me a scholarship and giving me this wonderful opportunity of pursuing my Ph.D. in Brazil.

I would like to express my deepest gratitude to my awesome advisor, Professor Mario Binelli, for his illuminating guidance and inspiring instruction during the development of this study. Professor Mario not only provided me with academic guidance but also gave me and my family a warm and sincere support. I am also grateful to Professor Mario’s family: Deby, Giga, Serena, and Jorginho, for always making us feel welcomed and for all the happy moments we have shared.

I am also indebted to all my laboratory colleagues: Claudia, Fernando, Guilherme, Sônia, Veerle, Emiliana, Roney, Saara, Estela, Everton, Moana, Milena, Mariana, Thiago, Bia, Mae, and Natalia. To Bárbara and Kaue: thank you for trusting me and accepting my advice.

Special thanks to Professors Luiz Coutinho, Ricardo Strefessi, Julio Balihero, Juliano Cohelio Silvera, Felipe Perecin, and Marcos Chiaratti for their assistance in laboratory procedures and data analysis.

I wish to thank CBRA's professors Rubens Paes de Arruda, Ed Hoffmann Madureira, Anneliese de Souza Traldi, Eneiva Carla Carvalho Celeghini, and André Furugen Cesar de Andrade for their solid advice, great conversations, coffees, and their willingness to always help me with my work.

Thanks to all colleagues of the Biosciences Department, especially the LMMD and the Pathology Lab.

I would like to express my sincere gratitude to Professor Augusto Hauber Gameiro and his family, Mariana, Manuela, Bruno, and "as meninas," for their friendship and support.

Thanks to Pati Cepellos and her family for offering me their home as my own. I hope we meet again soon.

Thanks to the Scolari family for the immeasurable love you had for me and my husband when we arrived in Brazil. We will never forget you.

I want to give a big thank you to my cousin, sister, friend, and “comadre” Carolina Castellanos Gonella. Thank you for always helping me with all my problems, for your great advice, and for helping me with my written English.

I want to thank my husband for joining me in this adventure, being always by my side, not letting me give up, and saying exactly what I needed to hear all the time. I also want to thank my daughter Nina for making my days happy and giving me a reason to smile every day. I love you both.

Finally, I want to thank all my family members. All of you have a special place in my heart and I am grateful for being part of our family. Specially, I want to thank my mother, for her love, guidance, patience, and many times financial support; my grandmother Nina Gonella Diaza who inspired me in many ways; and my beloved uncles (Guillermo, Yesid, Julio, and Armando) and aunts (Clara and Papapia) who have always been unconditional with me. I love you all!

¡¡¡Gracias...totales!!!

Gustavo Cerati, 1997.

RESUMO

GONELLA-DIAZA, A. M. **Efeito do ambiente endócrino peri-ovulatorio na fisiologia do oviduto de vacas de corte**: regulação do transcriptoma, morfologia do tecido, proliferação celular, remodelamento da matriz extracelular, perfil de abundância de microRNAs e composição do fluido ovidutal. [Effect of peri-ovulatory endocrine milieu in the oviductal physiology of beef cows: regulation of the transcriptome, tissue morphology, cell proliferation, extracellular matrix remodeling, microRNAs abundance profile, and oviductal fluid composition]. 2016. 244 f. Tese (Doutorado em Ciências) – Faculdade de Medicina Veterinária e Zootecnia, Universidade de São Paulo, Pirassununga, 2016.

Em fêmeas bovinas, o oviduto apresenta um importante papel no processo reprodutivo. As secreções ovidutais representam o ambiente onde ocorrem o armazenamento e a capacitação espermática, a fecundação e o desenvolvimento embrionário inicial. O controle molecular da receptividade do oviduto em bovinos é pouco conhecido. Na presente tese, empregou-se um modelo de receptividade baseado na manipulação do crescimento do folículo pré-ovulatório (FPO) para o estudo dos efeitos do perfil endócrino periovulatório na fisiologia do oviduto. O crescimento do FPO de vacas Nelore (*Bos indicus*) foi manipulado com o objetivo de produzir dois grupos: vacas com FPO e corpo lúteo (CL) grandes (FG-CLG; maior fertilidade) e vacas com FPO e CL pequenos (FP-CLP; menor fertilidade). Amostras da ampola e istmo foram coletadas no dia 4 após da indução da ovulação com GnRH. No primeiro estudo, o transcriptoma da ampola e istmo do lado ipsolateral ao CL foi determinado por RNAseq, à expressão gênica regional e a distribuição das proteínas PGR e ERα foram analisadas por qPCR e imunohistoquímica, respectivamente. Houve maior abundância de PGR e ERα no oviduto dos animais do grupo FG-CLG, o que indica uma maior disponibilidade de receptores e possivelmente, de mecanismos intracelulares de sinalização estimulados pelos esteroides em ambas as regiões. O perfil global de transcritos mostrou enriquecimento de características funcionais do

oviduto que poderiam afetar sua receptividade ao embrião. Tais características incluem mudanças morfológicas, como a ramificação morfogênica, e celulares, como a secreção, que foram aumentadas no grupo FG-CLG. No segundo estudo, após analisarem-se características morfológicas dos tecidos, concluiu-se que a ampola dos animais FG-CLG apresentou maior número de pregas primárias, maior perímetro do epitélio luminal, e maior proporção de células secretoras e de células em proliferação quando comparado aos animais do grupo FP-CLP. Não houve diferença na morfologia do istmo entre os grupos. No terceiro estudo, foi analisado o processo de remodelamento de matriz extracelular. Concluiu-se que no istmo dos animais do grupo FG-CLG existe menor quantidade de fibras de colágeno tipo 1 e maior abundância de proteínas envolvidas no remodelamento de matriz. No quarto estudo, determinou-se que o perfil endócrino periovulatório afeta a expressão de componentes da via de biossíntese e o perfil de microRNAs, que são diferentes entre os grupos. Finalmente, no quinto estudo, foram quantificados 205 metabólitos no fluido ovidutal dos animais. Destes, 37 encontram-se em concentrações diferentes entre os grupos. Concluiu-se que o oviduto de vacas de maior fertilidade apresenta um perfil de transcritos, proteínas e metabólitos que está associado a características morfológicas e funcionais favoráveis à sobrevivência e desenvolvimento do embrião.

Palavras-chave: Ampola, Istmo, Estradiol, Progesterona, Gado de Corte.

ABSTRACT

GONELLA-DIAZA, A. M. **Effect of peri-ovulatory endocrine milieu in the oviductal physiology of beef cows:** regulation of the transcriptome, tissue morphology, cell proliferation, extracellular matrix remodeling, microRNAs abundance profile, and oviductal fluid composition. [Efeito do ambiente endócrino peri-ovulatorio na fisiologia do oviduto de vacas de corte: regulação do transcriptoma, a morfologia do tecido, proliferação celular, remodelamento de matriz extracelular, pefil de abundancia de microRNAs e composição do fluido]. 2016. 244 p. Tese (Doutorado em Ciências) – Faculdade de Medicina Veterinária e Zootecnia, Universidade de São Paulo, Pirassununga, 2016.

In cattle, the oviduct plays an important role in the reproductive process. Oviductal secretions characterize the environment where storage and sperm capacitation, fertilization, and early embryo development take place. Because molecular control of bovine oviduct receptivity is poorly understood, this Thesis proposed a model of receptivity based on the manipulation of pre-ovulatory follicle growth (POF) used to study the effects of periovulatory endocrine profile on oviductal physiology. Growth of POF in Nelore cows (*Bos indicus*) was manipulated to produce two groups: cows with large POF and large corpus luteum (LF-LCL; higher fertility) and cows with small POF and small CL (SF-SCL; Lower fertility). Ampulla and isthmus samples were collected on day 4 after induction of ovulation with GnRH. In the first study, the transcriptome of the ipsilateral to CL ampulla and isthmus was determined by RNAseq, the regional expression of genes was studied by qPCR, and the distribution of the PGR and ERα proteins was assessed by immunohistochemistry. Greater abundance of PGR and ERα was found in the oviduct of the LF-LCL animals indicating that there is a greater availability of receptors and, possibly, of signaling-mechanisms stimulated by steroids in both oviductal regions. The transcripts profile showed enriched oviductal functional characteristics that could affect its embryo receptivity. These characteristics include

changes in morphology i.e. branching morphogenesis, and changes in cell functioning i.e. cell secretion, that were enriched in the LF-LCL group. In the second study, after morphological analyses, it was concluded that the ampulla of the LF-LCL animals presented more primary folds, a larger perimeter of the luminal epithelium, and a higher proportion of secretory and proliferating cells, when compared to SF-SCL group. There was no difference in isthmus morphology between groups. In the third study, the extracellular matrix remodeling was reserched. It was concluded that in the isthmus region of the LF-LCL animals, there is less type 1 collagen fibers and greater abundance of proteins involved in extracellular matrix remodeling. In the fourth study, it was determined that the periovulatory endocrine milieu affects the expression of components of the microRNAs biosynthesis pathway and the microRNAs profile, both different between groups. Finally, in the fifth study, 205 metabolites were quantified in the oviductal fluid and 37 were found to be in different concentrations when both groups were compared. It was concluded that oviduct of cows of higher fertility presents a profile of transcripts, proteins, and metabolites that is associated with morphological and functional characteristics favorable to the survival and development of the embryo.

Keywords: Ampulla. Isthmus. Estradiol. Progesterone. Beef Catlle.

LISTS OF ABBREVIATIONS

µL	Microliter
µm	Micrometer
µM	Micromolar
μm^2	Square Micrometer
ACTA2	Actin alpha 2
AGO1	Argonaute 1, RISC Catalytic Component
AGO2	Argonaute 2, RISC Catalytic Component
AGO3	Argonaute 3, RISC Catalytic Component
AGO4	Argonaute 4, RISC Catalytic Component
ANOVA	Analysis of variance
BE	Estradiol Benzoate
BGN	Biglycan
BMP4	Bone morphogenetic protein 4
cDNA	Complementary DNA
CL	Corpus Luteum
COC	Cumulus-oocyte complex
COL1A1	Collagen Type I Alpha 1 Chain
CTSS	Cathepsin S
CV	Coefficient of variation
CXCR4	C-X-C chemokine receptor type 4
DAVID	The Database for Annotation, Visualization and Integrated Discovery
DCN	Decorin
DE	Differentially expressed
DICER1	Dicer 1, Double-Stranded RNA-Specific Endoribonuclease
DICER1-cKO	Female mice with deletion of DICER1 in somatic cells of the reproductive tract
DROSHA	Drosha, Double-Stranded RNA-Specific Endoribonuclease
E2	Estradiol
ECM	Extracellular matrix

EGF	Epidermal growth factor
ERα	Estradiol Receptor Alpha
ERβ	Estradiol Receptor Beta
ESI	Electrospray ionization
FGF	Fibroblast growth factor
FIA	Flow injection analysis
FIGF	C-Fos Induced Growth Factor (Vascular Endothelial Growth Factor D)
GAPDH	Glyceraldehyde-3-Phosphate Dehydrogenase
GBA	Glucosidase Beta Acid
GEO	Gene Expression Omnibus
GF	Growth factor
GnRH	Gonadotropin-Releasing Hormone
H&E	Hematoxylin and eosin
HPSE	Heparanase
Im	Intramuscular
Ki67	Antigen Ki67
LC	Liquid chromatography
LF-LCL	Large Follicle Large Corpus Luteum
miRNA	microRNA
mL	Milliliter
MMP-1	Matrix metalloproteinase 1
MMP-10	Matrix metalloproteinase 10
MMP-13	Matrix metalloproteinase 13
MMP14	Matrix metalloproteinase 14
MMP-2	Matrix metalloproteinase 2
MMP-3	Matrix metalloproteinase 3
MMP-8	Matrix metalloproteinase 8
MMP-9	Matrix metalloproteinase 9
MRM	Multiple reaction monitoring
mRNA	Messenger RNA

MS/MS	Tandem mass spectrometry
NCBI	National Center for Biotechnology Information
nM	Nanomolar
NS	Not statistically significant
OVGP1	Oviductal Glycoprotein 1 (Oviductin 2)
P4	Progesterone
PAS	Periodic acid–Schiff
PBS	Phosphate buffered saline solution
PGF	Prostaglandin F2(alpha)
PGR	Progesterone Receptor
PITC	Phenylisothiocyanate
PLS-DA	Partial Least Squares Discriminant Analysis
PMSF	Phenylmethylsulfonyl fluoride
POF	Preovulatory Follicle
POSTN	Periostin
PPIA	Peptidylprolyl Isomerase A (C yclophilin A)
qPCR	Quantitative Real Time PCR
RER	Rough endoplasmic reticulum
RIN	RNA Integrity Number
RNAseq	RNA sequencing
RT	Room temperature
SEM	Standard Error of the Mean
SF-SCL	Small Follicle Small Corpus Luteum
TGFβ	Transforming growth factor-β
TIMP-1	Tissue Inhibitor Of Metalloproteinases 1
TIMP-2	Tissue Inhibitor Of Metalloproteinases 2
TIMP-4	Tissue Inhibitor Of Metalloproteinases 4
UTJ	Utero-tubal Junction
VCL	Vinculin
XPO5	Exportin 5

LIST OF FIGURES

LIST OF TABLES

SUMMARY

1 INTRODUCTION

The economic performance of dairy and beef herds is closely related to their reproductive efficiency (BRITT 1985; DE VRIES 2006; VASCONCELOS *et al*., 2014). This relationship is due in part to the fact that reproduction modulates important productive variables, some of which are directly related to main sources of income (BRITT 1985; BURNS *et al*., 2010). Based on this context, many decades of research on the reproductive physiology of the cow, led to the development of strategies that allow the synchronization of the estrous cycle, conventional or timed artificial insemination (TAI) and the production of embryos *in vitro* (BÓ *et al*., 2013; BO; BARUSELLI, 2014; VASCONCELOS *et al*., 2014). However, the reproductive efficiency of beef operations is still far from ideal and, despite these implementations, not all inseminated cows become pregnant. Thus, the study of the reproductive physiology and reproductive biology of the domestic animals is essential for overcoming challenges of reproductive efficiency.

The oviduct is a dynamic structure of the reproductive system, in which several important processes take place. The oviduct is divided in to anatomical regions that provide unique microenvironments that control specific physiological processes (ELLINGTON, 1991; HUNTER, 2012). Specifically, the infundibulum contains fimbriae that pick up the oocyte soon after fertilization and lead it to the lumen of the ampulla. In the ampulla lumen, which is a highly secretory region, the oocyte completes its process of nuclear and cytoplasmic maturation and fertilization and the first cell division of the zygote occurs. In the utero-tubal junction and isthmus, the spermatozoa are retained and capacitated. Also in the isthmus, the developing embryo is transported until its arrival in the uterus, which in cattle happens in a stage of 8-16 cells (HUNTER, 1998; HUNTER, 2012; BUHI *et al*., 2000; LEESE, 1988).

For embryos produced *in vitro*, the processes that normally happen in the oviductal lumen, happen artificially under laboratory conditions. The commercial success of these processes led to the idea that the oviduct is merely a conduit for the passage of gametes and embryos (MENEZO *et al*., 2015). However, multiple studies suggest that the oviduct participates actively in reproductive processes and engages

in biochemical communication with the structures that transit in its lumen. For example, the oviduct has the ability to recognize unfertilized oocytes and viable embryos thus modulating the transport of these structures. Betteridge *et al*., (1979) showed that in mares unfertilized structures are maintained at the utero-tubal junction whereas viable embryos can reach the uterine lumen. In addition, Wetscher *et al*., (2005) reported that bovine embryos of different qualities and developmental stages show distinct migration patterns after intra-tubal embryo transfer. Additionally, it was demonstrated that the porcine oviduct transcriptome is modulated differently to X- and Y-chromosome-bearing spermatozoa (ALMINANA *et al*., 2014).

When *in vivo* and *in vitro* embryo culture conditions are compared, the results of embryo implantation, conception rate, and survival rate after vitrification are superior for the *in vivo* conditions (RIZOS *et al*., 2002a, 2002b). Also, embryonic transcriptome (RIZOS *et al*., 2002c; NAGATOMO *et al*., 2015; PONSUKSILI *et al*., 2014) and epigenome (SALILEW-WONDIM *et al*., 2015) are different between *in vivo* and *in vitro* produced embryos. This difference suggests that *in vitro* conditions compromise embryo quality, mainly because it does not reflect the *in vivo* environment. This may be explained because the oviductal environment in high fertility cows is not fully characterized. Thus, it is essential to study in depth the oviductal physiology, not only to characterize the oviductal environment, but also to improve culture media for *in vitro* embryo production.

One main controller of the oviductal function is the endocrine system, especially the sex steroids estradiol and progesterone. The main role of estradiol and progesterone in regulating the functioning of the female reproductive tract is well known; also it is known that the elevated periovulatory concentrations of both hormones have been associated positively to fertility in beef cattle (PUGLIESI *et al*., 2014; VASCONCELOS *et al*., 2001; SA FILHO *et al*., 2009; SA FILHO *et al*., 2010). **The Central Hypothesis of this Thesis** is that animals with different periovulatory sex-steroid profiles have differences in their oviductal environment. To test this hypothesis an experimental model was developed, in which the growth of the periovulatory follicle was manipulated (MESQUITA *et al*., 2014). Specifically, two groups of cows were generated with distinct differences in the size of the periovulatory follicle and subsequent corpus luteum, as weel as corresponding concentrations of estradiol and progesterone. These two groups were named Large

Follicle – Large CL (LF-LCL) and Small Follicle – Small CL (SF-SCL) groups and were used in the series of studies described in the present Thesis.

The strategy used to determine differences in oviductal physiology between the two experimental groups can be found in Figure 1. Initially, the response to these two hormones was assessed by measuring their specific receptors on oviductal cells. Additionally, using RNA sequencing (RNAseq) and bioinformatics tools, molecular pathways that were different between groups were identified (Chapter 2). In the subsequent chapters of this Thesis, a selection of these pathways was studied extensively.

Figure 1– Flow chart of the studies and experiments performed to determine differences in oviductal physiology between the two experimental groups.

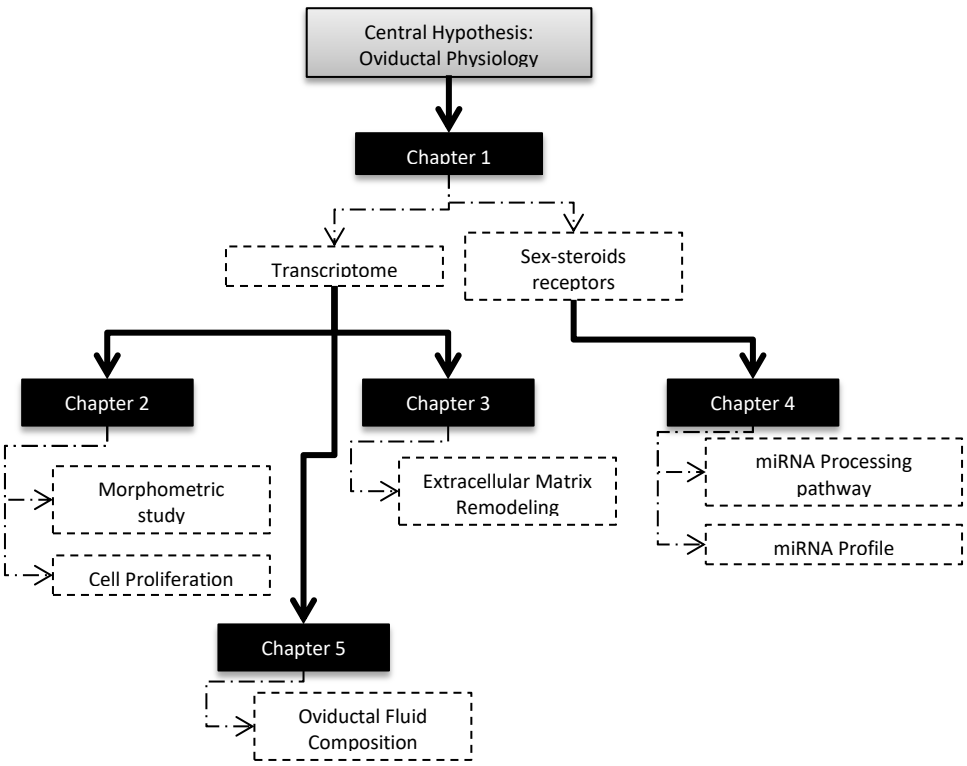

Source: Gonella-Diaza, 2017.

This Ph.D. Thesis has been divided in to six sections; each section was organized in a journal manuscript format. Section 1 is a summary of the relevant literature in oviductal physiology, and Chapters 1 to 5 are stand-alone manuscripts that contain the following subsections: introduction, materials and methodology,

results, discussion, and references. The manuscript of the first study (Chapter 1) was published in PloS One Journal in 2015 (GONELLA-DIAZA *et al*., 2017; Appendix A); The data set of the RNAseq reads and counts has been deposited in NCBI's Gene Expression Omnibus (GEO) and is accessible through GEO Series accession number GSE65681 and was published in the Genomic Data Journal (Appendix B). The manuscript of the second study (Chapter 2) was accepted for its publication in the Cell and Tissue Research Journal in july of 2017 (Accepntance letter in Appendix C). The final pages of this Ph.D. Thesis, introduce a general discussion, which summarizes the research and results of the previous chapters and provides directions for future research.

1.1 REFERENCES

ALMINANA, C.; CABALLERO, I.; HEATH, P.R.; MALEKI-DIZAJI, S.; PARRILLA, I.; CUELLO, C.; GIL, M.A.; VAZQUEZ, J.L.; VAZQUEZ, J. M.; ROCA, J.; MARTINEZ, E.A.; HOLT, W.V.; FAZELI, A. The battle of the sexes starts in the oviduct: modulation of oviductal transcriptome by X and Y-bearing spermatozoa. **BMC Genomics**, v. 15, p. 293, 2014.

BETTERIDGE, K.J.; EAGLESOME, M.D.; FLOOD, P.F. Embryo transport through the mare's oviduct depends upon cleavage and is independent of the ipsilateral corpus luteum. **Journal of Reproduction and Fertility Supplement**, v. 1979, n. 27, p. 387-394, 1979.

BO, G.A.; BARUSELLI, P.S. Synchronization of ovulation and fixed-time artificial insemination in beef cattle. **Animal**, v.8, Suppl. 1, p. 144-150, 2014.

BRITT, J.H. Enhanced reproduction and its economic implications. **Journal of Dairy Science**, v. 68, p. 1585-1592, 1985.

BUHI, W.C.; ALVAREZ, I.M.; KOUBA, A.J. Secreted proteins of the oviduct. **Cells Tissues Organs**, v. 166, p. 165-179, 2000.

BURNS, B.M.; FORDYCE, G.; HOLROYD, R.G. A review of factors that impact on the capacity of beef cattle females to conceive, maintain a pregnancy and wean a calf-Implications for reproductive efficiency in northern Australia. **Animal Reproduction Science**, v. 122, p. 1-22, 2010.

BÓ, G.; BARUSELLI, P.; MAPLETOFT, R. Synchronization techniques to increase the utilization of artificial insemination in beef and dairy cattle. **Animal Reproduction**, v. 10, p. 137-142, 2013.

DE VRIES, A. Economic value of pregnancy in dairy cattle. **Journal of Dairy Science**, v. 89, p. 3876-3885, 2006.

ELLINGTON, J. The bovine oviduct and its role in reproduction: a review of the literature. **The Cornell Veterinarian**, v. 81, p. 313-328, 1991.

HUNTER, R.H. Have the Fallopian tubes a vital role in promoting fertility?. **Acta Obstetricia et Gynecologica Scandinavica**, v. 77, p. 475-486, 1998.

HUNTER, R.H. Components of oviduct physiology in eutherian mammals. **Biological reviews of the Cambridge Philosophical Society**, v. 87, p. 244-255, 2012.

LEESE, H.J. The formation and function of oviduct fluid. **Journal of Reproduction and Fertility**, v. 82, p. 843-856, 1988.

MENEZO, Y.; GUERIN, P.; ELDER, K. The oviduct: a neglected organ due for re-assessment in IVF**. Reproductive BioMedicine Online**, v.30, p. 233-240, 2015.

MESQUITA, F.S.; PUGLIESI, G.; SCOLARI, S.C.; FRANCA, M.R.; RAMOS, R.S.; OLIVEIRA, M.; PAPA, P.C.; BRESSAN, F.F.; MEIRELLES, F.V.; SILVA, L.A.; NOGUEIRA, G.P.; MEMBRIVE, C.M.; BINELLI, M. Manipulation of the periovulatory sex steroidal milieu affects endometrial but not luteal gene expression in early diestrus Nelore cows. **Theriogenology**, v. 81, p. 861-869, 2014.

NAGATOMO, H.; AKIZAWA, H.; SADA, A.; KISHI, Y.; YAMANAKA, K.; TAKUMA, T.; SASAKI, K.; YAMAUCHI, N.; YANAGAWA, Y.; NAGANO, M.; KONO, T.; TAKAHASHI, M.; KAWAHARA, M. Comparing spatial expression dynamics of bovine blastocyst under three different procedures: in-vivo, in-vitro derived, and somatic cell nuclear transfer embryos. **Japanese Journal of Veterinary Research**, v. 63, p. 159-171, 2015.

PONSUKSILI, S.; TESFAYE, D.; SCHELLANDER, K.; HOELKER, M.; HADLICH, F.; SCHWERIN, M.; WIMMERS, K., Differential expression of miRNAs and their target mRNAs in endometria prior to maternal recognition of pregnancy associates with endometrial receptivity for *in vivo*- and *in vitro*-produced bovine embryos. **Biology of Reproduction**, v. 91, p. 135, 2014.

PUGLIESI, G.; SCOLARI, S.C.; MESQUITA, F.S.; MATURANA FILHO, M.; ARAUJO, E.R.; CARDOSO, D.; SALES, J.N.; MARTIN, I.; SA FILHO, M.; BERTAN, C.M.; BINELLI, M. Impact of Probing the Reproductive Tract During Early Pregnancy on Fertility of Beef Cows. **Reproduction in Domestic Animals**, v. 49, p. E35-E39, 2014.

RIZOS, D.; FAIR, T.; PAPADOPOULOS, S.; BOLAND, M.P.; LONERGAN, P. Developmental, qualitative, and ultrastructural differences between ovine and bovine embryos produced *in vivo* or *in vitro*. **Molecular Reproduction and Development**, v. 62, p. 320-327, 2002a.

RIZOS, D.; WARD, F.; DUFFY, P.; BOLAND, M.P.; LONERGAN, P. Consequences of bovine oocyte maturation, fertilization or early embryo development *in vitro* versus *in vivo*: implications for blastocyst yield and blastocyst quality. **Molecular Reproduction and Development**, v. 61, n. 2, p. 234-248. 2002b.

RIZOS, D.; LONERGAN, P.; BOLAND, M.P.; ARROYO-GARCIA, R.; PINTADO, B.; DE LA FUENTE, J.; GUTIERREZ-ADAN, A. Analysis of differential messenger RNA expression between bovine blastocysts produced in different culture systems: implications for blastocyst quality. **Biology of Reproduction**, v. 66, p. 589-595, 2002c.

SA FILHO, M.F.; CRESPILHO, A.M.; SANTOS, J.E.P.; PERRY, G. A.; BARUSELLI, P.S. Ovarian follicle diameter at timed insemination and estrous response influence likelihood of ovulation and pregnancy after estrous synchronization with progesterone or progestin-based protocols in suckled Bos indicus cows. **Animal Reproduction Science**, v. 120, p. 23-30, 2010.

SA FILHO, O.G.; MENEGHETTI, M.; PERES, R.F.G.; LAMB, G.C.; VASCONCELOS, J.L.M. Fixed-time artificial insemination with estradiol and progesterone for Bos indicus cows II: Strategies and factors affecting fertility. **Theriogenology**, v. 72, p. 210-218, 2009.

SALILEW-WONDIM, D.; FOURNIER, E.; HOELKER, M.; SAEED-ZIDANE, M.; THOLEN, E.; LOOFT, C.; NEUHOFF, C.; BESENFELDER, U.; HAVLICEK, V.; RINGS, F.; GAGNE, D.; SIRARD, M.A.; ROBERT, C.; SHOJAEI SAADI, H.A.; GAD, A.; SCHELLANDER, K.; TESFAYE, D. Genome-Wide DNA Methylation Patterns of Bovine Blastocysts Developed *In vivo* from Embryos Completed Different Stages of Development *In vitro*. **PLoS One**, v. 10, p. e0140467, 2015.

VASCONCELOS, J.L.; DE SA FILHO, O.G.; COOKE, R.F. Impacts of reproductive technologies on beef production in South America. **Advances in Experimental Medicine and Biology**, v. 752, p. 161-180, 2014.

VASCONCELOS, J.L.M.; SARTORI, R.; OLIVEIRA, H.N.; GUENTHER, J.G.; WILTBANK, M.C. Reduction in size of the ovulatory follicle reduces subsequent luteal size and pregnancy rate. **Theriogenology**, v. 56, p. 307-314. 2001.

WETSCHER, F.; HAVLICEK, V.; HUBER, T.; MULLER, M.; BREM, G.; BESENFELDER, U. Effect of morphological properties of transferred embryonic stages on tubal migration Implications for *in vivo* culture in the bovine oviduct. **Theriogenology**, v, 64. p. 41-48, 2005.

2 LITERATURE REVIEW: MORPHOPHISIOLOGY OF THE BOVINE OVIDUCT

2.1 INTRODUCTION

Since 1561, when Gabriele Falloppio discovered the oviduct, until the late 1900s, the oviduct was considered to be just a conduct for the passage of sperm and oocytes without any relevant metabolic or physiological function (BROWER; ANDERSON, 1969). However, it is now well accepted that the oviduct plays a major role in sperm storage and capacitation (BOILARD *et al*., 2004; LACHANCE *et al*., 2007), fertilization (CABALLERO *et al*., 2014), and early embryo development (LAI *et al*., 1996; SAINT-DIZIER *et al*., 2012). Based on its macro-anatomical characteristics, the oviduct can be divided into four regions: the infundibulum, the ampulla, the isthmus, and the utero-tubal junction. The infundibulum captures the oocyte after ovulation; the ampulla is site of fertilization; and the isthmus serves as a sperm reservoir in some species (HUNTER *et al*., 1991) and transports the embryo to the uterine lumen (KOLLE *et al*., 2009). These regions have a different function; they also have cellular and molecular characteristics different from each other (BROWER; ANDERSON, 1969; ABE, 1996; ITO *et al*., 2016).

It is also important to consider that oviductal secretions are composed of molecules originated from the peripheral circulation, as well as of molecules synthetized *de novo* by the luminal epithelial cells (WIJAYAGUNAWARDANE *et al*., 1998; ULBRICH *et al*., 2003; AVILES *et al*., 2010). These secretions include nutrients such as energy substrates, ions, amino acids, lipids, and proteins with structural, catalytic, and regulatory functions (BUHI *et al*., 2000; LI *et al*., 2007; HUGENTOBLER *et al*., 2010). In ruminants, the coordinated and sequential changes of ovarian steroids concentrations, estradiol (E2) and progesterone (P4) during the estrous cycle, regulate oviductal secretory function (GANDOLFI *et al*., 1989; BINELLI *et al*., 1999; BUHI *et al*., 2000). As a matter of fact, the volume of oviductal secretions increases around ovulation (MURRAY, 1995) and decreases during the luteal phase and pregnancy (CIGANKOVA *et al*., 1996). It is essential to study the oviductal physiology, the processes that take place in the oviductal lumen, and the environment where these processes occur. This literature review, therefore,

addresses a wide range of aspects of the oviduct's morphology and physiology, as well as the oviduct's interaction with gametes and embryo.

2.2 FUNCTIONAL MORPHOLOGY OF THE OVIDUCT

The oviduct or fallopian tube is the tubular organ that connects the ovary to the uterus and transports gametes and embryos. Starting near the ovary until entering the uterus, the oviduct has four segments: infundibulum, ampulla, isthmus, and the utero-tubal junction (UTJ; BACHA; BACHA, 2012). In cattle, the oviduct range from 20-25 cm in length and 1.5-3 mm in width, and it follows a path over the free edge of the broad ligament wrapping the ovary (GROSSMAN; SISSON, 1982). The infundibulum is funnel-like shaped. It has fimbriae inserted in the free margin of the broad ligament, and these fimbriae capture the oocyte after ovulation (GROSSMAN; SISSON, 1982; BACHA; BACHA, 2012). The ampulla participates in the transportation of the cumulus-oocyte complex (COC) and fertilization, while the isthmus and the UTJ are responsible for the formation of sperm reserves and embryo transportation to the uterus (HUNTER, 2012).

The oviductal wall is composed of a tunica serosa, a tunica muscularis, and a tunica mucosa (PRIEDKALNS; LEISER, 2006). These tunics present different characteristics depending of the oviductal region, i.e.: the tunica mucosa is more prominent in the ampulla and the tunica muscularis is thicker at the isthmus (Figure 1; PRIEDKALNS; LEISER, 2006; BACHA; BACHA, 2012). The tunica mucosa consists of a luminal columnar pseudostratified epithelium and the mucosal longitudinal folds. The number of folds decreases in the segments closest to the uterus. In cows, approximately 40 primary folds are present in the ampulla, each containing secondary and tertiary folds (PRIEDKALNS; LEISER, 2006; BACHA; BACHA, 2012). This complex organization can fill the lumen almost completely (McDANIEL *et al*., 1968; SAMUELSON, 2007). In the isthmus, tertiary folds begin to disappear. At the UTJ, only 4-8 primary folds remain while tertiary folds are absent (PRIEDKALNS; LEISER, 2006).

Figure 2– Illustration of the bovine oviduct

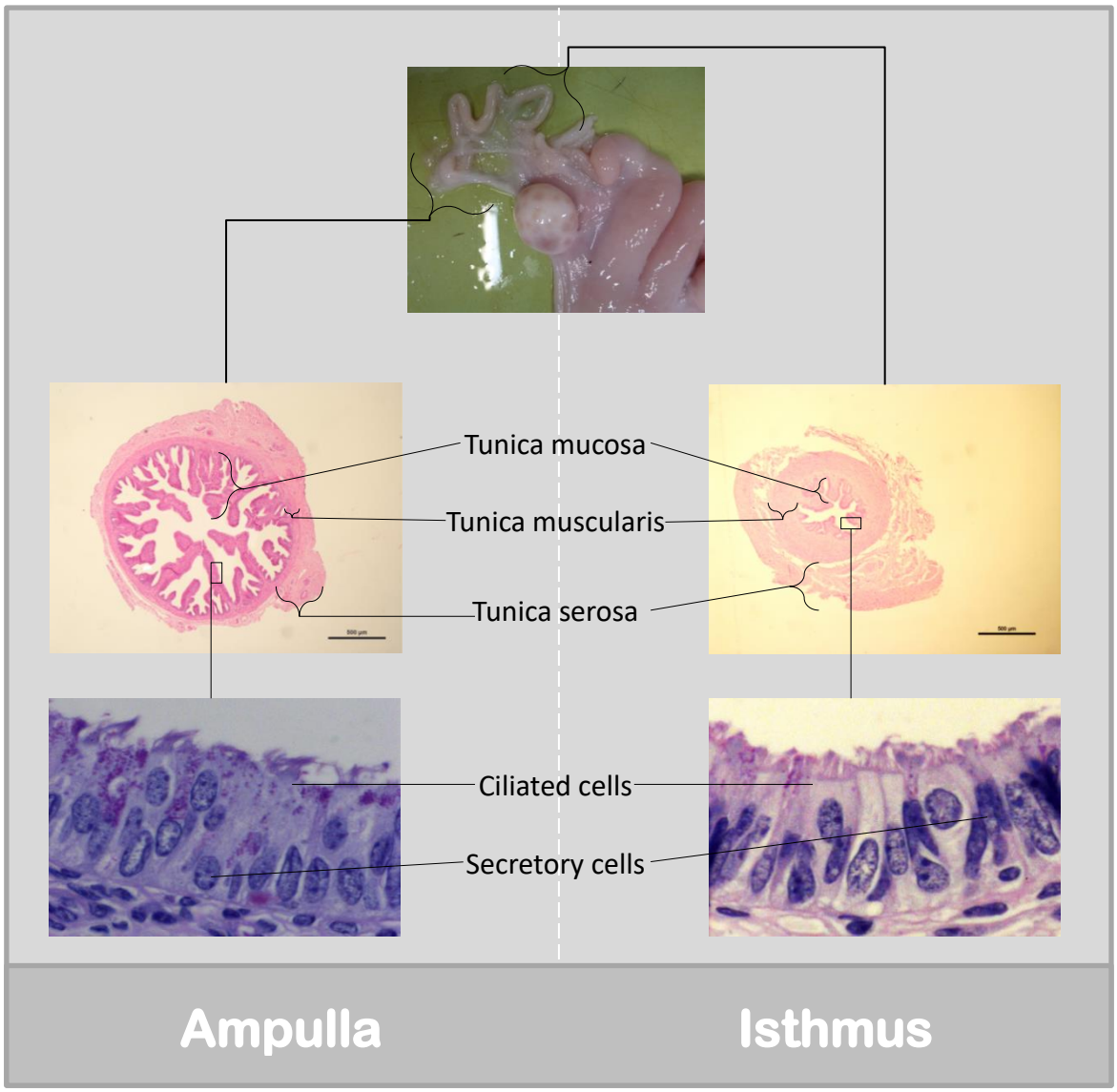

Source: Gonella-Diaza, 2017.

Legend: Top: Gross anatomy of the oviduct. Middle: microphotography of Hematoxilin-Eosine stained sections. Note the difference of the thickness of the structural layers. Bottom: microphotography of periodic acid-schiff stained sections. Note the difference in cellular morphology and cellular populations between the two regions.

2.2.1 Distribution and Population of Cells in the Oviductal Luminal Epithelium

The oviductal epithelium contains both columnar ciliated cells and non-ciliated secretory cells, also known as PEG cells (ERIKSEN *et al*., 1994; AYEN *et al*., 2012; BACHA; BACHA, 2012). It has been shown that there are cyclical and regional variations in the secretory cells ratio, which increases near the estrus. These cells are also present in greater proportion in the ampulla than in the isthmus (ESPINASSE, 1935; DONNEZ *et al*., 1985; LAUSCHOVA, 2003; AYEN *et al*., 2012).

Ciliated cells are more abundant in the infundibulum, where they favor the oocyte's movement. In the isthmus, these cells favor the embryo's transportation. The apical surface of these cells has many cilia and microvilli (BROWER; ANDERSON, 1969). Cilia have coordinated movements which move forward these structures (SAMUELSON, 2007). The nucleus of ciliated cells is spherical and located in the middle of the cell. The cytoplasm is slightly basophilic and rich in mitochondria (ERIKSEN *et al*., 1994). In rabbits, it was observed that the cytoplasm of ciliated cells has abundant mitochondria, ribosomes, and microtubules, which provide sufficient energy for ciliary movement (BROWER; ANDERSON, 1969). It is also believed that P4 concentrations can affect embryo development by regulating their transportation to the uterus (SAINT-DIZIER *et al*., 2012). In cows, it has been shown that P4 reduces the motility of the oviduct *in vivo* and the motility of cilia *ex vivo* by activating rapid genomic mechanisms (KOLLE *et al*., 2009).

Non-ciliated cells have a known secretory activity and may reach a larger size than ciliated cells. During follicular phase they develop characteristic cytoplasmic granules (ABE, 1996; SAMUELSON, 2007). It is known that the secretions of these cells provide nutrients for the oocyte and embryo (HUNTER, 1998; PRIEDKALNS; LEISER, 2006) and could favor sperm capacitation (HUNTER; WILMUT, 1984; HUNTER, 2012). Secretory cells are more basophilic and electron-dense than ciliated cells and could have a columnar or irregular morphology (ERIKSEN *et al*., 1994). The apical surface of the secretory cell can be found at the same height than the ciliated cell or even higher thus forming cellular protrusions in the lumen of the oviduct (ERIKSEN *et al*., 1994). However, this characteristic morphology may vary during the estrous cycle (AYEN *et al*., 2012). After ovulation, lower secretory cells are commonly found; they tend to increase its size and number of cytoplasmic

protrusions along the reproductive cycle (ERIKSEN *et al*., 1994). Protrusions may contain rough endoplasmic reticulum (RER) portions, mitochondria, and ribosomes. The nucleus of the secretory cell is located near the base of the cell, has an irregular shape, and is accompanied by RER generally. In electron microscopy, the secretory cell is electron-dense due to plenty RER and free ribosomes in the cytoplasm (BROWER; ANDERSON, 1969).

The most notable characteristic of secretory cells is the presence of secretory granules, whose number and distribution vary considerably among the days of the estrous cycle (BROWER; ANDERSON, 1969; ABE, 1996). In general terms, the secretory cell contains more granules during the follicular phase than during the luteal phase. Likewise, ampullary secretory cells have a greater number of granules than the isthmus, while the UTJ is practically free of granules. Inside the cell, two types of cytoplasmic granules can be found: the first kind is oval or circular granules that contain electron-lucent material and are located near the nucleus. The second type of granules is small, circular in shape, and contains electron-dense material (ABE, 1996). It is believed that the larger granules are transformed gradually into small granules. Cellular secretions are the main material contained inside these granules (BACHA; BACHA, 2012). It was reported that in rabbits, ten days after coitus, the cells expel almost all of its granules and recover their columnar shape and smaller size (BROWER; ANDERSON, 1969). The larger number of granules inside the secretory cells during the follicular phase could be related to nutrient supply during the migration and development of the embryo, and could provide an embryotrophic effect. Yet, the greater number of cellular protrusions in the luteal phase may be connected to epithelial renewal, when the epithelium prepares for the subsequent cycle (ERIKSEN *et al*., 1994; STEFFL *et al*., 2008).

2.2.2 Presence of Immune Cells

The oviduct is a sterile environment, but can be contaminated with pathogens from the uterus, the peritoneal cavity, and the follicular fluid (HERATH *et al*., 2007). The oviductal cells have the ability to provide efficient immune response, which can activate the arrival of immune system cells and trigger inflammatory processes if required (HERATH *et al*., 2007; KOWSAR *et al*., 2013; IBRAHIM *et al*., 2015). For

this reason, in physiological conditions, it is not common to find the presence of large amounts of immune cellular aggregates in the oviduct. Histological sections revealed that the presence of immune cells in the epithelium and stroma is uncommon. Additionally, contrary to what commonly happens in the gastrointestinal tract, these cells are not uniformly distributed (SAMUELSON, 2007; BACHA; BACHA, 2012).

Using flow cytometry for leukocytes quantification, Givan *et al*., (1997) have determined that these cells represent a small cell population in the tubal tissue in women (6-20%). Also, it was determined that the most commonly found leucocytes in the reproductive tract of women are T lymphocytes (CD3+ cells). Their ratio is higher in the cervix and vagina than in the uterus and tubes. Moreover, granulocytes (CD66b+ cells) were the second major leukocyte subpopulation found, and they had a greater presence in the fallopian tubes when compared to the uterus, cervix, and vagina. The number of monocytes/macrophages (CD14+ cells) and the number of B cells (CD19+ cells) represent each about 10% of the total number of leukocytes. Both subpopulations, CD14+ and CD19+ cells, were constant in all tissues/organs of the reproductive tract.

In another study, where immunohistochemistry was used to locate leukocytes, 147-743 cells per mm^2 of tissue were found. These cells were present in the epithelium, stroma, lamina propria, and tunica muscularis (ARDIGHIERI *et al*., 2014). Leukocytes were also mixed with the secretory cells and ciliated cells, and positioned above the basement membrane. In the stroma and in the muscular wall, leukocytes were only a few and dispersed, and occasionally formed small clusters around blood vessels (ARDIGHIERI *et al*., 2014).

2.2.3 Irrigation of the Oviduct

In the cow, a branch of the ovarian artery irrigates the infundibulum, ampulla, and distal isthmus. The uterine artery branch irrigates the proximal isthmus and UTJ (GROSSMAN; SISSON, 1982). The venous drainage occurs parallel to the arterial system. Thus, there is a possibility that molecules can be transferred from the ovary to the oviduct through the counter-current mechanism. That mechanism goes from the ovarian vein to the utero-ovarian artery and tubal artery (LEESE, 1988). This mechanism has also been studied by Hunter *et al*., (1983) in sows. They found that

the oviduct has a higher sex-steroids concentration than the serum, which can be explained by the local transportation of these hormones. Similar results were reported in cows (WIJAYAGUNAWARDANE *et al*., 1996; WIJAYAGUNAWARDANE *et al*., 1998), where E2 and P4 concentrations are higher in the oviductal tissue than in the peripheral blood.

2.3 SYNTHESIS AND SECRETION OF OVIDUCTAL FLUIDS

All the physiological processes that occur in the oviductal lumen depend mainly on the oviductal fluid and its components (BUHI *et al*., 2000). These processes could have two different origins: molecules secreted by the luminal epithelia or molecules coming from plasma (AVILES *et al*., 2010). Changes in concentrations of molecules derived from the biosynthetic activity of the oviduct are stimulated by E2 in a region-specific manner. In a study by Buhi *et al*., (1992), it was shown that the oviduct regions tend to have a different pattern of secretion and different forms to respond to E2. Using exogenous E2 to stimulate ovariectomized sows, they found an increase in the synthesis and secretion of macromolecules in the infundibulum and the ampulla, whereas the synthesis remains unchanged on the isthmus. Based on this work, the authors determined that the pattern of macromolecules secretion presents a "regional gradient". The ampulla secretes more quantity of macromolecules than the infundibulum, and the latter more than the isthmus. Similar results were also reported in sheep (BUHI *et al*., 1991).

The oviductal fluid is colorless and has a slightly alkaline pH (pH 7.7 to 8.2). The specific gravity of the fluid is less than 1.0 and osmolality is around 310 mOsm (LAUSCHOVA, 2003). In addition, it contains many metabolites such as glucose, lactate, pyruvate, and amino acids. The concentration of these metabolites concentration differs from those found in the uterine fluid or plasma. Also, oviductal fluid contains a large number of specific proteins with multiple functions (AVILES *et al*., 2010). BISHOP *et al*., (1956) used an experimental model in which the UTJ was ligated and the oviductal fluid was collected through the infundibulum in rabbits. They found that the oviduct produced 0.79 ml of fluid daily at a maximum pressure of 34 mmHg. Serum proteins were located in the oviductal lumen. The most abundant are albumin and immunoglobulins. Enzymes and cytokines that pass from the serum

through to the lumen by transudation were also found (LEESE, 1988; BUHI *et al*., 2000).

Multiple proteins secreted by the oviductal cells have been discovered using techniques such as one- or two-dimensional gel electrophoresis (BUHI *et al*., 2000). However, studying secreted proteins is a complex process because the most abundant proteins in the fluid are serum proteins. Binelli *et al*., (1999) employed an experimental model in which oviductal explants were cultured *in vitro* in a medium supplemented with radio-labeled leucine. Using samples from animals with or without persistent dominant follicles, they determined that the *de novo* protein synthesis made by oviduct cells varies depending on E2 concentrations. Among the proteins that are synthetized by the oviductal cells, the Oviductal Glycoprotein 1 (OVGP1) has been the most extensively studied (BOICE *et al*., 1990; BUHI, 2002). The OVGP1 is similar to members of the mucin and the glycosyl hydrolase 18 gene family, in which proteins with enzymatic activity are included. However, no enzymatic activity for OVGP1 has been reported. This protein is synthesized exclusively by non-ciliated secretory cells (BUHI, 2002), and the OVGP1 gene is present in the genome of various animals, such as all mammals (AVILES *et al*., 2010). It has been reported (BUHI *et al*., 2000; BUHI, 2002) that this protein interacts with gametes and embryos, and its maximum expression level occurs near the peak of E2 in cows (BUHI, 2002). Employing immunomicroscopy techniques, it was demonstrated that OVGP1 can penetrate the zona pellucida and enter the perivitelline space. It also interacts with the acrosomal membrane in the sperm (WEGNER; KILLIAN, 1991). However, it is still unknown the specific role of this protein during fertilization and embryonic development, as OVPG1 knockout mice have normal fertility (ARAKI *et al*., 2003).

2.4 OVIDUCTAL-GAMETE AND OVIDUCTAL-EMBRYO INTERACTIONS

The oviduct is an organ that allows the temporary accommodation and traffic of gametes and embryos, while providing different environments for the physiological events that take place in its lumen. The oocyte and the sperms cells enter in the oviduct by opposite sides and find each other in the final portion of the ampulla, where fertilization occurs (BESENFELDER *et al*., 2012). The oviduct offers all the

necessary conditions for the selective entry of sperm, sperm capacitation, and sperm hypermotility in order to protect the fertilization of the matured oocyte. These structures (gametes and embryos) modify local molecular mechanisms; this modification is the first exchange of biochemical signals with maternal tissues (SOSTARIC *et al*., 2008; BESENFELDER *et al*., 2012; ALMIÑANA *et al*., 2014). Multiple studies have been conducted to clarify the biochemical and molecular processes that occur during these processes.

2.4.1 Oviductal-Sperm Interactions

In mammals after mating, sperms migrate to the reproductive female tract and form the oviductal sperm reservoir in the caudal portion of the isthmus and UTJ. This formation happens because the sperm cells bind to the oviductal-cell's membranes. In cows, 6-8 hours are needed for the oviductal sperm reservoir to reach an optimal sperm concentration that ensures fertilization (HUNTER; WILMUT, 1983). Using video-microscopy, it was determined that the sperm cell binds exclusively to the ciliated cells thus forming a tangential angle (KOLLE *et al*., 2009). The bovine spermatozoa can remain adhered to the oviductal lumen more than 18 hours and be released only near the time of ovulation (De PAUW *et al*., 2002). Once the oocyte reaches the site of fertilization, the spermatic cells stored in the sperm reservoir begin the hyperactivation and early acrosome reaction; by releasing themselves form ciliated cells and resuming their migration to the site of fertilization (KOLLE *et al*., 2009). This sperm-ciliated cell interaction modifies the oviductal gene expression. The presence of sperm up-regulates the expression of adrenomedullin in oviductal cells. This transcript has been involved in ciliary motility in human (LI *et al*., 2010) and mouse (LIAO *et al*., 2011). Additionally, the sperm arrival increases the synthesis and secretion of prostaglandin E2, which is involved in smooth muscle contraction/relaxation (FAZELI *et al*., 2004). It could potentially intermediate in the establishment of an anti-inflammatory environment in the oviduct (YOUSEF *et al*., 2016). Moreover, it has been established that the oviductal cells could recognize between X- and Y-chromosome bearing spermatozoa. ALMIÑANA *et al*., 2014 found an oviductal sex-specific transcriptomic response when sows were inseminated with

sex-sorted semen. When compared to the presence of X-chromosome-bearing spermatozoa, they found that 501 genes were altered in the oviduct in the presence of Y-chromosome-bearing spermatozoa.

2.4.2 Oviductal-Oocyte Interaction

During ovulation, the cumulus-oocyte complex (COC) is expelled from the tertiary follicle and captured by the fimbriae through synchronic movements of its ciliated cells (ELLINGTON, 1991). The rhythmic contractions of the tunica muscularis of the infundibulum, the mesovarium, and the mesosalpinx are also involved in this process (HUNTER, 2012). The transportation of the COC to the fertilization local is rapid: 9-15 minutes in rabbits and 30-45 minutes in sows. This transportation is mediated by a combination of ciliary beats and muscular rhythmic contractions (HUNTER, 1998, 2012). Once the COC reaches the fertilization location, it makes a pause in its transportation. It happens because the cumulus cells establish a strong connection with the oviductal epithelial cells. This connection occurs undistinguished with mature or immature oocytes, and also with oocytes matured *in vitro* or *in vivo*. However, it does not happen with degenerated oocytes (KOLLE *et al*., 2009). During this transit, furthermore, the removal of cumulus cells exposes the zona pellucida to the oviductal fluid, and even components of the oviductal fluid penetrate the zona pellucida (WEGNER; KILLIAN, 1991). This process can promote the oocyte maturation and prevent polyspermy (COY *et al*., 2008, 2012).

2.4.3 Oviductal-Embryo Interactions

After fertilization, the new zygote undergoes mitotic process thus incrementing its cell number. This process is mediated mainly by oocyte components and by oviductal environment. The oviduct affects the embryo's development and the embryo, in turn, modulates the oviductal transcriptome and protein synthesis in a complex two-way communication. In mares, it was found that non-fertilized oocytes were retained in the oviduct while the fertilized embryo continues its transit to the uterus (VAN NIEKERK; GERNEKE, 1966). In hamsters, embryos were transported to

the uterus 1 day earlier than non-fertilized oocytes (ORTIZ *et al*., 1986). It has been assumed that this is mainly mediated by the embryo's capacity to produce prostaglandin E2 (WEBER *et al*., 1991).

The presence of the embryo modulates the oviductal transcriptome. Using mice, Lee *et al*., (2002) transferred viable embryos in one oviduct, and non-fertilized oocytes into the other oviduct. They showed that the presence of embryos upregulated the oviductal expression of specific genes like thymosin β4 and ribosomal protein L41. Chang *et al*., (2000) collected gilt's oviducts containing embryos at various stages of early development. They also collected oviductal epithelial cells and measured the abundance of specific transcripts. They found that 4-cell embryos 4-cell embryos and beyond 4-cell embryos have the capacity to modify the oviductal expression of specific genes (transforming growth factor-α and transforming growth factor-β binding protein II). Additionally, Almiñana *et al*., (2012) show that in the presence of embryos, the expression of genes related to the immune system was downregulated.

2.5 FINAL CONSIDERATIONS

The lumen of the oviduct should provide the correct environment for the occurrence of various reproductive processes. This environment varies depending on the region, the side of ovulation, and the estrous cycle. Changes in sex-steroid concentrations have a key role in this environment variation (BAUERSACHS *et al*., 2003; HUNTER, 2012; CERNY *et al*., 2015; GONELLA-DIAZA *et al*., 2015). E2 and P4 exert their function by activating specific receptors (CONNEELY *et al*., 2002; ULBRICH *et al*., 2003). How these processes can be modulated by different hormonal concentrations will be the subject of this Thesis.

2.6 REFERENCES

ABE, H. The mammalian oviductal epithelium: Regional variations in cytological and functional aspects of the oviductal secretory cells. **Histology and Histopathology**, v. 11, n. 3, p. 743-768, 1996.

ALMIÑANA, C. CABALLERO, I. HEATH, PR. MALEKI-DIZAJI, S. PARRILLA, I. CUELLO, C. GIL, MA. VAZQUEZ, JL. VAZQUEZ, JM. ROCA, J. MARTINEZ, EA. HOLT, WV. FAZELI, A. The battle of the sexes starts in the oviduct: modulation of oviductal transcriptome by X and Y-bearing spermatozoa. **BMC Genomics**. England, v.15, p.293, 2014.

ALMIÑANA, C. HEATH, PR. WILKINSON, S. SANCHEZ-OSORIO, J. CUELLO, C. PARRILLA, I. GIL, MA. VAZQUEZ, JL. VAZQUEZ, JM. ROCA, J. MARTINEZ, EA. FAZELI, A. Early developing pig embryos mediate their own environment in the maternal tract. **PLoS One**, v. 7, n. 3, p. e33625, 2012.

ARAKI, Y. NOHARA, M. YOSHIDA-KOMIYA, H. KURAMOCHI, T. ITO, M. HOSHI, H. SHINKAI, Y. SENDAI, Y. Effect of a null mutation of the oviduct-specific glycoprotein gene on mouse fertilization. **The Biochemical Journal**. England, v.374, p.551-7. 2003.

ARDIGHIERI, L. LONARDI, S. MORATTO, D. FACCHETTI, F. SHIH, IEM. VERMI, W. KURMAN, RJ. Characterization of the immune cell repertoire in the normal fallopian tube. **International journal of gynecological pathology**, v. 33, n. 6, p. 581-91, 2014.

AVILES, M. GUTIERREZ-ADAN, A. COY, P. Oviductal secretions: will they be key factors for the future ARTs? **Molecular Human Reproduction**, v. 16, n. 12, p. 896-906, 2010.

AYEN, E. SHAHROOZ, R. KAZEMIE, S. Histological and histomorphometrical changes of different regions of oviduct during follicular and lutealphases of estrus cycle in adult Azarbaijan buffalo. **Iranian Journal of Veterinary Research**: Shiraz University. v. 13. p. 42-48. 2012.

BACHA, WJ. BACHA, LM. **Color Atlas of Veterinary Histology.** Third edition. Wiley-blackwell. , June 2012. ISBN-13: 978-0470958513.

BAUERSACHS, S. BLUM, H. MALLOK, S. WENIGERKIND, H. RIEF, S. PRELLE, K. WOLF, E. Regulation of ipsilateral and contralateral bovine oviduct epithelial cell function in the postovulation period: a transcriptomics approach**. Biology of Reproduction**, v. 68, n. 4, p. 1170-7, 2003.

BESENFELDER, U. HAVLICEK, V. BREM, G. Role of the oviduct in early embryo development. **Reproduction of Domestic Animals**, v. 47 Suppl 4, p. 156-63, 2012.

BINELLI, M. HAMPTON, J. BUHI, WC. THATCHER, WW. Persistent dominant follicle alters pattern of oviductal secretory proteins from cows at estrus. **Biology of Reproduction**, v. 61, n. 1, p. 127-134, 1999.

BISHOP, DW. Active secretion in the rabbit oviduct. **The American Journal of Physiology**. v. 187, n. 2, p. 347-352, 1956.

BOICE, ML. GEISERT, RD. BLAIR, RM. VERHAGE, HG. Identification and characterization of bovine oviductal glycoproteins synthesized at estrus. **Biology of Reproduction**, v. 43, n. 3, p. 457-65, 1990.

BOILARD, M. REYES-MORENO, C. LACHANCE, C. MASSICOTTE, L. BAILEY, JL. SIRARD, MA. LECLERC, P. Localization of the chaperone proteins GRP78 and HSP60 on the luminal surface of bovine oviduct epithelial cells and their association with spermatozoa. **Biology of Reproduction**, v. 71, n. 6, p. 1879-1889, 2004.

BROWER, L. ANDERSON, E. Cytological Events Associated with the Secretory Process in the Rabbit Oviduct. **Biology of Reproduction**, v. 1, n.2, p.130-148, 1969.

BUHI, WC. Characterization and biological roles of oviduct-specific, oestrogen-dependent glycoprotein. **Reproduction**, v. 123, n. 3, p. 355-62, 2002.

BUHI, WC. ALVAREZ, IM. KOUBA, AJ. Secreted proteins of the oviduct. **Cells Tissues Organs**, v. 166, n. 2, p. 165-179, 2000.

BUHI, WC. ASHWORTH, CJ. BAZER, FW. ALVAREZ, IM. *In vitro* synthesis of oviductal secretory proteins by estrogen-treated ovariectomized gilts. **Journal of Experimental Zoology**, v. 262, n. 4, p. 426-35, 1992.

BUHI, WC. BAZER, FW. ALVAREZ, IM. MIRANDO, MA. *In vitro* synthesis of oviductal proteins associated with estrus and 17 beta-estradiol-treated ovariectomized ewes. **Endocrinology**, v. 128, n. 6, p. 3086-95, 1991.

CABALLERO, JN. GERVASI, MG. VEIGA, MF. DALVIT, GC. PEREZ-MARTÍNEZ, S. CETICA, PD. VAZQUEZ-LEVIN, MH. Epithelial cadherin is present in bovine oviduct epithelial cells and gametes, and is involved in fertilization-related events. **Theriogenology**, v. 81, n. 9, p. 1189-206, 2014.

CERNY, KL. GARRETT, E. WALTON, AJ. ANDERSON, LH. BRIDGES, PJ. A transcriptomal analysis of bovine oviductal epithelial cells collected during the follicular phase versus the luteal phase of the estrous cycle. **Reproductive Biology and Endocrinology**, v. 13, p. 84, 2015.

CHANG, HS. CHENG, WT. WU, HK. CHOO, KB. Identification of genes expressed in the epithelium of porcine oviduct containing early embryos at various stages of development. **Molecular reproduction and development**, v. 56, n. 3, p. 331-5, 2000.

CIGÁNKOVÁ, V. KRAJNICÁKOVÁ, H. KOKARDOVÁ, M. TOMAJKOVÁ, E. Morphological changes in the ewe uterine tube (oviduct) epithelium during puerperium. **Veterinarni Medicina**, v. 41, n. 11, p. 339-346, 1996.

CONNEELY, OM. MULAC-JERICEVIC, B. DEMAYO, F. LYDON, JP. O'MALLEY, BW. Reproductive functions of progesterone receptors. **Recent progress in hormone research**, v. 57, p. 339-55, 2002.

COY, P. CÁNOVAS, S. MONDÉJAR, I. SAAVEDRA, MD. ROMAR, R. GRULLÓN, L. MATÁS, C. AVILÉS, M. Oviduct-specific glycoprotein and heparin modulate sperm-zona pellucida interaction during fertilization and contribute to the control of

polyspermy. **Proceedings of the National Academy of Sciences**, v. 105, n. 41, p. 15809-14, 2008.

COY, P. JIMÉNEZ-MOVILLA, M. GARCÍA-VÁZQUEZ, FA. MONDÉJAR, I. GRULLÓN, L. ROMAR, R. Oocytes use the plasminogen-plasmin system to remove supernumerary spermatozoa. **Human Reproduction**, v. 27, n. 7, p. 1985-93, 2012

DE PAUW, IM. VAN SOOM, A. LAEVENS, H. VERBERCKMOES, S. DE KRUIF, A. Sperm binding to epithelial oviduct explants in bulls with different nonreturn rates investigated with a new *in vitro* model. **Biology of Reproduction**, v. 67, n. 4, p. 1073-1079, 2002.

DONNEZ, J. CASANAS-ROUX, F. CAPRASSE, J. FERIN, J. THOMAS, K. Cyclic changes in ciliation, cell height, and mitotic activity in human tubal epithelium during reproductive life. **Fertility and sterility**, v. 43, n. 4, p. 554-9, 1985.

ELLINGTON, J. The bovine oviduct and its role in reproduction: a review of the literature. **The Cornell veterinarian**, v. 81, n. 3, p. 313-328, 1991.

ERIKSEN, T. TERKELSEN, O. HYTTEL, P. GREVE, T. Ultrastructural features of secretory-cells in the bovine oviduct epithelium. **Anatomy and Embryology**, v. 190, n. 6, p. 583-590, 1994.

ESPINASSE, PG. The oviducal epithelium of the mouse. **Journal of Anatomy**, v. 69, p. 363-368, 1935.

FAZELI, A. AFFARA, NA. HUBANK, M. HOLT, WV. Sperm-induced modification of the oviductal gene expression profile after natural insemination in mice. **Biology of Reproduction**, v. 71, n. 1, p. 60-5, 2004.

GANDOLFI, F. BREVINI, TA. RICHARDSON, L. BROWN, CR. MOOR, RM. Characterization of proteins secreted by sheep oviduct epithelial-cells and their function in embryonic-development. **Development**, v. 106, n. 2, p. 303-312, 1989.

GIVAN, AL. WHITE, HD. STERN, JE. COLBY, E. GOSSELIN, EJ. GUYRE, PM. WIRA, CR. Flow cytometric analysis of leukocytes in the human female reproductive tract: comparison of fallopian tube, uterus, cervix, and vagina. **American journal of reproductive immunology**, v. 38, n. 5, p. 350-9, 1997.

GONELLA-DIAZA, AM. ANDRADE, SC. SPONCHIADO, M. PUGLIESI, G. MESQUITA, FS. VAN HOECK, V. STREFEZZI, RDEF. GASPARIN, GR. COUTINHO, LL. BINELLI, M. Size of the Ovulatory Follicle Dictates Spatial Differences in the Oviductal Transcriptome in Cattle. **Plos One**. v. 10, n. 12, e0145321. 2015.

GETTY, R. GROSSMAN, JD. SISSON, S. **Anatomía de los animales domesticos : Sisson y Grossman.** 5th edition. Barcelona, Salvat, 1982. ISBN 8434516098.

HERATH, S. WILLIAMS, EJ. LILLY,ST. GILBERT, RO. DOBSON, H. BRYANT, CE. SHELDON, IM. Ovarian follicular cells have innate immune capabilities that modulate their endocrine function. **Reproduction**. v.134, p.683-93. 2007.

HUGENTOBLER, SA. SREENAN, JM. HUMPHERSON, PG. LEESE, HJ. DISKIN, MG. MORRIS, DG. Effects of changes in the concentration of systemic progesterone on ions, amino acids and energy substrates in cattle oviduct and uterine fluid and blood. **Reproduction Fertility and Development**, v. 22, n. 4, p. 684-694, 2010.

HUNTER, R. WILMUT, I. The rate of functional sperm transport into the oviducts of mated cows. **Animal Reproduction Science**, v. 5, n. 3, p. 167-173, 1983.

HUNTER, RH. Have the Fallopian tubes a vital role in promoting fertility? **Acta Obstetricia et Gynecologica Scandinavica**, v. 77, n. 5, p. 475-86, 1998.

HUNTER, RHF. Components of oviduct physiology in eutherian mammals**.** **Biological Reviews**, v. 87, n. 1, p. 244-55, 2012.

HUNTER, RH. COOK, B. POYSER, NL. Regulation of oviduct function in pigs by local transfer of ovarian steroids and prostaglandins: a mechanism to influence

sperm transport. **European Journal of Obstetrics, Gynecology, and Reproductive Biology**, v. 14, n. 4, p. 225-32, 1983.

HUNTER, RHF. FLECHON, B. FLECHON, JE. Distribution, morphology and epithelial interactions of bovine spermatozoa in the oviduct before and after ovulation - a scanning electron-microscope study. Tissue & Cell, v. 23, n. 5, p. 641-656, 1991.

HUNTER, RHF. WILMUT, I. Sperm transport in the cow - peri-ovulatory redistribution of viable cells within the oviduct. **Reproduction Nutrition Development**, v. 24, n. 5, p. 597-608, 1984.

IBRAHIM, S. SALILEW-WONDIM, D. RINGS, F. HOELKER, M. NEUHOFF, C. THOLEN, E. LOOFT, C. SCHELLANDER, K. TESFAYE, D. Expression Pattern of Inflammatory Response Genes and Their Regulatory MicroRNAs in Bovine Oviductal Cells in Response to Lipopolysaccharide: Implication for Early Embryonic Development. **PLoS One**. v.10, p.e0119388. 2015.

ITO, S. KOBAYASHI, Y. YAMAMOTO, Y. KIMURA, K. OKUDA, K. Remodeling of bovine oviductal epithelium by mitosis of secretory cells. **Cell and tissue research**, v. 366. n. 2, p. 403-410, 2016.

KÖLLE, S. DUBIELZIG, S. REESE, S. WEHREND, A. KÖNIG, P. KUMMER, W. Ciliary Transport, Gamete Interaction, and Effects of the Early Embryo in the Oviduct: Ex Vivo Analyses Using a New Digital Videomicroscopic System in the Cow. **Biology of Reproduction**, v. 81, n. 2, p. 267-274, 2009.

KOWSAR, R. HAMBRUCH, N. LIU, J. SHIMIZU, T. PFARRER, C. MIYAMOTO, A. Regulation of innate immune function in bovine oviduct epithelial cells in culture: the homeostatic role of epithelial cells in balancing Th1/Th2 response. **Journal of Reproduction and Development**. v. 59, 2013. p.470-478, 2013.

LACHANCE, C. BAILEY, JL. LECLERC, P. Expression of Hsp60 and Grp78 in the human endometrium and oviduct, and their effect on sperm functions. **Human Reproduction**, v. 22, n. 10, p. 2606-2614, 2007.

LAI, YM. WANG, HS. LEE, CL. LEE, JD. HUANG, HY. CHANG, FH. LEE, JF. SOONG, YK. Insulin-like growth factor-binding proteins produced by Vero cells, human oviductal cells and human endometrial cells, and the role of insulin-like growth factor-binding protein-3 in mouse embryo co-culture systems. **Human Reproduction**, v. 11, n. 6, p. 1281-1286, 1996.

LAUSCHOVA, I. Secretory cells and morphological manifestation of secretion in the mouse oviduct. **Scripta Medica (BRNO)**, v. 76, n. 4, p. 203-214, 2003.

LEE, KF. YAO, YQ. KWOK, KL. XU, JS. YEUNG, WS. Early developing embryos affect the gene expression patterns in the mouse oviduct. **Biochemical and biophysical research communications**, v. 292, n. 2, p. 564-70, 2002.

LEESE, HJ. The formation and function of oviduct fluid. **Journal of Reproduction and Fertility**, v. 82, n. 2, p. 843-856, 1988.

LI, HW. LIAO, SB. CHIU, PC. TAM, WW. HO, JC. NG, EH. HO, PC. YEUNG, WS, TANG F, O WS. Expression of adrenomedullin in human oviduct, its regulation by the hormonal cycle and contact with spermatozoa, and its effect on ciliary beat frequency of the oviductal epithelium. In: (Ed.). **The Journal of Clinical Endocrinology and Metabolism**. v.95, p.E18-25. 2010.

LI, R. WHITWORTH, K. LAI, L. WAX, D. SPATE, L. MURPHY, CN. RIEKE, A. ISOM, C. HAO, Y. ZHONG, Z. KATAYAMA, M. SCHATTEN, H. PRATHER, RS. Concentration and composition of free amino acids and osmolalities of porcine oviductal and uterine fluid and their effects on development of porcine IVF embryos. **Molecular Reproduction and Development**, v. 74, n. 9, p. 1228-1235, 2007.

LIAO, SB. HO, JC. TANG, F. O, WS. Adrenomedullin increases ciliary beat frequency and decreases muscular contraction in the rat oviduct. **Reproduction**, v. 141, n. 3, p. 367-72, 2011.

MCDANIEL, JW. SCALZI, H. BLACK, D. Influence of ovarian hormones on histology and histochemistry of the bovine oviduct. **Journal of Dairy Science**, v. 51, n. 5, p. 754-761, 1968.

MURRAY, MK. Epithelial lining of the sheep ampulla oviduct undergoes pregnancy-associated morphological-changes in secretory status and cell height. **Biology of Reproduction**, v. 53, n. 3, p. 653-663, 1995.

ORTIZ, ME. BEDREGAL, P. CARVAJAL, MI. CROXATTO, HB. Fertilized and unfertilized ova are transported at different rates by the hamster oviduct. **Biology of Reproduction**, v. 34, n. 4, p. 777-81, 1986.

PRIEDKALNS, J. LEISER, R. Female Reproductive System. In: **Dellmann's Textbook of veterinary histology**; edited by Eurell, JA. and Frappier, BL. Sixth edition: Blackwell publishing, 2013. ISBN 978-1-118-68582-2.

SAINT-DIZIER, M. SANDRA, O. PLOYART, S. CHEBROUT, M. CONSTANT, F. Expression of nuclear progesterone receptor and progesterone receptor membrane components 1 and 2 in the oviduct of cyclic and pregnant cows during the post-ovulation period. **Reproductive Biology and Endocrinology**, v. 10, p. 76. 2012.

SAMUELSON, DA. **Textbook of veterinary histology**. 1st edition. Saunders-Elsevier, 2007. ISBN 0721681743.

SOSTARIC, E. DIELEMAN, SJ. VAN DE LEST, CH. COLENBRANDER, B. VOS, PL. GARCIA-GIL, N. GADELLA, BM. Sperm binding properties and secretory activity of the bovine oviduct immediately before and after ovulation. **Molecular Reproduction and Development**, v. 75, n. 1, p. 60-74, 2008.

STEFFL, M. SCHWEIGER, M. SUGIYAMA, T. AMSELGRUBER, WM. Review of apoptotic and non-apoptotic events in non-ciliated cells of the mammalian oviduct. **Annals of Anatomy-Anatomischer Anzeiger**, v. 190, n. 1, p. 46-52, 2008.

ULBRICH, SE. KETTLER, A. EINSPANIER, R. Expression and localization of estrogen receptor alpha, estrogen receptor beta and progesterone receptor in the bovine oviduct *in vivo* and *in vitro*. **Journal of Steroid Biochemistry and Molecular Biology**, v. 84, n. 2-3, p. 279-289, 2003.

VAN NIEKERK, CH. GERNEKE, WH. Persistence and parthenogentic cleavage of tubal ova in the mare. **The Onderstepoort journal of veterinary research**, v. 33, n. 1, p. 195-232. 1966.

WEBER, JA. FREEMAN, DA. VANDERWALL, DK. WOODS, GL. Prostaglandin E2 secretion by oviductal transport-stage equine embryos. **Biology of Reproduction**, v. 45, n. 4, p. 540-3, 1991.

WEGNER, CC. KILLIAN, GJ. *In vitro* and *in vivo* association of an oviduct estrus-associated protein with bovine zona pellucida. **Molecular reproduction and development**, v. 29, n. 1, p. 77-84, 1991.

WIJAYAGUNAWARDANE, MP.CERBITO, WA. MIYAMOTO, A. ACOSTA, TJ. TAKAGI, M. MIYAZAWA, K. SATO, K. Oviductal progesterone concentration and its spatial distribution in cyclic and early pregnant cows. **Theriogenology**, v. 46, n. 7, p. 1149-1158, 1996.

WIJAYAGUNAWARDANE MP1, MIYAMOTO A, CERBITO WA, ACOSTA TJ, TAKAGI M, SATO K. Local distributions of oviductal estradiol, progesterone, prostaglandins, oxytocin and endothelin-1 in the cyclic cow. **Theriogenology**, v. 49, n. 3, p. 607-618, 1998.

YOUSEF, MS. MAREY, MA. HAMBRUCH, N. HAYAKAWA, H. SHIMIZU, T. HUSSIEN, HA. ABDEL-RAZEK, AK. PFARRER, C. MIYAMOTO, A. Sperm Binding to Oviduct Epithelial Cells Enhances TGFB1 and IL10 Expressions in Epithelial Cells as Well as Neutrophils *In vitro*: Prostaglandin E2 As a Main Regulator of Anti-Inflammatory Response in the Bovine Oviduct. **PLoS One**, v. 11, n. 9, p. e0162309, 2016.

3 CHAPTER 1: SIZE OF THE OVULATORY FOLLICLE DICTATES SPATIAL DIFFERENCES IN THE OVIDUCTAL TRANSCRIPTOME IN CATTLE[1]

In cattle, molecular control of oviduct receptivity to the embryo is poorly understood. Here, we used a bovine model for receptivity based on size of the pre-ovulatory follicle to compare oviductal global and candidate gene transcript abundance on day 4 of the estrous cycle. Growth of the pre-ovulatory follicle (POF) of Nelore (*Bos indicus*) cows was manipulated to produce two groups: large POF large corpus luteum (CL) group (LF-LCL; greater receptivity) and small POF-small CL group (SF-SCL). Oviductal samples were collected four days after GnRH-induced ovulation. Ampulla and isthmus transcriptome was obtained by RNAseq, regional gene expression was assessed by qPCR, and PGR and ERα protein distribution was evaluated by immunohistochemistry. There was a greater abundance of PGR and ERα in the oviduct of LF-LCL animals thus indicating a greater availability of receptors and possibly sex steroids stimulated signaling in both regions. Transcriptomic profiles indicated a series of genes associated with functional characteristics of the oviduct that are regulated by the periovulatory sex steroid milieu and that potentially affect oviductal receptivity and early embryo development. They include tissue morphology changes (extra cellular matrix remodeling), cellular changes (proliferation), and secretion changes (growth factors, ions and metal transporters), and were enriched for the genes with increased expression in the LF-LCL group. In conclusion, differences in the periovulatory sex steroid milieu lead to different oviductal gene expression profiles that could modify the oviductal environment to affect embryo survival and development.

[1] The full version of this study was published in the journal PLoS One (Gonella et al., 2015. Size of the ovulatory follicle dictates spatial differences in the oviductal transcriptome in cattle. Plos One, v.10, n.12, p. e0145321) and it is attached in the Appendix A.

4 CHAPTER 2: SEX STEROIDS MODULATE MORPHOLOGICAL AND FUNCTIONAL FEATURES OF THE BOVINE OVIDUCT[2]

4.1 INTRODUCTION

The oviduct, the anterior-most tubular segment of the female reproductive tract, is composed of three specialized regions, infundibulum, ampulla, and isthmus, each with distinct morphological, cellular, molecular and functional characteristics (HUNTER, 2012; LEESE, 1988; HUNTER, 1998). The oviduct must provide a suitable environment for the transport of gametes, fertilization, and early embryo development (HUNTER, 2012; BESENFELDER *et al*., 2012). During pre-natal development of the reproductive tract, the oviductal lumen is defined by a fairly flat epithelial lining, without appreciable folding. Only in the postnatal life the complexity of mucosal folds starts to develop. In the adult animal, oviductal folds develop a complex organization exhibiting primary, secondary and tertiary folds are observed (KENNGOTT; SINOWATZ 2007; KONISHI *et al*., 1987; AGDUHR, 1927). At this point, the oviductal epithelium forms longitudinal folds that increase the epithelial surface area, allowing for an improved interaction with gametes and embryos during their transit through the organ. However, this organization varies according to the oviductal region (BACHA; BACHA 2012, ABE, 1996) and the phase of the estrous cycle (McDANIEL *et al*., 1968, MOKHTAR, 2015; RESTALL, 1966). In general, the infundibulum and ampulla present greater number and complexity of folds than the isthmus; additionally, during estrus, the number of folds, as well as their degree of folding is increased (RESTALL, 1966). Furthermore, the oviductal epithelium contains two main cell types: ciliated and secretory cells. Ciliated cells are involved in sperm capacitation, transport of sperm cells and embryo, and to some extent, secretion of molecules into the lumen (DONNEZ *et al*., 1985; HUNTER 2012). On the other hand, unlike ciliated cells, secretory cells have their cellular machinery specifically organized for the synthesis and secretion of substances into the oviductal lumen (GANDOLFI *et al*., 1989; BROWER; ANDERSON, 1969). The proportion of these

[2] This manuscript was submitted to the Cell& Tissue research jjournal and was accepted for its publication on July of 2017. The acceptance letter is on Apendix C.

cells varies across the oviductal regions; with the ampulla exhibiting grater secretory activity compared to the other two regions owing to its greater proportion of secretory cells (BUHI *et al*., 2000).

Several studies showed that appropriate timing and prominence of sex-steroid hormones is important to ensure maternal receptivity (DEMETRIO *et al*., 2007; ASHWORTH *et al*., 1989; MORRIS; DISKIN, 2008). It has also been established that cows ovulating larger follicles can attain greater proestrus estradiol (E2) plasma concentrations, form a larger corpus luteum (CL) and produce greater progesterone (P4) concentrations during early diestrus (MESQUITA *et al*., 2014; VASCONCELOS *et al*., 2001; DEMETRIO *et al*., 2007; PERES *et al*., 2009). Furthermore, cows with such a periovulatory endocrine profile present increased fertility when compared to cows ovulating smaller follicles and forming smaller CLs (PUGLIESI *et al*., 2016). This increase in fertility is associated with changes in the endometrial (MESQUITA *et al*., 2015) and oviductal (GONELLA-DIAZA *et al*., 2015) transcriptome. However, very little is known about whole-organ, cellular and molecular mechanisms that could regulate oviductal functions, and that are associated with fertility. In a recent study, Gonella-Diaza *et al*., 2015 used an experimental model to modulate pre-ovulatory follicle growth to produce two groups of animals with distinctly different endocrine and ovarian phenotypes, the large follicle, large CL (LF-LCL) and the small follicle, small CL (SF-SCL) groups. On day 4 of the estrous cycle, LF-LCL cows presented 692 and 590 differentially expressed genes in the ampulla and isthmus, respectively, when compared to SF-SCL cows. Among these differentially expressed genes, several enriched cellular and metabolic processes such as branching morphogenesis, cellular proliferation and secretion were identified. However, whether such changes in transcript abundance resulted in phenotypic changes that could be related to oviductal functions remains unknown. Enrichment of transcripts associated with the aforementioned processes in the oviducts of LF-LCL cows suggests an increased proliferative activity of oviductal luminal epithelium, leading to folding and, consequently, increased surface area of the epithelial lining and secretion capacity. This phenotype might represent an advantage for the oviductal environment of cows via the local circulation of a more favorable endocrine profile arising from the ovulation of larger follicles and CLs thus resulting in improved production and secretion of nutrients and growth factors by the oviduct ultimately leading to greater

embryo quality and development potential (WETSCHER *et al*., 2005; AHUMADA *et al*., 2013). Thus, the objectives of this study were to compare (1) the oviduct morphology, (2) abundance of transcripts related to branching morphogenesis and cellular secretion, and (3) cellular proliferation between cows treated to ovulate larger or smaller follicles.

4.2 METHODOLOGY

4.2.1 Animal handling, reproductive management, and tissue processing

All animal procedures were approved by the Ethics and Animal Handling Committee of the School of Veterinary Medicine and Animal Science of the University of São Paulo (USP) in São Paulo, Brazil (CEUA/FMVZ; protocols numbers 2281-2011 and 4293160916). The hormonal manipulation procedures described here have been validated and previously published (MESQUITA *et al*., 2014, 2015; GONELLA-DIAZA *et al*., 2015). Briefly, prior to starting the experiment, 56 multiparous and non-lactating Nelore cows (*Bos indicus*) were selected, kept in grazing conditions (*Brachiaria brizantha* pasture), and supplemented with mineralized salt to fulfill their maintenance requirements. After a gynecological examination, cows were selected according to three criteria: no gross reproductive abnormalities, a body condition score between 3 and 4 (0, emaciated; 5, obese), and normal estrous cyclic activity.

Animals were randomly divided into two groups: LF-LCL and SF-SCL. Briefly, animals were pre-synchronized by intramuscular injection of GnRH agonist (1 µg of buserelin acetate; Sincroforte, Ouro Fino, Cravinhos, Brazil) and, 7 days later an injection of Prostaglandin F2 alpha analog (PGF; 0.5 mg of sodium cloprostenol; Sincrocio, Ouro Fino, Cravinhos, Brazil). At this day [day -20 (D-20)] animals received an ESTROTECT Heat detector patch (Rockway, Inc. Spring Valley,WI, USA) and estrus detection was performed twice daily from D-20 to D-10. Only animals with a fresh, PGF responsive CL (at least 5 days old) on D-10 stayed in the

experiment. Remaining cows (n = 41) received a new intravaginal P4 releasing device (1 g; Sincrogest, Ourofino) on D-10 and an intramuscular injection of 2 mg E2 benzoate (Sincrodiol, Ourofino). Only cows of LF-LCL group received an im injection of PGF. P4-releasing devices were removed after 8.25 and 8.75 days in the LF-LCL and SF-SCL groups, respectively. The differential animal handling (PGF injection at the time of P4-device insertion and timing of device removal) during the synchronization protocol was designed to enable animals of the LF-LCL group: 1) to develop a new follicular wave under a low P4 environment; and 2) to have more time to grow the preovulatory follicle during the proestrus. All animals received two PGF injections 6 h apart at P4 device removal. Ovulation was induced by an injection of 10 µg Buserelin on D0 (Sincroforte, Ourofino). Animals that responded to treatments were slaughtered on D4 after induction of ovulation (LFLCL, n = 13; SF-SCL, n= 10).

Immediately after slaughter, the reproductive tract was transported on ice to the laboratory; the oviducts ipsilateral and contralateral to the ovary containing the CL were identified and dissected to obtain samples of ampulla and isthmus (Figure 1). From each oviductal region, two sub-samples were extracted. These sub-samples were either fixed in buffered formalin or frozen in liquid nitrogen for histological or molecular analyzes, respectively.

Figure 3 – Experimental model.

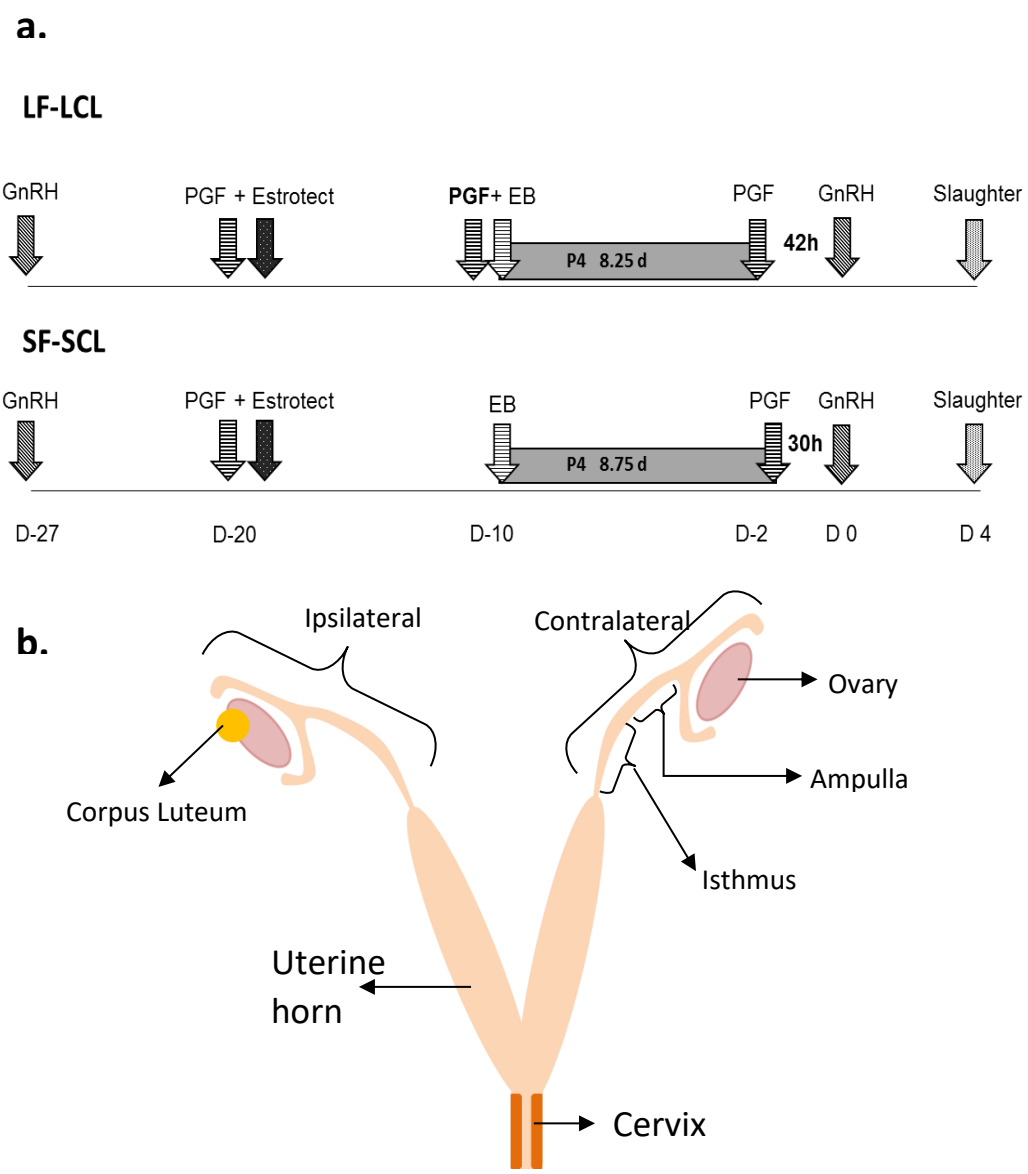

Source: Gonella-Diaza (2017)

Legend. **A.** Hormonal manipulation protocol used in the present study. Animals (n = 41) were pre-synchronized by intramuscular injection of GnRH agonist and, 7 days later an injection of Prostaglandin F2 alpha (PGF) analog. At this day [day -20 (D-20)] animals received an ESTROTECT Heat detector device and estrus detection was performed twice daily from D-20 to D-10. All animals received a new intravaginal P4-releasing device on D-10 along with an intramuscular injection of 2 mg estradiol benzoate. Simultaneously, cows in the LF-LCL received an intramuscular injection of PGF. The P4 devices were removed on day -2, 42 h and 30 h before the GnRH injection in the LF-LCL and the SF-SCL groups, respectively. All animals received a PGF injection at P4 device removal and a second PGF injection 6 h later. Ovulation was induced by an injection of GnRH agonist on D0. **B.** Reproductive tract of the cow showing the local of the sample collection. Immediately after slaughter, the reproductive tract was removed, transported on ice and the ipsilateral and contralateral oviducts were dissected. Later, ampulla and isthmus samples from each side were preserved for histological or molecular analysis.

4.2.2 Histological analysis

Freshly dissected tissues remained in formalin for 24 hours then were dehydrated in a gradient of increasing ethanol concentrations, and cleared in a gradient of increasing concentrations of xylene before embedding in paraffin. Cross-sections were obtained at 4 µm of thickness and from each sample; at least 5 non-consecutive sections, 8 µm apart, were obtained. Three sections were stained with Harris-Haematoxylin and Eosin (H&E), and two were stained with periodic acid-Schiff (PAS). The H&E stained sections were photographed using a stereomicroscope coupled to a digital camera and computer with specialized software to capture the entire tissue section in the same image. PAS-stained luminal epithelium tissue sections were photographed with an optical microscope (Zeiss Axioplan 2, Zeiss, Oberkochen, Germany) coupled with a digital camera (Zeiss MC 80 DX, Zeiss) using 100x magnification with oil immersion. Initially, the pictures were analyzed to assess the quality and integrity of the tissue sample. Samples lacking unimpaired structural layer (tunica mucosa, tunica muscularis, and/or tunica serosa) or with strong signals of epithelial detachment were discarded. The remaining samples from both regions (ampulla and isthmus) were used to perform the following analyses:

Thickness of the tunica mucosa and tunica muscularis: Using images of the H&E-stained sections loaded on the Image Pro Plus 4.5 software (Media Cybernetics, Silver Spring, USA), the thickness (µm) of both tunicae was determined (Figures 2A and 2B, respectively). For each tissue sample, this procedure was performed 5 times in each of three non-consecutive tissue sections. The arithmetic mean of the 15 values was used for statistical analysis.

Number of primary and secondary mucosal folds and folding grade: Using images of H&E-stained sections, the number of primary (Figure 2C) and secondary (Figure 2D) folds were counted using the "Cell Counter" plugin of the Image J 1.48 software (National Institutes of Health, Bethesda, USA). For each tissue sample, this procedure was performed in three non-consecutive sections. The arithmetic mean of the values was used for statistical analysis. The ratio of the number of secondary

folds divided by the number of primary folds was assessed as a new variable named folding grade. Due to the absence of tertiary folds in all isthmus samples, this variable was not considered in the study.

Luminal epithelium perimeter: In the H&E-stained sections, the "trace-wand" tool of the Image Pro Plus software was used to draw the luminal epithelial lining. Tissue fragments that were detached from the luminal epithelium were ignored (Figure 2E). For each tissue sample, this procedure was repeated on three non-consecutive tissue sections and the arithmetic mean of the three values was used for statistical analysis.

Number of secretory cells: Images of PAS-stained tissue sections were loaded on the Image J software and the number of ciliated and secretory cells of the luminal epithelium was determined using the "Cell Counter" plugin. In order to identify each cell type, the following morphological characteristics were considered: the presence of cilia, the presence of cytoplasmic protrusions and PAS-positive granules in the secretory cells, and the position of the nuclei: basal for secretory cells and apical for ciliated cells (Figure 3). Counting was continued until a total of 500 cells per sample were counted.

Figure 4 – Illustration of the morphometric analysis performed on cross-sections of the isthmus and ampulla stained with hematoxylin-eosin.

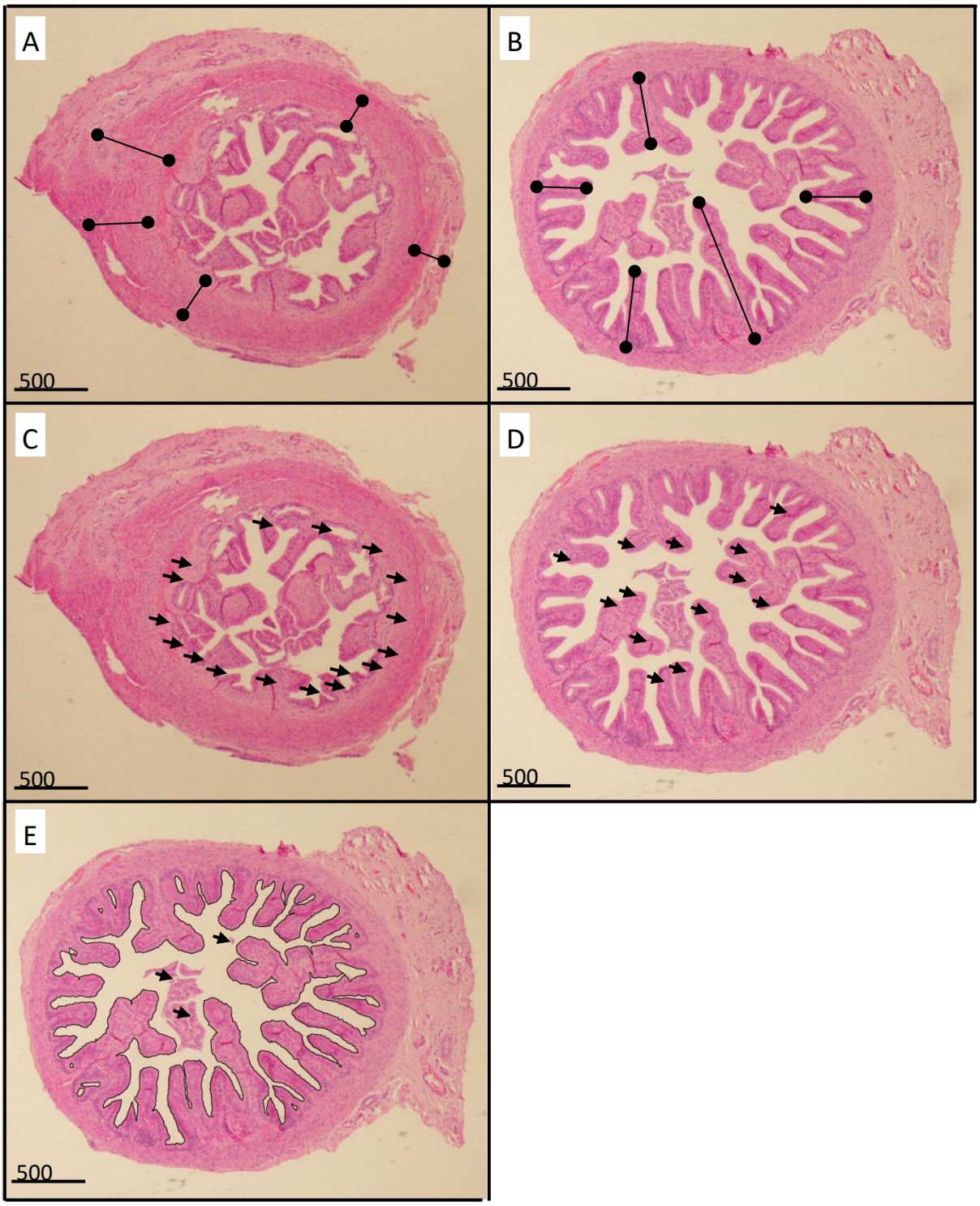

Source: Gonella-Diaza (2017).

Legend: Morphometric analysis performed on cross-sections of the isthmus (a, c) and ampulla (b, d, e) stained with hematoxylin-eosin. Height of muscular (a) and mucosa (b) layers. Number of primary (c) and secondary folds (d). Luminal epithelial perimeter (e). Arrows: cell accumulations that were detached and not in direct contact with the tissue were ignored from the analysis..

Figure 5 – Luminal epithelium of an ampulla cross-section stained with periodic acid-Schiff (PAS)

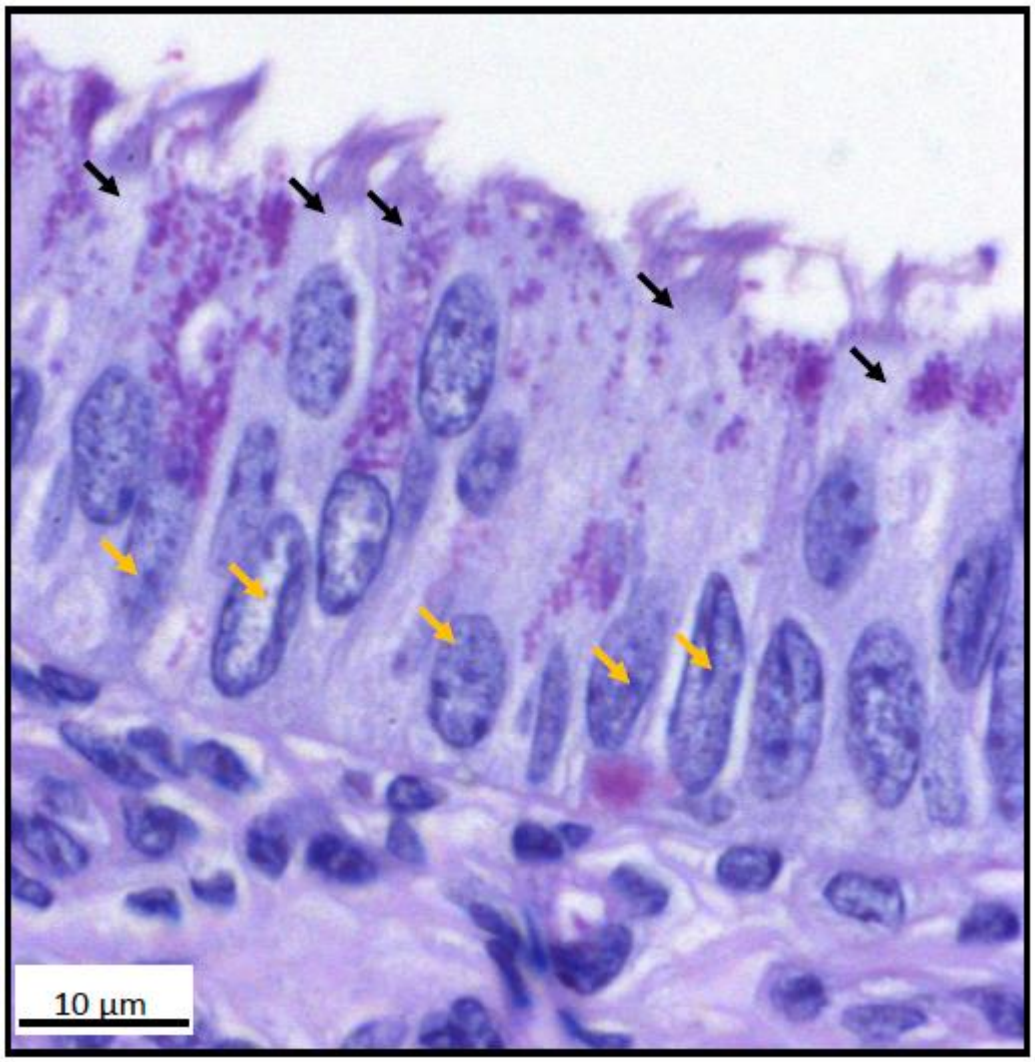

Source: Gonella-Diaza (2017).

Legend. Black arrows: ciliated cells; Yellow arrows: secretory cells.

4.2.3 Determination of the cellular proliferation

Paraffin-embedded oviductal samples were stained with antibodies against KI67 in order to identify proliferating oviductal luminal epithelial cells. Four µm thick tissue sections were deparaffinized in xylene and rehydrated in an ethanol series. These sections were then subjected to antigen retrieval by pressure cooking in citrate buffer (10 mM citric acid, pH 6.0), preheated to 80°C for 1 min, allowed to cool down for 20 min, and rinsed with PBS (1.09 g of Na2HPO4 anhydrous, 0.32 g of NaH2PO4

anhydrous, 9 g of NaCl, 1 ml of Tween 20, 1000 ml of distilled water, pH7.4). Endogenous peroxidase activity was blocked by incubation with Peroxidase Block kit (code K0679, DAKO, Denmark) for 15 minutes at room temperature. After 3 consecutive washes with PBS, slides were incubated with Protein Block (Code X0909, DAKO). Immediately, slides were incubated with monoclonal mouse anti-human KI67 primary antibody, Clone MIB-1 (code M7240; DAKO) (CHANROT *et al*., 2017; MESQUITA *et al*., 2015; YOSHIOKA *et al*., 2015), diluted in PBS (1:100, which corresponds to 0.52 µg/ml). Negative control slides were incubated with normal mouse IgG (sc-2025; Santa Cruz Biotechnology, Santa Cruz, CA) with the same concentration of primary antibody. Both incubations were performed overnight at 4°C. After the PBS wash series, slides were incubated with Advance Kit (Code K4069; DAKO) for 15 min at room temperature with the HRP link and then with the HRP enzyme. After washing with PBS, 3,3-diaminobenzidine tetrahydrochloride (K3468; DAKO) was used as chromogen. The sections were counterstained with hematoxylin, dehydrated, cleared in xylene, and mounted on glass slides. Images were captured with a Nikon Eclipse TS100 microscope (Nikon Corporation, Tokyo, Japan) adapted to a digital camera (Moticam 580, Motic Asia, Hong Kong, China) and uploaded to the Image J software. Cells with a dense nuclear staining for KI67 were considered proliferating. The number of these cells was determined after counting a total of 500 cells per sample, using the "Cell Counter" plugin of Image J.

4.2.4 Transcript abundance by Quantitative PCR.

Frozen samples (≈ 20 mg) were ground in liquid nitrogen using a mortar and pestle and immediately mixed with buffer RLT from AllPrep® DNA/RNA/Protein Mini kit (No. 80004, Qiagen, São Paulo, São Paulo, Brazil), as recommended by manufacturer's instructions. After homogenization with needle (18G) and syringe, the tissue suspension was centrifuged at 13,000 x g for 3 min for debris removal and the supernatant was loaded in silica columns. Finally, the silica columns were eluted with 30 µL of RNase-free water and RNA was kept at −80°C. Concentration of total RNA extracts was measured using the NanoVue spectrophotometer (GE Healthcare). Total RNA (1 µg) was reverse transcribed (High Capacity cDNA Reverse

Transcription Kit, Life Technologies) according to manufacturer's instructions; Briefly, samples were incubated at 25°C for 10 min, followed by incubation at 37°C for 2 h and reverse transcriptase inactivation at 85°C for 5 min and storage at −20°C. The cDNA obtained was used for gene expression assays by qPCR. Step-One Plus (Life Technologies, Carlsbad, CA) with SYBR Green Chemistry was used for the amplification analysis. Primers were designed based on GenBank Ref-Seq mRNA sequences of target genes. Sequences were masked to remove repetitive sequences with RepeatMasker (http://www.repeatmasker.org/) (SMIT *et al*., 1996, 2010) and, then, the masked sequences were used to design primers using the PrimerQuest software (IDT1, http://www.idtdna.com/primerquest/Home/Index). Primer characteristics were checked with Oligo Analyzer 3.1 software (IDT1, http://www.idtdna.com/analyzer/Applications/OligoAnalyzer/), while the specificity was compared by BLAST1 (NCBI, http://blast.ncbi.nlm.nih.gov). Quantitative PCR products from reactions containing designed primers were analyzed by agarose gel electrophoresis and SANGER sequencing, and identities were confirmed. Details of primers are provided in Table 1. Determination of qPCR efficiency and Cq (quantification cycle) values per sample were performed with LinRegPCR software (V2014.2; http://linregpcr.nl/). Cyclophilin A (PPIA) and Glyceraldehyde-3-Phosphate Dehydrogenase (GAPDH) were used as reference genes and their geometric mean was used to normalize the target transcript abundance values (Cq values). These reference genes were selected previously for stability of expression in oviduct tissues (GONELLA-DIAZA *et al*., 2015). The following candidate genes were selected because they were representative of ontology terms enriched in our previous study and considered relevant to oviductal biology: Branching morphogenesis [Bone morphogenetic protein 4 (BMP4); C-X-C chemokine receptor type 4 (CXCR4); Matrix metalloproteinase 14 (MMP14); Vinculin (VCL)], and cellular secretion [Cathepsin S (CTSS); C-Fos Induced Growth Factor (Vascular Endothelial Growth Factor D, FIGF); Glucosidase Beta Acid (GBA); Heparanase (HPSE)].

Table 1 - Primer sequences of target and reference genes analyzed using qPCR.

Target Gene	Gene Bank Number	Forward primer sequence(5'-3')	Reverse primer sequence (5'-3')	Primer efficiency (%)	Amplicon length (bp)
BMP4	NM_001045877.1	AGAGCGCAGTCATCCCGGAT	TCCAGATGTTCTTCGTGGTGGAAGC	1.96	160
CTSS *	NM_001033615.2	AGAAGCCGTGGCCAATAAA	CTTCCCGTCAAGGTTACCATAG	2.10	157
CXCR4	NM_174301.3	AAAGTGACCCTGAGGACTTGAGTAG	CCGGAAGCAGGGTTCCTT	2.03	153
FIGF	NM_001101043.2	CACCTGCAGCTGTGAGGAC	GACATGGATGGGGAACTGGG	1.91	169
GBA	NM_001046421.2	GATTTCCTTTCGCCTCCGGT	AGGCATAGGATACTCCTCTCTGG	1.99	141
GAPDH *	NM_001034034.2	GCCATCAATGACCCCTTCAT	TGCCGTGGGTGGAATCA	1.93	69
HPSE *	NM_174082.2	CGGATTGTTGAGAAGATCAGA	AAGGTGTTGGACAGGAAGGG	1.92	94
MMP14	NM_174390.2	TGCCTACTGACAGGATTGA	GGGTATTCGCTTTCCACTATC	1.97	121
PPIA *	NM_178320.2	GCCATGGAGCGCTTTGG	CCACAGTCAGCAATGGTGATCT	2.02	64
VCL	NM_001191370.1	GCTGTTCAAGGGAGTAATAGG	TTCTGGCTTTGGGAAGAAATA	2.07	153

Source: Gonella-Diaza (2017)
* Primers for genes labeled * have been previously reported in Gonella-Diaza *et al*., (2015).

4.2.5 Statistical analyses

In all statistical analyses performed, the animal was considered as the experimental unit. All data are reported as mean ± standard error of the mean. Data was analyzed using Proc GLIMMIX of the SAS software (SAS 9.2; SAS Institute). The fixed effects of group (LF-LCL vs. SF-SCL), region (ampulla vs. isthmus), and side (ipsilateral vs. contralateral to the CL), as well as two-way interactions (group x region, group x side; region x side) and the three-way interaction (group x region x side) were analyzed using a three-way nested ANOVA. Animal, animal within the group, animal within the interaction group x region, and animal within the interaction group x side were considered random effects. The model was adjusted in order to consider the distribution of the data of each dependent variable. The significance of the effects was determined using the type III sum of squares F test.

4.3 RESULTS

4.3.1 Histological analysis

The thickness of the tunica mucosa (*P* <0.01) and the tunica muscularis (*P* <0.01) were different between regions (Figure 5; Table 2). The ampulla has a thicker mucosa (676.74 ± 72.27 µm) compared to the isthmus (271.86 ± 42.49 µm), while the isthmus had a thicker tunica muscularis (197.11 ± 19.33 µm) than the ampulla (96.36 ± 15.56 µm). There was a significant three-way interaction in the number of primary mucosal folds (Figure 6; Table 2; *P* = 0.01). The number of primary mucosal folds was always greater in the ampulla than the isthmus. However, in the ampulla it was greater for the LF-LCL group in the ipsilateral side, but not in the contralateral side. There were also no differences across all isthmus samples. The number of secondary folds was greater in the ampulla (15.16 ± 2.62 secondary folds) than in the isthmus (1.91 ± 2.30 secondary folds; *P* <0.01). Due to the interest in studying the morphogenic processes, the ratio between the number of secondary folds and the number of primary folds was analyzed as a new dependent variable, called folding grade, for which a three-way interaction (*P* = 0.03) was detected (Figure 6, Table 2). Although folding grade was always greater in the ampulla than the isthmus, in the ampulla it was greater for the LF-LCL group in the ipsilateral side, but not in the contralateral side, while it was similar across all isthmus samples. The luminal epithelial perimeter was affected by a group x side interaction (*P*=0.06). In the ipsilateral side, the luminal perimeter was similar for both groups in the isthmus, but significantly greater in the ampulla of cows in the LF-LCL group, while in the contralateral side mean perimeter was similar across regions and between groups. A three-way interaction was identified when the number of secretory cells was analyzed (P = 0.01; Figure 7; Table 2). Similar to number of primary folds and folding grade, number of secretory cells was always greater in the ampulla than the isthmus; in the ampulla it was greater for the LF-LCL group in the ipsilateral side, but not in the contralateral side, while it was similar across all isthmus samples.

Figure 6 – Mean ± S.E.M. values of the thick of the tunica muscularis and mucosa and perimeter of the lumen in ipsilateral or contralateral to the CL oviducts for cows of the LF-LCL and SF-SCL groups.

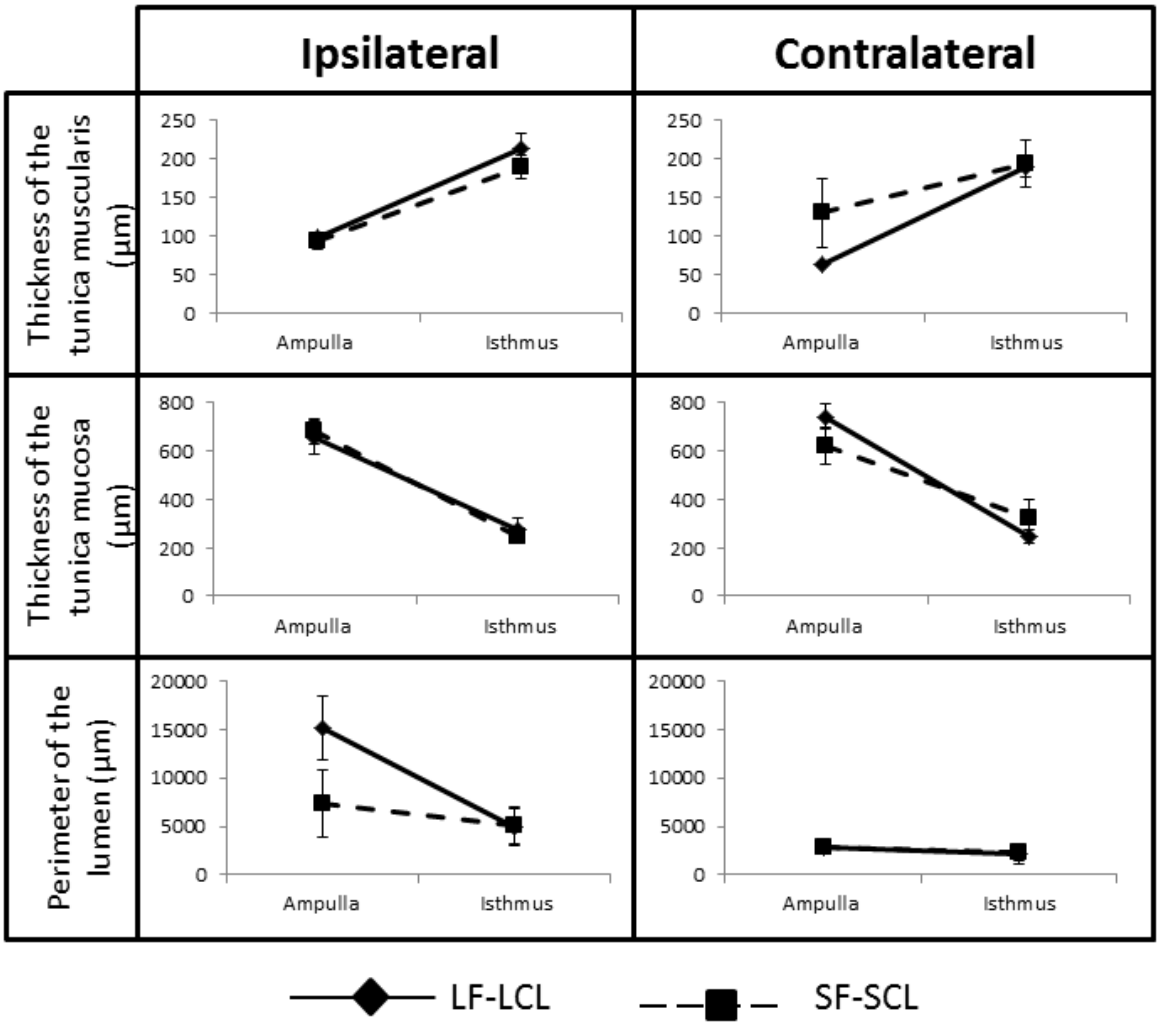

Source: Gonella-Diaza (2017).

Table 2 *P* value (Pr > F) of the fixed effects: Group (LF-LCL vs. SF-SCL), Region (ampulla vs. isthmus), and Side (ipsilateral vs. contralateral) with their respective double and triple interactions for the morphological variables evaluated.

Dependent variable	**Group**	**Region**	**Side**	**Group x Region**	**Group x Side**	**Region x Side**	**Group x Region x Side**
Thick of the tunica mucosa (µm)	NS	<0.01	NS	NS	NS	NS	NS
Thick of the tunica muscularis (µm)	NS	<0.01	NS	NS	0.09	NS	NS
Number of primary mucosa folds	0.09	<0.01	NS	0.03	NS	0.09	0.01
Number of secondary mucosal folds	NS	<0.01	NS	NS	NS	NS	NS
Folding grade	NS	<0.01	NS	NS	NS	NS	0.03
Luminal Epithelium perimeter (µm)	NS	<0.01	NS	NS	0.04	0.08	0.06
Ratio of secretory cells	0.02	<0.01	NS	NS	<0.01	<0.01	0.01
Number of Ki67 positive cells	0.02	0.03	NS	NS	NS	NS	NS

Source: Gonella-Diaza (2017).

Legend: Statistically significant differences were determined by three-way nested ANOVA where NS depicts not statistically significant. .

Figure 7 – Mean ± S.E.M.; Values of the number of primary and secondary mucosal folds, and folding grade in ipsilateral or contralateral to the CL oviducts for cows of the LF-LCL and SF-SCL groups.

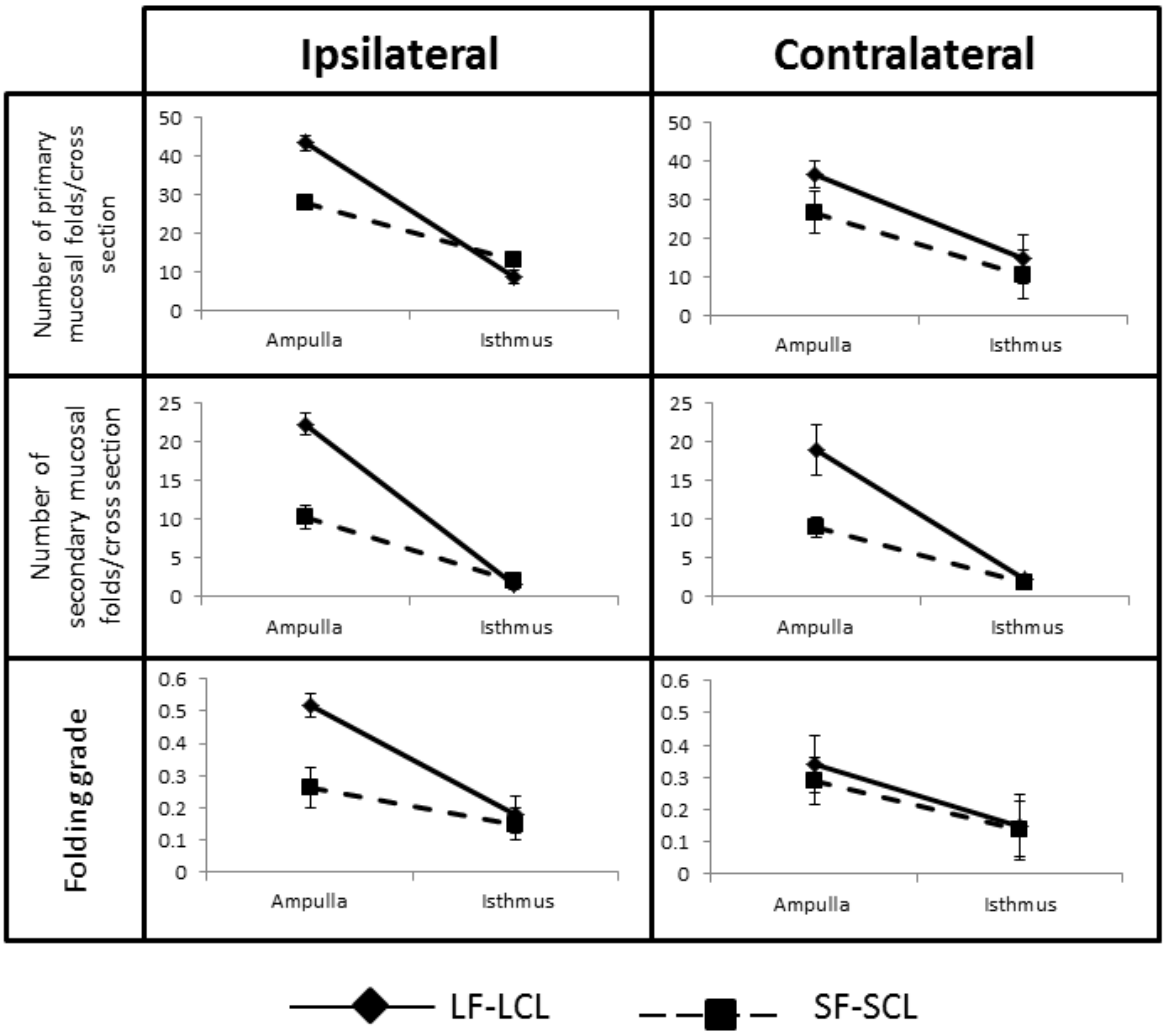

Source: Gonella-Diaza (2017).

Figure 8 – Mean ± S.E.M.; Number of secretory cells Ki67 positive cells in ipsilateral or contralateral to the CL oviducts of cows of the LF-LCL and SF-SCL groups.

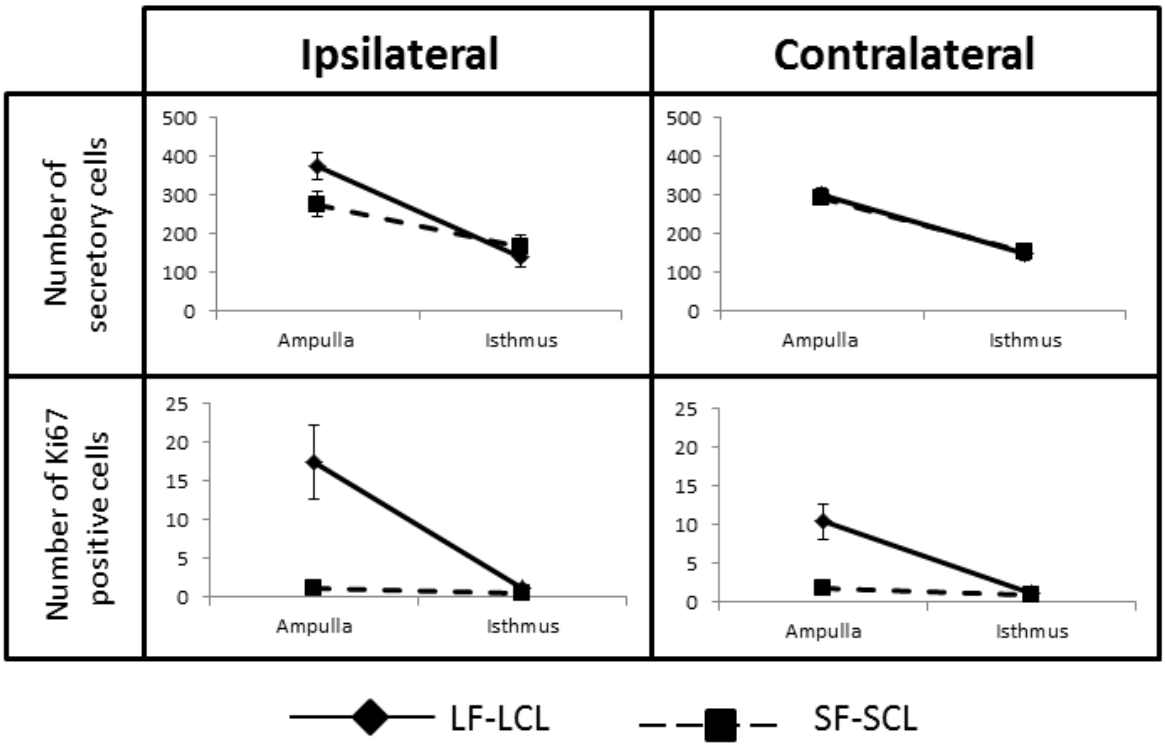

Source: Gonella-Diaza (2017).

Staining for KI67 on the oviductal samples revealed the presence of proliferative activity in the luminal epithelium of all samples. After Ki-67-positive nuclei counting, a significant effect of region (*P* = 0.03) and group (*P*=0.02; Figure 7) was observed. The proliferation activity was stronger in the ampulla (7.72 ± 2.22 KI67-positive cells) than the isthmus (0.92 ± 0.34 cells KI67 positive cells) and in the LF-LCL group (7.60 ±1.90 KI67-positive cells) than in the SF-SCL group (1.03 ± 0.66 KI67-positive cells).

4.3.2 Gene expression

The *P* values of fixed effects and their interactions for the transcripts abundance of candidate genes are shown on Table 3. A three-way interaction was

detected for transcript abundance of GBA (*P* = 0.02; Figure 8) and CTSS (*P* = 0.01; Figure 8). While GBA transcript abundance in the SF-SCL group was less in the isthmus than in the ampulla in both sides, abundance in the LF-LCL animals slightly increased in the ipsilateral isthmus and slightly decreased in the contralateral isthmus, compared to the respective ampullae. CTSS transcript abundance was up-regulated in the ipsilateral isthmus and the contralateral ampulla of the LF-LCL group. Group means were similar in the ipsilateral ampulla and in the contralateral isthmus.

Table 3 - *P* value (Pr > F) of the fixed effects: Group (LF-LCL vs. SF-SCL), Region (ampulla vs. isthmus), and Side (ipsilateral vs. contralateral) with their respective double and triple interactions for the abundance of transcripts evaluated by qPCR

Dependent variable	**Group**	**Region**	**Side**	**Group x Region**	**Group x Side**	**Region x Side**	**Group x Region x Side**
BMP4	0.05	NS	0.02	NS	NS	NS	NS
CTSS	0.03	<0.01	0.03	NS	NS	NS	0.01
CXCR4	NS	0.09	NS	NS	NS	NS	NS
FIGF	NS	0.01	<0.01	NS	NS	NS	NS
GBA	0.06	0.02	NS	0.02	NS	0.03	0.02
HPSE	NS	<0.01	NS	NS	NS	NS	NS
MMP14	NS	<0.01	0.07	NS	NS	0.04	NS
VCL	0.09	<0.01	NS	0.09	NS	NS	NS

Source: Gonella-Diaza (2017).
Legend: Statistically significant differences were determined by three-way nested ANOVA where NS depicts not statistically significant.

Figure 9 – Mean ± S.E.M; transcript abundance of CTSS, GBA, MMP14, and VCL.

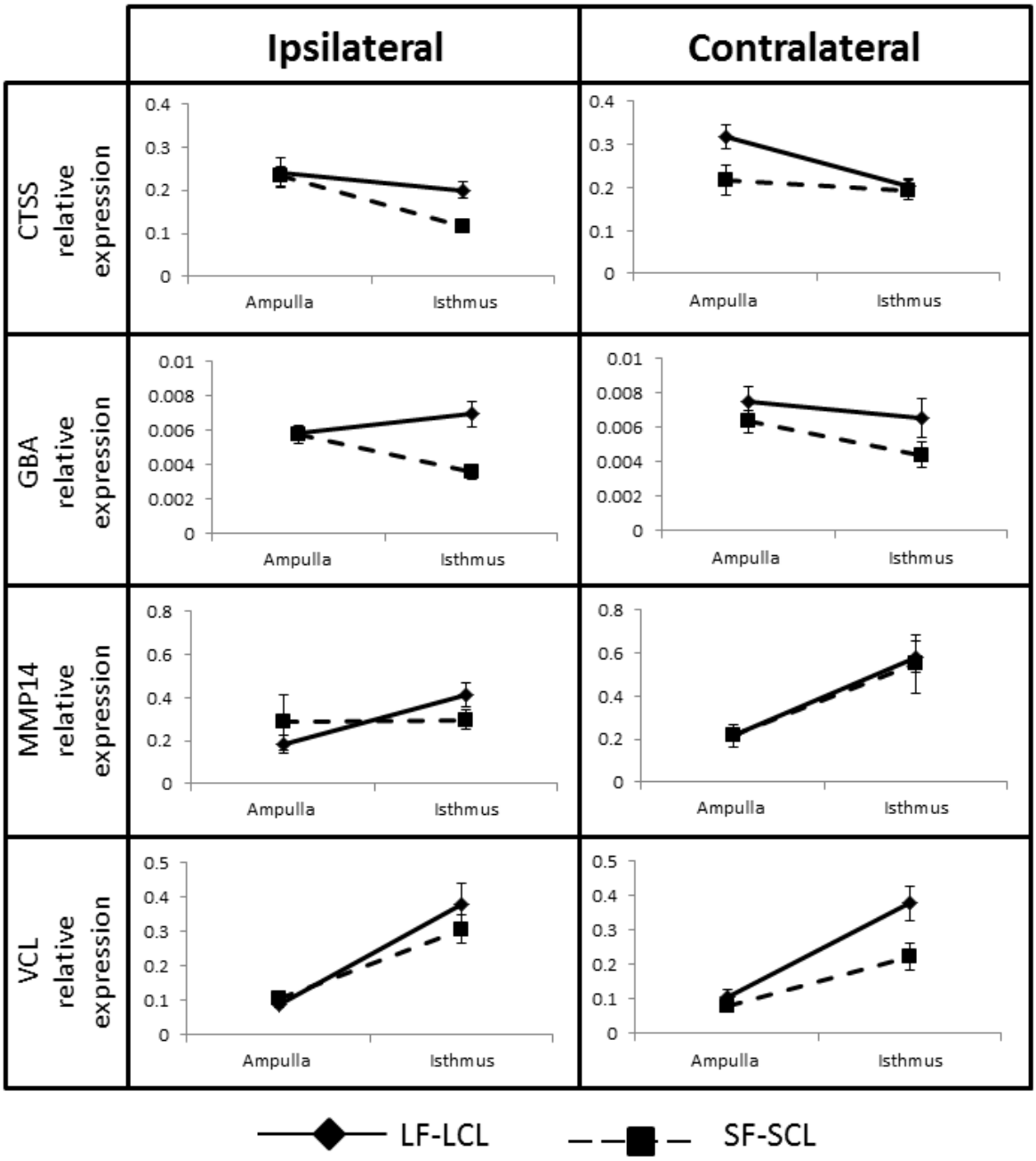

Source: Gonella-Diaza (2017).
Legend: Gene expression was normalized to PPIA and GAPDH in the oviducts ipsilateral and contralateral to the CL from beef cows synchronized to ovulate a large (LF-LCL) or small follicles (SF-SCL) an day 4 of the estrous cycle.

There was a Region by Side interaction on the transcript abundance of MMP14 (*P* = 0.04; Figure 8). Abundance was greater in the contralateral isthmus compared with the other regions, but similar between regions in the ipsilateral oviduct. The group by region interaction of VCL transcript abundance (*P*=0.09; Figure 8) indicated that while group means were similar in the ampulla, LF-LCL group presented upregulated VCL expression in the isthmus.

There was a significant effect of the side in the BMP4 (*P* = 0.02; Figure 9) and FIGF (*P* = <0.01; Figure 9) transcript abundance, both of them being up-regulated in the contralateral side. The transcript abundance of CXCR4 (*P* = 0.09; Figure 9), FIGF (*P* = 0.01) and, HPSE (*P* = < 0.01; Figure 9) was affected by region; transcripts were more abundant in the ampulla than in the isthmus. BMP4 transcript abundance was greater in the LF-LCL group (*P* = 0.05).

Figure 10 – Mean ± S.E.M; transcript abundance of BMP4, FIGF, CXCR4, and HPSE.

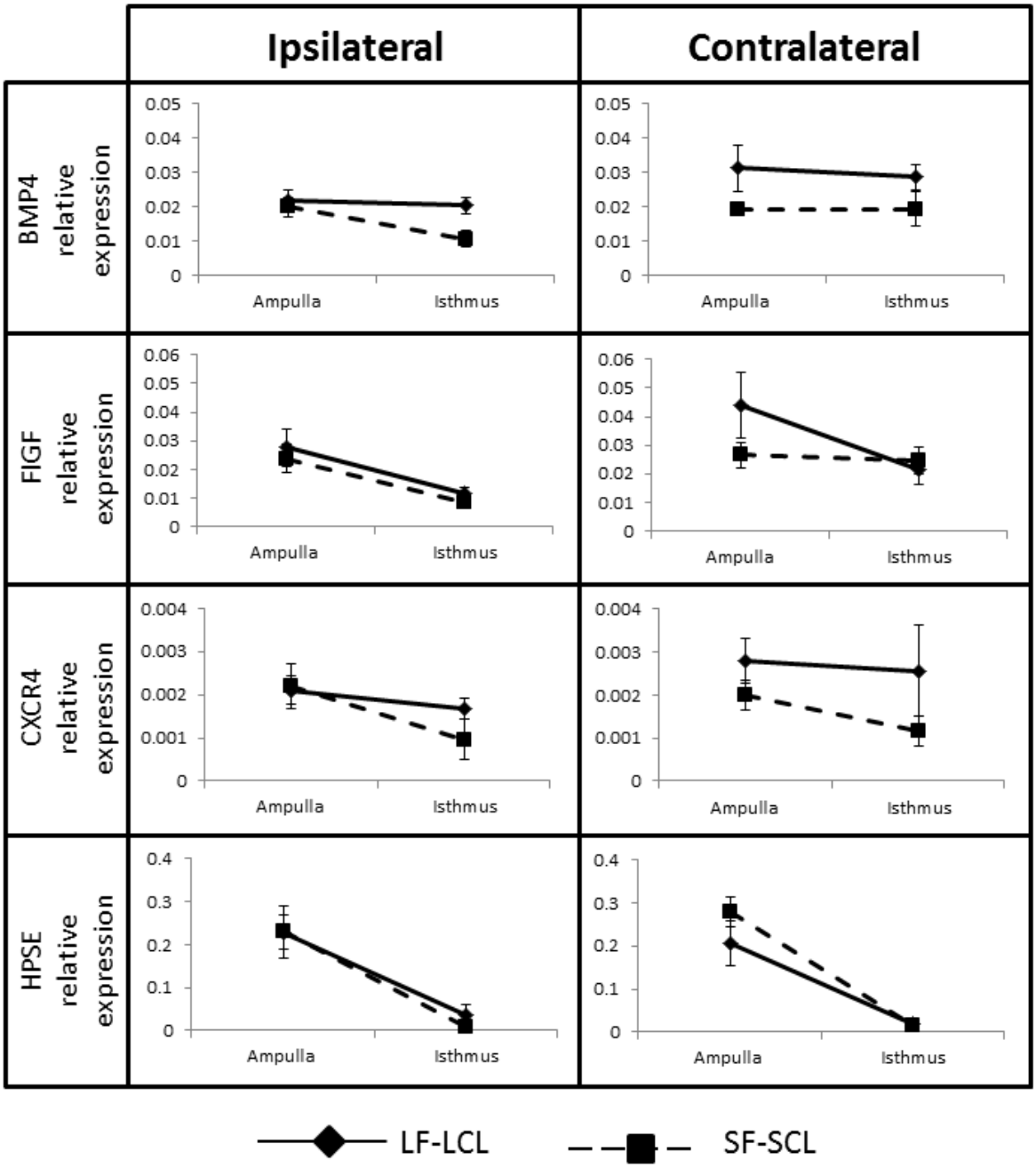

Source: Gonella-Diaza (2017).

Legend. Gene expression was normalized to PPIA and GAPDH in the oviducts ipsilateral and contralateral to the CL from beef cows synchronized to ovulate a large (LF-LCL) or small follicles (SF-SCL) on day 4 of the estrous cycle.

4.4 DISCUSSION

The positive role of the oviduct in embryo quality is well accepted. For example, it is clear that quality and developmental potential of *in vivo*-produced embryos is greater than *in vitro*-produced embryos (RIZOS *et al*., 2002a; 2002b; 2002c). However, there is a poor understanding of cellular and molecular mechanisms that affect oviduct functions to impact embryo development and quality. Previous assessment of the oviductal transcriptome have elucidated a number of mechanisms regulated by the periovulatory endocrine milieu, i.e., proestrus and estrus increase in E2 and diestrus increase in P4 concentrations, potentially involved in oviductal function (GONELLA-DIAZA *et al*., 2015). Such pathways included branching morphogenesis, cellular proliferation, and secretion. More importantly, genes in theses pathways were upregulated in the LF-LCL group, associated with a greater receptivity to the embryo. It was expected that in response to pre-ovulatory E2, the oviduct initiates morphogenic and proliferative processes, resulting in invasion of the epithelium into the lumen and modifying the number of secretory cells, finally increasing the functional epithelial area. The main objective of this study was to compare the morphology, gene expression, and cellular proliferation of two regions (ampulla and isthmus) of the ipsilateral and contralateral oviducts between groups of cows showing distinctly different periovulatory endocrine milieus associated with greater (LF-LCL group) or lower (SF-SCL group) fertility.

Growth and ovulation of a larger follicle stimulate development of the oviductal secretory mucosa. In the present study, the number of primary folds, folding grade and the luminal epithelium perimeter were greater in the oviduct of animals of the LF-LCL group. In the endometrium, after an E2 stimulus, cells are stimulated to proliferate and endometrial glands reorganize, resulting in greater glandular epithelium area (WANG *et al*., 2007, GRAY *et al*., 2001). The oviductal mucosa, due to structural simplicity and its lack of glands, depends mainly on the luminal epithelial cells to synthesize oviductal fluid (LEESE 1988, ABE 1996). It is expected that a greater secretory capacity is better able to provide molecules important to support embryo development (AVILES *et al*., 2010, HUNTER 1998, SIMINTIRAS *et al*., 2016). As described previously, variables associated with the secretory mucosa were

better developed in the ampulla than in the isthmus (BUHI *et al*., 1991, 1992). Interestingly, mucosal development was also greater in the ipsilateral compared to the contralateral oviduct. Vascular arrangements in the cranial portion of the uterus and the oviduct direct greater amounts of gonadal steroids to this region of the reproductive tract. Thus, the side ipsilateral to the pre-ovulatory follicle and the subsequent CL is exposed to greater concentration of sex-steroids (WIJAYAGUNAWARDANE *et al*., 1996, 1998; HUNTER *et al*., 1983). This may explain increased folding of the luminal epithelium of the ipsilateral in comparison to the contralateral side. Morphology of the oviduct compartments was consistent with previous transcriptomic data indicating enrichment of transcripts related to branching morphogenesis in the oviduct of LF-LCL cows (GONELLA-DIAZA *et al*., 2015). Taking these findings together, it was hypothesized that the greater luminal epithelial surface developed by the LF-LCL cows would result in a greater secretory capacity. However, because not all of the epithelial cells secrete components of the oviductal fluid, it was necessary to measure the numbers of secretory cells.

Growth and ovulation of a larger follicle increased the number of secretory cells and KI67-positive, proliferating cells. The ampulla of LF-LCL cows has a greater amount of both secretory and proliferating cells (Figure 6 and Table 2). The secretory cells actively produce and secrete specific glycoproteins into the lumen and their secretions form the oviductal fluid (AGUILAR; REYLEY 2005, ERIKSEN *et al*., 1994, LEESE 1988). These cells are more abundant in the ampulla and, during the estrous cycle, the number of secretory cells varies. Indeed, during the follicular phase the number of secretory cells, as well as the volume of oviductal fluid increase (LEESE 1988, AYEN *et al*., 2012, ITO *et al*., 2016). Therefore, it can be assumed that cows ovulating larger follicles would exhibit greater proliferation rates and, therefore, have more secretory cells therein producing more oviductal fluid. Also, the KI67-positive cells were almost ten times more frequent in the LF-LCL group than in the SF-SCL group. These results are in agreement with a recent study published by Ito *et al*., (2016), who concluded that the proportions of ciliated and secretory epithelial cells change during the estrous cycle and that only the secretory cells proliferate. Data also suggest that the remodeling of the bovine oviductal epithelium provides the optimal environment for gamete transport, fertilization and embryonic development. Furthermore, remodeling is mainly regulated by proliferation of secretory cells.

Morphological changes induced by growth and ovulation of a larger follicle were not associated with changes in abundance of selected transcripts. In this study, regulation of transcript abundance among treatments, regions and sides was complex. In the ipsilateral ampullae, abundance of all transcripts studied was similar between groups. It is possible that transcript regulation associated with the morphological differences between groups, described above for that region, occurred at an earlier point in time, not sampled in the present study. Conversely, despite the absence of morphological changes between groups in the ipsilateral isthmus, there was a greater abundance of transcripts associated with secretion (CTSS, GBA) and branching morphogenesis (BMP4, MMP14) in cows from the LF-LCL group. On D4 it is expected that embryo will be in the isthmus, in transit to the uterus (KOLLE *et al*., 2009). Thus, morphological changes observed in the ampulla may be important for processes that occurred prior to the moment samples were collected, such as fertilization, the initial embryo divisions and transport to the isthmus. The D4 isthmus role is to support the final embryo divisions before entering the uterus and to transport the embryo. Based on the isthmus morphological variables that we measured, changes in the secretory epithelium were probably not associated with a functional advantage for cows on the LF-LCL group. Conversely, changes in transcript abundance are suggestive of LF-LCL-stimulated secretory activity per individual, pre-existing cells because there was no evidence of proliferation. Furthermore, tissue remodeling involving MMP14 and BMP4 may be critical to transport the embryo to the uterus.

In summary, exposure to greater proestrus-estrus concentrations of E2 and early diestrus concentrations of P4 dramatically changes ampullary morphology to a highly secretory phenotype that may be critical to support embryo early development. Additional analyses to evaluate whether these morphological and gene expression differences are associated with greater bioavailability of nutrients and growth factors to the embryo are necessary. In the isthmus, similar morphological changes were not regulated, indicating that they were not required to support isthmic function. However, changes in critical transcript abundance suggest that this region is also under sex-steroid regulation, which is further supported by the detection of cognate receptors reported earlier. Future experiments are warranted to determine the role of the periovulatory endocrine milieu on tissue remodeling. Collectively, these observations

may help to explain the greater fertility of cows ovulating larger follicles and developing larger CLs. In conclusion, the present data provide functional connections between a fertility model and the oviduct transcriptome in beef cattle. We propose that sex-steroids act in an oviduct region-specific fashion to support early embryo development.

4.5 REFERENCES

ABE, H. The mammalian oviductal epithelium: Regional variations in cytological and functional aspects of the oviductal secretory cells. **Histology and Histopathology**, v. 11, p. 743-768, 1996.

AGDUHR, E. Studies on the structure and development of the bursa ovarica and the tuba uterina in the mouse. **Acta Zoologica**, v. 8, p. 1-133, 1927.

AGUILAR, J.; REYLEY, M. The uterine tubal fluid: secretion, composition and biological effects. **Animal Reproduction**, v. 2, p. 91-105, 2005.

AHUMADA, C.J.; SALVADOR, I.; CEBRIAN-SERRANO, A.; LOPERA, R.; SILVESTRE, M.A. Effect of supplementation of different growth factors in embryo culture medium with a small number of bovine embryos on *in vitro* embryo development and quality. **Animal**, v. 7, p. 455-462, 2013.

ASHWORTH, C.J; SALES, D.I.; WILMUT, I. Evidence of an association between the survival of embryos and the periovulatory plasma progesterone concentration in the ewe. **Journal of Reproduction and Fertility**, v. 87, p. 23-32, 1989.

AVILES, M.; GUTIERREZ-ADAN, A.; COY, P. Oviductal secretions: will they be key factors for the future ARTs?. **Molecular Human Reproduction**, v. 16, p. 896-906, 2010.

AYEN, E.; SHAHROOZ, R.; KAZEMIE, S. Histological and histomorphometrical changes of different regions of oviduct during follicular and lutealphases of estrus

cycle in adult Azarbaijan buffalo. **Iranian Journal of Veterinary Research**, v. 13, p. 42-48, 2012.

BACHA, W.J.; BACHA, L.M. **Color Atlas of Veterinary Histology**, Third edition. Wiley-blackwell. ISBN-13: 978-0470958513. 356 pages, 2012.

BESENFELDER, U.; HAVLICEK, V.; BREM, G. Role of the oviduct in early embryo development. **Reproduction in Domestic Animals**, v. 47, p. 156-163, 2012.

BROWER, L.; ANDERSON, E.; Cytological Events Associated with the Secretory Process in the Rabbit Oviduct. **Biology of Reproduction**, v. 1, p. 130-148. 1969.

BUHI, W.C.; ALVAREZ, I.M.; KOUBA, A.J. Secreted proteins of the oviduct. **Cells, Tissues, Organs**, v. 166, p. 165-179, 2000.

BUHI, W.C.; ASHWORTH, C.J.; BAZER, F.W.; ALVAREZ, I.M. *In vitro* synthesis of oviductal secretory proteins by estrogen-treated ovariectomized gilts. **Journal of Experimental Zoology**, v. 262, p. 426-435, 1992.

BUHI, W.C.; BAZER, F.W.; ALVAREZ, I.M.; MIRANDO, M.A. *In vitro* synthesis of oviductal proteins associated with estrus and 17 beta-estradiol-treated ovariectomized ewes. **Endocrinology**, v. 128, p. 3086-3095, 1991.

CHANROTA, M; GUOA, Y. DALINA, A.M.; PERSSONB, E.; BÅGEA, R.; SVENSSONA, A.; GUSTAFSSONA, H.; HUMBLOTA, P. Dose related effects of LPS on endometrial epithelial cell populations from dioestrus cows. **Animal Reproduction Science**, v. 177, p. 12-24, 2017.

DEMETRIO, D.G.; SANTOS, R.M.; DEMETRIO, C.G.; VASCONCELOS, J.L. Factors affecting conception rates following artificial insemination or embryo transfer in lactating Holstein cows. **Journal of Dairy Science**, v. 90, p. 5073-5082, 2007.

DONNEZ, J.; CASANAS-ROUX, F.; CAPRASSE, J.; FERIN, J.; THOMAS, K. Cyclic changes in ciliation, cell height, and mitotic activity in human tubal epithelium during reproductive life. **Fertility and Sterility**, v. 43, p. 554-559, 1985.

ERIKSEN, T.; TERKELSEN, O.; HYTTEL, P.; GREVE, T. Ultrastructural features of secretory-cells in the bovine oviduct epithelium. **Anatomy and embryology**, v. 190, p. 583-590, 1994.

GANDOLFI, F.; BREVINI, T.A.L.; RICHARDSON, L.; BROWN, C.R.; MOOR, R.M. Characterization of proteins secreted by sheep oviduct epithelial-cells and their function in embryonic-development. **Development**. v. 106, p. 303-12, 1989.

GONELLA-DIAZA, A.; ANDRADE, S.; SPONCHIADO, M.; PUGLIESI, G.; MESQUITA, F.; VAN HOECK, V.; STREFEZZI, R.; GASPARIN, G.; COUTINHO, L.; BINELLI, M. Size of the ovulatory follicle dictates spatial differences in the oviductal transcriptome in cattle. **Plos One**. v. 10, e0145321, 2015.

GRAY, C.A.; BARTOL, F.F.; TARLETON, B.J.; WILEY, A.A.; JOHNSON, G.A.; BAZER, F.W.; SPENCER, T.E. Developmental biology of uterine glands. **Biology of Reproduction**. v. 65, p. 1311-1323, 2001.

HUNTER, R.H. Have the Fallopian tubes a vital role in promoting fertility?. **Acta Obstetricia et Gynecologica Scandinavica**. v. 77, p. 475-486, 1998.

HUNTER, R.H. Components of oviduct physiology in eutherian mammals. **Biological reviews of the Cambridge Philosophical Society**. v. 87, p. 244-255, 2012.

HUNTER, R.H.; COOK, B.; POYSER, N.L. Regulation of oviduct function in pigs by local transfer of ovarian steroids and prostaglandins: a mechanism to influence sperm transport. **European Journal of Obstetrics Gynecology And Reproductive Biology**, v. 14, p. 225-232, 1983.

ITO, S.; KOBAYASHI, Y.; YAMAMOTO, Y.; KIMURA, K.; OKUDA, K. Remodeling of bovine oviductal epithelium by mitosis of secretory cells. **Cell and Tissue Research**, v. 366, p. 403-410, 2016.

KENNGOTT, R.A.; SINOWATZ, F. Prenatal development of the bovine oviduct. **Anatomia, Histologia, Embryologia**, v. 36, p. 272-283, 2007.

KOLLE, S.; DUBIELZIG, S.; REESE, S.; WEHREND, A.; KONIG, P.; KUMMER, W. Ciliary Transport, Gamete Interaction, and Effects of the Early Embryo in the Oviduct: Ex Vivo Analyses Using a New Digital Videomicroscopic System in the Cow. **Biology of Reproduction**, v. 81, p. 267-274, 2009.

KONISHI, I.; FUJII, S.; PARMLEY, T.H.; MORI, T. Development of ciliated cells in the human fetal oviduct: an ultrastructural study. **The Anatomical Record**, v. 219, p. 60-68, 1987.

LEESE, H.J. The formation and function of oviduct fluid. **Journal of Reproduction and Fertility**, v. 82, p. 843-856, 1988.

MCDANIEL, J.W.; SCALZI, H.; BLACK, D. Influence of ovarian hormones on histology and histochemistry of the bovine oviduct. **Journal of Dairy Science**, v. 51, p. 754-761, 1968.

MESQUITA, F.S.; PUGLIESI, G.; SCOLARI, S.C.; FRANCA, M.R.; RAMOS, R.S.; OLIVEIRA, M.; PAPA, P.C.; BRESSAN, F.F.; MEIRELLES, F.V.; SILVA, L.A.; NOGUEIRA, G.P.; MEMBRIVE, C.M.; BINELLI, M. Manipulation of the periovulatory sex steroidal milieu affects endometrial but not luteal gene expression in early diestrus Nelore cows. **Theriogenology**, v. 81, p. 861-869, 2014.

MESQUITA, F.S.; RAMOS, R.S.; PUGLIESI, G.; ANDRADE, S.C.; VAN HOECK, V.; LANGBEEN, A.; OLIVEIRA, M.L.; GONELLA-DIAZA, A.M.; GASPARIN, G.; FUKUMASU, H.; PULZ, L.H.; MEMBRIVE, C.M.; COUTINHO, L.L.; BINELLI, M. The Receptive Endometrial Transcriptomic Signature Indicates an Earlier Shift from

Proliferation to Metabolism at Early Diestrus in the Cow. **Biology of Reproduction**, v. 93. p. 52. 2015.

MOKHTAR, DM. Microscopic and histochemical characterization of the bovine uterine tube during the follicular and luteal phases of estrous cycle. **Journal of Microscopy and Ultrastructure**, v. 3, p. 44-52, 2015.

MORRIS, D.; DISKIN, M. Effect of progesterone on embryo survival. **Animal**, v. 2, p. 1112-1119, 2008.

PERES, R.F.; CLARO, I.J.R.; SA FILHO, O.G.; NOGUEIRA, G.P.; VASCONCELOS, J.L.; Strategies to improve fertility in Bos indicus postpubertal heifers and non-lactating cows submitted to fixed-time artificial insemination. **Theriogenology**, v. 72, p. 681-689, 2009.

PUGLIESI, G.; SANTOS, F.B.; LOPES, E.; NOGUEIRA, É.; MAIO, J.R.; BINELLI, M. Improved fertility in suckled beef cows ovulating large follicles or supplemented with long-acting progesterone after timed-AI. **Theriogenology**, v. 85, p. 1239-1248, 2016.

RESTALL, B.J. Histological observations on the reproductive tract of the ewe. **Australian Journal of Biological Sciences**, v.19, p. 673-686, 1966.

RIZOS, D.; FAIR, T.; PAPADOPOULOS, S.; BOLAND, M.P.; LONERGAN, P. Developmental, qualitative, and ultrastructural differences between ovine and bovine embryos produced *in vivo* or *in vitro*. **Molecular Reproduction and Development**, v. 62, p. 320-327, 2002a.

RIZOS, D.; LONERGAN, P.; BOLAND, M.P.; ARROYO-GARCIA, R.; PINTADO, B. DE LA FUENTE, J.; GUTIERREZ-ADAN, A. Analysis of differential messenger RNA expression between bovine blastocysts produced in different culture systems: implications for blastocyst quality. **Biology of Reproduction**, v. 66, p. 589-595, 2002b.

RIZOS, D.; WARD, F.; DUFFY, P.; BOLAND, M.P.; LONERGAN, P. Consequences of bovine oocyte maturation, fertilization or early embryo development *in vitro* versus *in vivo*: implications for blastocyst yield and blastocyst quality. **Molecular Reproduction and Development**, v. 61, p. 234-248, 2002c.

SIMINTIRAS, C.A.; FRÖHLICH, T.; SATHYAPALAN, T.; ARNOLD, G.J.; ULBRICH, S.E.; LEESE, H.J.; STURMEY, R.G. Modelling oviduct fluid formation *in vitro*. **Reproduction**, v. 153, p. 23-33, 2016.

SMIT, A.; HUBLEY, R.; GREEN, P. (1996-2010) **RepeatMasker Open-3.0**. http://www.repeatmasker.org.

VASCONCELOS, J.L.M.; SARTORI, R.; OLIVEIRA, H.N.; GUENTHER, J.G.; WILTBANK, M.C. Reduction in size of the ovulatory follicle reduces subsequent luteal size and pregnancy rate. **Theriogenology**, v. 56, p. 307-314, 2001.

WANG, C.K.; ROBINSON, R.S.; FLINT, A.P.F.; MANN, G.E. Quantitative analysis of changes in endometrial gland morphology during the bovine oestrous cycle and their association with progesterone levels. **Reproduction**, v. 134, p. 365-371, 2007.

WETSCHER, F.; HAVLICEK, V.; HUBER, T.; MULLER, M.; BREM, G.; BESENFELDER, U. Effect of morphological properties of transferred embryonic stages on tubal migration Implications for *in vivo* culture in the bovine oviduct. **Theriogenology**, v. 64, p. 41-48, 2005.

WIJAYAGUNAWARDANE, M.P.B.; CERBITO, W.A.; MIYAMOTO, A.; ACOSTA, T.J.; TAKAGI, M.; MIYAZAWA, K.; SATO, K. Oviductal progesterone concentration and its spatial distribution in cyclic and early pregnant cows. **Theriogenology**, v. 46, p. 1149-1158, 1996.

WIJAYAGUNAWARDANE, M.P.B.; MIYAMOTO, A.; CERBITO, W.A.; ACOSTA, T.J.; TAKAGI, M.; SATO, K. Local distributions of oviductal estradiol, progesterone, prostaglandins, oxytocin and endothelin-1 in the cyclic cow. **Theriogenology**, v. 49, p. 607-618, 1998.

YOSHIOKA, S.; ABE, H.; SAKUMOTO, R.; OKUDA, K. Proliferation of Luteal Steroidogenic Cells in Cattle. **Plos One**, v. 8, e84186, 2013.

5 CHAPTER 3: SEX STEROIDS DRIVE THE REMODELING OF OVIDUCTAL EXTRACELLULAR MATRIX AND REGULATE EMBRYO RECEPTIVITY IN CATTLE

5.1 INTRODUCTION

The proper environment for fertilization and early embryonic development is provided by the oviduct (BESENFELDER *et al*., 2012; ELLINGTON 1991), which depends on the sex-steroid endocrine milieu for its proper functioning. For example, under an estradiol stimulus the oviductal epithelial cells start to proliferate and secrete metabolic components changing the environment in the oviductal lumen (ERIKSEN *et al*., 1994; HUNTER *et al*., 1983; LAUSCHOVA 2003). Previous assessment of the oviductal transcriptome has elucidated a number of transcripts regulated by the periovulatory endocrine milieu thus suggesting a relevant role of proestrus-estrus estradiol (E2) and metaestrus-diestrus progesterone (P4) concentrations in regulating oviductal function (GONELLA-DIAZA *et al*., 2015). Enriched pathways included cellular proliferation, secretion, and extracellular matrix (ECM) remodeling. Additionally, it was recently reported that the sex steroid-mediated changes in the oviductal transcriptome were intimately associated with variations in oviductal morphology. Cows ovulating larger follicles presented a greater number of secretory cells and oviductal folds, greater proportion of proliferating cells, and greater epithelial area when compared to cows ovulating smaller follicles (GONELLA-DIAZA *et al*., 2017). Global transcriptional regulation and phenotypic changes of oviductal tissue may help to explain the positive impact of a larger preovulatory follicle size on fertility during FTAI protocols (PUGLIESI *et al*., 2016; SA FILHO *et al*., 2010; PERRY *et al*., 2014; LU *et al*., 2011). However, sex-steroid effects on oviductal ECM remodeling dynamics in cattle are poorly understood.

The ECM is a group of extracellular molecules that offers structural and biochemical support to cells and tissues (BONNANS *et al*., 2014; LU *et al*., 2011). ECM interacts with the surrounding cells and signal to regulate important processes such as migration, proliferation, apoptosis, and/or differentiation of cells. Also, growth

factors (GF) can be stored in the ECM and locally released during the remodeling process through ECM cleavage (BONNANS *et al*., 2014; COX; ERLER, 2011; TAIPALE; KESKI-OJA, 1997). Growth factors identified in the ECM include: epidermal growth factor (EGF), fibroblast growth factor (FGF), WNTs, transforming growth factor-β (TGFβ), and amphiregulin (HYNES, 2009). Furthermore, growth factors play a central role in the regulation of ECM remodeling itself by promoting cellular proliferation. ECM remodeling process occurs under a complex regulation and depends on the balance of abundance and activity between numerous proteinases and their inhibitors (HYNES, 2009; COX; ERLER, 2011). ECM remodeling occurs in the endometrium during embryo implantation and has been described in humans, mice, and ruminants (COUTIFARIS *et al*., 1998; ABRAHAMSOHN; ZORN, 1993; BURGHARDT *et al*., 2002). Furthermore, we showed clear effects of the peri-ovulatory sex-steroids concentrations in the endometrial ECM remodeling (SCOLARI *et al*., 2016). Here, we hypothesize that the abundance of ECM components and remodelers is different in the oviduct of cows treated to ovulate larger or smaller follicles.

5.2 MATERIALS AND METHODOLOGY

5.2.1 Animals

Animal procedures were approved by the Ethic Committee on Animal Use of the School of Veterinary Medicine and Animal Science of the University of São Paulo (CEUA/FMVZ; protocols numbers 2281-2011 and 4293160916). Experiments were conducted at the University of São Paulo, campus Pirassununga (São Paulo, Brazil) using adult, pluriparous, cyclic, and non-lactating Nelore (*Bos indicus*) cows, without reproductive disorders according to gynecological examination and body condition score between 3 and 4 (0 emaciated; 5 obese). All animals were kept in grazing conditions and to fulfill their maintenance requirements, they were supplemented with sugar cane and/or corn silage, concentrate, minerals, and water *ad libitum*.

5.2.2 Reproductive Management and Experimental Design

Ovulations were synchronized as described previously by Mesquita and coworkers (2014) and Gonella and coworkers (2015). Cows were manipulated to ovulate smaller [Small Follicle-Small CL group (SF-SCL)] or larger [Large Follicle-Large CL group (LF-LCL)] follicles. Our previous studies have reported contrasting peri-ovulatory endocrine milieus with distinct proestrus/estrus concentrations of E2 and metaestrus concentrations of P4, as well as different receptivity and fertility between the above mentioned experimental groups (PUGLIESI *et al*., 2016; MESQUITA *et al*., 2014; GONELLA-DIAZA *et al*., 2015; MESQUITA *et al*., 2015). Briefly, animals were pre-synchronized by two intramuscular (im) injections of prostaglandin F2α analogue (PGF; 0.5 mg of sodium cloprostenol; Sincrocio, Ourofino Saúde Animal, Cravinhos, Brazil), 14 days apart. At the second PGF injection of Presynch (D-20), animals received an Estrotect Heat detector patch device (Rockway, Inc., Spring Valley, WI, USA), and estrus detection was performed twice a day every day from D-19 to D-10. Only animals that presented estrus after the second PGF treatment and with a new PGF-responsive CL (at least 5 days old) on D-10 stayed in the experiment. On D-10, the remaining cows (n = 41) received a new intravaginal P4-releasing device (1 g; Sincrogest, Ourofino) and an im injection of 2 mg estradiol benzoate (Sincrodiol, Ourofino Saúde Animal; Figure 10). Cows were randomly assigned into one of the experimental groups, and on D-10 cows from the LF-LCL group received a single im treatment of PGF. Eight days later, the P4 devices were removed 42–60 h or 30–36 h before the gonadotropin-releasing hormone (GnRH) treatment in the LF-LCL (n = 20) and SF-SCL (n = 21) groups, respectively. All animals received a PGF2 injection at P4 device removal. Ovulations were induced in all cows on D0 using GnRH agonist (Buserelin acetate, 10 µg, im; Sincroforte, Ourofino Saúde Animal). Expectation was that POF growth would be reduced in the presence of greater circulating P4 concentrations in cows from the SF-SCL group because of P4 from both exogenous (device) and endogenous (CL) sources.

Figure 11 – Hormonal manipulation protocol used in the present study.

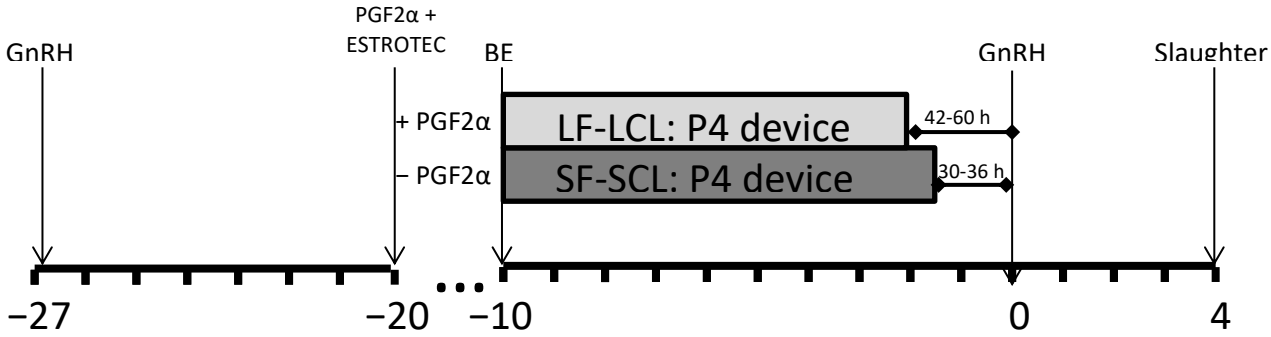

Source: Gonella-Diaza (2017).

Legend: Please see text for details. BE, injection of 2 mg of estradiol benzoate (Sincrodiol; Ourofino); GnRH, injection of 0.01 mg of buserelin acetate (Sincroforte; Ourofino); P4 device, P4-releasing device containing 1 g of P4 (Sincrogest; Ourofino, Cravinhos, SP, Brazil); PGF2α, injection of 0.5 mg of sodium cloprostenol (Sincrocio; Ourofino); Slaughter, endpoint for sample collection.

To assess follicle growth and ovulation of the POF as well as CL area and blood flow, transrectal ultrasound examinations were carried out on D-10 and D-6, daily from D-2 to D4. Ultrasound exams were performed with the aid of a duplex B-mode (gray-scale) and Color-Doppler instrument (MyLab30 Vet Gold; Esaote Healthcare, São Paulo, SP, Brazil) equipped with a multifrequency linear transducer. Blood samples were collected via jugular venipuncture in tubes containing heparin (BD, São Paulo, SP, Brazil) on D-1 and D4. Blood samples were immediately stored on ice. To obtain plasma, blood was centrifuged at 1500g for 30 minutes (min) at 4°C. The plasma was then aliquoted and stored at −20°C. On D4 of the estrous cycle (day 0 = injection of GnRH to induce ovulation), cows from LF-LCL (n = 16) and SF-SCL (n = 8) groups were stunned by a captive bolt and slaughtered by jugular exsanguination. The reproductive tract was transported on ice to the laboratory, ovarian structures were measured and weighed, and the oviduct ipsilateral to the ovary bearing the CL was dissected. Samples from ampulla and isthmus were snap-frozen in liquid nitrogen and then transferred to −80°C until processing for RNA or protein extraction. Another portion of samples was fixed by immersion in 4% buffered formalin for 24 h at 4°C, followed by several washings in PBS. Subsequently, samples were embedded in paraffin.

5.2.3 Hormonal Quantification

Concentrations of P4 were measured by radioimmunoassay (Coat-A-Count kit progesterone, Siemens Medical Solutions Diagnostics) validated previously for bovine plasma samples (GARBARINO *et al*., 2004). Estradiol concentrations were measured using a commercial RIA kit (Double Antibody Estradiol, DPC, Los Angeles, CA, USA) validated previously for bovine plasma samples (SIDDIQUI *et al*., 2009). The intra-assay CV and sensitivity were 1.7% and 0.13 pg/mL for E2 and 0.8% and 0.05 ng/mL for P4, respectively.

5.2.4 RNA Isolation

RNA was isolated using the kit AllPrep DNA/RNA/Protein Mini kit (No. 80004, Qiagen, São Paulo, São Paulo, Brazil). Frozen ampulla and isthmus samples were ground in liquid nitrogen using a mortar and pestle, and were mixed with buffer RLT. Tissue suspension was homogenized with a 21-g needle, centrifuged at 13,000 x g for 3 min and supernatant was loaded and processed in silica columns. Columns were eluted with 30 µL of RNase-free water, and RNA was kept at −80°C. Concentration of total RNA extracts was measured using the Nano-Vue spectrophotometer (GE Healthcare Europe, Munich, Germany).

5.2.5 mRNA Libraries, Sequencing, and Bioinformatics.

Methods and general results from transcriptomic analysis of tissues were published previously (GONELLA-DIAZA *et al*., 2015). Ampulla and isthmus samples from 3 animals of each group were selected for individual RNA-Seq. RNA quality was assessed with the Nano-Vue spectrophotometer (GE Healthcare; 260/280 and 260/230 nm ratios) and with the Agilent Bioanalyzer (Agilent Technologies, Palo Alto, USA; 28S/18S ratio and RNA integrity number (RIN) data). All samples had a RIN ≥8

and were considered suitable for RNAseq analysis. For the analysis of expression profiles, libraries were generated using a routine RNA library preparation TruSeq protocol developed by Illumina Technologies (San Diego, CA) using 1 µg of total RNA as input. Briefly, polyA selected RNA was cleaved as per Illumina protocol and the cleaved fragments were used to generate first strand cDNA using SuperScript II reverse transcriptase and random hexamers. Subsequently, second strand cDNA was synthesized with RNaseH and DNA polymerase enzyme. Adapter ligation and end repair steps followed second strand synthesis. Resulting products were amplified via PCR and cDNA libraries were then purified and validated using the Bioanalyzer 2100 (Agilent Technologies). Paired-end sequencing of 101bp reads was performed using the Illumina HiSeq 2000 (ampulla samples) and Illumina HiSeq 2500 (isthmus samples) platforms. The quality filtering was performed by seqyClean v1.3.12. (https://bitbucket.org/izhbannikov/seqyclean/get/stable.zip) using a minimum of 26 Phred quality vector. Adaptor sequences from the Univec database (https://www.ncbi.nlm.nih.gov/tools/vecscreen/univec/) were used as guides to remove possible contaminants. Only high quality paired-end sequences were kept for further analyses. Reads were mapped with Tophat v.2.0.8 (KIM *et al*., 2013) and Bowtie2 v2.1.0 (LANGMEAD; SALZBERG, 2012) on the masked bovine genome assembly (*Bos taurus,* UMD 3.1, NCBI). The mapping file was sorted using SAMTools v 0.1.18 (LI *et al*., 2009) and read counts were obtained using the script from HTSeq-count v0.5.4p2 (http://www-huber.embl.de/users/anders/HTSeq/doc/count.html). Differential expression analysis was performed with DESEq v1.12.1 (ANDERS; HUBER, 2010) from R/Bioconductor (GENTLEMAN *et al*., 2004). Using the function “estimate Size Factors”, the normalized counts were obtained (baseMean values are the number of reads divided by the size factor or normalization constant). The standard deviation along the baseMean values was also calculated for each transcript. In order to avoid artifacts caused by low expression profiles and high expression variance, only transcripts that had an average of baseMean > 5 and mean greater than the standard variation were analyzed. The method to test for differential expression was the negative binomial distribution, through the nbinom Test function on DESeq. The threshold for evaluating significance was obtained by applying a *P* value of 0.05 FDR- Benjamini-Hochberg (BENJAMINI; HOCHBERG, 1995). Gene enrichment analysis was performed

separately for each region, using the functional annotation tool of the Database for Annotation, Visualization, and Integrated Discovery (DAVID; DENNIS *et al*., 2003).

5.2.6 Protein Extraction and Multiplexed MMP Array

Protein analyses were conducted only in isthmus samples because transcriptome analyses indicates that most changes in transcript abundance of ECM remodeling-genes were detected in this region. About 20 mg of frozen isthmus samples (n = 4 for each group) were ground in liquid nitrogen using a mortar and pestle. Tissue homogenates were weighed and diluted (1 to 10 weight/volume) with cell lysis buffer (Abcam: ab152163) supplemented with 1:100 protease inhibitor (GE Healthcare; UK) and Phenylmethylsulfonyl fluoride (PMSF, final concentration of 1 mM). Total protein concentration was measured using the Pierce™ BCA Protein Assay Kit (Cat. Number: 23225; Thermo Scientific). Human MMP Antibody Array (Abcam: ab134004) was used to detect and quantify several proteins in parallel, namely MMP-1, MMP-2, MMP-3, MMP-8, MMP-9, MMP-10, MMP-13, TIMP-1, TIMP-2 and TIMP-4. All procedures were performed according to the manufacturer's recommendation, and all incubation and washing steps were performed with gentle shaking. To summarise, membranes were blocked by incubating with 2 mL of 1X Blocking buffer at room temperature (RT) for 30 min. The buffer was aspirated and, then 1 ml of diluted sample containing 300 µg of total protein was pipetted into each membrane and incubated overnight at 4°C. Membranes were transferred to clean containers and were washed with 20 ml of Wash Buffer I at RT for 45 min. Next, buffer was removed and three additional washes with 2 ml of 1X Wash Buffer I, followed by 2 washes with 2 ml of 1X Wash Buffer II for 5 min at RT were performed. Afterward, 1 ml of 1X Biotin-Conjugated Anti-Cytokines was then added to each membrane and incubated for 2 hours at RT. Membranes were washed again (3 x 1X Wash Buffer I and 2 x 1X Wash Buffer II) and next, 2 ml of 1X HRP-Conjugated Streptavidin were added and incubated for 2 hours at RT. After washing steps (3 x 1X Wash Buffer I and 2 x 1X Wash Buffer II), membranes were transferred into a clean container and the excess of wash buffer was removed by blotting the

membrane edges with tissue paper. Membranes were transferred again onto a plastic sheet (included in the kit) and were incubated with 500 µl of a mix of equal volumes (1:1) of Detection Buffer C and D for 2 min at RT. Each membrane was placed between two plastic sheets and all air bubbles were smoothed out. Immediately, membranes were imaged using a ChemiDoc MP imaging system (Biorad, Hercules, Ca, USA). Finally, images were analyzed using spot-recognition analysis software (ImageJ). Signal intensities of each protein were normalized with the mean value of the positive control signals. The amino acid sequences of the human and bovine proteins were aligned using the EMBOSS Pairwise Sequence Alignment Algorithm at the EMBL-EBI Web site (http://www.ebi.ac.uk/Tools/psa/emboss_needle/) with the “needle” method and default settings selected. Results of these alignments are shown on Appendix D.

5.2.7 Immunohistochemistry for Collagen Type I

Histological sections (4 µm) of both the ampula (n = 5 of each group) and the isthmus (n = 5 of each group) were deparaffinized, rehydrated, and subjected to enzymatic digestion with 0.4% pepsin (Sigma, USA) diluted in 0.5 N acetic acid for 30 min at 37°C. After blocking endogenous peroxidase with 6% H2O2 solution (Merck, USA) for 30 min, the slides were incubated in a humidified chamber overnight at 4°C with the rabbit primary anti- type I collagen (#600-401-103, Rockland, USA; 1:3000). Slides were then incubated with the complex Super Picture Polymer Detection kit (Life Technologies, USA) for 30 min at 37°C. After incubation, the reaction was visualized with 3’3 diaminobenzidine chromogen and counterstaining with Harris hematoxylin. Negative controls were performed replacing the primary antibody with normal rabbit IgG (#sc-2027, Santa Cruz Biotechnology, USA). Sections were finally observed by light microscopy using the 10× objective and five optical fields from at least three tissue sections were photographed. Digital morphometric analysis for type I collagen quantification was performed using Image J and the Color deconvolution plugin (RUIFROK; JOHNSTON, 2001), as reported previously (BRIANEZI *et al*., 2015; Figure 11). Thus, identification of the immunostaning signal was performed in

the whole tissue (i.e., ampulla or isthmus) as well as for each structural layer separately (i.e., tunica mucosa, tunica muscularis, and tunica serosa). Data is presented as the percentage of the whole tissue or mucosal area that only had positive staining for type I collagen.

Figure 12 – Image analysis for collagen type I quantification.

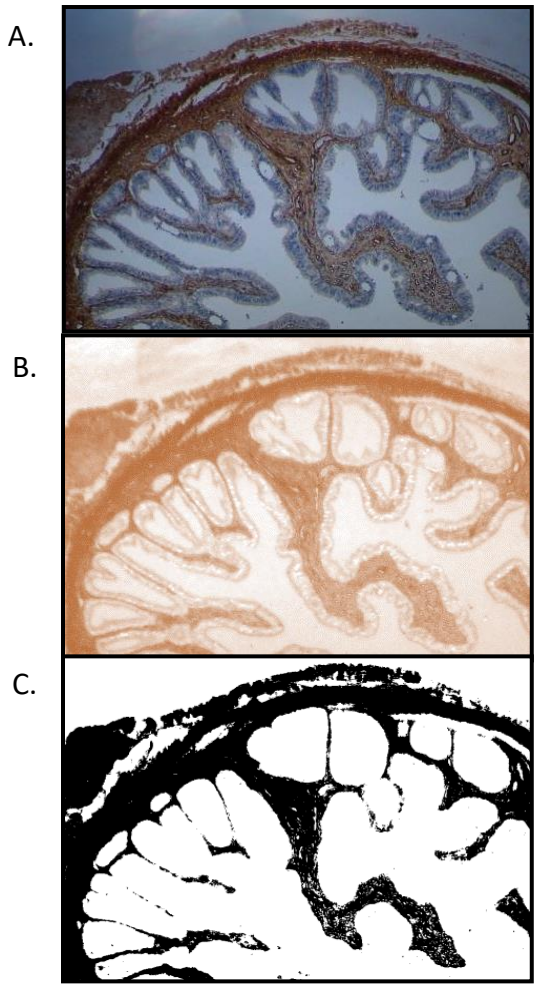

Source: Gonella-Diaza (2017).

Legend: The original image (Panel A) was proceed using the “Color deconvolution” algorithm and the product in channel 2 (Panel B), corresponding to the DAB staining, was selected and transformed to binary (Panel C). Finally, total black area and mucosal black area were quantified.

5.2.8 Statistical Analysis.

The experiment was conducted as a completely randomized design. All statistical analyses were performed using SAS computational software, version 9.3 for Microsoft Windows (SAS Institute Inc., Cary, NC). Plasma concentrations of E2 and P4, follicle diameter, CL area, and protein quantification of the MMPs array were analyzed by ANOVA using the GLM procedure of SAS. Analyses of percentage of positive type I collagen areas was analyzed using the GLIMMIX procedure of SAS. The model included the fixed effects of group, region, and their interaction. Due to repeated measures within each cow (i.e. ampulla and isthmus), a repeated statement was used. A significant difference between groups was considered when $P \leq 0.05$, whereas differences between $P > 0.05$ and $P \leq 0.10$ were considered as approaching significance.

5.3 RESULTS

5.3.1 Animal Model

Results from the animal model used here were reported previously (GONELLA-DIAZA *et al*., 2015). The hormonal manipulation protocol was successful in generating two groups of cows with distinct ovarian features and ovarian steroid endocrine profiles. To summarize, follicle diameter and E2 plasma concentration on D-1 and CL area and P4 plasma concentration on D4 were 38.81, 275.54, 65.68, and 75% greater for the LF-LCL compared to the SF-SCL group, respectively ($P < 0.01$).

5.3.2 ECM-Related Gene Expression

A comprehensive analysis of the ampulla and isthmus transcriptome of cows in the LF-LCL and SF-SCL groups was reported previously (GONELLA-DIAZA *et al*., 2015). A total of 692 and 590 genes showed differential expression between groups in ampulla and isthmus samples, respectively (adjusted *P* value <0.1). Functional enrichment analysis revealed clusters with overrepresented ontology terms and activation of pathways associated with extracellular matrix region, organization, and remodeling in the LF-LCL group, especially in the isthmus region (Table 4). In particular, molecules up-regulated in the isthmus region of cows ovulating larger follicles could be further classified as ECM components (Collagens), ECM remodelers (ADAMs and MMPs), and ECM-related growth factors (potentially released from the ECM during the remodeling process). A list of these genes, their Log2Fold Change, and adjusted *P* value is available on table 5.

Table 4 - Functional enrichment of pathways related to extracellular matrix region, organization and, remodeling upregulated in the isthmus of LF-LCL cows (n = 3/group) on D4

Category	Term	Count	*P* Value	Fold Enrichment	FDR
GOTERM_CC_FAT	Extracellular matrix	22	3.19E-15	9.56629213	3.93E-12
GOTERM_CC_FAT	Extracellular region part	28	1.14E-12	5.07540984	1.40E-09
GOTERM_CC_FAT	Proteinaceous extracellular matrix	19	1.25E-12	9.02208589	1.52E-09
GOTERM_CC_FAT	Extracellular region	38	9.23E-12	3.29730942	1.13E-08
GOTERM_CC_FAT	Extracellular matrix part	10	2.36E-08	14.0727273	2.89E-05
GOTERM_CC_FAT	Collagen	7	6.02E-08	30.1	7.35E-05
GOTERM_MF_FAT	Extracellular matrix structural constituent	6	4.73E-06	22.7807882	0.00624005
GOTERM_BP_FAT	Extracellular structure organization	8	2.75E-05	8.91425672	0.04379667
GOTERM_BP_FAT	Extracellular matrix organization	7	6.22E-05	9.9894412	0.09905482
GOTERM_BP_FAT	Cell adhesion	13	3.29E-04	3.45573106	0.52295268
GOTERM_BP_FAT	Biological adhesion	13	3.29E-04	3.45573106	0.52295268
GOTERM_BP_FAT	Collagen fibril organization	4	5.80E-04	23.2407407	0.9205409
GOTERM_BP_FAT	Cell-matrix adhesion	5	9.08E-04	11.2975823	1.43742997
GOTERM_CC_FAT	Basement membrane	5	0.00107329	10.75	1.30283791
GOTERM_BP_FAT	Cell-substrate adhesion	5	0.00135688	10.1678241	2.14128781
GOTERM_CC_FAT	Fibrillar collagen	3	0.00234181	38.7	2.82254928
GOTERM_MF_FAT	Extracellular ligand-gated ion channel activity	5	0.00686542	6.53547202	8.69262497
GOTERM_CC_FAT	Extracellular space	8	0.05384605	2.31910112	49.1316462
GOTERM_BP_FAT	Cell-cell adhesion	5	0.08232873	3.01268861	74.5800692
GOTERM_MF_FAT	Actin binding	5	0.09101805	2.90995469	71.6264489

Source: Gonella-Diaza (2017).

Table 5 - ECM-related genes detected in the RNAseq data of the isthmus of cows with distinct peri-ovulatory milieus (SF-SCL vs LF-LCL; n = 3 cows/group).

Group of compounds	Gene	LF-LCL Mean	SF-SCL Mean	log2 Fold Change	*P* adj
ECM components	COL16A1	6293.56	3660.96	-0.78165387	0.04
	COL18A1	8542.26	5214.03	-0.71221989	0.00
	COL1A1	93788.33	43054.85	-1.12323288	0.00
	COL3A1	155148.37	73926.80	-1.06947922	0.00
	COL4A1	26365.29	11385.09	-1.21149419	0.01
	COL4A2	17563.09	6746.39	-1.38035914	0.00
	COL4A4	289.55	65.42	-2.1459759	0.02
	COL4A6	1286.96	520.30	-1.30656213	0.02
	COL5A2	10238.78	4809.16	-1.09018779	0.00
	COL5A3	1396.72	647.93	-1.10813799	0.02
	COL6A2	29451.41	17259.63	-0.77093504	0.03
	COL6A5	105.59	22.42	-2.23586941	0.01
	COL6A6	167.07	39.88	-2.06677633	0.02
	COL8A1	822.11	307.91	-1.4167993	0.01
ECM remodelers	ADAM23	78.11	27.18	-1.52271622	0.02
	ADAMTS2	1437.79	625.71	-1.2002885	0.00
	ADAMTS4	330.22	124.43	-1.40806423	0.00
	MMP14	5535.61	2445.40	-1.17867064	0.01
	MMP24	45.53	9.27	-2.29571126	0.00
	MMP7	9.80	68.70	2.80982956	0.02
Growth Factors	ANGPTL1	394.26	106.91	-1.88281558	0.02
	BMI1	696.43	458.59	-0.60278294	0.02
	BMP4	670.38	399.37	-0.74725945	0.05
	EGR2	24.74	5.27	-2.23047745	0.03
	EGR3	25.17	3.68	-2.77334971	0.00
	FGF9	98.45	49.92	-0.97976472	0.02
	GRIP1	386.87	124.55	-1.63518452	0.00
	IGF-I	1805.95	748.14	-1.27137824	0.02
	NGFR	87.48	30.74	-1.50899029	0.01
	PDGFD	245.46	148.50	-0.72502686	0.02
	TF	153.17	34.15	-2.16515123	0.00
	WISP1	49.67	13.92	-1.83495449	0.03

Source: Gonella-Diaza (2017).

Legend: Fold changes were the ratio of the mean expression values of SF-SCL/LF-LCL.

5.3.3 MMPs and TIMPs Protein Expression

The results of the amino acid sequence alignment between human and bovine proteins resulted in adequate identities (ranging from 71 to 91%), similarities (79.8 to 95.9%) and gaps (0 to 7.7%) for the commercial kit target proteins, supporting the use of the human platform for detecting bovine orthologs. As for MMP10 bovine protein, no sequence information was found on the NCBI protein database; Therefore, its quantification was not considered in the present study. Signal intensities for MMP3, MMP8, MMP9, MMP13, and TIMP4 were 65.84, 43.50, 44.30, 76.08, and 65.23% greater for the LF-LCL compared to the SF-SCL group, respectively ($P < 0.05$). Additionally, the protein expression of MMP1 and TIMP2 tended to differ between groups, and was greater in the LF-LCL group (71.48 and 63.39% greater intensity in comparison to SF-SCL; $P < 0.10$; Figure 12).

Figure 13 – MMP Antibody Array analysis in isthmus samples form LF-LCL and SF-SCL cows.

A.

	A	B	C	D	E	F	G	H
1	POS	POS	NEG	NEG	MMP-1	MMP-2	MMP-3	MMP-8
2	POS	POS	NEG	NEG	MMP-1	MMP-2	MMP-3	MMP-8
3	MMP-9	MMP-10	MMP-13	TIMP-1	TIMP-2	TIMP-4	NEG	POS
4	MMP-9	MMP-10	MMP-13	TIMP-1	TIMP-2	TIMP-4	NEG	POS

B.

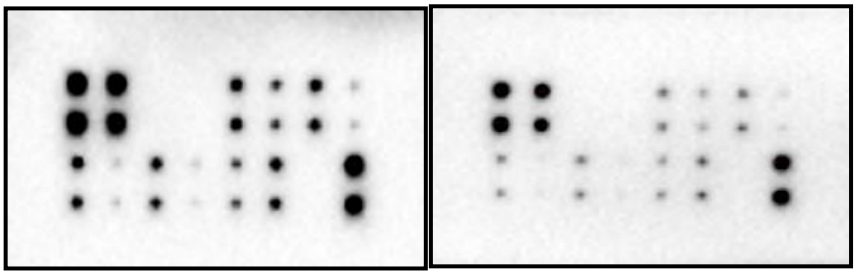

C.

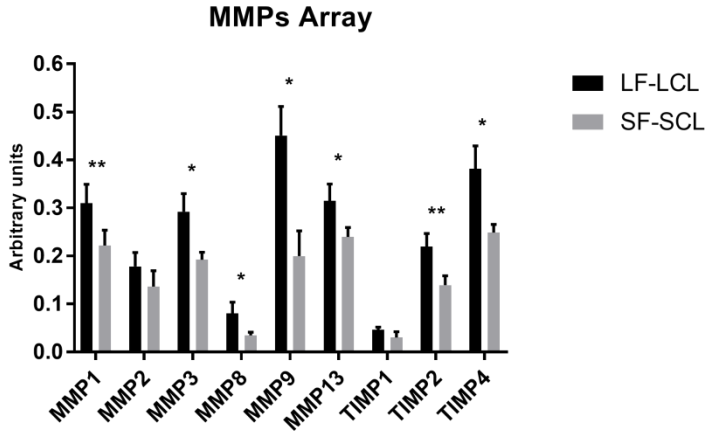

Source: Gonella-Diaza (2017).

Legend: (Panel A) Map for the location of antibodies in the membranes. (Panel B) Representative photographs of membranes from LF-LCL group (left) and SF-SCL group (right). (Panel C) Quantification of signal density for each antibody. Signal intensities of each protein were normalized with the mean value of the positive controls signals. Values are the mean ± SEM of independent samples. MMP, matrix metalloproteinases; TIMP, tissue inhibitor of metalloproteinase. *Significant difference from control (* $P < 0.05$; ** $P < 0.10$).

5.3.4 Immunohistochemical Evaluation of Collagen Content and Tissue Distribution

Immunohistochemistry analyses were performed to determine the distribution of type I collagen in the oviduct (Figure 13). In both groups, type I collagen was detected in all the structural tunicae (mucosa, muscular, and serosa) as thicker fibers. There were no differences in the type I collagen content when the tunica muscular and the tunica serosa were compared between groups or regions (data not shown). However, when type I collagen content was quantified in the tunica mucosa, even though no region effect was observed, a significant group effect was detected with stronger signal in SF-SCL in comparison to LF-LCL samples on both regions (LF-LCL ampulla: 14.48 ± 5.21% and isthmus: 17.05 ± 2.52%; SF-SCL ampulla: 27.77 ± 1.70% and isthmus: 29.55 ± 3.58%).

Figure 14 – Representative photomicrographs of Collagen type I immunostaining in ampulla and isthmus samples of animals from the LF-LCL and SF-SCL groups.

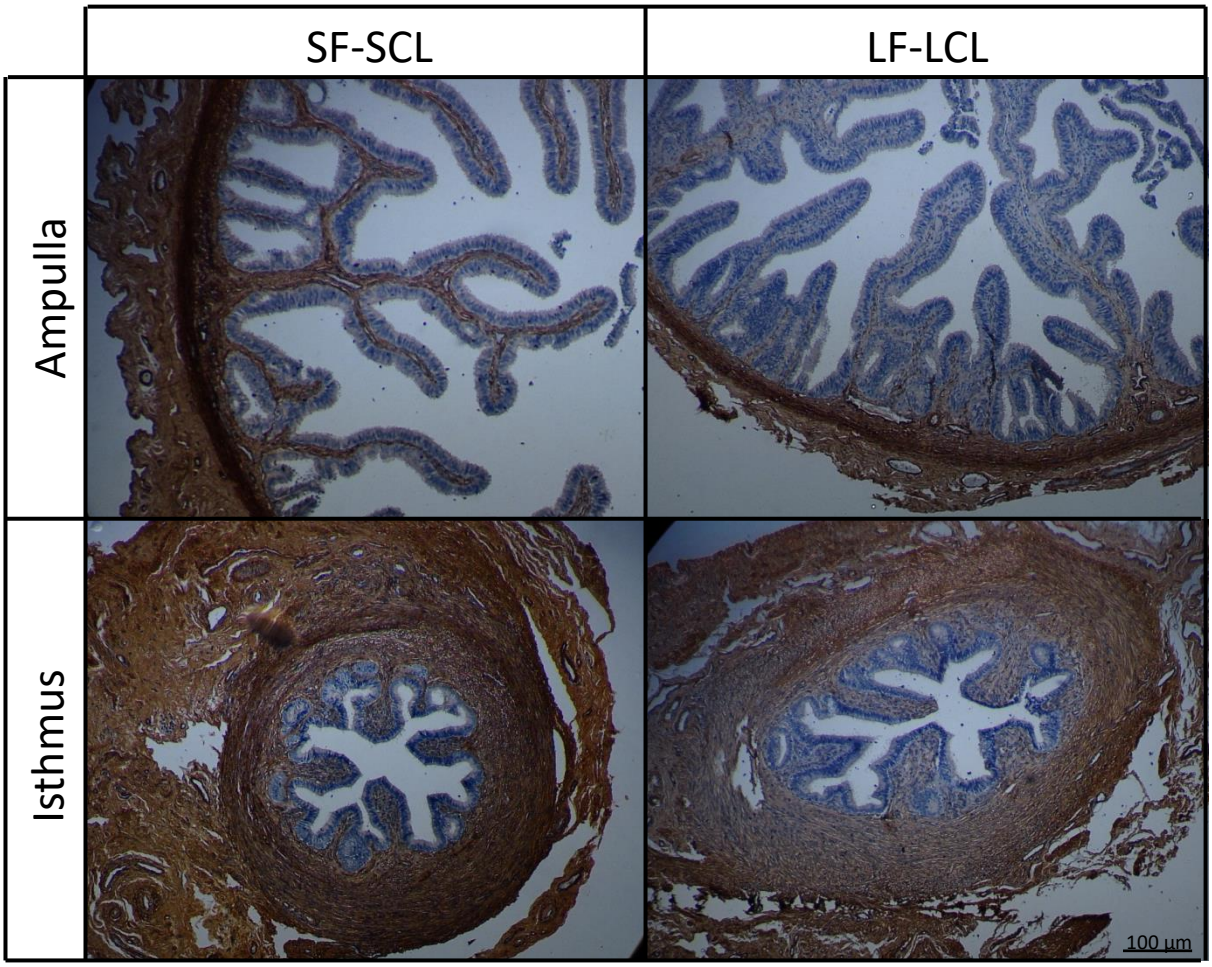

Source: Gonella-Diaza (2017).

5.4 DISCUSSION

During the estrous cycle, hormonal changes prepare the reproductive tract for estrus, ovulation, fertilization, embryo development, and implantation. In cattle, changes in endometrial morphology, (WANG *et al*., 2007), transcriptome (MESQUITA *et al*., 2015; FORDE *et al*., 2011), secretome, and proteome (MULLEN *et al*., 2012; FAULKNER *et al*., 2012), among others, have been reported to be mediated by sex-steroids. In particular, the oviduct plays an important role during the reproductive process. Fertilization and early embryo development take place in the

oviductal lumen. However, the molecular processes that occurr in the oviduct during the estrous cycle and their relation to embryo receptivity have been thotouhgly established. The objective of this study was to evaluate gene and protein expression of ECM components and remodelers in cows treated to ovulate larger or smaller follicles.

Growth and ovulation of a larger follicle stimulates transcription of molecules related to ECM remodeling. In the present study, transcript abundance of ECM-related genes was greater in the LF-LCL group. Other studies have described changes in the bovine oviductal transcriptome using different experimental models. Bauersachs *et al*., (2003) compared the transcriptome of ipsilateral and contralateral oviducts at D 3.5 after standing heat. They reported a series of molecular functional categories that were up-regulated in the ipsilateral side, including cell-surface proteins, cell-cell interaction proteins, members of signal transduction pathways, immune-related proteins, and enzymes. While investigating the changes in oviductal gene expression during the estrous cycle in a subsequent study, Bauersachs *et al*., (2004) discovered reported enrichment of molecular process such as protein modification and secretion, endocytosis, regulation of transcription, signaling pathways, and immune-related functions. Additionally, Cerny *et al*., (2015) reported a series of molecular pathways related to cholesterol biosynthesis, oxidative phosphorylation, cancer and cell cycle, receptor signaling pathway, and cell-cell adhesion, among others, which were altered either by the estrous-cycle stage (i.e., follicular vs. luteal) or by the oviductal region (i.e., ampulla vs. isthmus). Moreover, other studies have shown that the oviductal transcriptome is also responsive to the presence of sperm cells or embryos (ALMINANA *et al*., 2014; ALMINANA *et al*., 2012; MAILLO *et al*., 2016; MAILLO *et al*., 2015; GABLER *et al*., 2008). Nevertheless, none of the experimental models employed in the above-mentioned studies have shown a relationship between the factors tested and regulation of ECM remodeling genes. Considering the model of the current study, two interconnected factors offer potential biological explanation for the differential regulation observed. First, modulation of the size of the ovulatory follicle led to two distinct patterns of ovarian steroid hormones secretion (i.e., cows ovulating larger follicles had earlier and more prominent rise in estradiol and, consequently, higher progesterone concentrations). Therefore, imposing both, temporal and concentration-related effects

that are related to the moment in which the oviduct is exposed to the referred endocrine milieu. Second, an overall performance phenotype is also imposed by the current model, in which cows ovulating larger follicles reached greater fertility rates, as reported by Pugliesi *et al*. (2016). In that regard, up-regulation of ECM-related genes in the LF-LCL group may suggest that (1) ECM remodeling initiates earlier in response to the earlier and more prominent rise in ovarian steroids, and/or that (2) the early onset of ECM remodeling in the oviduct is necessary for preparating a more receptive female reproductive tract. Interestingly, changes in the expression of ECM-related genes were also observed in a study where the oviductal transcriptome of young (30-50 months; high fertility) and aged (more than 120 months; low fertility) cows were compared. Tanaka *et al*., (2016) reported that in aged oviductal epithelial cells there was an inhibition of ECM-related genes, such as decorin (DCN), periostin (POSTN), COL1A1, actin alpha 2 (ACTA2), and biglycan (BGN), supporting the proposed relationship between the regulation of ECM-related molecules in the oviduct and fertility. According to the literature, the oviductal transcriptome could be altered by many factors, such as oviductal region, side relative to the POF or CL, presence of embryo and gametes, and fertility. However, disturbances in the expression of ECM-related genes were only observed when distinct fertility phenotypes in cows were compared.

Growth and ovulation of a larger follicle stimulate protein expression of MMPs and TIMPs in the isthmus. In the present study, the protein expression of several members of the ECM remodeling pathway was measured simultaneously using an antibody array. Out of the nine proteins were evaluated, seven were more abundant (five showed statistical differences and two statistical tendencies) in the LF-LCL group, thus being consistent with the RNA-seq data. ECM remodeling occurs in several tissues during physiological and pathological processes as well as during tissue development (BONNANS *et al*., 2014; LU *et al*., 2011). During early embryo development, the endometrial ECM undergoes remodeling by changing its composition as part of a necessary mechanism to promote embryo implantation (BURGHARDT *et al*., 2002; ABRAHAMSOHN; ZORN, 1993). Among the potential biological implications of regulating ECM composition, the ECM has been described as a compartment for local storage of growth factors (TAIPALE; KESKI-OJA, 1997) that during the matrix breakdown are released and may favor embryo development,

particularly during the pre-implantation stage (ALEXANDER *et al*., 1996; DIMITRIADIS *et al*., 2005). Gabler *et al*., (2001) reported that protein expression and activity of ECM remodelers in the bovine oviduct is affected by the estrous cycle stage. These authors showed the active presence of two major ECM remodeling pathways: the Matrix metalloproteinase system and the plasminogen system. It was concluded that enzymes such as uPA, PAI-1, TIMPs, MMP-1 and MMP-2 are produced and secreted by bovine oviductal cells. Those enzymes could act by protecting gametes and the early embryo from proteolytic degradation and releasing heparin-binding GF from the epithelium surface, thus stimulating embryo development. Therefore, one may presume that oviduct cells from cows of the LF-LCL group, which express greater abundance of ECM-remodeling molecules, could provide an oviductal luminal environment of greater exposure potential of the embryo and oviduct cells themselves to numerous GF.

Growth and ovulation of a larger follicle stimulate type I collagen degradation in the tunica mucosa of ampulla and isthmus. In the present study, the type I collagen content was quantified in the tunica mucosa. While no differences were observed in type I collagen content between regions, the tunica mucosa of LF-LCL cows expressed approximately 50% less collagen than that of SF-SCL cows. This result is highly correlated with the MMP protein profiling obtained in the current study. Out of the four major type I collagen proteases (MMP1, MMP2, MMP8 and, MMP13), three of them were more abundant in the oviduct of LF-LCL cows suggesting that the observed low abundance of type I collagen is a consequence of the greater abundance of type I collagen proteases reported in this study. Additionally, the relationship between sex-steroids and oviductal MMPs expression has also been shown in several species (DIAZ *et al*., 2012; GABLER *et al*., 2001; LESNIAK-WALENTYN; HRABIA, 2016). In particular, Gabler *et al*., (2001) evaluated activity and quantity of MMPs using gelatin zymograms in cows, and showed that these proteins are more active during the follicular phase (days 1-5 and 19-21 of the estrous cycle), when estradiol circulating concentrations are greater, thus suggesting a positive regulation of MMPs by estradiol and supporting our data. In this context, modulating the composition and arrangement of the ECM may also represent a mechanism of phenotype regulation for the surrounding cell types, becaouse it provides an environment that is more or less permissive to biological processes such

as proliferation, migration, and differentiation (MESQUITA *et al*., 2015; THYBERG; HULTGARDH-NILSSON, 1994; KOOHESTANI *et al*., 2013).

Although currently it is common to produce embryos in the laboratory using *in vitro* conditions, it is clear that quality and developmental potential of *in vivo*-produced embryos is greater than that of *in vitro*-produced embryos (RIZOS *et al*., 2002b; RIZOS *et al*., 2002c; RIZOS *et al*., 2002a). However, little is known about oviductal environment and oviductal-derived molecules that could improve embryo quality. The present study showed that ECM remodeling process takes place in the oviduct of high fertility cows when the embryo is being transported from the oviductal lumen into the uterine environment. This remodeling process is more intense and probably occurs earlier in these cows, when compared with low fertility cows. Additionally, the remodeling process could help release GF from the ECM benefiting the development and survival of the embryo. New studies are needed to compare the composition of the oviductal fluid, especially GF availability, in models or conditions that simulate distinct fertility conditions in cattle.

5.5 REFERENCES

ABRAHAMSOHN, P. A.; ZORN, T. M. Implantation and decidualization in rodents. **Journal of Experimental Zoology**, v. 266, p. 603-628, 1993.

ALEXANDER, C. M.; HANSELL, E. J.; BEHRENDTSEN, O.; FLANNERY, M. L.; KISHNANI, N. S.; HAWKES, S. P.; WERB, Z. Expression and function of matrix metalloproteinases and their inhibitors at the maternal-embryonic boundary during mouse embryo implantation. **Development**, v. 122, p. 1723-1736, 1996.

ALMINANA, C.; CABALLERO, I.; HEATH, P. R.; MALEKI-DIZAJI, S.; PARRILLA, I.; CUELLO, C.; GIL, M. A.; VAZQUEZ, J. L.; VAZQUEZ, J. M.; ROCA, J.; MARTINEZ, E. A.; HOLT, W. V.; FAZELI, A. The battle of the sexes starts in the oviduct:

modulation of oviductal transcriptome by X and Y-bearing spermatozoa. **BMC Genomics**, v. 15, p. 293, 2014.

ALMINANA, C.; HEATH, P. R.; WILKINSON S.; SANCHEZ-OSORIO J.; CUELLO C.; PARRILLA I.; GIL M. A.; VAZQUEZ J. L.; VAZQUEZ J. M.; ROCA J.; MARTINEZ E. A.; FAZELI A. Early developing pig embryos mediate their own environment in the maternal tract. **PLoS One**, v. 7, e33625, 2012.

ANDERS, S.; HUBER, W. Differential expression analysis for sequence count data. **Genome Biology**, v. 11, R106, 2010.

BAUERSACHS, S.; BLUM, H.; MALLOK, S.; WENIGERKIND, H.; RIEF, S.; PRELLE, K.; WOLF, E. Regulation of ipsilateral and contralateral bovine oviduct epithelial cell function in the postovulation period: a transcriptomics approach. **Biology of** Reproduction, v. 68, p. 1170-1177, 2003.

BAUERSACHS, S.; REHFELD, S.; ULBRICH, S. E.; MALLOK, S.; PRELLE, K.; WENIGERKIND, H.; EINSPANIER, R.; BLUM, H.; WOLF, E. Monitoring gene expression changes in bovine oviduct epithelial cells during the oestrous cycle. **Journal of Molecular Endocrinology**, v. 32, p. 449-466, 2004.

BENJAMINI, Y.; HOCHBERG, Y. Controlling the false discovery rate: A practical and powerful approach to multiple testing. **Journal of the Royal Statistical Society Series B-Methodological,** v. 57, p. 289-300, 1995.

BESENFELDER, U.; HAVLICEK, V.; BREM, G. Role of the oviduct in early embryo development. **Reproduction in Domestic Animals**, v. 47 (Suppl 4), p. 156-163, 2012.

BONNANS, C.; CHOU, J.; WERB, Z. Remodelling the extracellular matrix in development and disease. **Nature Reviews Molecular Cell** Biology, v. 15, p. 786-801, 2014.

BRIANEZI, G.; GRANDI, F.; BAGATIN, E.; ENOKIHARA, M. M.; MIOT, H. A. Dermal type I collagen assessment by digital image analysis. **Brazilian Annals of Dermatology**, v. 90, p. 723-727, 2015.

BURGHARDT, R. C.; JOHNSON, G. A.; JAEGER, L. A.; KA, H.; GARLOW, J. E.; SPENCER, T. E.; BAZER, F. W. Integrins and extracellular matrix proteins at the maternal-fetal interface in domestic animals. **Cells Tissues Organs,** v. 172, p. 202-217, 2002.

CERNY, K. L.; GARRETT, E.; WALTON, A. J.; ANDERSON, L. H.; BRIDGES, P. J. A transcriptomal analysis of bovine oviductal epithelial cells collected during the follicular phase versus the luteal phase of the estrous cycle. **Reproductive Biology and Endocrinology**, v. 13, p. 84, 2015.

COUTIFARIS, C.; OMIGBODUN, A.; COUKOS, G. Integrins, endometrial maturation, & human embryo implantation. **Seminars in Reproductive Endocrinology**, v. 16, p. 219-229, 1998.

COX, T. R.; ERLER, J. T. Remodeling and homeostasis of the extracellular matrix: implications for fibrotic diseases and cancer. **Disease Models & Mechanisms.** v. 4, p. 165-178, 2011.

DENNIS, G.Jr.; SHERMAN, B. T.; HOSACK, D. A.; YANG, J.; GAO, W.; LANE, H. C.; LEMPICKI, R. A. DAVID: Database for Annotation, Visualization, and Integrated Discovery. **Genome Biology**, v.4(5), P3, 2003.

DIAZ, P. S.; SOLAR, P. A.; JUICA, N. E.; ORIHUELA, P. A.; CARDENAS, H.; CHRISTODOULIDES, M.; VARGAS, R.; VELASQUEZ, L. A. Differential expression of extracellular matrix components in the Fallopian tubes throughout the menstrual cycle. **Reproductive Biology and Endocrinology** , v. 10, p. 56, 2012.

DIMITRIADIS, E.; WHITE, C. A.; JONES, R. L.; SALAMONSEN, L. A. Cytokines, chemokines and growth factors in endometrium related to implantation. **Human Reproduction Update,** v. 11, p. 613-630, 2005.

ELLINGTON, J. The bovine oviduct and its role in reproduction: a review of the literature. **The Cornell veterinarian**, v. 81, p. 313-328, 1991.

ERIKSEN, T.; TERKELSEN, O.; HYTTEL, P.; GREVE, T. Ultrastructural features of secretory-cells in the bovine oviduct epithelium. **Anatomy and Embryology**, v. 190, p. 583-590, 1994.

FAULKNER, S.; ELIA, G.; MULLEN, M. P.; O'BOYLE, P.; DUNN, M. J.; MORRIS, D. A comparison of the bovine uterine and plasma proteome using iTRAQ proteomics. **Proteomics**, v. 12, p. 2014-2023, 2012.

FORDE, N.; BELTMAN, M. E.; DUFFY, G. B.; DUFFY, P.; MEHTA, J. P.; O'GAORA, P.; ROCHE, J. F.; LONERGAN, P.; CROWE, M. A. Changes in the Endometrial Transcriptome During the Bovine Estrous Cycle: Effect of Low Circulating Progesterone and Consequences for Conceptus Elongation. **Biology of Reproduction**, v. 84, p. 266-278, 2011.

GABLER, C.; KILLIAN, G. J.; EINSPANIER, R. Differential expression of extracellular matrix components in the bovine oviduct during the oestrous cycle. **Reproduction,** v. 122, p. 121-130, 2001.

GABLER, C.; ODAU, S.; MULLER, K.; SCHON, J.; BONDZIO, A.; EINSPANIER, R. Exploring cumulus-oocyte-complex-oviductal cell interactions: gene profiling in the bovine oviduct. **Journal of Physiology and Pharmacology**, v. 59 (Suppl. 9), p. 29-42, 2008.

GARBARINO, E. J.; HERNANDEZ, J. A.; SHEARER, J. K.; RISCO, C. A.; THATCHER, W. W. Effect of lameness on ovarian activity in postpartum Holstein cows. **Journal of Dairy Science**, v. 87, p. 4123-4131, 2004.

GENTLEMAN, R. C.; CAREY, V. J.; BATES, D. M.; BOLSTAD, B.; DETTLING, M.; DUDOIT, S.; ELLIS, B.; GAUTIER, L.; GE, Y. C.; GENTRY, J.; HORNIK, K.; HOTHORN, T.; HUBER, W.; IACUS, S.; IRIZARRY, R.; LEISCH, F.; LI, C.;

MAECHLER, M.; ROSSINI, A. J.; SAWITZKI, G.; SMITH, C.; SMYTH, G.; TIERNEY, L.; YANG, J. Y. H.; ZHANG, J. H. Bioconductor: open software development for computational biology and bioinformatics. **Genome Biology**, v. 5(10), R80, 2004.

GONELLA-DIAZA, A. M.; ANDRADE, S. C.; SPONCHIADO, M.; PUGLIESI, G.; MESQUITA, F. S.; VAN HOECK, V.; STREFEZZI, R.F.; GASPARIN, G. R.; COUTINHO, L. L.; BINELLI, M. Size of the Ovulatory Follicle Dictates Spatial Differences in the Oviductal Transcriptome in Cattle. **PLoS One**, v. 10, e0145321, 2015.

GONELLA-DIAZA, A. M.; MESQUITA, F. S.; DA SILVA, K. R.; DE CARVALHO BALIEIRO, J. C.; DOS SANTOS, N. P.; PUGLIESI, G.; STREFEZZI, R.F.; BINELLI, M. Sex Steroids Modulate Morphological and Functional Features of the Bovine Oviduct. **Submitted to Cell and Tissue Research**. 2017.

HUNTER, R. H.; COOK, B.; POYSER, N. L. Regulation of oviduct function in pigs by local transfer of ovarian steroids and prostaglandins: a mechanism to influence sperm transport. **European Journal of Obstetrics and Gynecology**, v. 14, p. 225-232, 1983.

HYNES, R. O. The extracellular matrix: not just pretty fibrils. **Science,** v. 326, p. 1216-1219, 2009.

KIM, D.; PERTEA, G.; TRAPNELL, C.; PIMENTEL, H.; KELLEY, R.; SALZBERG, S. L. TopHat2: accurate alignment of transcriptomes in the presence of insertions, deletions and gene fusions. **Genome Biology**, v. 14, R36, 2013.

KOOHESTANI, F.; BRAUNDMEIER, A. G.; MAHDIAN, A.; SEO, J.; BI, J.; NOWAK, R. A. Extracellular matrix collagen alters cell proliferation and cell cycle progression of human uterine leiomyoma smooth muscle cells. **PLoS One**, v. 8, e75844, 2013.

LANGMEAD, B.; SALZBERG, S. L. Fast gapped-read alignment with Bowtie 2. **Nature Methods**, v. 9, p. 357-359, 2012.

LAUSCHOVA, I. Secretory cells and morphological manifestation of secretion in the mouse oviduct. **Scripta Medica (BRNO)**, v. 76, p. 203-214, 2003.

LESNIAK-WALENTYN A.; HRABIA A. Involvement of matrix metalloproteinases (MMP-2, -7, -9) and their tissue inhibitors (TIMP-2, -3) in the chicken oviduct regression and recrudescence. **Cell and Tissue Research**, v. 366, p. 443-454, 2016.

LI, H.; HANDSAKER, B.; WYSOKER, A.; FENNELL, T.; RUAN, J.; HOMER, N.; MARTH, G.; ABECASIS, G.; DURBIN, R. The Sequence Alignment/Map format and SAMtools. **Bioinformatics**, v. 25, p. 2078-2079, 2009.

LU, P.; TAKAI, K.; WEAVER, V. M.; WERB, Z. Extracellular matrix degradation and remodeling in development and disease. **Cold Spring Harbor perspectives in biology**, v. 3, a005058, 2011.

MAILLO, V.; DE FRUTOS, C.; O'GAORA, P.; FORDE, N.; BURNS, G. W.; SPENCER, T. E.; GUTIERREZ-ADAN, A.; LONERGAN, P.; RIZOS D. Spatial differences in gene expression in the bovine oviduct. **Reproduction**, v. 152, p. 37-46, 2016.

MAILLO, V.; GAORA, P. O.; FORDE, N.; BESENFELDER, U.; HAVLICEK, V.; BURNS, G. W.; SPENCER, T. E.; GUTIERREZ-ADAN, A.; LONERGAN, P.; RIZOS, D. Oviduct-Embryo Interactions in Cattle: Two-Way Traffic or a One-Way Street?. **Biology of Reproduction**, v. 92, p. 144, 2015.

MESQUITA, F. S.; PUGLIESI, G.; SCOLARI, S. C.; FRANCA, M. R.; RAMOS, R. S.; OLIVEIRA, M.; PAPA, P. C.; BRESSAN, F. F.; MEIRELLES, F. V.; SILVA, L. A.; NOGUEIRA, G. P.; MEMBRIVE, C. M.; BINELLI, M. Manipulation of the periovulatory sex steroidal milieu affects endometrial but not luteal gene expression in early diestrus Nelore cows. **Theriogenology**, v. 81, p. 861-869, 2014.

MESQUITA, F. S.; RAMOS, R. S.; PUGLIESI, G.; ANDRADE, S. C.; VAN HOECK, V.; LANGBEEN, A.; OLIVEIRA, M. L.; GONELLA-DIAZA, A. M.; GASPARIN, G.; FUKUMASU, H.; PULZ, L. H.; MEMBRIVE, C. M.; COUTINHO, L. L.; BINELLI, M.

The Receptive Endometrial Transcriptomic Signature Indicates an Earlier Shift from Proliferation to Metabolism at Early Diestrus in the Cow. **Biology of Reproduction**, v. 93, p. 52, 2015.

MULLEN, M. P.; ELIA, G.; HILLIARD, M.; PARR, M. H.; DISKIN, M. G.; EVANS, A. C.; CROWE, M. A. Proteomic characterization of histotroph during the preimplantation phase of the estrous cycle in cattle. **Journal of Proteome Research**, v. 11, p.3004-3018, 2012.

PERRY, G. A.; SWANSON, O. L.; LARIMORE, E. L.; PERRY, B. L.; DJIRA, G. D.; CUSHMAN, R. A. Relationship of follicle size and concentrations of estradiol among cows exhibiting or not exhibiting estrus during a fixed-time AI protocol. **Domestic Animal Endocrinology**, v. 48, p. 15-20, 2014.

PUGLIESI, G.; SANTOS, F. B.; LOPES, E.; NOGUEIRA, É.; MAIO, J. R.; BINELLI, M. Improved fertility in suckled beef cows ovulating large follicles or supplemented with long-acting progesterone after timed-AI. **Theriogenology**, v. 85, p. 1239-1248, 2016.

RIZOS, D.; FAIR, T.; PAPADOPOULOS, S.; BOLAND, M. P.; LONERGAN, P. Developmental, qualitative, and ultrastructural differences between ovine and bovine embryos produced *in vivo* or *in vitro*. **Molecular Reproduction and Development**, v. 62, p. 320-327, 2002a.

RIZOS, D.; LONERGAN, P.; BOLAND, M. P.; ARROYO-GARCIA, R.; PINTADO, B.; DE LA FUENTE, J.; GUTIERREZ-ADAN, A. Analysis of differential messenger RNA expression between bovine blastocysts produced in different culture systems: implications for blastocyst quality. **Biology of Reproduction**, v. 66, p. 589-595, 2002b:

RIZOS, D.; WARD, F.; DUFFY, P.; BOLAND, M. P.; LONERGAN, P. Consequences of bovine oocyte maturation, fertilization or early embryo development *in vitro* versus *in vivo*: implications for blastocyst yield and blastocyst quality. **Molecular Reproduction and Development**, v. 61, p. 234-248, 2002c.

RUIFROK, A. C.; JOHNSTON, D. A. Quantification of histochemical staining by color deconvolution. **Analytical and Quantitative Cytology and Histology**, v. 23, p. 291-299, 2001.

SA FILHO, M. F.; CRESPILHO, A. M.; SANTOS, J. E. P.; PERRY, G. A.; BARUSELLI, P. S., Ovarian follicle diameter at timed insemination and estrous response influence likelihood of ovulation and pregnancy after estrous synchronization with progesterone or progestin-based protocols in suckled Bos indicus cows. **Animal Reproduction Science**, v. 120, p. 23-30, 2010.

SIDDIQUI, M. A. R.; GASTAL, E. L.; GASTAL, M. O.; ALMAMUN, M.; BEG, M. A.; GINTHER, O. J. Relationship of vascular perfusion of the wall of the preovulatory follicle to *in vitro* fertilisation and embryo development in heifers. **Reproduction**, v. 137, p. 689-697, 2009.

TAIPALE, J.; KESKI-OJA, J. Growth factors in the extracellular matrix. **The FASEB Journal**, v. 11, p. 51-59, 1997.

TANAKA, H.; OHTSU, A.; SHIRATSUKI, S.; KAWAHARA-MIKI, R.; IWATA, H.; KUWAYAMA, T.; SHIRASUNA, K. Age-dependent changes in inflammation and extracellular matrix in bovine oviduct epithelial cells during the post-ovulatory phase. **Molecular Reproduction and Development**, v. 83, p. 815-826, 2016.

THYBERG, J.; HULTGARDH-NILSSON, A. Fibronectin and the basement membrane components laminin and collagen type IV influence the phenotypic properties of subcultured rat aortic smooth muscle cells differently. **Cell and Tissue Research**, v. 276, p. 263-271, 1994.

WANG, C. K.; ROBINSON, R. S.; FLINT, A. P. F.; MANN, G. E. Quantitative analysis of changes in endometrial gland morphology during the bovine oestrous cycle and their association with progesterone levels. **Reproduction**, v. 134, p. 365-371, 2007.

6 CHAPTER 4: STEROIDAL REGULATION OF OVIDUCTAL MICRORNAS IS ASSOCIATED WITH MODULATION OF THE MICRORNA-PROCESSING PATHWAY COMPONENTS

6.1 INTRODUCTION

Female sex-steroid hormones, such as estradiol and progesterone, play pivotal roles in the reproductive tract by allowing a proper environment for pregnancy establishment. They modulate the abundance of factors, such as extracellular matrix proteins, growth factors, cytokines, and sex-steroids receptors. Modulation is complex and follows spatio-temporal patterns that are not fully understood (SPENCER; BAZER, 1995; SHIMIZU *et al*., 2010; AKBALIK *et al*., 2011; SAGSOZ *et al*., 2011; ARAUJO *et al*., 2014; CERNY *et al*., 2015). A likely ingredient of such complex regulation is microRNA (miRNAs) modulation of gene expression. miRNAs are short non-coding RNAs (19-24 nucleotides in length in their mature form) that are involved in the control several aspects of cellular function. They act regulating protein translation by promoting messenger RNA (mRNA) degradation (DAVIS-DUSENBERY; HATA, 2010; OLIVETO *et al*., 2017). Based on computational prediction, it has been estimated that more than 60% of mammalian mRNAs could be targeted by at least one miRNA (FRIEDMAN *et al*., 2009). Similar to mRNAs, some miRNAs are differentially expressed (DE) among tissues, developmental stages, and diseases. Additionally, the miRNA biosynthesis and processing cellular machinery are also regulated by sex-steroids (DAVIS-DUSENBERY; HATA, 2010; NOTHNICK *et al*., 2010; COCHRANE *et al*., 2012; KLINGE, 2012). As a matter of fact, it has been shown that sex-steroids regulate the protein expression of DICER1, DROSHA, XPO5, and Argonaut (AGO) proteins in human breast cancer (CASTELLANO *et al*., 2009; COCHRANE *et al*., 2010) and endometrium (NOTHNICK *et al*., 2010).

Biogenesis of miRNAs starts with the transcription of a primary RNA transcript (pri-miRNA) from a specific gene. This pri-miRNA is processed to a precursor miRNA (pre-miRNA, 70–100 nucleotides) by a protein complex orchestrated by DROSHA (a class 2 RNAse III-type enzyme). Pre-miRNAs are then transported from the nucleus

to the cytoplasm through exportin-5 (XPO5). Next, DICER1 cleaves the pre-miRNA to the mature form of the miRNA. Mature miRNAs form an RNA-induced silencing complex (RISC) along with DICER1 and AGO proteins. RISC then binds target mRNA and regulates their translation by either cleaving or degrading the target transcript. This regulatory mechanism mediated by miRNAs has brought a new degree of complexity to the study of the regulation of cellular processes and has been proved to be essential for the proper functioning of cells and organisms. For instance, female mice with deletion of DICER1 in somatic cells of the reproductive tract (DICER1-cKO) are sterile. These DICER1-cKO females have decreased ovulation rates, compromised oocyte and embryo integrity, and presented defects in the oviducts and uterus (NAGARAJA *et al*., 2008). Despite the critical role of miRNAs on the regulation of reproductive processes, to the best of our knowledge, no reports that characterize miRNA population or miRNA biosynthesis machinery in the bovine oviduct have been published.

Therefore, in the present study, we evaluated two hypotheses regarding the periovulatory endocrine profile: (1) it affects the miRNA processing pathway and (2) it changes in the miRNAs expression profile in bovine oviductal tissues. We used an experimental model in which growth of the pre-ovulatory follicle (POF) is controlled. This model allowed us to obtain two groups of cows (large follicle and large corpus luteum, LF-LCL group; and small follicle and small corpus luteum, SF-SCL). These groups differ in the size of the POF and CL and, consequently, they also have differences in the periovulatory plasmatic concentrations of estradiol and progesterone. We have demonstrated previously that this manipulation of POF and CL size induces differences in P4 and E2 levels. Additionally in a previous study, we demonstrated that LF-LCL animals have a greater abundance of PGR and ERα in the oviduct suggesting greater sex-steroids-stimulated signaling (GONELLA-DIAZA *et al*., 2015). The main objective of the study was to establish if there was also a steroidal regulation of oviductal miRNAs expression in the oviduct of cattle.

6.2 MATERIALS AND METHODOLOGY

6.2.1 Animals and Reproductive Management

All animal procedures were approved by the Ethics and Animal Handling Committee of the college of veterinary (CEUA/FMVZ-USP; protocols numbers 2281-2011 and 4293160916). Experiments were carried out at the University of São Paulo, Pirassununga campus, State of São Paulo, Brazil. The hormonal manipulation procedures described here have been validated and published in previous studies (MESQUITA *et al*., 2014, 2015; GONELLA-DIAZA *et al*., 2015). To summarize, prior to starting the experiment, multiparous and non-lactating Nelore cows (*Bos indicus*) were selected, kept in grazing conditions (*Brachiaria brizantha* pasture), and supplemented with mineralized salt to fulfill their maintenance requirements. After a gynecological examination, cows were selected according to three criteria: no gross reproductive abnormalities, a body condition score between 3 and 4 (0, emaciated; 5, obese), and normal cyclic estrous activity (Presence of CL). Animals were randomly divided into two groups: large follicle and large CL group (LF-LCL) and small follicle and small CL group (SF-SCL). A total of 56 cows were presynchronized (Presynch) by two intramuscular injections of prostaglandin F2 alpha analog (PGF; 0.5 mg of sodium cloprostenol; Sincrocio, Ouro Fino, Cravinhos, Brazil), 14 days apart. Ten days after the second PGF injection, cows that had a fresh and PGF-responsive CL (at least 5 days old) were selected. Remaining animals were removed from the experiment. Cows (n = 41) received a new intravaginal P4- releasing device (1 g; Sincrogest, Ourofino) as well as 2 mg estradiol benzoate (EB; Sincrodiol, Ouro Fino Saude Animal) injected intramuscularly (im). Only cows in the LF-LCL group received an intramuscular injection of PGF. P4-releasing devices were removed prior to GnRH injection from LF-LCL (n=20) and the SF-SCL (n=21) cows. All animals received two PGF injections 6 hours apart at P4 device removal. The differential animal handling (PGF at P4 device insertion and timing of device removal) during the synchronization protocol was designed to enable animals of the LF-LCL group: 1) to develop a new follicular wave under a low P4 environment; and 2) to have more time to grow the

preovulatory follicle during the proestrus. In order to induce ovulation, a GnRH analogue (1 µg of buserelin acetate; Sincroforte, Ouro Fino Saude Animal) was administered (im) either 30 or 42 hours after removal of the P4 devices in SF-SCL groups and LF-LCL, respectively. Animals were slaughtered on Day 4 (Day 0 = treatment with GnRH). Throughout the experiment, animals were evaluated daily by transrectal ultrasonography in order to record follicular dynamics and luteal development.

6.2.2 Tissue Processing

Immediately after slaughter, the reproductive tract was transported on ice to the laboratory and the oviduct ipsilateral to CL was dissected. Samples from ampulla and isthmus were frozen in liquid nitrogen and stored at −80°C until RNA extraction.

6.2.3 RNA Extraction

Approximately 30 mg of tissue was macerated in liquid nitrogen using a stainless-steel apparatus and immediately homogenized in 200 µl of Trizol reagent (Invitrogen Life Technologies, Carlsbad, CA, USA). The homogenate was incubated for 5 min at room temperature to permit the complete dissociation of nucleoprotein complexes and then, 128 µl of chloroform were added. The homogenate was shaken vigorously for 3 min and incubated again for 5 min at room temperature. After incubation, the homogenate was centrifuged at 12000 x g for 15 min at 4°C. The aqueous phase was transferred to a fresh tube, 400 µl of isopropanol were added, and the tube was stored at -80°C overnight. Total RNA was precipitated by centrifugation at 18000g for 8 min at 4°C. The pellet was washed twice with 1 ml of 75% ethanol, dried under air at room temperature, and dissolved in 10 µl of diethylprocarbonate-treated water. Concentration and quality of total RNA was measured by a spectrophotometer (NanoDrop; Thermo Scientific, Wilmington, DE).

6.2.4 Reverse Transcription of mRNAs Molecules

Transcript abundance of miRNAs processing pathway-components was evaluated using qPCR. After total RNA extraction, 500 ng of RNA were reverse transcribed (High Capacity cDNA Reverse Transcription Kit, Life Technologies) according to manufacturer's instructions. Briefly, RNA was incubated at 25°C for 10 min, followed by incubation at 37°C for 2 h and reverse transcriptase inactivation at 85°C for 5 min and storage at −20°C. The cDNA obtained was used for gene expression assays by qPCR. Step-One Plus (Life Technologies, Carlsbad, CA) with SYBR Green Chemistry was used for transcript abundance analysis. Primers were designed based on GenBank Ref-Seq mRNA sequences of Drosha ribonuclease type III (DROSHA), Exportin 5 (XPO5), Dicer ribonuclease type III (DICER1), and AGO proteins (Argonaute RISC catalytic components [AGO1, AGO2, AGO3, and AGO4]). Sequences were masked to remove repetitive sequences with Repeat-Masker (http://www.repeatmasker.org/) and the masked sequences were used for primer design using the PrimerQuest software (IDT1, http://www.idtdna.com/primerquest/Home/Index). The characteristics of the primers were checked in Oligo Analyzer 3.1 software (IDT1, http://www.idtdna.com/analyzer/Applications/OligoAnalyzer/), while the specificity was compared by BLAST1 (NCBI, http://blast.ncbi.nlm.nih.gov). qPCR products from reactions containing designed primers were submitted to agarose gel electrophoresis and sequencing in order to confirm identities. Details of primers are provided on Table 6. LinRegPCR software (V2014.2; http://linregpcr.nl/) was employed to determine qPCR efficiency and Cq (quantification cycle) values per sample. Quantification was obtained after normalization of the target genes expression values (Cq values) by the geometric mean of the endogenous control expression values Cyclophilin A (PPIA) and Glyceraldehyde- 3-Phosphate Dehydrogenase (GAPDH).

Table 6 - Primer sequences and amplicon characteristics of transcripts from members of the miRNA biosynthesis machinery.

GenBank ID	Gene	Primer Sequence (5′–3′) Forward/Reverse	Amplicon Length (bp)	PCR Efficiency
XM_005196186.2	Drosha ribonuclease type III (DROSHA)	AAGGCAGTGCATGTCACAGAA GCTGGGAGGTTCGTATTGGT	170	
NM_203359.1	Dicer ribonuclease type III (DICER1)	TCACGATCAACACGGCCATTG TTGGGGGACCAACAATGGAG	177	
NM_001205899.1	Argonaute RISC catalytic component 1 (AGO1)	ATTGATGTCTCAGCCACTGCCT CTTGATCTCCTTGGTGAAGCGTAC	140	
NM_205794.1	Argonaute RISC catalytic component 2 (AGO2)	TTACAAGTCGGACAGGAGCAGA AGTCGCTCTGATCATGGTTGAG	121	
NM_001001133.1	Argonaute RISC catalytic component 3 (AGO3)	GGGCAGTTCAGGCAGGTATTA GTCTGTGTCCACCGTCGTT	197	
XM_002686552.4	Argonaute RISC catalytic component 4 (AGO4)	CATCAGTCTGTGAGACCTGCCAT TTGACACGCTGGGAGTCTGTTAG	163	
XM_002697301.3	Exportin 5 (XPO5)	AGGCTACATTGACTGGGTGC TCCAACTTGCCTTTCCTGCT	150	

Source: Gonella-Diaza (2017).

6.2.5 qPCR Analysis of miRNAs

Abundance of miRNAs was evaluated in two phases. First, the abundance of 348 miRNA, including 3 housekeeping miRNAs (RNT43 snoRNA, Hm/Ms/Rt T1 snRNA, and bta-miR-99b), was evaluated in the ampulla and isthmus regions, using a pool of samples from 6 animals of each of the two groups (LF-LCL and SF-SCL). Abundance was evaluated using “Bovine Profiler plates” containing specific primers designed using mature miRNA sequences downloaded from mirBase database (http://www.mirbase.org). Briefly, cDNA was synthesized from 200 ng of total RNA using the miScript Reverse Transcription Kit (Qiagen). Each reverse transcription (RT) reaction contained 1 µl of miScript Reverse Transcriptase Mix, 1 µl of 10x

miScript Nucleics Mix, 2µl of 5x miScript HiFlex Buffer, and RNase-free water, in order to complete 10 µl of total reaction volume. Tubes were incubated for 60 min at 37°C, and then for 5 min at 95°C to inactivate enzyme and were placed on ice. The miScript HiFlex Buffer was chosen because it permits the amplification of mature miRNA, pre-miRNA, and mRNA from the same reverse transcription reaction. Quantification of miRNAs was performed using the miScript SYBR Green PCR kit (Qiagen). PCR assays with specific primers for each miRNA and an universal reverse primer, were performed in 10 µl reactions and set up with an automated pipetting station (Hamilton Microlab 4200). Reactions without the addition of any specific primer were used as negative controls to verify no specific amplification. qPCR was conducted using the Step-One Plus (Life Technologies, Carlsbad, CA) PCR system with 96-well plates. The 10 µL PCR reaction contained 0,1 µl of RT product, 5 µl of 2 X QuantiTect SYBR Green PCR Master Mix, 1 µl of 10× miScript Universal Primer, 1 µl of specific forward primer, and 2,9 µl of RNase-free water. The qPCR cycle conditions were as follows: 95°C for 15 min, 45 cycles of 94°C for 15 sec, 55°C for 30 sec, and 70°C for 15 sec followed by a melt curve analysis. Relative expression was calculated from Ct values following the 2−ΔΔCt method (SCHMITTGEN; LIVAK, 2008) after normalization with the geometric mean of the housekeeping miRNAs (RNT43 snoRNA, Hm/Ms/Rt T1 snRNA, and bta-miR-99b).

In the second phase of the study, 88 miRNA were selected to study their expression in the individual ampulla and isthmus samples (n=5 animals per group) based on results from phase 1. In order to select miRNAs, the following criteria were established: 1) the Cq value (number of cycles it takes to detect a fluorescence signal above background) was ≤ 37 and 2) identification of a single (mature miRNA) or double (mature miRNA + pre-miRNA) peak in the meting curve. All the qPCR procedures were performed as described for step one.

6.2.6 Bioinformatics Analysis

Initially, the bovine sequence of the DE-miRNA and the human sequences (available in miRbase; SCHMITTGEN; LIVAK, 2008) were aligned using the Pairwise

Sequence Alignment algorithm of Clustal Omega (v. 1.2.3; GOUJON *et al*., 2010; MCWILLIAM *et al*., 2013; http://www.ebi.ac.uk/Tools/msa/clustalo/) at EMBL-EBI. Results of these alignments can be found in Appendix E. After confirming the bovine-human miRNAs homology, DIANA-mirPath (VLACHOS *et al*., 2015), a web-based computational tool developed to identify molecular pathways potentially altered by the expression of multiple miRNAs, was used to incorporate the DE-miRNAs into molecular pathways. The list of DE-miRNAs for each group and region was uploaded to the mirPath and the list of potentially regulated pathways was saved in Microsoft office Excel spreadsheets. Because there were a great number of regulated pathways, the most representative ones, according to their biological role, were selected.

6.2.7 Statistical Analysis

The experiment was conducted as a completely randomized design. All statistical analyses were performed using SAS computational software, version 9.3 for Microsoft Windows (SAS Institute Inc., Cary, NC). Concentrations of E2 and P4, follicle diameter, CL area, and transcript abundance of miRNAs processing pathway-components were analyzed by ANOVA using MIXED procedure of SAS. The model included the fixed effects of group, region and their interaction. Due to repeated measures within each cow (i.e. ampulla and isthmus), a repeated statement was used.

miRNA relative expression was calculated from Ct values after normalization with the geometric mean of housekeeping miRNAs and represented using the $2^{-\Delta Ct}$ method. To identify differential miRNA expression between LF-LCL and SF-SCL groups, t-test in an Excel Spreadsheet was performed. A significant difference between groups was considered when $P \leq 0.01$. All data will be shown from here on as mean ± standard error of mean.

6.3 RESULTS

6.3.1 Animal Model

Results from the animal model used here have been reported previously (GONELLA *et al*. 2015). The experimental model used was successful in creating two distinct groups of cows: LF-LCL and SF-SCL. As a result, follicle diameter and E2 plasma concentration on D-1 as well as CL area and P4 plasma concentration on D4 were 39%, 276%, 66% and, 75% greater for the LF-LCL compared to the SF-SCL group ($P < 0.01$), respectively.

6.3.2 Expression of miRNA Processing Pathway-components

In order to investigate the impact of the two different endocrine environments on the miRNAs abundance on the oviduct, we started by evaluating the levels of miRNA processing components. Transcripts abundance of miRNA processing pathway-components is located in Figure 15. DROSHA is the enzyme involved in processing pri-miRNA to pre-miRNA (DAVIS-DUSENBERY; HATA, 2010) and was increased in the SF-SCL group ($P = 0.04$) as well as in the ampulla of both groups ($P = 0.001$). XPO5 is a protein that exports pre-miRNAs from the nucleus to the cytoplasm (DAVIS-DUSENBERY; HATA, 2010), and was similarly expressed between groups and regions. DICER1 is an RNase responsible for pre-miRNAs cleavage producing double-stranded miRNAs (CARTHEW; SONTHEIMER, 2009). We identified a significant interaction group*region (P = 0.08) in DICER1 expression. This interaction reflected an abundance of 18.7 and 3.0 times higher in the ampulla and isthmus of SF-SCL group compared to LF-LCL group, respectively. The AGO family plays a catalytic role in the RNA-induced silencing complex (RISC) (CARTHEW; SONTHEIMER, 2009). Only a region effect was detected for AGO1 and AGO2, as represented by the greater abundance of AGO1 in the ampulla (8.3 fold; P

= 0.02) and AGO2 in the isthmus (4.2 fold; *P* = 0.01). For AGO4 a significant interaction of region by group (*P* = 0.03) was detected. The abundance of transcript was 2.1 times higher in ampulla than isthmus of the SF-SCL group and 1.2 times higher in isthmus than ampulla of the LF-LCL group. Finally, AGO3 transcript abundance was not influenced by group or region.

Figure 15 –Transcript abundance of genes involved in the miRNA biosynthetic machinery, expression normalized to Peptidylprolyl isomerase A (PPIA) and Glyceraldehyde 3-phosphate dehydrogenase (GAPDH) in the ampulla (AMP) and isthmus (IST) ipsilateral to the CL from beef cows synchronized to ovulate a large (LF-LCL) or a small follicle (SF-SCL) on day 4 of the estrous cycle. Mean ± SEM.

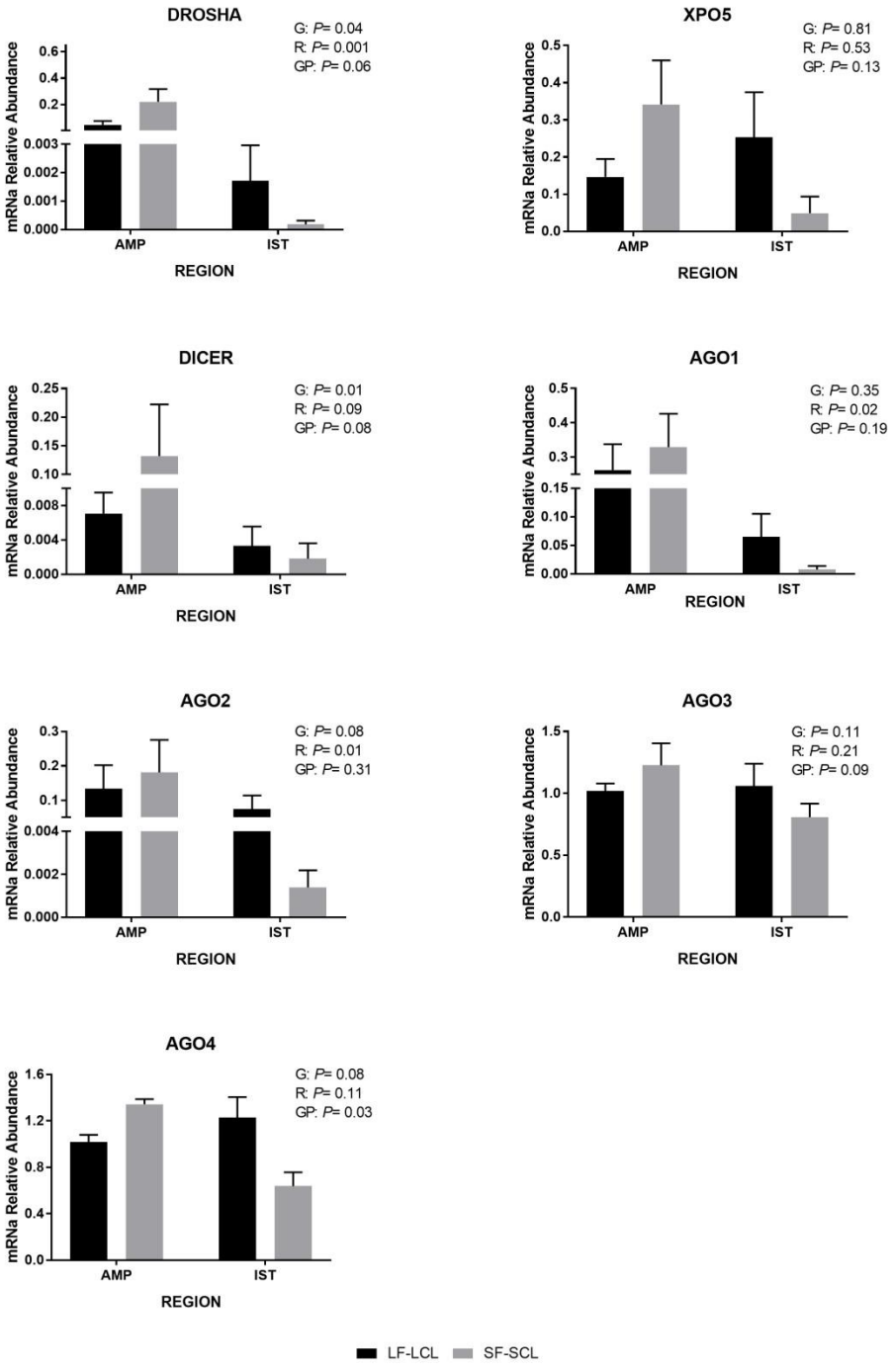

Source: Gonella-Diaza (2017).

Legend: Effect of Group (G), Region (R), and interaction of Group-by-Region (GR) are indicated. Genes: Drosha Ribonuclease III (DROSHA), Exportin 5 (XPO5), Dicer 1, Ribonuclease III (DICER), RISC Catalytic Components: Argonaute 1, 2, 3, and 4 (AGO1, AGO2, AGO3, AGO4).

6.3.3 miRNA Abundance Profiles in Ampulla and Isthmus.

In the ampulla, 78, 146, and 92 miRNAs showed low (Cq ≥ 30), intermediate (Cq ≥ 25 to 30), and high (Cq < 25) expression, respectively. In the isthmus 144, 104, and 18 miRNAs showed low, intermediate, and high expression (Appendix F). Additionally, 32 and 82 miRNAs were undetected in ampulla and isthmus, respectively (Figure 16). Moreover, 67 miRNAs were exclusively detected in the ampulla and 17 were exclusively detected in the isthmus, while 249 miRNAs were detected in both regions.

Figure 16 – Venn diagram indicating the microRNAs detected in the ampulla and isthmus or undetected in both regions.

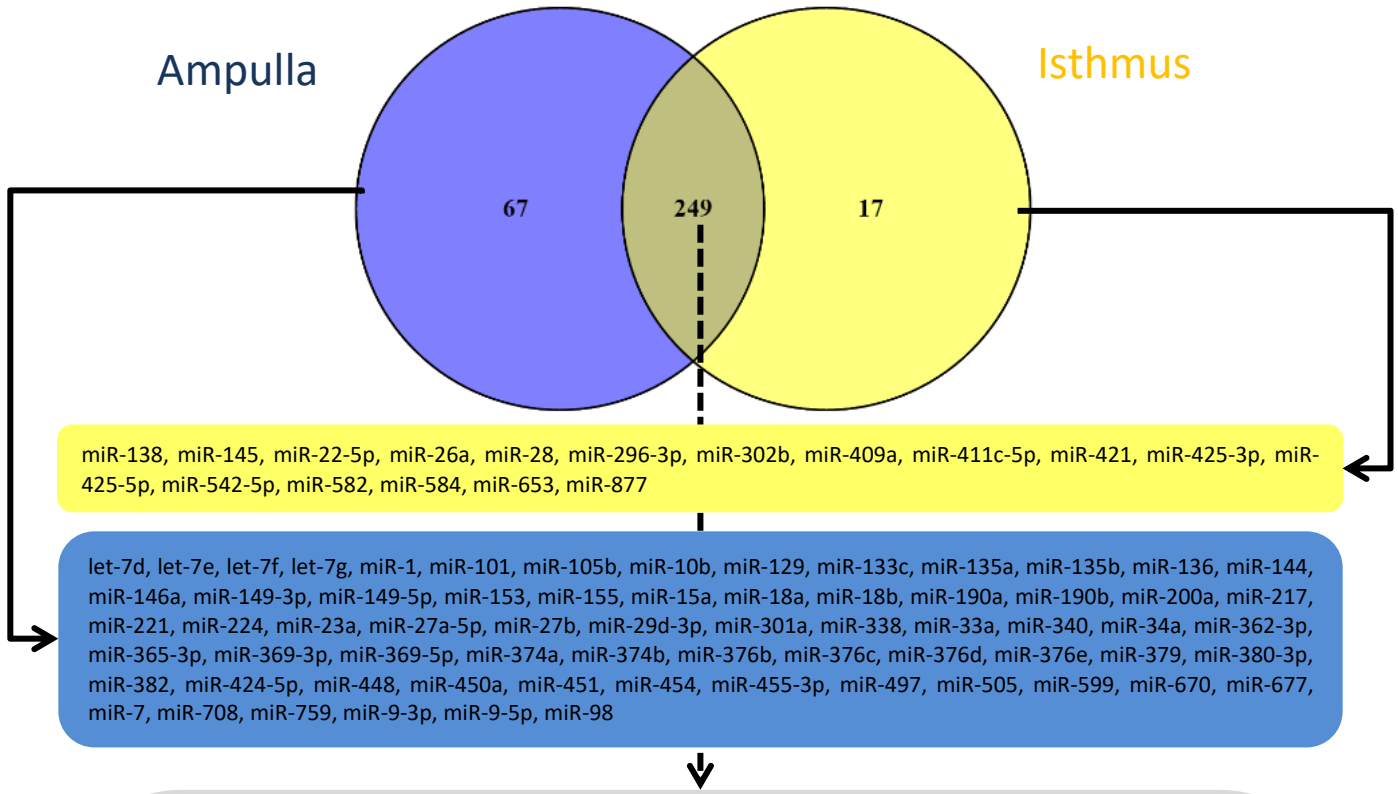

Source: Gonella-Diaza (2017).

6.3.4 miRNAs Abundance in LF-LCL and SF-SCL Groups.

The abundance of the 88 selected miRNAs was evaluated using individual samples of ampulla and isthmus. Volcano plots showing ampulla (n = 10) and isthmus (n = 10) miRNA abundance of LF/LCL and SF/SCL groups were constructed in terms of the differentially expressed miRNAs (Figure 17). For ampulla, 15 out of 88 miRNAs were DE (P < 0,01) between groups (Table 7). In the LF-LCL animals, 5 miRNAs were up-regulated (miR-106b, miR-200b, miR-375, miR-92a, and miR-99a-5p) and 9 were down-regulated (let-7b, miR-106a, miR-181d, miR-30c, miR-339b, miR-378, miR-631, miR-92b, and miR-940).

Figure 17 – Volcano Plot showing ampulla (Panel A; n = 10 samples) and isthmus (Panel B; n = 10 samples) microRNA abundance of LF/LCL and SF/SCL groups, in terms of the differentially expressed microRNAs ($p < 0.05$).

A.

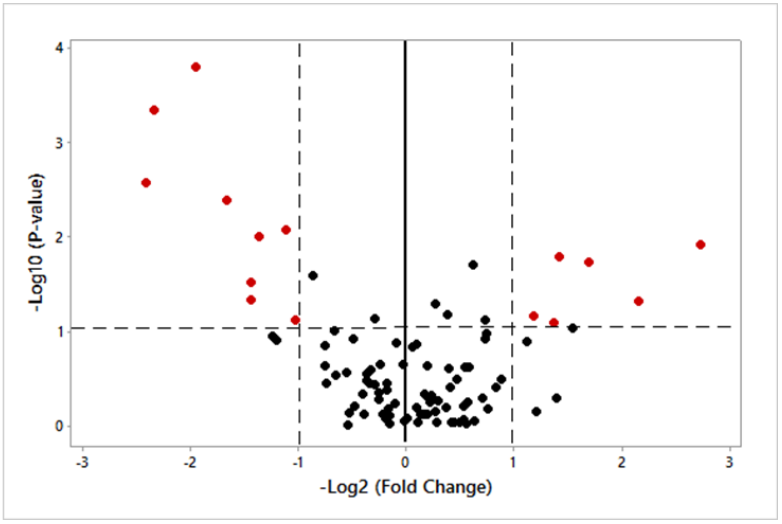

B.

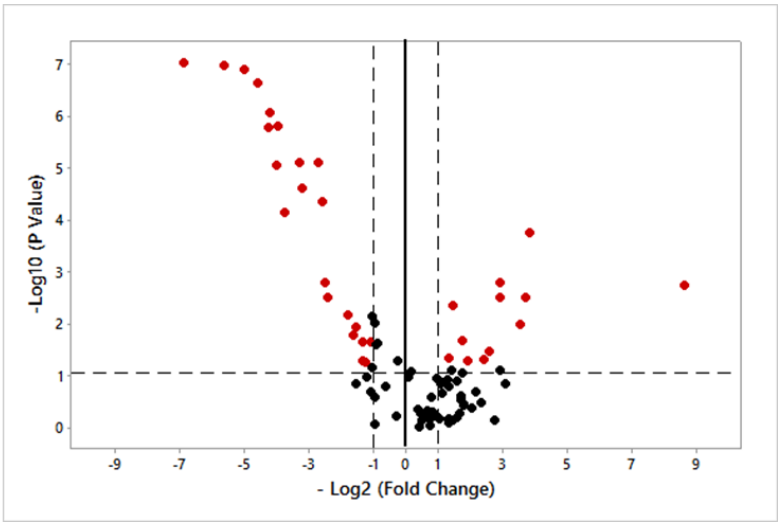

Source: Gonella-Diaza (2017).

Table 7 - Relative abundance of differentially expressed microRNAs in ampulla of LF-LCL and SF-SCL groups (n = 10).

microRNA	LF-LCL	SF-SCL	*P* value	Log2 (Fold Change)
let-7b	0.271 ± 0.046	1.052 ± 0.634	≤ 0.001	1.955
miR-106a	0.008 ± 0.002	0.020 ± 0.009	0.010	1.362
miR-106b	0.047 ± 0.038	0.015 ± 0.009	0.019	-1.692
miR-181d	0.028 ± 0.010	0.088 ± 0.058	0.004	1.668
miR-200b	0.193 ± 0.078	0.159 ± 0.025	0.042	-0.273
miR-30c	0.026 ± 0.005	0.056 ± 0.034	0.008	1.114
miR-339b	0.164 ± 0.053	0.301 ± 0.261	0.026	0.870
miR-375	0.241 ± 0.085	0.036 ± 0.013	0.012	-2.732
miR-378	0.046 ± 0.015	0.125 ± 0.107	0.031	1.448
miR-631	5.740 ± 2.225	15.586 ± 8.933	0.047	1.441
miR-92a	0.142 ± 0.068	0.032 ± 0.003	0.049	-2.150
miR-92b	0.521 ± 0.250	2.785 ± 2.683	0.003	2.417
miR-940	0.928 ± 0.414	4.714 ± 4.399	≤ 0.001	2.346
miR-99a-5p	0.200 ± 0.079	0.130 ± 0.020	0.020	-0.623

Source: Gonella-Diaza (2017).

Legend: Fold changes were the ratio of the mean expression values of SF-SCL/LF-LCL.

For the isthmus, 34 out of 88 miRNAs were DE ($P < 0,01$) between groups (Table 8). Of these DE-miRNAs, 12 were up-regulated (miR-106a, miR-122, miR-192, miR-193b, miR-378, miR-383, miR-423-5p, miR-425-3p, miR-431, miR-654, miR-671, and miR-769) and 22 were down-regulated (miR-125b, miR-132, miR-138, miR-143, miR-154b, miR-17-3p, miR-17-5p, miR-181b, miR-188, miR-193a-5p, miR-196b, miR-199a-3p, miR-200b, miR-211, miR-219, miR-30b-5p, miR-30d, miR-345-5p, miR-409b, miR-432, miR-532, and miR-631) in the LF-LCL animals.

Table 8 - Relative abundance of differentially expressed microRNAs in isthmus of LF-LCL and SF-SCL groups (n = 10).

microRNA	LF-LCL	SF-SCL	*P* value	Log2 (Fold Change)
miR-106a	0.038 ± 0.018	0.011 ± 0.004	0.020	-1.818
miR-122	1.838 ± 1.363	0.244 ± 0.153	0.002	-2.910
miR-125b	0.036 ± 0.007	0.239 ± 0.202	0.000	2.736
miR-132	0.393 ± 0.126	9.506 ± 9.013	0.000	4.598
miR-138	0.406 ± 0.144	13.037 ± 11.970	0.000	5.005
miR-143	0.317 ± 0.174	15.701 ± 15.104	0.000	5.628
miR-154b	0.297 ± 0.097	5.649 ± 5.003	0.000	4.247
miR-17-3p	0.022 ± 0.009	0.119 ± 0.096	0.003	2.454
miR-17-5p	0.147 ± 0.101	0.466 ± 0.425	0.017	1.661
miR-181b	0.017 ± 0.005	0.272 ± 0.215	0.000	3.961
miR-188	0.186 ± 0.049	0.372 ± 0.273	0.010	0.999
miR-192	0.230 ± 0.037	0.084 ± 0.002	0.004	-1.457
miR-193a-5p	0.111 ± 0.049	0.289 ± 0.192	0.022	1.375
miR-193b	0.050 ± 0.022	0.004 ± 0.002	0.003	-3.686
miR-196b	0.032 ± 0.011	0.296 ±0.253	0.000	3.222
miR-199a-3p	0.007 ± 0.002	0.822 ± 0.818	0.000	6.885
miR-200b	0.019 ± 0.009	0.307 ± 0.256	0.000	4.032
miR-211	0.048 ± 0.028	0.168 ± 0.152	0.007	1.818
miR-219	0.060 ± 0.019	0.590 ± 0.555	0.000	3.295
miR-30b-5p	0.028 ± 0.012	0.374 ± 0.365	0.000	3.754
miR-30d	0.119 ± 0.031	0.734 ± 0.587	0.000	2.620
miR-345-5p	0.597 ± 0.257	11.439 ± 11.292	0.000	4.260
miR-378	0.184 ± 0.068	0.025 ± 0.010	0.003	-2.892
miR-383	0.324 ± 0.151	0.130 ± 0.027	0.046	-1.318
miR-409b	0.021 ± 0.006	0.039 ± 0.032	0.025	0.925
miR-423-5p	0.210 ± 0.052	0.024 ± 0.013	0.047	-3.149
miR-425-3p	0.639 ± 0.180	0.109 ± 0.053	0.035	-2.556
miR-431	0.086 ± 0.036	0.026 ± 0.008	0.021	-1.743
miR-432	0.153 ± 0.038	0.327 ± 0.301	0.023	1.099
miR-532	0.352 ± 0.086	0.647 ± 0.593	0.024	0.877
miR-631	105.937 ± 28.771	316.714 ± 131.871	0.012	1.580
miR-654	0.386 ± 0.220	0.034 ± 0.019	0.011	-3.509
miR-671	0.023 ± 0.022	0.000 ± 0.000	0.002	-8.618
miR-769	1.896 ± 1.746	0.134 ± 0.112	0.000	-3.824

Source: Gonella-Diaza (2017).

Legend: Fold changes were the ratio of the mean expression values of SF-SCL/LF-LCL.

6.3.5 Molecular Pathways Altered in Ampulla and Isthmus of LF-LCL and SF-SCL Animals

In the ampulla region, a total of 61 and 63 pathways were enriched in LF-LCL and SF-SCL animals, respectively (Appendices G and H). Pathways related to cell cycle, lysine degradation, fatty acid biosynthesis, bacterial invasion of epithelial cells, TGF-beta, estrogen, ErbB, and Wnt signaling were commonly enriched in both groups. ERβ signaling pathway was only enriched in the LF-LCL animals while fatty acid metabolism and sphingolipid signaling pathways were enriched only in SF-SCL animals. For all the enriched pathways, the number of affected genes and the *P* value was always greater in the SF-SCL animals indicating a potentially greater miRNAs-mediated suppression of these cellular processes (Figure 18).

In the isthmus region, 70 and 69 pathways were predicted in the LF-LCL and SF-SCL groups, respectively (Appendices I and J). There were commonly enriched pathways between groups, namely cell cycle, ECM-receptor interaction, fatty acid biosynthesis, lysine degradation, bacterial invasion of epithelial cells, TGF-beta, estrogen, ERβ, ErbB, and Wnt signalization. Also, insulin, TNF, and VEGF signaling pathways were enriched in the SF-SCL animals. Similarly to the ampulla region, the number of affected miRNAs was greater in the SF-SCL animals (Figure 19).

Figure 18 – Number of genes (Panels A and B) and *P* value (Panels C and D) of selected KEGG pathways affected by putative targets of differentially expressed miRNAs in ampulla of LF-LCL (Panels A and C) and SF-SCL (Panels B and D) animals.

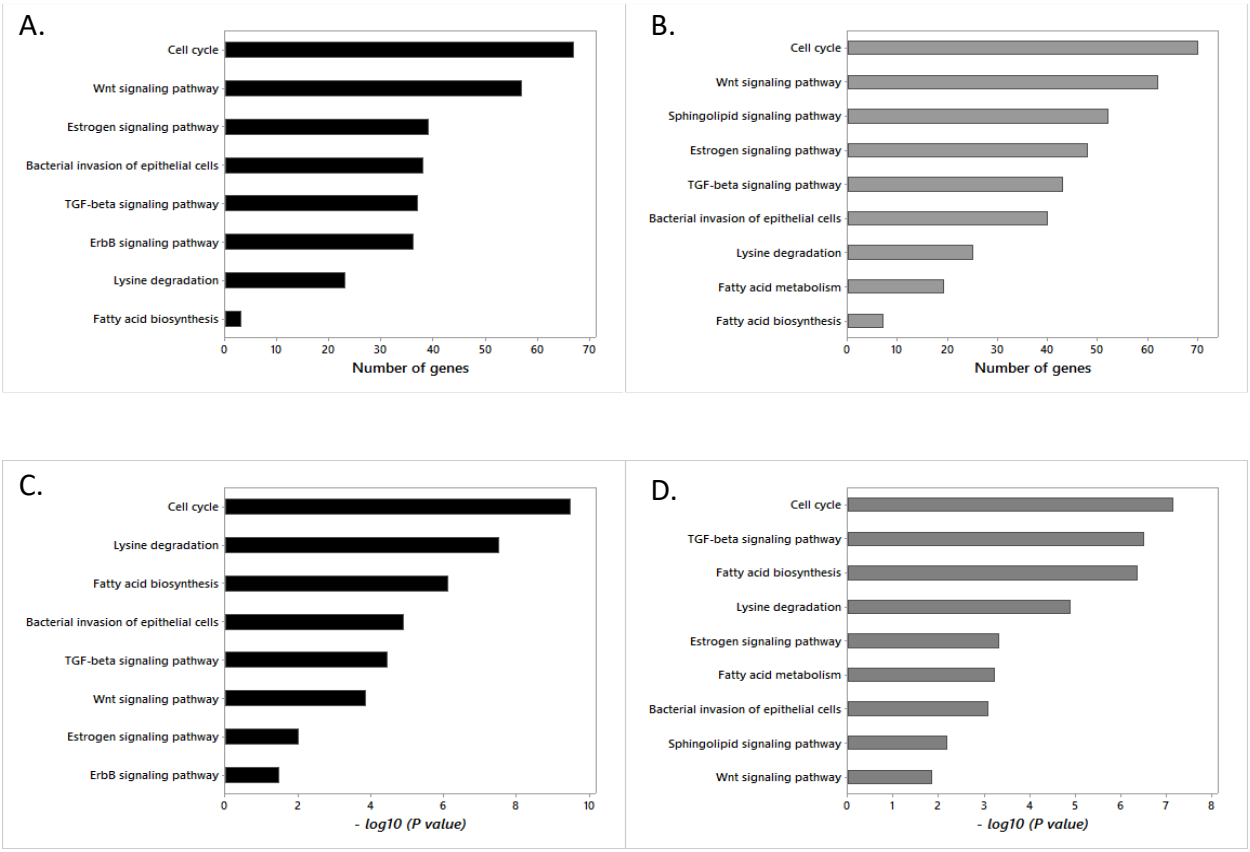

Source: Gonella-Diaza (2017).

Legend: Pathways were selected according to relevance to oviductal biology. The *P* values were transformed using negative Log10 to facilitate the visualization of the results.

Figure 19 – Number of genes (Panels A and B) and *P* value (Panels C and D) of selected KEGG pathways affected by putative targets of differentially expressed miRNAs in isthmus of LF-LCL (Panels A and C) and SF-SCL (Panels B and D) animals.

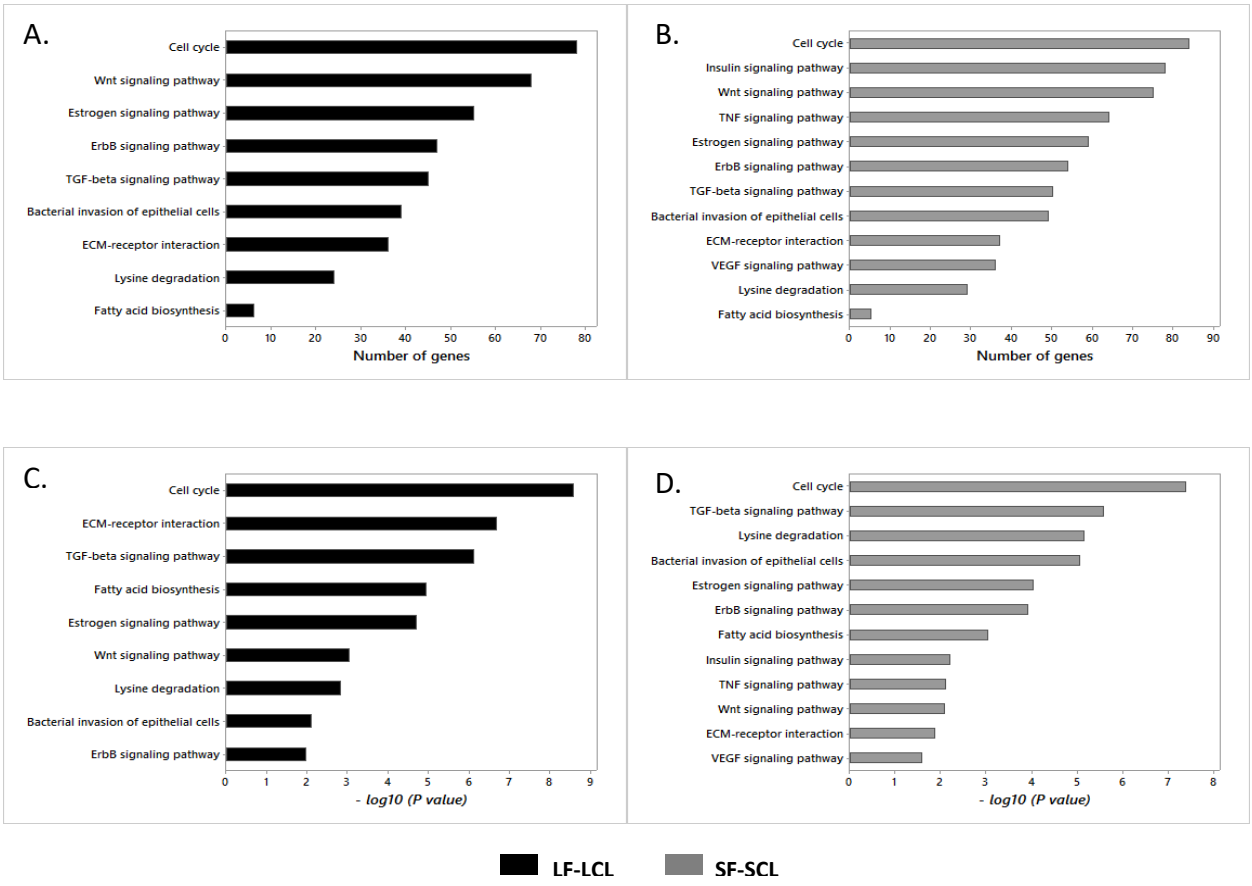

Source: Gonella-Diaza (2017).

Legend: Pathways were selected according to relevance to oviductal biology. The *P* values were transformed using negative Log10 to facilitate the visualization of the results.

6.4 DISCUSSION

In the present study, we tested the hypotheses that the periovulatory endocrine profile affects the miRNA processing pathway and change the miRNAs expression profile in bovine oviductal tissues. We used an experimental model in which the growth of the POF is controlled to generate two groups of cows (LF-LCL and SF-SCL) with distinct periovulatory endocrine profiles. The differences between groups were in the size of the POF and CL and in the pre-ovulatory estradiol and post-ovulatory progesterone concentrations. We also demonstrated that LF-LCL animals have a greater abundance of PGR and ERα in the oviduct thus indicating a

greater availability of receptors and possibly sex-steroid stimulated signaling in both regions (GONELLA-DIAZA *et al*., 2015). We showed previously sex-steroid-induced changes in the oviductal transcriptome (GONELLA-DIAZA *et al*., 2015). These changes were specific to the isthmus or the ampulla regions. Regional transcriptome differences are consistent with regional specializations. Indeed, these two oviductal regions present distinct morphological (CIGANKOVA *et al*., 1996; AYEN *et al*., 2012; GONELLA-DIAZA *et al*., 2017), cellular (BROWER; ANDERSON, 1969; ABE, 1996; ITO *et al*., 2016), molecular (GONELLA-DIAZA, A. M. *et al*., 2015; MAILLO *et al*., 2016), and functional (HUNTER, 1998, 2012; KOLLE *et al*., 2009) characteristics. The ampulla is the site of fertilization characterized by a prominent presence of secretory cells, while the isthmus, the caudal end of the oviduct, is important for embryo transport an early development and is equiped with a large population of ciliated cells (HUNTER, 1998). Regulation of transcription is complex and include the active participation of miRNAs. Therefore, we aimed to study the sex-steroidal regulation of oviductal miRNAs expression in cattle. Since their discovery, miRNAs have added another degree of complexity to the study of how cells regulate their gene expression and their functioning (DAVIS-DUSENBERY; HATA, 2010; VAN ROOIJ, 2011). miRNAs present differential transcriptional profiles in specific tissues, developmental stages, and diseases (OLIVETO *et al*., 2017). Indeed, in the last few years, many studies have focused in the use of miRNAs as potential biomarkers for physiologic and pathologic conditions (WANG *et al*., 2013; CORREIA *et al*., 2017; HAJIZAMANI *et al*., 2017). In the present study, we used a qPCR-based screening of 348 miRNAs to identify a regional signature of miRNA abundance in the oviduct. As it was expected, we characterized sex-steroid-induced changes in the oviductal miRNAome. Furthermore, we discovered specific miRNAs only expressed in the ampulla or isthmus showing that the functional differences of these two regions could be regulated by miRNAs.

Sex-steroids regulate the expression of miRNA-processing pathway components in the oviduct of cattle (COCHRANE *et al*., 2010; KLINGE, 2012). Specifically, abundance of DROSHA, DICER1, AGO1, and AGO2 were up-regulated in the ampulla compared to the isthmus, while XPO5, AGO3, and AGO4 were not affected by region effect. Cochrane *et al*. (2010) showed that miRNAs are differentially expressed in ERα+ and ERα− breast cancers (human cells) and that

miRNAs control the expression and functioning of several genes such as ERα itself, DICER1, and some growth factor receptors. Additionally, Nothnick *et al*. (2010) concluded that sex-steroids could modulate miRNA expression in two different ways. First, sex-steroids could affect miRNA at the transcription level, possibly by direct binding with hormone response elements that have been identified in specific miRNAs promoter regions (BHAT-NAKSHATRI *et al*., 2009). Second, sex-steroids could influence miRNA expression through regulation of the miRNA processing machinery. In the present study, the abundance of DROSHA, DICER1, and AGO4 was greater in SF-SCL than in LF-LCL suggesting a collectively greater inhibition of transcription associated with the ovulation of a smaller follicle. This is the first time that control of the miRNA-processing components mediated by sex-steroids has been shown in cattle, and specifically in the female reproductive tract. Moreover, in the present study, 15 miRNAs in ampulla and 34 miRNAs in isthmus were differentially expressed between LF-LCL and SF-SCL animals, respectively. Based on these results it is tempting to speculate that miRNA abundance is affected by the periovulatory endocrine milieu, at least partly due to effects modulating the expression of the miRNA processing pathway.

Using bioinformatics tools, a series of enriched pathways regulated by DE-miRNAs were described in ampulla and isthmus of both groups. These pathways have important biological roles controlling oviductal processes. In all cases, enriched pathways predicted by DE miRNAs of SF-SCL appear to have an increased suppression of a larger number of genes and a higher *P* value showing that in these animals this molecular process could be inhibited. These results are consistent with those of previous studies. For instance, Gonella *et al*. (GONELLA-DIAZA *et al*., 2017) showed that SF-SCL animals have less Ki67 positive cells (marker for cellular proliferation) in the oviductal epithelium than LF-LCL animals. In the present study, SF-SCL animals also have a large number of genes potentially suppressed on the cell cycle pathway. Moreover, tissues from the SF-SCL group have less immunostaining for ERα (GONELLA-DIAZA *et al*., 2015). In the current study, this group showed a greater number of suppressed genes in the estrogen signaling pathway. Although further studies are necessary to clarify the roles of miRNA in the oviductal function, it is clear that control differs in animals subjected to different periovulatory milieus.

In conclusion, the oviductal miRNA-synthesizing machinery and miRNAome are controlled by the peri-ovulatory sex-steroid milieu in a complex and regionally-specific way.

6.5 REFERENCES

ABE, H. The mammalian oviductal epithelium: Regional variations in cytological and functional aspects of the oviductal secretory cells. **Histology and Histopathology**, v. 11, p. 743-768, 1996.

AKBALIK, M.E.; SAGSOZ, H.; SARUHAN, B.G. Localization of Estrogen Receptor Alpha and Progesterone Receptor B in the Bovine Ovary During the Follicular and Luteal Phase of the Sexual Cycle. **Kafkas Universitesi Veteriner Fakultesi Dergisi**, v. 17, p. 795-802, 2011.

ARAUJO, E.R.; SPONCHIADO, M.; PUGLIESI, G.; VAN HOECK, V.; MESQUITA, F. S.; MEMBRIVE, C. M.; BINELLI, M. Spatio-specific regulation of endocrine-responsive gene transcription by periovulatory endocrine profiles in the bovine reproductive tract. **Reproduction, Fertility and Development**, v. 28, n. 10, p. 1533-1544, 2014.

AYEN, E.; SHAHROOZ, R.; KAZEMIE, S. Histological and histomorphometrical changes of different regions of oviduct during follicular and lutealphases of estrus cycle in adult Azarbaijan buffalo. **Iranian Journal of Veterinary Research**, v. 13, p. 42-48, 2012.

BHAT-NAKSHATRI, P.; WANG, G.; COLLINS, N.R.; THOMSON, M.J.; GEISTLINGER, T.R.; CARROLL, J.S.; BROWN, M.; HAMMOND, S.; SROUR, E.F.; LIU, Y.; NAKSHATRI, H. Estradiol-regulated microRNAs control estradiol response in breast cancer cells. **Nucleic Acids Research**, v. 37, p. 4850-4861, 2009.

BROWER, L.; ANDERSON, E. Cytological Events Associated with the Secretory Process in the Rabbit Oviduct. **Biology of Reproduction**, v. 1, p. 130-148, 1969.

CARTHEW, R.W.; SONTHEIMER, E.J. Origins and Mechanisms of miRNAs and siRNAs. **Cell**, v. 136, p. 642-655, 2009.

CASTELLANO, L.; GIAMAS, G.; JACOB, J.; COOMBES, R.C.; LUCCHESI, W.; THIRUCHELVAM, P.; BARTON, G.; JIAO, L.R.; WAIT, R.; WAXMAN, J.; HANNON, G.J.; STEBBING, J. The estrogen receptor-alpha-induced microRNA signature regulates itself and its transcriptional response. **Proceedings of the National Academy of Sciences of the United States of America**, v. 106, n. 37, p. 15732-15737, 2009.

CERNY, K.L.; GARRETT, E.; WALTON, A.J.; ANDERSON, L.H.; BRIDGES, P.J. A transcriptomal analysis of bovine oviductal epithelial cells collected during the follicular phase versus the luteal phase of the estrous cycle. **Reproductive Biology and Endocrinology**, v. 13, p. 84, 2015.

CIGANKOVA, V.; KRAJNICAKOVA, H.; KOKARDOVA, M.; TOMAJKOVA, E. Morphological changes in the ewe uterine tube (oviduct) epithelium during puerperium. **Veterinarni Medicina**, v. 41, p. 339-346, 1996.

COCHRANE, D.R.; CITTELLY, D. M.; HOWE, E.N.; SPOELSTRA, N.S.; MCKINSEY, E.L.; LAPARA, K.; ELIAS, A.; YEE, D.; RICHER, J.K. MicroRNAs link estrogen receptor alpha status and Dicer levels in breast cancer. **Hormones and Cancer**, v. 1 p. 306-319, 2010.

COCHRANE, D.R.; SPOELSTRA, N.S.; RICHER, J.K. The role of miRNAs in progesterone action. **Molecular and Cellular Endocrinology**, v. 357, p. 50-59, 2012.

CORREIA, C.N.; NALPAS, N.C.; MCLOUGHLIN, K.E.; BROWNE, J.A.; GORDON, S.V.; MACHUGH, D.E.; SHAUGHNESSY, R.G. Circulating microRNAs as Potential Biomarkers of Infectious Disease. **Frontiers in Immunology**, v. 8, p. 118, 2017.

DAVIS-DUSENBERY, B.N.; HATA, A. Mechanisms of control of microRNA biogenesis. **Journal of Biochemistry**, v. 148, p. 381-392, 2010.

FRIEDMAN, R.C.; FARH, K.K.; BURGE, C.B.; BARTEL, D.P. Most mammalian mRNAs are conserved targets of microRNAs. **Genome Research**, v. 19, p. 92-105, 2009.

GONELLA-DIAZA, A.M.; ANDRADE, S.C.; SPONCHIADO, M.; PUGLIESI, G.; MESQUITA, F.S.; VAN HOECK, V.; STREFEZZI, R.F.; GASPARIN, G.; COUTINHO, L.L.; BINELLI, M. Size of the Ovulatory Follicle Dictates Spatial Differences in the Oviductal Transcriptome in Cattle. **PLoS One**, v. 10, p. e0145321, 2015.

GONELLA-DIAZA, A.M.; MESQUITA, F.S.; DA SILVA, K.R.; DE CARVALHO BALIEIRO, J.C.; DOS SANTOS, N.P.; PUGLIESI, G.; STREFEZZI, R.F.; BINELLI, M. Sex Steroids Modulate Morphological and Functional Features of the Bovine Oviduct. **Submitted to Cell and Tissue Research**, 2017.

GOUJON, M.; MCWILLIAM, H.; LI, W.; VALENTIN, F.; SQUIZZATO, S.; PAERN, J.; LOPEZ, R. A new bioinformatics analysis tools framework at EMBL-EBI. **Nucleic Acids Research**, v. 38, p. W695-699, 2010.

HAJIZAMANI, S.; SHAHJAHANI, M.; SHAHRABI, S.; SAKI, N. MicroRNAs as prognostic biomarker and relapse indicator in leukemia. **Clinical and Translational Oncology**. doi: 10.1007/s12094-017-1638-x. 2017.

HUNTER, R.H. Have the Fallopian tubes a vital role in promoting fertility? **Acta Obstetricia et Gynecologica Scandinavica**, v. 77, p. 475-486, 1998.

HUNTER, R.H. Components of oviduct physiology in eutherian mammals. **Biological reviews of the Cambridge Philosophical Society**, v. 87, p. 244-255, 2012.

ITO, S.; KOBAYASHI, Y.; YAMAMOTO, Y.; KIMURA, K.; OKUDA, K. Remodeling of bovine oviductal epithelium by mitosis of secretory cells. **Cell and Tissue Research**, v. 366, p. 403-410, 2016.

KLINGE, C.M. miRNAs and estrogen action. **Trends in Endocrinology and Metabolism**, v. 23, p. 223-233, 2012.

KOLLE, S.; DUBIELZIG, S.; REESE, S.; WEHREND, A.; KONIG, P.; KUMMER, W. Ciliary Transport, Gamete Interaction, and Effects of the Early Embryo in the Oviduct: Ex Vivo Analyses Using a New Digital Videomicroscopic System in the Cow. **Biology of Reproduction**, v. 81, p. 267-274, 2009.

MAILLO, V.; DE FRUTOS, C.; O'GAORA, P.; FORDE, N.; BURNS, G.W.; SPENCER, T.E.; GUTIERREZ-ADAN, A.; LONERGAN, P.; RIZOS, D., Spatial differences in gene expression in the bovine oviduct. **Reproduction**, 152 37-46. 2016:

MCWILLIAM, H.; LI, W.; ULUDAG, M.; SQUIZZATO, S.; PARK, Y.M.; BUSO, N.; COWLEY, A.P.; LOPEZ, R. Analysis Tool Web Services from the EMBL-EBI. **Nucleic Acids Research**, 41 W597-600. 2013:

MESQUITA, F.S.; PUGLIESI, G.; SCOLARI, S.C.; FRANCA, M.R.; RAMOS, R.S.; OLIVEIRA, M.; PAPA, P.C.; BRESSAN, F.F.; MEIRELLES, F.V.; SILVA, L.A.; NOGUEIRA, G.P.; MEMBRIVE, C.M.; BINELLI, M. Manipulation of the periovulatory sex steroidal milieu affects endometrial but not luteal gene expression in early diestrus Nelore cows. **Theriogenology**, 81 861-869. 2014:

MESQUITA, F.S.; RAMOS, R.S.; PUGLIESI, G.; ANDRADE, S.C.; VAN HOECK, V.; LANGBEEN, A.; OLIVEIRA, M.L.; GONELLA-DIAZA, A.M.; GASPARIN, G.; FUKUMASU, H.; PULZ, L.H.; MEMBRIVE, C.M.; COUTINHO, L.L.; BINELLI, M., The Receptive Endometrial Transcriptomic Signature Indicates an Earlier Shift from Proliferation to Metabolism at Early Diestrus in the Cow. **Biology of Reproduction**, 93 52. 2015:

NAGARAJA, A.K.; ANDREU-VIEYRA, C.; FRANCO, H.L.; MA, L.; CHEN, R.; HAN, D.Y.; ZHU, H.; AGNO, J.E.; GUNARATNE, P.H.; DEMAYO, F.J.; MATZUK, M.M. Deletion of Dicer in somatic cells of the female reproductive tract causes sterility. **Molecular Endocrinology**, 22 2336-2352 2008.

NOTHNICK, W.B.; HEALY, C.; HONG X. Steroidal regulation of uterine miRNAs is associated with modulation of the miRNA biogenesis components Exportin-5 and Dicer1. **Endocrine**, 37 265-273. 2010:

OLIVETO, S.; MANCINO, M.; MANFRINI, N.; BIFFO, S. Role of microRNAs in translation regulation and cancer. World. **Journal of Biological Chemistry**, 8 45-56. 2017:

SAGSOZ H.; AKBALIK M. E.; SARUHAN B. G.; KETAI, M.A. Localization of estrogen receptor alpha and progesterone receptor B in bovine cervix and vagina during the follicular and luteal phases of the sexual cycle. **Biotechnic & Histochemistry**, 86 262-271. 2011:

SCHMITTGEN, T.D.; LIVAK, K.J. Analyzing real-time PCR data by the comparative C(T) method. **Nature Protocols**, 3 1101-1108. 2008:

SHIMIZU, T.; KREBS, S.; BAUERSACHS, S.; BLUM, H.; WOLF, E.; MIYAMOTO, A. Actions and interactions of progesterone and estrogen on transcriptome profiles of the bovine endometrium. **Physiological Genomics**, 42A 290-300. 2010:

SPENCER, T.E.; BAZER, F.W., Temporal and spatial alterations in uterine estrogen-receptor and progesterone-receptor gene-expression during the estrous-cycle and early-pregnancy in the ewe. **Biology of Reproduction**, 53 1527-1543. 1995:

VAN ROOIJ, E. The Art of MicroRNA Research. **Circulation Research**, 108 219-234. 2011:

VLACHOS, I.S.; ZAGGANAS, K.; PARASKEVOPOULOU, M.D.; GEORGAKILAS, G.; KARAGKOUNI, D.; VERGOULIS, T.; DALAMAGAS, T.; HATZIGEORGIOU, A.G.,

DIANA-miRPath v3.0: deciphering microRNA function with experimental support. **Nucleic Acids Research**, 43 W460-466. 2015:

WANG, X.; GU, Z.; JIANG H. MicroRNAs in farm animals. **Animal**, 7 1567-1575. 2013:

7 CHAPTER 5: THE PERIOVULATORY ENDOCRINE MILIEU AFFECTS THE COMPOSITION OF THE OVIDUCTAL FLUID IN BEEF COWS - Preliminary Results

7.1 INTRODUCTION

In cattle, important reproductive processes take place in the oviductal lumen: sperm transport and capacitation, fertilization, early embryo development and transport. An adequate oviductal microenvironment is essential for all these processes to occur successfully (BUHI *et al*., 2000). The oviductal microenvironment is composed by molecules secreted by the luminal epithelium and molecules selectively transported from blood plasma (AVILES *et al*., 2010; HUNTER 2012). Our working hypothesis is that success of processes that occur in the oviductal lumen depends on the nature and quantity of molecules that comprise the luminal microenvironment. However, regulation of the biochemical composition of the uterine fluid is poorly studied. For example, it is known that sex-steroids affect function and morphology of oviductal epithelial cells (BUHI *et al*., 1992; BINELLI *et al*., 1999), but nature and concentration of specific molecules regulated by these hormones are not clear. In Chapters 2 and 3 of the present Thesis, it was reported that the size of the preovulatory follicle modulates both the oviductal transcriptome and morphology, respectively. Regarding the transcriptome, it is reasonable to assume that changes in transcription will lead to changes in oviductal molecular composition and activity, and these changes will ultimately modify the composition of secretions in the uterine lumen. Regarding Morphology, cows ovulating larger follicles have a greater proportion of secretory cells and a larger epithelial area in the ampulla compared to cows ovulating smaller follicles. This result supports the notion of a greater overall secretory capacity in this group of cows. The hypothesis of this study is that the size of the preovulatory follicle modulates the periovulatory endocrine milieu affecting the composition of the oviductal fluid.

7.2 MATERIALS AND METHODOLOGY

7.2.1 Animals and Reproductive Management

Animal procedures were approved by the Ethic Committee on Animal Use of the School of Veterinary Medicine and Animal Science of the University of São Paulo (CEUA/FMVZ; protocols numbers 2281-2011 and 4293160916). The experiments were conducted at the University of São Paulo (Pirassununga campus, State of São Paulo, Brazil). The hormonal manipulation was performed as described previously (MESQUITA *et al*., 2014; GONELLA-DIAZA *et al*., 2015) and aimed to obtain cows ovulating smaller [Small Follicle-Small CL group (SF-SCL)] or larger [Large Follicle-Large CL group (LF-LCL)] follicles. As a result, in addition to differences in the follicular size, these experimental groups differ in their periovulatory endocrine milieus with distinct proestrus/estrus concentrations of E2 and metaestrus concentrations of P4, as well as differences in receptivity and fertility (PUGLIESI *et al*., 2016; MESQUITA *et al*., 2014, 2015; GONELLA-DIAZA *et al*., 2015, 2017).

7.2.2 Oviductal Fluid Collection and Storage

On D4 of the estrous cycle (day 0 = injection of GnRH to induce ovulation), cows were stunned by a captive bolt and slaughtered by jugular exsanguination in the campus abattoir. The complete reproductive tract was collected and immediately transported on ice to the laboratory (5 minutes approximately). The ovary containing the CL was identified and the oviduct ipsilateral to the ovary bearing the CL was dissected. The oviductal lumen was washed with 2 ml of sterile PBS for the removal of oviductal fluid. A syringe attached to a sterile tip was inserted through the infundibulum and the fluid was recovered by the opposite end (uterus-tubal junction). A gentle massage was performed on the oviduct to direct the PBS to the caudal end

of the organ. The fluid was centrifuged (7000 g, 10 min, 4 ° C) for removal of cells and debris. Afterward, the supernatant was stored in a sterile cryotube, frozen in liquid Nitrogen, and storage at -80°C for further analysis.

7.2.3 Metabolite, Prostaglandins, and Related Compounds Measurements in Oviductal Fluid

Oviductal fluid samples (n = 7 per group) were processed in the Biocrates INC laboratory (Innsbruck, Austria) for the quantification of metabolites, eicosanoids and prostaglandins. The experimental metabolomics measurement technique is described in detail by patent US 2007/0004044 (accessible online at http://www.freepatentsonline.com/20070004044.html). For the quantification of concentrations of metabolites, we employed the commercial Biocrates q180 Assay. This essay quantifies amino acids, biogenic amines, acylcarnitines, lysophosphatidylcholines, phosphatidylcholines, sphingomyelins, and hexoses. A complete list of metabolites quantified is provided in Appendices K to P. The fully automated essay is based on derivatization of PITC (phenylisothiocyanate) in the presence of internal standards followed by FIA-MS / MS (acylcarnitines, lysophosphatidylcholines, phosphatidylcholines, sphingomyelins, and hexoses) and LC-MS / MS (amino acids). SCIEX 4000 QTRAP® equipment (SCIEX, Darmstadt, Germany) and ThermoFisher Scientific Waltham USA with electrospray ionization (ESI) were used for the analyses. Results are provided as individual metabolite concentration in micromolar (µM).

Analyses of prostaglandins and related compounds were performed as described previously by Unterwurzacher *et al*., (2008). Briefly, eicosanoids and other oxidized polyunsaturated fatty acids were extracted from 20 µl of oviductal fluid with a methanolic protein precipitating solution. The analysis was performed by the SPE-HPLC-MS/MS on a SCIEX 5500 QTRAP™ (AP SCIEX, Darmstadt, Germany) instrument. Detection was carried out in multiple reaction monitoring (MRM) mode using negative electrospray ionization (ESI). Several deuterated eicosanoids and polyunsaturated fatty acid metabolites were used as internal standards. Quantitation was performed with a seven point calibration. The use of three levels of quality

controls ensures a consistent high-quality analysis. The results are showed as analyte concentration in nanomolar (nM).

7.2.4 Statistical Analyses

Biocrates had no access to phenotype or experimental group information that would have permitted any data pre-filtering other than objective quality control for measurement errors based on internal controls and duplicates. All metabolomic data was used as received from Biocrates. We neither applied any data correction, nor removed any data points. Initially, multivariate analyses were performed with two objectives: to identify which metabolites explain the separation of experimental groups and which could be potentially used as markers of fertility. These analyses were performed using the Web server MetaboAnalyst 3.0 (www.metaboanalyst.ca; XIA; WISHART, 2011, 2016). Variables with 50% or more of missing data were excluded from analyses. Preanalysis filtering was then performed based on the interquartile range to remove outlier values. Data was then normalized by the sample median, log transformed, and scaled by the auto scaling method. Partial Least Squares Discriminant Analysis (PLS-DA) was used to create a Scores plot between the two groups and to identify the most important explanatory variables.

Next, univariate analyses of the metabolite composition were performed using SAS for Windows (SAS 9.3 Institute Inc., Cary, NC, USA, 2003). After evaluating the fulfillment of the statistical assumptions, SAS PROC MIXED was used to evaluate mean differences between the LF-LCL and the SF-SCL groups and to calculate the interclass correlation coefficient. Significant statistical effects were considered when $P < 0.10$. Graphs were plotted with Minitab® 17.1.0 Minitab Inc., PA, USA.

7.3 RESULTS

7.3.1 Multivariate Analyses

The PLS-DA score plot showed that the overall metabolite profiles of the LF-LCL and SF-SCL groups are significantly different and that samples from each group were divided clearly into two non-overlapping clusters. Additionally, the most influential variables to separate the two groups, identified by the PLS-DA, were: PC ae C364, Leu, lysoPC a C160, AA, C121, PC aa C240, PC ae C421, PC aa C366, C18, and Glu.

Figure 20 – PLS-DA score plot of the metabolic profiles in the oviductal fluid of the LF-LCL and SF-SCL groups.

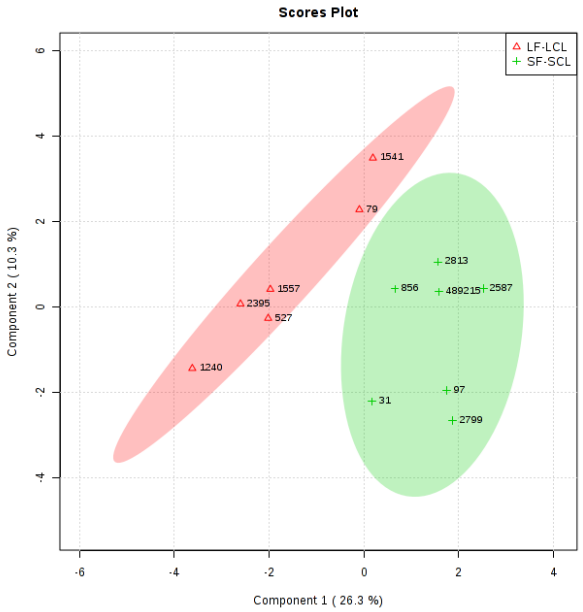

Source: Gonella-Diaza (2017).

Figure 21 – Important variables identified by PLS-DA.

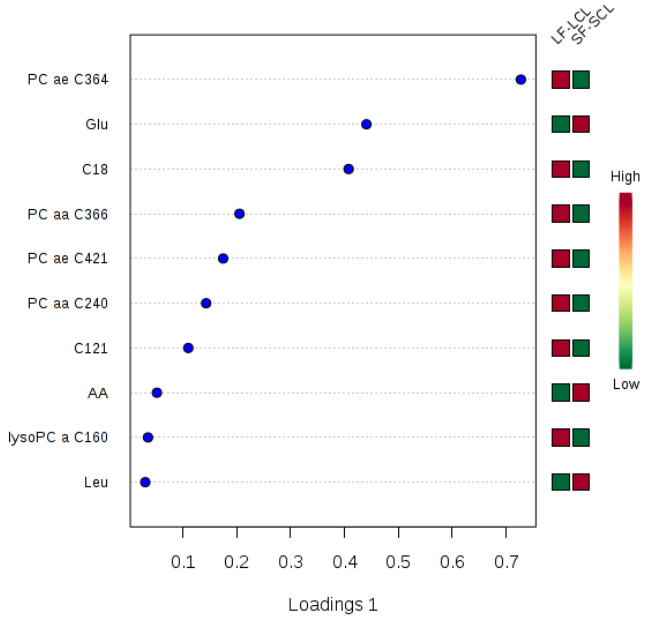

Source: Gonella-Diaza (2017).

Legend: The colored boxes on the right indicate the relative concentrations of the corresponding metabolite in each group.

7.3.2 Amino Acids and Biogenic Amines

Amino acids are organic compounds containing amine (-NH2) and carboxyl (-COOH) functional groups. They play key roles both as composing proteins and as intermediaries in metabolism. In the present study, a total of 21 amino acids were quantified in the oviductal washing (Appendix K). Eight amino acids were not detected; three amino acids were more abundant in the oviductal washings of the SF-SCL group (Aspartate, Citrulline and Glutamate) and one in the LF-LCL group (Phenylalanine).

Biogenic amines are biogenic substances with one or more amine groups. They are basic nitrogenous compounds formed mainly by decarboxylation of amino acids or by amination and transamination of aldehydes and ketones. Biogenic amines are involved in a variety of regulatory functions. Out of the 21 biogenic amines that were measured, two were more abundant in the oviductal washings of the SF-SCL group (Creatinine and Taurine; Figure 19).

Figure 22 – Box plot graph of amino acids concentration (µM) values in oviductal washings collected from cows in the LF-LCL and SF-SCL groups.

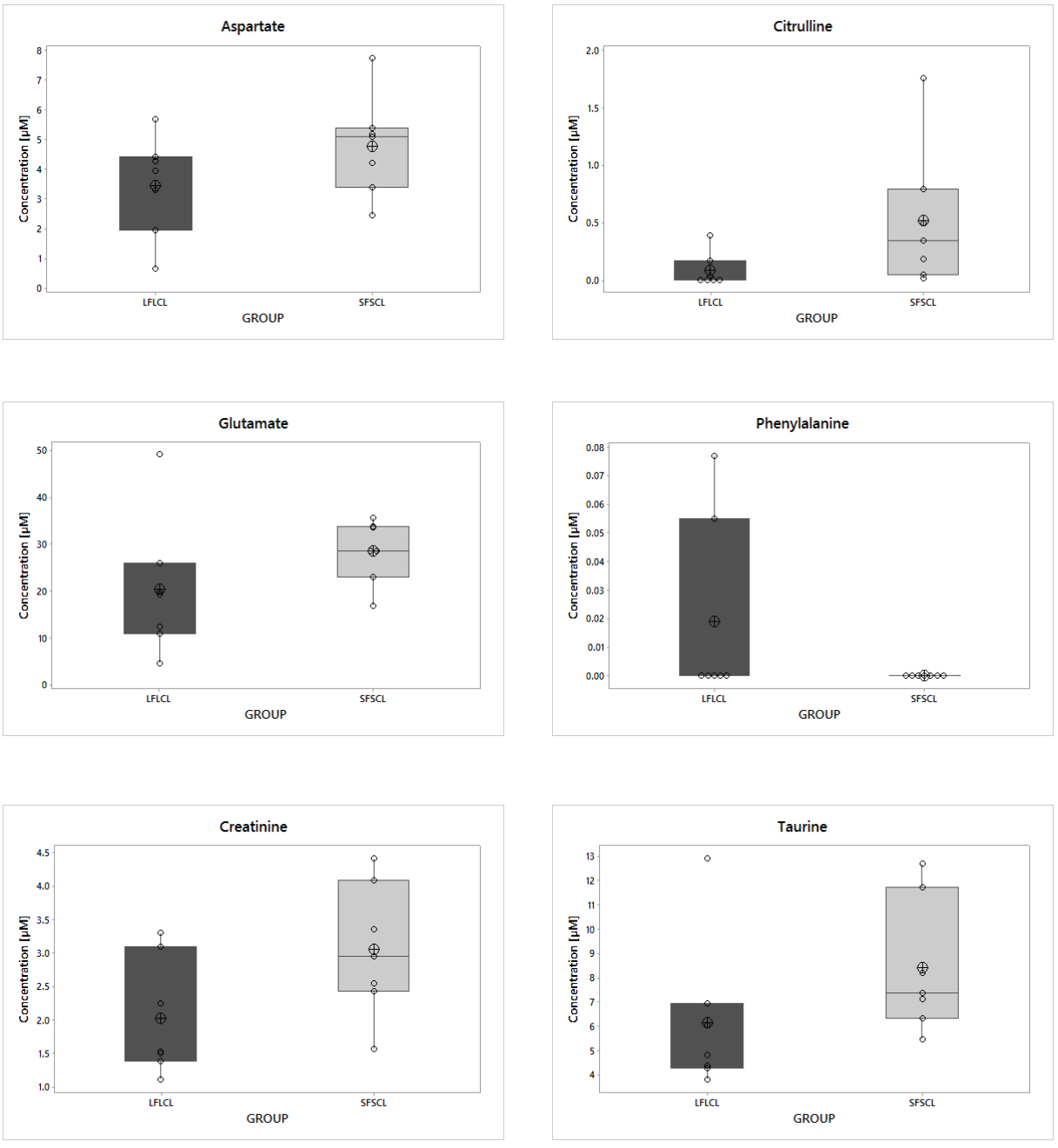

Source: Gonella-Diaza (2017).

Legend: Box-and-wisker plots of amino acids presenting concentrations significantly different between groups ($P < 0.1$) are shown. Individual values (circles), the mean value (cross circle) and the boxes and wiskers represent the interquartile amplitude.

7.3.3 Acylcarnitines

Acylcarnitines are defined as the condensation product of a carboxylic acid and carnitine, and they transport fatty acid crossing the inner mitochondrial membrane (LEHNINGER *et al*., 2000). Concentrations of forty acylcarnitines were measured in oviductal fluid (Appendix L) and 10 resulted to be different between groups (Figure 20). Acetylcarnitine, Butenoylcarnitine, Glutarylcarnitine, Hydroxyhexadecadienoylcarnitine, and Valerylcarnitine were more abundant in the oviductal washings of the SF-SCL group, while Hexadecadienoylcarnitine, Malonylcarnitine, Hydroxytetradecenoylcarnitine, Stearylcarnitine, and Oleylcarnitine were more abundant in LF-LCL group.

Figure 23 – Box plot graph of acylcarnitines concentration (µM) values in oviductal washings collected from cows in the LF-LCL and SF-SCL groups.

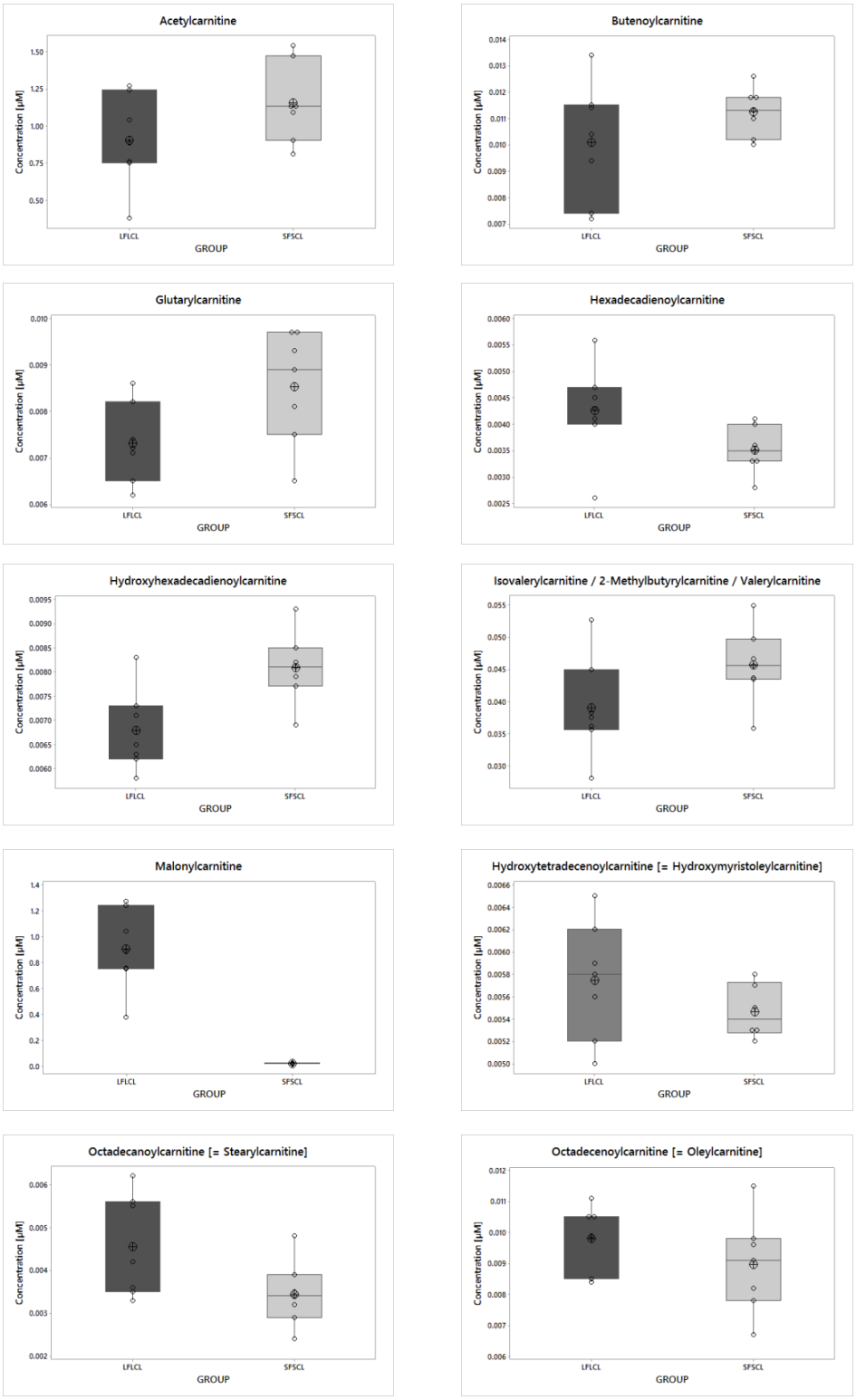

Source: Gonella-Diaza (2017).

Legend: Box-and-wisker plots of Acylcarnitines presenting concentrations significantly different between groups ($P < 0.1$) are shown. Individual values (circles), the mean value (cross circle) and the boxes and wiskers represent the interquartile amplitude.

7.3.4 Phosphatidylcholines and Lysophosphatidylcholines

Phosphatidylcholines are classified as phospholipids; they possess a choline as a head group and are the most abundant lipid class in mammalian cell-membranes (LEHNINGER *et al*., 2000). Lysophosphatidylcholines are the result of the partial hydrolysis of phosphatidylcholines, generally when one of the fatty acid groups is removed. In the present study concentrations of 76 phosphatidylcholines were measured in the oviductal fluid (Appendix M) and 13 were different between groups. Four Phosphatidylcholines were more abundant in the oviductal washings of the SF-SCL group (Phosphatidylcholine with acyl-alkyl residue sum C30:2 [PC ae C30:2], PC ae C36:0, PC ae C40:2, Phosphatidylcholine with diacyl residue sum C32:2 [PC aa C32:2]) and eight in the LF-LCL group (Lf PC ae C36:4, PC ae C42:3, PC ae C44:3 , PC aa C24:0, PC aa C28:1, PC aa C36:6, PC aa C38:1, PC aa C40:2).

Out of the 14 Lysophosphatidylcholines that were measured (Appendix N), only two were found in different concentrations between groups. These two were more abundant in the oviductal washings of the LF-LCL group: Lysophosphatidylcholine with acyl residue C16:0 (lysoPC a C16:0) and lysoPC a C18:2 (Figure 22).

Figure 24 – Box plot graph of phosphatidylcholines concentration (µM) values in oviductal washings collected from cows in the LF-LCL and SF-SCL groups

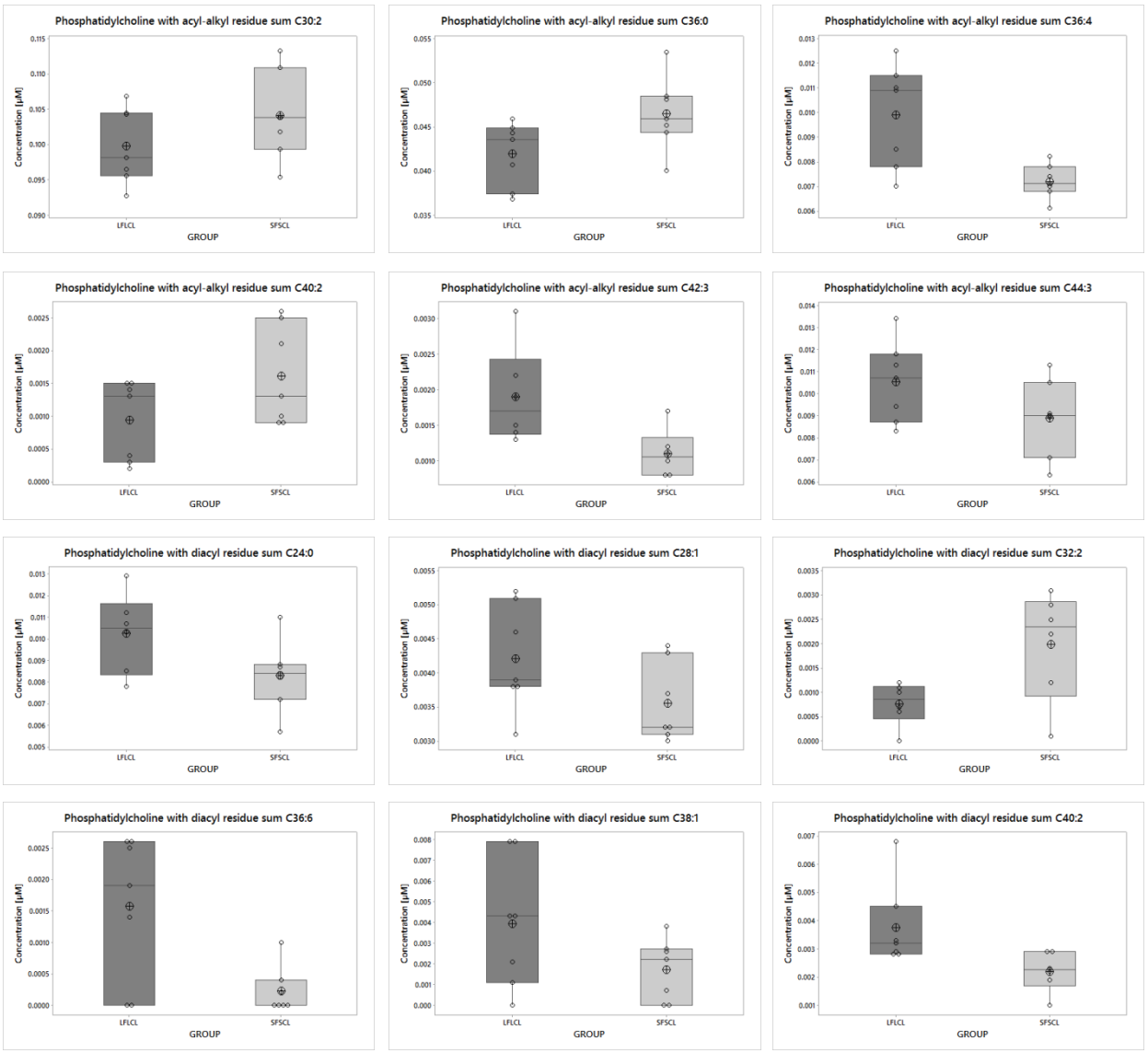

Source: Gonella-Diaza (2017).

Legend: Box-and-wisker plots of Phosphatidylcholines presenting concentrations significantly different between groups ($P < 0.1$) are shown. Individual values (circles), the mean value (cross circle) and the boxes and wiskers represent the interquartile amplitude.

Figure 25 – Box plot graph of lysophosphatidylcholines concentration (µM) values in oviductal washings collected from cows in the LF-LCL and SF-SCL groups.

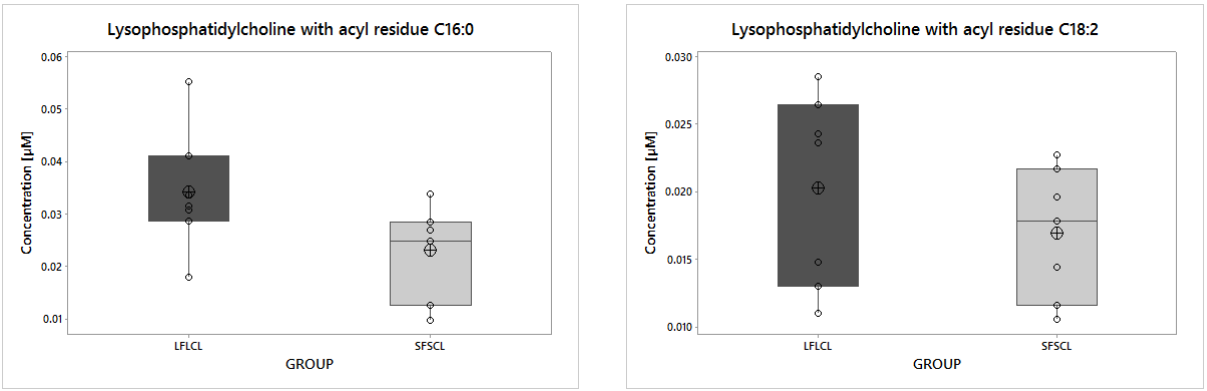

Source: Gonella-Diaza (2017).

Legend: Box-and-wisker plots of Lysophosphatidylcholines presenting concentrations significantly different between groups ($P < 0.1$) are shown. Individual values (circles), the mean value (cross circle) and the boxes and wiskers represent the interquartile amplitude.

7.3.5 Sphingomyelins

Sphingomyelins are part of the sphingolipids components; they can be found in plasma membrane, the endocytic recycling compartment, and the Golgi apparatus (LEHNINGER *et al*., 2000). In the present study, concentrations of a total of 15 sphingomyelins were measured in the oviductal washings (Appendix O). Concentration of Hydroxysphingomyelin with acyl residue sum C24:1 [SM (OH) C24:1] was abundant in the LF-LCL washings and concentration of SM with acyl residue sum C22:3 (SM C22:3), and SM C24:0 were most abundant in the SF-SCL group (Figure 23).

Figure 26 – Box plot graph of sphingomyelins concentration (µM) values in oviductal washings collected from cows in the LF-LCL and SF-SCL groups.

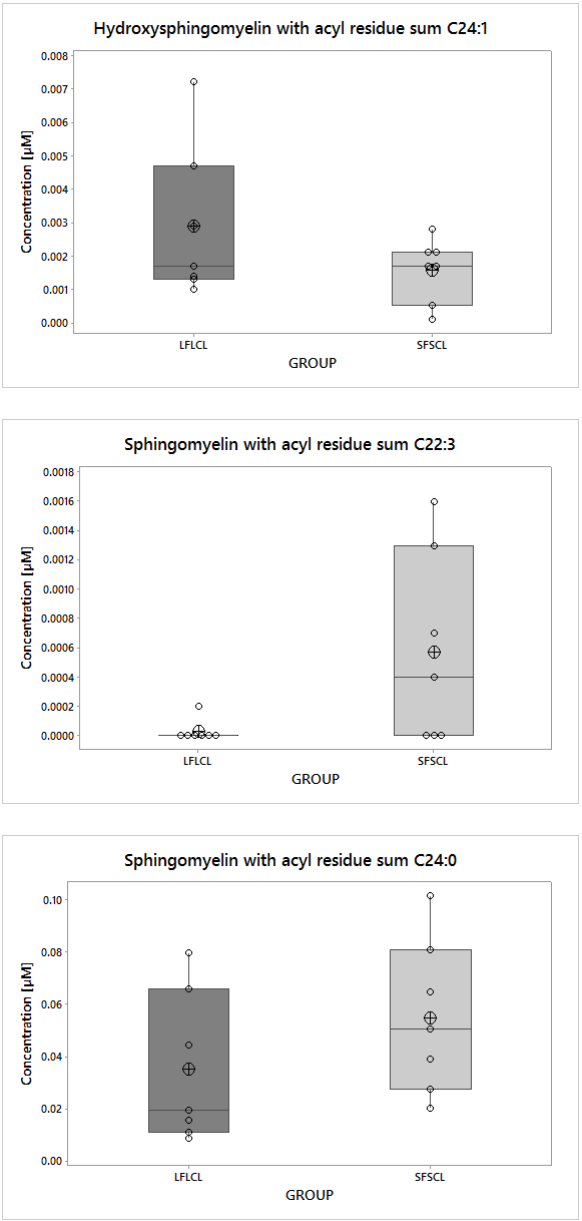

Source: Gonella-Diaza (2017).

Legend: Box-and-wisker plots of Sphingomyelins presenting concentrations significantly different between groups ($P < 0.1$) are shown. Individual values (circles), the mean value (cross circle) and the boxes and wiskers represent the interquartile amplitude.

7.3.6 Hexoses

Hexoses includes monosaccharides containing 6 carbons (e.g. glucose, fructose, and galactose, among others). In the present study, all hexoses were quantified together as a sum of all hexoses. The hexoses concentration in the oviductal washing of SF-SCL group was greater than in the LF-LCL group (Figure 24).

Figure 27 – Box plot graph of hexoses concentration (µM) values in oviductal washings collected from cows in the LF-LCL and SF-SCL groups

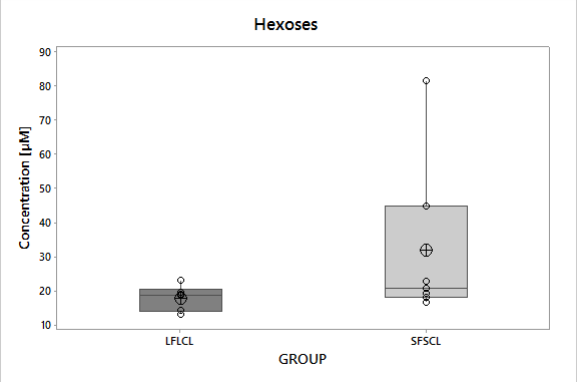

Source: Gonella-Diaza (2017).

Legend: Box-and-wisker plots of Hexoses showing significant differences between groups ($P < 0.1$). Individual values (circles), the mean value (cross circle) and the boxes and wiskers represent the interquartile amplitude.

7.3.7 Prostaglandins and Related Compounds

Prostaglandins and related compounds are collectively known as eicosanoids. They are derived from the arachidonic acid and serve as local signaling molecules with specific effects on target cells close to their site of synthesis (LEHNINGER *et al*., 2000). Concentrations of 17 analytes from this category were measured. Only Arachidonic acid and Prostaglandin F2alpha were statistically different between groups, being more abundant in the SF-SCL group (Figure 25; Appendix P).

Figure 28 – Box plot graph of arachidonic acid and Prostaglandin F2alpha concentrations (nM) values in oviductal washings collected from cows in the LF-LCL and SF-SCL groups.

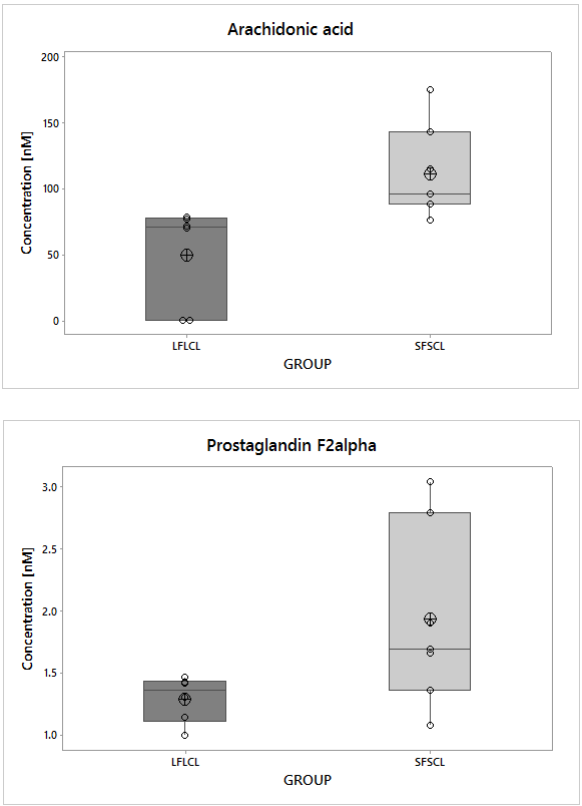

Source: Gonella-Diaza (2017).

Legend: Box-and-wisker plots of Prostaglandins and related compounds presenting concentrations significantly different between groups ($P < 0.1$) are shown. Individual values (circles), the mean value (cross circle) and the boxes and wiskers represent the interquartile amplitude.

7.4 DISCUSSION

The central hypothesis of this study was that the size of the periovulatory follicle modulates the periovulatory endocrine milieu affecting the composition of the oviductal fluid. To test this hypothesis, a metabolomics approach was used to compare the composition of the oviductal fluid of LF-LCL and SF-SCL cows. A total of 191 analytes were quantified using a commercial metabolome platform. Analytes of all biochemical categories assayed presented different concentrations between experimental groups. These results lead us to accept the hypothesis and to conclude that the composition of the oviductal fluids is different between cows with contrasting receptivity and fertility status. Although further studies and analyses are needed, it

could be assumed that analytes presenting different concentrations between groups can be used as biomarkers of fertility. Additionally, it would be interesting to identify the function of each of these compounds during the early embryo development and their potential use during in vitro embryo production.

7.5 REFERENCES.

AVILES, M.; GUTIERREZ-ADAN, A.; COY, P. Oviductal secretions: will they be key factors for the future ARTs?. **Molecular Human Reproduction**, v. 16, p. 896-906, 2010.

BINELLI, M.; HAMPTON, J.; BUHI, W.C.; THATCHER, W.W. Persistent dominant follicle alters pattern of oviductal secretory proteins from cows at estrus. **Biology of Reproduction**, v. 61, p. 127-134, 1999.

BUHI, W.C.; ALVAREZ, I. M.; KOUBA A.J. Secreted proteins of the oviduct. **Cells Tissues Organs**, v. 166, p. 165-179, 2000.

BUHI, W.C.; ASHWORTH, C.J.; BAZER, F.W.; ALVAREZ, I.M. In vitro synthesis of oviductal secretory proteins by estrogen-treated ovariectomized gilts. **Journal of Experimental Zoology**, v. 262, p. 426-435, 1992.

GONELLA-DIAZA, A.M.; ANDRADE, S.C.; SPONCHIADO, M.; PUGLIESI, G.; MESQUITA, F.S.; VAN HOECK, V.; STREFEZZI, R.F.; GASPARIN, G.R.; COUTINHO, L.L.; BINELLI, M. Size of the Ovulatory Follicle Dictates Spatial Differences in the Oviductal Transcriptome in Cattle. **PLoS One**, v. 10, p. e0145321, 2015.

GONELLA-DIAZA, A.M.; MESQUITA, F.S.; DA SILVA, K.R.; DE CARVALHO BALIEIRO, J.C.; DOS SANTOS, N.P.; PUGLIESI, G.; STREFEZZI, R.F.; BINELLI, M. Sex Steroids Modulate Morphological and Functional Features of the Bovine Oviduct. **Submitted to Cell and Tissue Research.** 2017:

HUNTER, R.H. Components of oviduct physiology in eutherian mammals. **Biological reviews of the Cambridge Philosophical Society**, v. 87, p. 244-255, 2012.

LEHNINGER, A.; NELSON, D.; COX, M., **Lehninger principles of biochemistry**. 6th edition. Worth Publishers, New York, 2000.

MESQUITA, F.S.; PUGLIESI, G.; SCOLARI, S.C.; FRANCA, M.R.; RAMOS, R.S.; OLIVEIRA, M.; PAPA, P.C.; BRESSAN, F.F.; MEIRELLES, F.V.; SILVA, L.A.; NOGUEIRA, G.P.; MEMBRIVE, C.M.; BINELLI, M., Manipulation of the periovulatory sex steroidal milieu affects endometrial but not luteal gene expression in early diestrus Nelore cows. **Theriogenology**, v. 81, p. 861-869, 2014.

MESQUITA, F.S.; RAMOS, R.S.; PUGLIESI, G.; ANDRADE, S.C.; VAN HOECK, V.; LANGBEEN, A.; OLIVEIRA, M.L.; GONELLA-DIAZA, A.M.; GASPARIN, G.; FUKUMASU, H.; PULZ, L.H.; MEMBRIVE, C.M.; COUTINHO, L.L.; BINELLI, M. The Receptive Endometrial Transcriptomic Signature Indicates an Earlier Shift from Proliferation to Metabolism at Early Diestrus in the Cow. **Biology of Reproduction**, v. 93, p. 52, 2015.

PUGLIESI, G.; SANTOS, F.B.; LOPES, E.; NOGUEIRA, É.; MAIO, J.R.; BINELLI, M. Improved fertility in suckled beef cows ovulating large follicles or supplemented with long-acting progesterone after timed-AI. **Theriogenology**, v. 85, p. 1239-1248, 2016.

UNTERWURZACHER, I.; KOAL, T.; BONN, G.K.; WEINBERGER, K.M.; RAMSAY, S.L. Rapid sample preparation and simultaneous quantitation of prostaglandins and lipoxygenase derived fatty acid metabolites by liquid chromatography-mass spectrometry from small sample volumes. **Clinical Chemistry and Laboratory Medicine**, v. 46, p. 1589-1597, 2008.

XIA, J. WISHART, D.S. Using MetaboAnalyst 3.0 for Comprehensive Metabolomics Data Analysis. **Current Protocols in Bioinformatics**, v. 55, p.14.10.1-14.10.91, 2016.

XIA, J WISHART, D.S. Web-based inference of biological patterns, functions and pathways from metabolomic data using MetaboAnalyst. **Nature Protocols**, v. 6, n. 6, p. 743-760, 2011.

8 GENERAL DISCUSSION AND CONCLUSION

The functional control of the oviductal environment depends on the circulating concentrations of estradiol (E2) and progesterone (P4) (CRISMAN *et al*., 1980; HUNTER, 2012). These sex-steroid hormones diffuse through the plasma membrane of target cells and signal through intra-cellular hormone-specific receptors to regulate cellular physiology (CONNEELY *et al*., 2002; MATTHEWS; GUSTAFSSON, 2003). There are two different modes of sex-steroid intracellular signaling, which are often referred to as genomic and non-genomic pathways. In the genomic pathway, steroids bind to their nuclear receptors inducing them to change their three-dimensional structures, which cause dissociation from chaperones, dimerization, and activation of the receptor transcriptional domain (CONNEELY *et al*., 2002). The active receptors bind directly to the DNA, specifically in the promoter of specific genes containing hormone response elements. Additionally, active receptors can be indirectly associated with promoters through protein-protein interactions with other DNA-binding transcription factors (HARRIS, 2007). In either case, interaction of sex-steroids with their specific receptors leads to transcriptional activation of specific genes. In addition to the nuclear receptors, E2 and P4 also possess membrane receptors which can alter cell signaling via modulation of intracellular cascades, e.g. via G protein and adenylate cyclase activation (PROSSNITZ; BARTON, 2014). In the oviduct, it has been established that the activation of sex-steroids signaling pathways causes changes in cell function, mainly through modulation of gene expression, i.e., through the genomic pathway (ULBRICH *et al*., 2003). Overall, changes in gene expression precede synthesis of new proteins that modulate cell function. It is well known that in the oviduct, proestrus-estrus E2 promotes secretion and transport processes of gametes and the embryo (BISHOP, 1956; AKIRA *et al*., 1993), while P4 promotes epithelial remodeling during the metestrus-diestrus (RUCKEBUSCH; BAYARD, 1975; EINSPANIER et al., 1999). However, until now it was unknown whether cows with different concentrations of E2 and P4 during these periods had differences in additional oviductal functions. The main objective of this Thesis was to investigate the effects of different peri-ovulatory endocrine milieus in oviductal functions relevant for receptivity and fertility.

To properly study the oviduct, several factors must be taken into consideration. First, the oviduct has different regions that fulfill specific functions (McDANIEL *et al*., 1968; ABE, 1996). Thus, these regions should be studied separately in order to understand their functions and characteristics. Second, in monovulatory species such as cattle, the sex steroid concentrations achieved in the tissue are different when comparing the two oviducts (ipsilateral and contralateral to the side of ovulation) (HUNTER *et al*., 1983; WIJAYAGUNAWARDANE *et al*., 1998). Thus, sides should be studied individually. Third, the oviduct is an organ of difficult access. Unlike other tissues, which can be explored by different techniques such as biopsies, cytobrush, or in vivo flushings, in order to collect oviduct tissue samples the animals need to be submitted to surgery or slaughtered, which is one of the causes of the few studies in that organ (KOLLE *et al*., 2010; MENEZO *et al*., 2015). During the planning and implementation of this Thesis, all these considerations were taken into account. First, ampulla and isthmus samples from the ipsilateral and contralateral sides were collected separately. This procedure is in contrast with some of the most recent publications in this area, in which gene expression studies were conducted in luminal epithelial cells scraped after exposing of the lumen and do not take into account the different oviductal regions (ALMIÑANA *et al*., 2014; BAUERSACHS *et al*., 2004; CERNY *et al*., 2015). Second, in our experiments, the animals were slaughtered on day 4. This day was selected because, if an embryo was present in our model, on this day the embryo would be transiting inside the isthmus (CRISMAN *et al*., 1980; KOLLE *et al*., 2009). Third, after slaughter, the oviducts were washed and tissue samples from specific oviductal regions were both frozen and fixed in formalin. This procedure gave us the opportunity to acquire valuable information from the same individual animals through the use of multiple analytical techniques. Thus, transcripts abundance, immunohistochemistry, and tissue morphology were analyzed in the same animal, allowing a comprehensive overview of the oviductal physiology. This was clearly represented, for example, when transcriptome information acquired in Chapter 1 was confronted with morphometric analyzes described in Chapter 2.

A summary of all the results of the present Ph.D. Thesis is in Figure 29. In Chapter 1, it was hypothesized that different proestrus-estrus concentrations of E2 and metestrus concentrations of P4 specifically regulate expression of oviductal genes that support pregnancy. In order to test this hypothesis, the RNA sequencing

technology was used and the transcriptome of ampulla and isthmus of the ipsilateral side was determined. In both regions, the LF-LCL tissues showed enrichment in transcripts associated with cellular processes such as cell proliferation, morphogenesis, and ECM remodeling. Transcripts from genes coding for intercellular adhesion proteins, ECM constituents, degradation and remodeling enzymes, and growth factors were more abundant in LF-LCL cows. These pathways, enriched in the group of greater fertility, could potentially bring direct benefits on the development of the embryo and were further studied in subsequent chapters.

In Chapter 2, the molecular pathways related to branching morphogenesis, cellular secretion, and cellular proliferation were studied. In the ampulla, differences were detected between the groups, both in their gross morphology and in their cellular populations. It was observed that LF-LCL cows presented more primary folds, a greater folding grade, and a larger luminal epithelium perimeter (gross morphology changes), and also LF-LCL cows possess more secretory cells and proliferating cells. These results were consistent with previous transcriptomic data. However, no morphological differences were detected when comparing the morphology of the isthmus between the two groups. Because the ampulla has a larger contribution to the oviductal secretions, it was hypothesized that the LF-LCL cows would have a greater secretory capacity. Probably, this capacity would impact the composition of the oviductal fluid and, consequently, embryo development.

In Chapter 3, the gene and protein expression of ECM components and remodelers was evaluated. The results showed that in both ampulla and isthmus, transcript abundance of ECM-related genes was greater in the LF-LCL group and, in the isthmus, the protein expression of MMPs and TIMPs was also stimulated in the LF-LCL cows. Both results confirm the RNA-seq data. When immunostaining for type I collagen was assessed, the LF-LCL animals showed lower scores indicating that the ECM was indeed undergoing a remodeling process. Taking this together, it can be assumed that the oviduct of LF-LCL cows could have a greater quantity of free growth factors (released form the ECM). These GF could affect the oviduct cells themselves and the structures transiting inside the oviductal lumen. Once again, these results lead one to think that the oviductal lumen of the LF-LCL cows is better suited for embryo development.

In Chapter 1, it was concluded that oviducts from LF-LCL animals were under a strong sex-steroids signaling. In Chapter 4 we studied if there was a sex-steroidal regulation of oviductal miRNAs expression in the oviduct, as reported previously in other tissues. For the first time, it was shown that sex-steroids can mediate control of miRNA-processing components, potentially leading to differences in the microRNAome in cattle. This control could modify molecular pathways that affect cellular function. However, it is unknown yet how these alterations can affect the embryo. There is evidence suggest that microRNAs could be transported outside the cell (inside microvesicles and exosomes) and captured by the embryo thus altering its gene expression. Then, it is likely that differences in microRNAome between the LF-LCL and SF-SCL groups have a direct effect on the embryo, its gene expression, and its development and survival.

In Chapter 5, the composition of the oviductal fluid in high and low fertility cows was studied. Many evidences took us to the study of the composition of this fluid. First, in chapter 1 the oviductal transcriptome of LF-LCL cows showed secretion as an enriched process. Second, in Chapter 2, it was found that the ampulla of LF-LCL cows has differences in morphology that support differences in the secretory patterns. Finally, because LF-LCL cows also have an active ECM remodeling and probably growth factors released after matrix breakdown, to study the oviductal fluid composition in was the reasonable next step to follow. It was found that there were differences in the metabolites composition of the oviductal fluid between LF-LCL and SF-SLC cows. Although, it is still necessary to study and understand the role of each of these metabolites in oviductal biology and how they might affect the development of the embryo, these differences between groups already indicate that the oviduct of high fertility cows provides a different environment. This environment was prompted by differences in the composition of its oviductal fluid.

Collectivelly, these results lead me to **accept the central hypothesis of this Thesis** and to conclude that animals with different periovulatory sex-steroid profiles have differences in their oviductal environment.

Figure 29 – Summary of the main results of the present PhD Thesis.

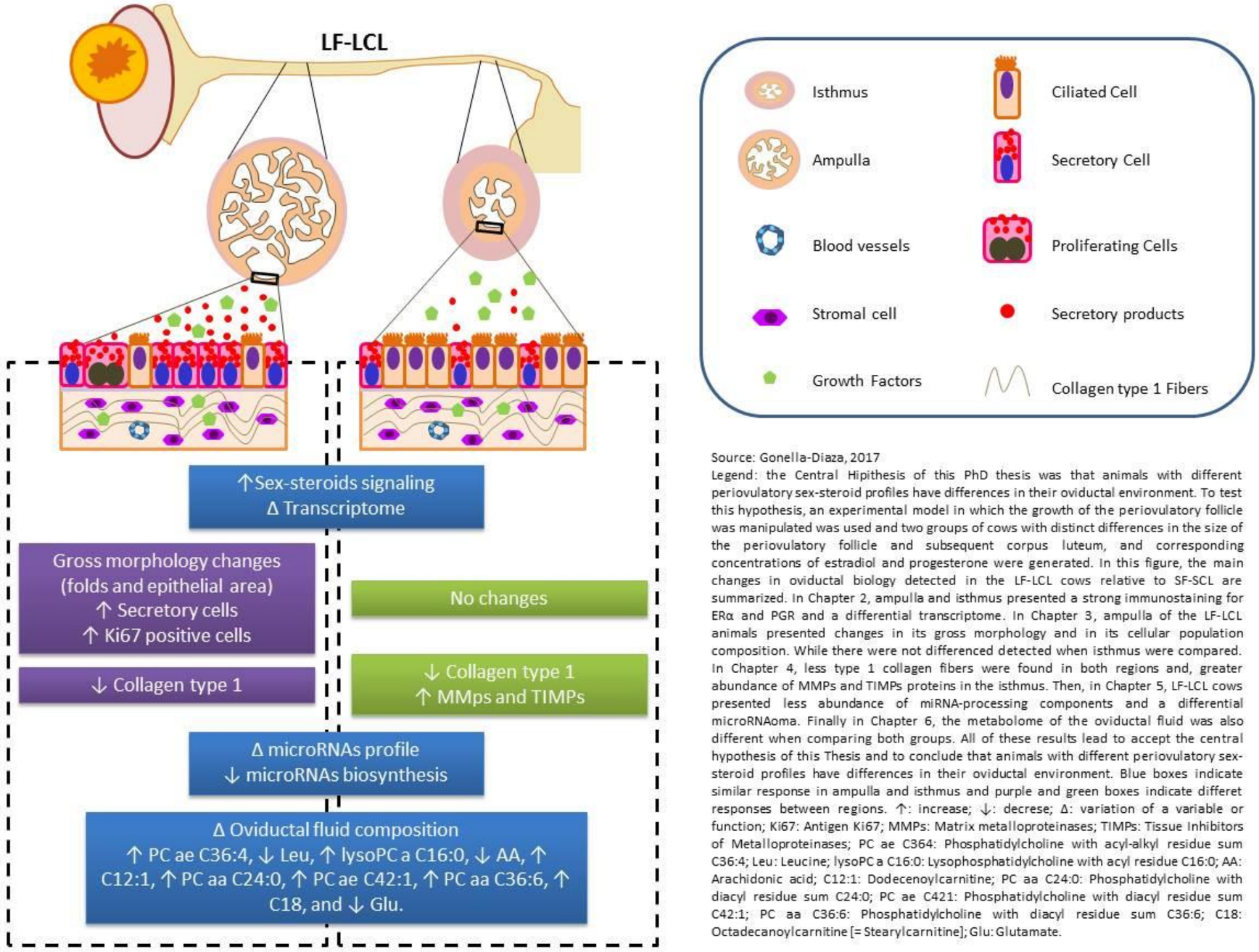

Source: Gonella-Diaza, 2017

Legend: the Central Hipithesis of this PhD thesis was that animals with different periovulatory sex-steroid profiles have differences in their oviductal environment. To test this hypothesis, an experimental model in which the growth of the periovulatory follicle was manipulated was used and two groups of cows with distinct differences in the size of the periovulatory follicle and subsequent corpus luteum, and corresponding concentrations of estradiol and progesterone were generated. In this figure, the main changes in oviductal biology detected in the LF-LCL cows relative to SF-SCL are summarized. In Chapter 2, ampulla and isthmus presented a strong immunostaining for ERα and PGR and a differential transcriptome. In Chapter 3, ampulla of the LF-LCL animals presented changes in its gross morphology and in its cellular population composition. While there were not differenced detected when isthmus were compared. In Chapter 4, less type 1 collagen fibers were found in both regions and, greater abundance of MMPs and TIMPs proteins in the isthmus. Then, in Chapter 5, LF-LCL cows presented less abundance of miRNA-processing components and a differential microRNAoma. Finally in Chapter 6, the metabolome of the oviductal fluid was also different when comparing both groups. All of these results lead to accept the central hypothesis of this Thesis and to conclude that animals with different periovulatory sex-steroid profiles have differences in their oviductal environment. Blue boxes indicate similar response in ampulla and isthmus and purple and green boxes indicate differet responses between regions. ↑: increase; ↓: decrese; Δ: variation of a variable or function; Ki67: Antigen Ki67; MMPs: Matrix metalloproteinases; TIMPs: Tissue Inhibitors of Metalloproteinases; PC ae C364: Phosphatidylcholine with acyl-alkyl residue sum C36:4; Leu: Leucine; lysoPC a C16:0: Lysophosphatidylcholine with acyl residue C16:0; AA: Arachidonic acid; C12:1: Dodecenoylcarnitine; PC aa C24:0: Phosphatidylcholine with diacyl residue sum C24:0; PC ae C421: Phosphatidylcholine with diacyl residue sum C42:1; PC aa C36:6: Phosphatidylcholine with diacyl residue sum C36:6; C18: Octadecanoylcarnitine [= Stearylcarnitine]; Glu: Glutamate.

8.1 REFERENCES

ABE, H. The mammalian oviductal epithelium: Regional variations in cytological and functional aspects of the oviductal secretory cells. **Histology and Histopathology**, v. 11, p. 743-768, 1996.

AGDUHR, E. Studies on the structure and development of the bursa ovarica and the tuba uterina in the mouse. **Acta Zoologica**, v. 8, p. 1-133, 1927.

AGUILAR, J.; REYLEY, M. The uterine tubal fluid: secretion, composition and biological effects. **Animal Reproduction**, v. 2, p. 91-105, 2005.

AHUMADA, C.J.; SALVADOR, I.; CEBRIAN-SERRANO, A.; LOPERA, R.; SILVESTRE, M.A. Effect of supplementation of different growth factors in embryo culture medium with a small number of bovine embryos on *in vitro* embryo development and quality. **Animal**, v. 7, p. 455-462, 2013.

ASHWORTH, C.J; SALES, D.I.; WILMUT, I. Evidence of an association between the survival of embryos and the periovulatory plasma progesterone concentration in the ewe. **Journal of Reproduction and Fertility**, v. 87, p. 23-32, 1989.

AVILES, M.; GUTIERREZ-ADAN, A.; COY, P. Oviductal secretions: will they be key factors for the future ARTs?. **Molecular Human Reproduction**, v. 16, p. 896-906, 2010.

AYEN, E.; SHAHROOZ, R.; KAZEMIE, S. Histological and histomorphometrical changes of different regions of oviduct during follicular and lutealphases of estrus cycle in adult Azarbaijan buffalo. **Iranian Journal of Veterinary Research**, v. 13, p. 42-48, 2012.

BACHA, W.J.; BACHA, L.M. **Color Atlas of Veterinary Histology**, Third edition. Wiley-blackwell. ISBN-13: 978-0470958513. 356 pages, 2012.

BESENFELDER, U.; HAVLICEK, V.; BREM, G. Role of the oviduct in early embryo development. **Reproduction in Domestic Animals**, v. 47, p. 156-163, 2012.

BROWER, L.; ANDERSON, E.; Cytological Events Associated with the Secretory Process in the Rabbit Oviduct. **Biology of Reproduction**, v. 1, p. 130-148. 1969.

BUHI, W.C.; ALVAREZ, I.M.; KOUBA, A.J. Secreted proteins of the oviduct. **Cells, Tissues, Organs**, v. 166, p. 165-179, 2000.

BUHI, W.C.; ASHWORTH, C.J.; BAZER, F.W.; ALVAREZ, I.M. *In vitro* synthesis of oviductal secretory proteins by estrogen-treated ovariectomized gilts. **Journal of Experimental Zoology**, v. 262, p. 426-435, 1992.

BUHI, W.C.; BAZER, F.W.; ALVAREZ, I.M.; MIRANDO, M.A. *In vitro* synthesis of oviductal proteins associated with estrus and 17 beta-estradiol-treated ovariectomized ewes. **Endocrinology**, v. 128, p. 3086-3095, 1991.

CHANROTA, M; GUOA, Y. DALINA, A.M.; PERSSONB, E.; BÅGEA, R.; SVENSSONA, A.; GUSTAFSSONA, H.; HUMBLOTA, P. Dose related effects of LPS on endometrial epithelial cell populations from dioestrus cows. **Animal Reproduction Science**, v. 177, p. 12-24, 2017.

DEMETRIO, D.G.; SANTOS, R.M.; DEMETRIO, C.G.; VASCONCELOS, J.L. Factors affecting conception rates following artificial insemination or embryo transfer in lactating Holstein cows. **Journal of Dairy Science**, v. 90, p. 5073-5082, 2007.

DONNEZ, J.; CASANAS-ROUX, F.; CAPRASSE, J.; FERIN, J.; THOMAS, K. Cyclic changes in ciliation, cell height, and mitotic activity in human tubal epithelium during reproductive life. **Fertility and Sterility**, v. 43, p. 554-559, 1985.

ERIKSEN, T.; TERKELSEN, O.; HYTTEL, P.; GREVE, T. Ultrastructural features of secretory-cells in the bovine oviduct epithelium. **Anatomy and embryology**, v. 190, p. 583-590, 1994.

GANDOLFI, F.; BREVINI, T.A.L.; RICHARDSON, L.; BROWN, C.R.; MOOR, R.M. Characterization of proteins secreted by sheep oviduct epithelial-cells and their function in embryonic-development. **Development**. v. 106, p. 303-12, 1989.

GONELLA-DIAZA, A.; ANDRADE, S.; SPONCHIADO, M.; PUGLIESI, G.; MESQUITA, F.; VAN HOECK, V.; STREFEZZI, R.; GASPARIN, G.; COUTINHO, L.; BINELLI, M. Size of the ovulatory follicle dictates spatial differences in the oviductal transcriptome in cattle. **Plos One**. v. 10, e0145321, 2015.

GRAY, C.A.; BARTOL, F.F.; TARLETON, B.J.; WILEY, A.A.; JOHNSON, G.A.; BAZER, F.W.; SPENCER, T.E. Developmental biology of uterine glands. **Biology of Reproduction**. v. 65, p. 1311-1323, 2001.

HUNTER, R.H. Have the Fallopian tubes a vital role in promoting fertility?. **Acta Obstetricia et Gynecologica Scandinavica**. v. 77, p. 475-486, 1998.

HUNTER, R.H. Components of oviduct physiology in eutherian mammals. **Biological reviews of the Cambridge Philosophical Society**. v. 87, p. 244-255, 2012.

HUNTER, R.H.; COOK, B.; POYSER, N.L. Regulation of oviduct function in pigs by local transfer of ovarian steroids and prostaglandins: a mechanism to influence sperm transport. **European Journal of Obstetrics Gynecology And Reproductive Biology**, v. 14, p. 225-232, 1983.

KOLLE, S.; REESE, S.; KUMMER, W. New aspects of gamete transport, fertilization, and embryonic development in the oviduct gained by means of live cell imaging. **Theriogenology**, v. 73, p. 786–795, 2010.

ITO, S.; KOBAYASHI, Y.; YAMAMOTO, Y.; KIMURA, K.; OKUDA, K. Remodeling of bovine oviductal epithelium by mitosis of secretory cells. **Cell and Tissue Research**, v. 366, p. 403-410, 2016.

KENNGOTT, R.A.; SINOWATZ, F. Prenatal development of the bovine oviduct. **Anatomia, Histologia, Embryologia**, v. 36, p. 272-283, 2007.

KOLLE, S.; DUBIELZIG, S.; REESE, S.; WEHREND, A.; KONIG, P.; KUMMER, W. Ciliary Transport, Gamete Interaction, and Effects of the Early Embryo in the Oviduct: Ex Vivo Analyses Using a New Digital Videomicroscopic System in the Cow. **Biology of Reproduction**, v. 81, p. 267-274, 2009.

KONISHI, I.; FUJII, S.; PARMLEY, T.H.; MORI, T. Development of ciliated cells in the human fetal oviduct: an ultrastructural study. **The Anatomical Record**, v. 219, p. 60-68, 1987.

LEESE, H.J. The formation and function of oviduct fluid. **Journal of Reproduction and Fertility**, v. 82, p. 843-856, 1988.

MCDANIEL, J.W.; SCALZI, H.; BLACK, D. Influence of ovarian hormones on histology and histochemistry of the bovine oviduct. **Journal of Dairy Science**, v. 51, p. 754-761, 1968.

MESQUITA, F.S.; PUGLIESI, G.; SCOLARI, S.C.; FRANCA, M.R.; RAMOS, R.S.; OLIVEIRA, M.; PAPA, P.C.; BRESSAN, F.F.; MEIRELLES, F.V.; SILVA, L.A.; NOGUEIRA, G.P.; MEMBRIVE, C.M.; BINELLI, M. Manipulation of the periovulatory sex steroidal milieu affects endometrial but not luteal gene expression in early diestrus Nelore cows. **Theriogenology**, v. 81, p. 861-869, 2014.

MESQUITA, F.S.; RAMOS, R.S.; PUGLIESI, G.; ANDRADE, S.C.; VAN HOECK, V.; LANGBEEN, A.; OLIVEIRA, M.L.; GONELLA-DIAZA, A.M.; GASPARIN, G.; FUKUMASU, H.; PULZ, L.H.; MEMBRIVE, C.M.; COUTINHO, L.L.; BINELLI, M. The Receptive Endometrial Transcriptomic Signature Indicates an Earlier Shift from Proliferation to Metabolism at Early Diestrus in the Cow. **Biology of Reproduction**, v. 93. p. 52. 2015.

MOKHTAR, DM. Microscopic and histochemical characterization of the bovine uterine tube during the follicular and luteal phases of estrous cycle. **Journal of Microscopy and Ultrastructure**, v. 3, p. 44-52, 2015.

MORRIS, D.; DISKIN, M. Effect of progesterone on embryo survival. **Animal**, v. 2, p. 1112-1119, 2008.

PERES, R.F.; CLARO, I.J.R.; SA FILHO, O.G.; NOGUEIRA, G.P.; VASCONCELOS, J.L.; Strategies to improve fertility in Bos indicus postpubertal heifers and non-lactating cows submitted to fixed-time artificial insemination. **Theriogenology**, v. 72, p. 681-689, 2009.

PUGLIESI, G.; SANTOS, F.B.; LOPES, E.; NOGUEIRA, É.; MAIO, J.R.; BINELLI, M. Improved fertility in suckled beef cows ovulating large follicles or supplemented with long-acting progesterone after timed-AI. **Theriogenology**, v. 85, p. 1239-1248, 2016.

RESTALL, B.J. Histological observations on the reproductive tract of the ewe. **Australian Journal of Biological Sciences**, v.19, p. 673-686, 1966.

RIZOS, D.; FAIR, T.; PAPADOPOULOS, S.; BOLAND, M.P.; LONERGAN, P. Developmental, qualitative, and ultrastructural differences between ovine and bovine embryos produced *in vivo* or *in vitro*. **Molecular Reproduction and Development**, v. 62, p. 320-327, 2002a.

RIZOS, D.; LONERGAN, P.; BOLAND, M.P.; ARROYO-GARCIA, R.; PINTADO, B. DE LA FUENTE, J.; GUTIERREZ-ADAN, A. Analysis of differential messenger RNA expression between bovine blastocysts produced in different culture systems: implications for blastocyst quality. **Biology of Reproduction**, v. 66, p. 589-595, 2002b.

RIZOS, D.; WARD, F.; DUFFY, P.; BOLAND, M.P.; LONERGAN, P. Consequences of bovine oocyte maturation, fertilization or early embryo development *in vitro* versus *in vivo*: implications for blastocyst yield and blastocyst quality. **Molecular Reproduction and Development**, v. 61, p. 234-248, 2002c.

SIMINTIRAS, C.A.; FRÖHLICH, T.; SATHYAPALAN, T.; ARNOLD, G.J.; ULBRICH, S.E.; LEESE, H.J.; STURMEY, R.G. Modelling oviduct fluid formation *in vitro*. **Reproduction**, v. 153, p. 23-33, 2016.

SMIT, A.; HUBLEY, R.; GREEN, P. (1996-2010) **RepeatMasker Open-3.0**. http://www.repeatmasker.org.

VASCONCELOS, J.L.M.; SARTORI, R.; OLIVEIRA, H.N.; GUENTHER, J.G.; WILTBANK, M.C. Reduction in size of the ovulatory follicle reduces subsequent luteal size and pregnancy rate. **Theriogenology**, v. 56, p. 307-314, 2001.

WANG, C.K.; ROBINSON, R.S.; FLINT, A.P.F.; MANN, G.E. Quantitative analysis of changes in endometrial gland morphology during the bovine oestrous cycle and their association with progesterone levels. **Reproduction**, v. 134, p. 365-371, 2007.

WETSCHER, F.; HAVLICEK, V.; HUBER, T.; MULLER, M.; BREM, G.; BESENFELDER, U. Effect of morphological properties of transferred embryonic stages on tubal migration Implications for *in vivo* culture in the bovine oviduct. **Theriogenology**, v. 64, p. 41-48, 2005.

WIJAYAGUNAWARDANE, M.P.B.; CERBITO, W.A.; MIYAMOTO, A.; ACOSTA, T.J.; TAKAGI, M.; MIYAZAWA, K.; SATO, K. Oviductal progesterone concentration and its spatial distribution in cyclic and early pregnant cows. **Theriogenology**, v. 46, p. 1149-1158, 1996.

WIJAYAGUNAWARDANE, M.P.B.; MIYAMOTO, A.; CERBITO, W.A.; ACOSTA, T.J.; TAKAGI, M.; SATO, K. Local distributions of oviductal estradiol, progesterone, prostaglandins, oxytocin and endothelin-1 in the cyclic cow. **Theriogenology**, v. 49, p. 607-618, 1998.

YOSHIOKA, S.; ABE, H.; SAKUMOTO, R.; OKUDA, K. Proliferation of Luteal Steroidogenic Cells in Cattle. **Plos One**, v. 8, e84186, 2013.

APPENDICES & SUPPLEMENTAL MATERIAL

APPENDIX A

PLOS | ONE

RESEARCH ARTICLE

Size of the Ovulatory Follicle Dictates Spatial Differences in the Oviductal Transcriptome in Cattle

Angela María Gonella-Diaza[1], Sónia Cristina da Silva Andrade[2], Mariana Sponchiado[1], Guilherme Pugliesi[1], Fernando Silveira Mesquita[3], Veerle Van Hoeck[1], Ricardo de Francisco Strefezzi[4], Gustavo R. Gasparin[2], Luiz L. Coutinho[2], Mario Binelli[1]*

1 Faculdade de Medicina Veterinária e Zootecnia, Universidade de São Paulo, Pirassununga, São Paulo, Brazil, **2** Laboratório de Biotecnologia Animal, Escola Superior de Agricultura Luiz de Queiroz, Universidade de São Paulo, Av Pádua Dias, 11, Piracicaba, SP, Brazil, **3** Faculdade de Medicina Veterinária, Universidade Federal do Pampa, Uruguaiana, Brazil, **4** Faculdade de Zootecnia e Engenharia de Alimentos, Universidade de São Paulo, Pirassununga, São Paulo, Brazil

* binelli@usp.br

OPEN ACCESS

Citation: Gonella-Diaza AM, da Silva Andrade SC, Sponchiado M, Pugliesi G, Mesquita FS, Van Hoeck V, et al. (2015) Size of the Ovulatory Follicle Dictates Spatial Differences in the Oviductal Transcriptome in Cattle. PLoS ONE 10(12): e0145321. doi:10.1371/journal.pone.0145321

Editor: Wilfried A. Kues, Friedrich-Loeffler-Institute, GERMANY

Received: August 31, 2015

Accepted: December 1, 2015

Published: December 23, 2015

Data Availability Statement: An overview of this data has been deposited in NCBI's Gene Expression Omnibus (GEO) and is accessible through GEO Series accession number GSE65681.

Funding: This research was funded by Coordenação de Aperfeiçoamento de Pessoal de Nível Superior (CAPES); PEC-PG program: AMGD grant number 15068-12-9; National Counsel of Technological and Scientific Development (CNPq); Fundação de Amparo à Pesquisa do Estado de São Paulo (FAPESP): MB grant number 2011/03226-4. The funders had no role in study design, data collection

Abstract

In cattle, molecular control of oviduct receptivity to the embryo is poorly understood. Here, we used a bovine model for receptivity based on size of the pre-ovulatory follicle to compare oviductal global and candidate gene transcript abundance on day 4 of the estrous cycle. Growth of the pre-ovulatory follicle (POF) of Nelore (*Bos indicus*) cows was manipulated to produce two groups: large POF large corpus luteum (CL) group (LF-LCL; greater receptivity) and small POF-small CL group (SF-SCL). Oviductal samples were collected four days after GnRH-induced ovulation. Ampulla and isthmus transcriptome was obtained by RNA-seq, regional gene expression was assessed by qPCR, and PGR and ERa protein distribution was evaluated by immunohistochemistry. There was a greater abundance of PGR and ERa in the oviduct of LF-LCL animals thus indicating a greater availability of receptors and possibly sex steroids stimulated signaling in both regions. Transcriptomic profiles indicated a series of genes associated with functional characteristics of the oviduct that are regulated by the periovulatory sex steroid milieu and that potentially affect oviductal receptivity and early embryo development. They include tissue morphology changes (extra cellular matrix remodeling), cellular changes (proliferation), and secretion changes (growth factors, ions and metal transporters), and were enriched for the genes with increased expression in the LF-LCL group. In conclusion, differences in the periovulatory sex steroid milieu lead to different oviductal gene expression profiles that could modify the oviductal environment to affect embryo survival and development.

Introduction

From the discovery of the oviduct by Gabriele Falloppio in 1561 until the late 1900s, it was believed that the oviduct was simply a conduit for the passage of sperm and oocyte without

and analysis, decision to publish, or preparation of the manuscript.

Competing Interests: The authors have declared that no competing interests exist.

relevant metabolic or physiological functions [1]. However, it is now well accepted that the oviduct plays a major role in sperm storage and capacitation, fertilization and early embryo development [2–5]. Based on its macro-anatomical characteristics, the oviduct can be divided into three portions: the infundibulum which captures the oocyte after ovulation, the ampulla, which is site of fertilization, and the isthmus, which serves as a sperm reservoir in some species [6] and also transports the embryo to the uterine lumen [7]. Consistent with the functional specialization, cellular and molecular characteristics of the oviduct vary according to region [1, 8]. The oviduct epithelial lumen has two types of cells: ciliated and non-ciliated (secretory) cells [9]. In buffaloes [10] and cattle [8], the relative numbers of secretory cells are significantly greater in the ampulla than in the infundibulum and the isthmus. Additionally, the proportion of secretory cells increases during the follicular phase as compared to the luteal phase of the estrous cycle. Oviductal secretions are comprised of molecules originated from the peripheral circulation as well as molecules synthesized de novo by the luminal epithelial cells [11–13]. Oviductal secretions include nutrients, such as energy substrates, ions and amino acids, and lipids and proteins with structural, catalytic and regulatory functions [14–16].

The function of the female reproductive tract is under constant influence of sex steroidal hormones; they define morphology and physiology of tract components and, ultimately, the ability to support pregnancy. In ruminants, the coordinated and sequential changes of concentrations of ovarian steroids, estradiol (E2) and progesterone (P4) during the estrous cycle regulate oviductal secretory function [17–19]. Indeed, volume of oviductal secretions increases around ovulation [20] and decreases during the luteal phase and pregnancy [21]. More importantly, it has been shown that, in cattle, the proestrus-estrus concentrations of E2 and metaestrus-diestrus concentrations of P4 are positively associated with the probability of pregnancy success [22–24]. There are probably multiple targets of sex-steroid actions that affect fertility, such as the oocyte, oviduct, and endometrium. For example, P4 supplementation during early diestrus regulated the endometrial transcriptome, secretions, and elongation of the conceptus [25–27]. Furthermore, our recent work described a model in which ovulation of larger follicles, and consequent greater proestrus E2 concentrations and early diestrus P4 concentrations, modulated global and specific transcription of endometrial genes in *Bos taurus indicus* cattle [28–30]. However, the modulation of oviductal function by the periovulatory sex steroid milieu remains unstudied in cattle. Here, we hypothesize that distinctly different proestrus-estrus concentrations of E2 and metestrus concentrations of P4 specifically regulate expression of oviductal genes that support pregnancy. To test this hypothesis, we use an in vivo experiment that aimed to 1., produce groups of animals with distinctly different periovulatory endocrine milieus and to discover their effect on: 2., the oviductal regional regulation of gene and protein expression of sex-steroid receptors; 3., the transcriptome of the ampulla and the isthmus and, 4., the regional expression of candidate genes associated with oviductal function in Nelore cows four days after induction of ovulation.

Materials and Methodology

Animals

All animal procedures were approved by the Ethics and Animal Handling Committee of the School of Veterinary Medicine and Animal Science of the University of São Paulo. Experiment was carried out at the University of São Paulo, Pirassununga Campus (São Paulo, Brazil). Forty one multiparous and non-lactating Nelore (Bos indicus) cows with no gross reproductive abnormalities by gynecological examination, with a body condition score between 3 and 4 (0, emaciated; 5, obese), were kept in grazing conditions (*Brachiaria brizantha* pastures),

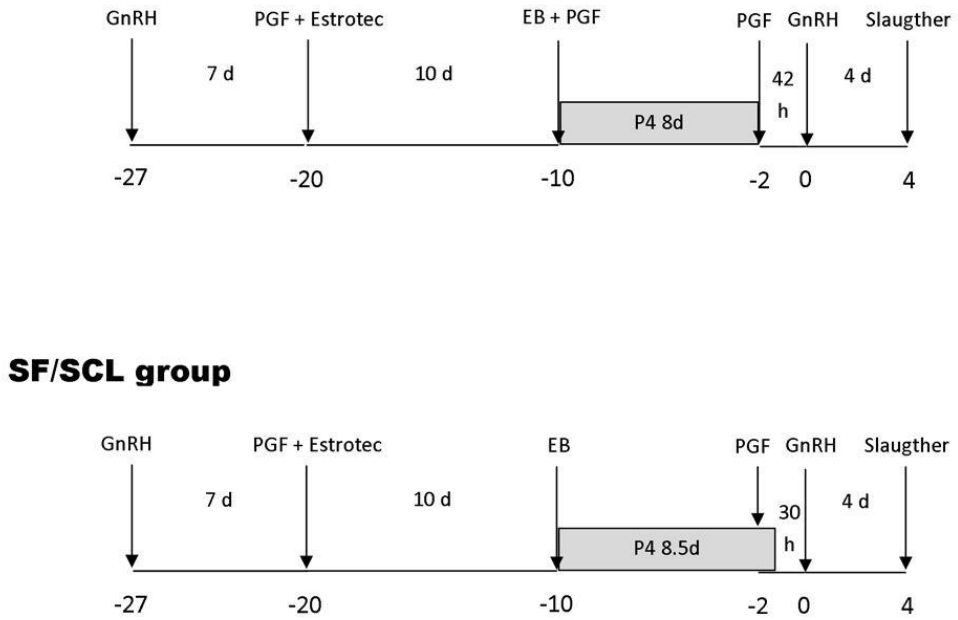

Fig 1. Schematic of the hormonal manipulation protocol used in the present study. Animals (n = 41) were pre-synchronized by intramuscular injection of GnRH agonist and, 7 days later an injection of Prostaglandin F2 alpha (PGF) analog. At this day [day -20 (D-20)] animals received an ESTROTECT Heat detector device and estrus detection was performed twice daily from D-20 to D-10. All animals received a new intravaginal P4-releasing device on D-10 along with an intramuscular injection of 2 mg estradiol benzoate. Simultaneously, cows in the LF-LCL received an intramuscular injection of PGF. The P4 devices were removed on day -2, 42 h and 30 h before the GnRH injection in the LF-LCL and the SF-SCL groups, respectively. All animals received a PGF injection at P4 device removal and a second PGF injection 6 h later. Ovulation was induced by an injection of GnRH agonist on D0.

doi:10.1371/journal.pone.0145321.g001

supplemented with mineralized salt to fulfill their maintenance requirements, and had free access to fresh water.

Reproductive management and experimental design

Animal and reproductive management was performed as described previously [28, 29] to generate animals ovulating a larger follicle and presenting a subsequent larger CL (LF-LCL group, associated with greater receptivity and fertility) or smaller follicles (SF-SCL group; Fig 1). Briefly, animals were pre-synchronized by intramuscular injection of GnRH agonist (1 μg of buserelin acetate; Sincroforte, Ouro Fino, Cravinhos, Brazil) and, 7 days later an injection of Prostaglandin F2 alpha analog (PGF; 0.5 mg of sodium cloprostenol; Sincrocio, Ouro Fino, Cravinhos, Brazil). At this day [day -20 (D-20)] animals received an ESTROTECT Heat detector patch (Rockway, Inc. Spring Valley, WI, USA) and estrus detection was performed twice daily from D-20 to D-10. All animals received an intravaginal P4-releasing device (1g; Sincrogest) on D-10 along with an intramuscular injection of 2 mg estradiol benzoate (Sincrodiol, Ouro Fino). Simultaneously, cows in the LF-LCL received an intramuscular injection of PGF. The P4 devices were removed on day -2, 42 h and 30 h before the GnRH injection in the LF-LCL and the SF-SCL groups, respectively. All animals received a PGF injection at P4 device removal and a second PGF

injection 6 h later. Ovulation was induced by an injection of GnRH agonist on D0. In order to assess growth and ovulation of the pre-ovulatory follicle (POF) and CL area, transrectal ultrasound examinations were carried out on D-10 and daily from D-2 to D4, and color Doppler mode was used to detect signals of CL blood flow. Ultrasonography was performed with the aid of a duplex B-mode (gray-scale) and pulsed-wave color Doppler ultrasound instrument (MyLab30 Vet Gold; Esaote Healthcare, São Paulo, São Paulo, Brazil) equipped with a multifrequency linear transducer. All Doppler scans were performed at a constant gain setting for color. Retrospective interpretation of changes in follicular diameters over time allowed the identification of the dominant follicle of the estradiol benzoate-induced wave, the determination of the POF diameter, and the day of ovulation. Ovulation was defined as the disappearance of the previously identified POF followed by the observation of a CL on the same approximate topographical location on the ovary. The diameter of follicles was calculated as the average between measurements of two perpendicular axes of each structure. The maximum CL area was determined using a B-mode still image and the tracing function [31]. For CL with an anechoic fluid-filled cavity, the area of the cavity was subtracted from the total area [32].

Blood sampling and hormone measurements

Blood sampling for determination of P4 and E2 concentrations was performed once daily from D-2 to D4. Blood samples were collected by jugular venipuncture in tubes containing Heparin (BD, São Paulo, São Paulo, Brazil). Plasma was separated using centrifugation at 4°C, 1500x g for 30 minutes (min), and stored at −20°C. Plasma P4 concentrations were measured in all samples using a solid-phase radioimmunoassay (Coat-a-Count; Siemens, Los Angeles, CA, USA), as validated previously [33]. Plasma E2 concentrations were determined using a commercial RIA kit (Double Antibody Estradiol; Siemens) as reported previously [34]. The intra-assay CV and sensitivity for P4 and E2, respectively, were 0.8% and 0.05 ng/mL, and 1.7% and 0.13 pg/mL.

Tissue collection and processing

On D4, cows were stunned using a captive bolt and euthanized by jugular exsanguination at the University slaughterhouse. Reproductive tracts were transported on ice and dissected within 15 min of slaughter. The oviduct ipsilateral to the ovary containing the CL was dissected and the ampulla and isthmus regions separated. The ipsilateral side was chosen because it is the side in which oocyte, sperm, zygote, and early embryos will transit during the initial days after estrus. Furthermore, there is evidence suggesting that the ipsilateral and the contralateral sides are controlled by different transcription mechanisms [12, 35, 36].

Tissue from ampulla and isthmus regions, covering all the oviductal thickness, were either frozen in liquid nitrogen or fixed in buffered formalin prior to paraffin embedding. Transcriptome of ampulla and isthmus were evaluated because previous evidence suggested that they were morphologically [8], physiologically [2], and molecularly [37, 38] different. Furthermore regions play distinct roles in the reproductive process.

The D4 was selected because at this point, the oocyte transport, sperm transport, and fertilization have already occurred, and, if successful, an early embryo is expected to be in transit between the ipsilateral ampulla and isthmus. Our interest was to gain understanding of how the differences in the E2 and P4 concentrations during the periovulatory period affect the ampulla and isthmus transcriptome.

Immunohistochemistry

Paraffin-embedded ampulla and isthmus samples were sectioned into 4 μm sections and mounted onto an adhesive slide (StarFrost, Knittel Glass, Braunschweig, Germany). Sections

were deparaffinized in xylene, and rehydrated in a series of increasing dilutions of ethanol. Sections were incubated for 5 min in 10nM citrate buffer (pH 6) at room temperature, and then processed for 4 cycles of 5 min at 750 watts in a microwave for antigen retrieval. Slides were cooled at room temperature for 20 min and washed three times for 5 min in PBS containing 0.3% Triton (PBS/Triton; pH 7.4). Endogenous peroxidase activity was blocked by incubation in 1.5% hydrogen peroxide in methanol for 30 min at room temperature. Sections were washed in PBS/Triton (3 x 5 min). To block nonspecific binding, protein block was carried out using 2% non-fat dry milk for 15 min at room temperature. Tissue sections were incubated in a humid chamber with a mouse monoclonal anti-Progesterone Receptor (PGR) primary antibody (Clone PR10A9; 1:75 dilution; Beckman Coulter PN IM1546; France) overnight at 4°C or anti-Estrogen Receptor alpha mouse monoclonal (ER alpha; clone 1D5, 1:50 dilution; Dako; Denmark) 60 min at room temperature. Technical negative control reactions contained normal mouse IgG instead of primary antibody. Tissue sections were then washed (3x5 min) in PBS/Triton. The Biotinylated Link Universal Solution (DK0690, Dako) was used as secondary antibody, and the incubation was conducted for 15 min at room temperature in a humid chamber. Next, slides were washed in PBS/Triton buffer (3x5 min), incubated with a streptavidin- peroxidase complex (Streptavidin-HRP, K0690, DAKO) for 15 min in a humid chamber, and washed again in PBS/Triton. Sections were then incubated in diaminobenzidine (DAB, K3468, DAKO) solution for 5 min and washed in distilled water (3x5 min). Finally, sections were counterstained with hematoxylin, washed in running water for 10 min, dehydrated in a series of increasing concentrations of ethanol, cleared in xylene, and mounted on coverslips. The immunostaining procedure for each primary antibody was performed in a single run. The slides were photographed using light microscopy and immunostaining was subjectively analyzed (strong, mild, weak or no staining) in the luminal epithelium (LE), stromal cells (SC), muscular layer (ML) and serous membrane (SM).

RNA and protein isolation

Frozen ampulla and isthmus samples were ground in liquid nitrogen using a mortar and pestle and immediately mixed with buffer RLT from AllPrep® DNA/RNA/Protein Mini kit (No. 80004, Qiagen, São Paulo, São Paulo, Brazil), as recommended by manufacturer's instructions. Tissue suspension was passed at least 5 times through a 21-ga needle, and centrifuged at 13,000 x g for 3 min for removal of debris, before supernatant loading and processing in silica columns. RNeasy columns were eluted with 30 μL of RNase-free water and both, RNA and protein, were kept at −80°C. Concentration of total RNA extracts was measured using the NanoVue spectrophotometer (GE Healthcare).

RNA Sequencing (RNA-Seq): procedures and data analysis

Ampulla and isthmus samples of the three top-ranked animals in the LF-LCL group and the three bottom ranked animals in the SF-SCL group were selected for individual RNA-Seq (please see details in the Statistical Analyses section). RNA quality was assessed with the NanoVue spectrophotometer (GE Healthcare Europe, Munich, Germany; 260/280 and 260/230 nm ratios) and with the Agilent Bioanalyzer (Agilent Technologies, Palo Alto, USA; 28S/18S ratio and RNA integrity number (RIN) data). All samples had a RIN $\geq$8 and were considered suitable for RNAseq analysis. For the analysis of expression profiles in LF-LCL and SF-SCL animals, libraries were generated using a routine RNA library preparation TruSeq protocol developed by Illumina Technologies (San Diego, CA) using 1 μg of total RNA as input. Briefly, polyA selected RNA was cleaved as per Illumina protocol and the cleaved fragments were used to generate first strand cDNA using SuperScript II reverse transcriptase and random hexamers. Subsequently, second strand cDNA was synthesized with RNaseH and DNA polymerase

enzyme. Adapter ligation and end repair steps followed second strand synthesis. Resulting products were amplified via PCR and cDNA libraries were then purified and validated using the Bioanalyzer 2100 (Agilent Technologies). Paired-end sequencing of 101bp reads was performed using the Illumina HiSeq 2000 (ampulla samples) and Illumina HiSeq 2500 (isthmus samples) platforms. The quality filtering was performed by seqyClean v1.3.12. (https://bitbucket.org/izhbannikov/seqyclean/get/stable.zip) using a minimum of 26 Phred quality vector, and adaptor sequences from the Univec database (https://www.ncbi.nlm.nih.gov/tools/vecscreen/univec/) were used as guide to remove possible contaminants and minimum read length of 65 bases. Only high quality paired-end sequences were kept for further analyses. The reads were mapped with Tophat v.2.0.8 [39] and Bowtie2 v2.1.0 [40] on the masked bovine genome assembly (Bos taurus UMD 3.1, NCBI). The isoforms were obtained with the package Cufflinks v.2.1.1 [41], with the annotation file (.gtf) as guide through the option -G (the RABT assembly) and specifically the PGR gene isoforms were searched.

The mapping file was sorted using SAMTools v 0.1.18 [42] and read counts were obtained using the script from HTSeq-count v0.5.4p2 (http://www-huber.embl.de/users/anders/HTSeq/doc/count.html). The differential expression analysis was performed with package DESEq v1.12.1 [43], from R/Bioconductor [44]. Using the function "estimate Size Factors", the normalized counts were obtained (baseMean values, which are the number of reads divided by the size factor or normalization constant). The standard deviation along the baseMean values was also calculated for each transcript. In order to avoid artifacts caused by low expression profiles and high expression variance, only transcripts that had an average of baseMean > 5 and the mean greater than the standard variation were analyzed. The method to test for differential expression was the negative binomial distribution, through the nbinom Test function on DESeq. The threshold for evaluating significance was obtained by applying a p-value of 0.05 FDR- Benjamini-Hochberg [45]. The gene enrichment analysis was performed separately for each region, using the functional annotation tool of the Database for Annotation, Visualization, and Integrated Discovery (DAVID; [46] using as background the set of genes that passed through the differential expression analysis filter. In order to avoid overrepresentation of some GO similar categories, GO terms were grouped when having more than 3 common genes.

Quantitative PCR

RNA quality and quantity was measured with the NanoVue spectrophotometer and 1 μg was reverse transcribed (High Capacity cDNA Reverse Transcription Kit, Life Technologies) according to manufacturer's instructions; samples were incubated at 25°C for 10 min, followed by incubation at 37°C for 2 h and reverse transcriptase inactivation at 85°C for 5 min and storage at −20°C. The cDNA obtained was used for gene expression assays by qPCR.

Step-One Plus (Life Technologies, Carlsbad, CA) with SYBR Green Chemistry was used for the amplification analysis. Primers were designed based on GenBank Ref-Seq mRNA sequences of target genes. Sequences were masked to remove repetitive sequences with RepeatMasker (http://www.repeatmasker.org/) [47] and, then, the masked sequences were used to primer design using the PrimerQuest software (IDT1, http://www.idtdna.com/primerquest/Home/Index). The characteristics of the primers were checked in Oligo Analyzer 3.1 software (IDT1, http://www.idtdna.com/analyzer/Applications/OligoAnalyzer/), while the specificity was compared by BLAST1 (NCBI, http://blast.ncbi.nlm.nih.gov). qPCR products from reactions containing designed primers were submitted to agarose gel electrophoresis and sequencing and identities were confirmed. Details of primers are provided on Table 1.

In order to select reference genes, the GeNorm Microsoft Excel applet was used. This applet provides a measure of gene expression stability (M) [48]. Histone 2, Glyceraldehyde-

Table 1. Primer sequences of target and reference genes analyzed using qPCR.

Target gene	Gene Bank Number	Forward primer sequence (5′–3′)	Reverse sequence (5′–3′)	Primer efficiency (%)	Amplicon length (bp)
ACTB	NM_173979.3	GGATGAGGCTCAGAGCAAGAGA	TCGTCCCAGTTGGTGACGAT	2.03	77
ANGPT2	NM_001098855.1	ACCCTTCAGGTGAACACTGG	CGTGAGGCCTTTAAGGTGAA	2.03	178
ANGPT4	NM_001076483.2	ACCCTCATTCAGCGCCGTGA	GCTGGGTTGCCAAAGCCCTGTT	2.06	83
CADM3	NM_001075946.1	AACCTCTCCCAGGACGACAGT	TCTGCTGGGCAGGGTTAGAC	1.93	133
C-MET	NM_001012999.2	AGGTCGATTCATGCAGGTTGT	TTTAGCGGGTGCTCCACAAT	1.98	114
CTGF	NM_174030.2	CGTGTGCACCGCTAAAGATG	TCCGCTCTGGTACACAGTTCCT	2.06	61
CTSS	NM_001033615.2	AGAAGCCGTGGCCAATAAA	CTTCCCGTCAAGGTTACCATAG	2.10	157
CXCR4	NM_174301.3	AAAGTGACCCTGAGGACTTGAGTAG	CCGGAAGCAGGGTTCCTT	2.03	153
EDN1	NM_181010.2	GAGTGTGTCTACTTCTGCCATC	CTAGCACACTGGCATCTCTTC	2.10	158
ESR1	XM_002690343.1	CAGGCACATGAGCAACAAAG	TCCAGCAGCAGGTCGTAGAG	2.05	82
ESR2	NM_174051.3	GTAGAGAGCCGCCATGAATAC	CAATGGATGGCTAAAGGAGAGA	1.96	161
GAPDH	NM_001034034.2	GCCATCAATGACCCCTTCAT	TGCCGTGGGTGGAATCA	1.93	69
HISTONA 2	AY835842.1	GAGGAGCTGAACAAGCTGTTG	TTGTGGTGGCTCTCAGTCTTC	1.93	103
HPSE	NM_174082.2	CGGATTGTTGAGAAGATCAGA	AAGGTGTTGGACAGGAAGGG	1.92	94
HSPA1A	NM_203322.2	CACCATCACCAACGACAA	CTTGTCCAGCACCTTCTTC	2.08	181
OVGP1	NM_001080216.1	CCGCTGGACCTTTGTCTTCT	GAAATCCAGGAGTCTGCCCA	1.93	166
PCNA	NM_001034494.1	TTGGCTCCCAAGATCGAGGATGAA	TGTGCTGGCATCTCAGAAGCAGTT	1.95	98
PDGF	NM_001083706.1	TCTCTGATCCCAATGCACCG	TCGGTACAAGTCATCTCGCC	1.99	147
PGR	NM_001205356.1	GCCGCAGGTCTACCAGCCCTA	GTTATGCTGTCCTTCCATTGCCCTT	1.97	199
PGR1	NM_001202474.3	ACTACCTGAGGCCGGATT	CCCTTCCATTGCCCTCTTAAA	2.03	163
PGRMC2	NM_001099060.1	CAGGGGAAGAACCGTCAGAA	ATGAAGCCCCACCAGACATT	1.98	168
PPIA	NM_178320.2	GCCATGGAGCGCTTTGG	CCACAGTCAGCAATGGTGATCT	2.02	64
RGS20	NM_001076327.1	CGTCTAGGACAGGGACTTTAGA	GAACACACTACTGCCACCATAA	2.09	198
RPL15	NM_001077866.1	TGGAGAGTATTGCGCCTTCTC	CACAAGTTCCACCACACTATTGG	1.99	64
TGFB2	NM_001113252.1	AATTTGGTGAAGGCCGAGTTC	GGTTTTCACGACTTTGCTCCA	1.95	149
TGFB3	NM_001101183.1	TTACTGCTTCCGCAATTTCA	TCTGAGCTGCGGAGGTATG	1.94	149
TGFBR1	NM_174621.2	GATTCGGCCACGGATACAA	GTCGAGCTACTTCCCAGAATAC	1.94	165
TGFBR2	NM_001159566.1	AAGTCGGTTAACAGCGATATGATG	TCCGGCTTCTCGCAGATG	2.04	154
VCL	NM_001191370.1	GCTGTTCAAGGGAGTAATAGG	TTCTGGCTTTGGGAAGAAATA	2.07	153

doi:10.1371/journal.pone.0145321.t001

3-Phosphate Dehydrogenase (GAPDH), Actin Beta (ACTB), Cyclophilin A (PPIA), Ribosomal Protein L15 (RPL15) Ct values were converted to scale expression quantities using the delta-Ct method and entered into geNorm. Genes were ranked based on M values, where the genes with the most stable expression had the lowest values. Data was analyzed in geNorm initially using all five genes and then the two most stable genes (PPIA, GAPDH) were selected. Determination of qPCR efficiency and Cq (quantification cycle) values per sample were performed with LinRegPCR software (V2014.2; http://linregpcr.nl/). Quantification was obtained after normalization of the target genes expression values (Cq values) by the geometric mean of the endogenous control expression values PPIA and GAPDH. In order to validate RNAseq analysis results, qPCR was conducted on a subset of 23 genes. We selected genes from the following functional categories, relevant to oviductal biology: sex-steroid receptors [Estrogen Receptor 1 (ESR1) and 2 (ESR2), progesterone receptor (PGR), progesterone receptor membrane component 2 (PGRMC2), and Regulator Of G-Protein Signaling 20 (RGS20)], angiogenesis [angiopoietin 2 (ANGTP2) and 4 (ANGTP4), and endothelin 1 (EDN1)], cellular proliferation [connective tissue growth factor (CTGF), MET proto-oncogene receptor tyrosine kinase

(C-MET), proliferating cell nuclear antigen (PCNA), platelet derived growth factor D (PDGFD), transforming growth factor beta 2 (TGFB2) and 3 (TGFB3), transforming growth factor beta receptor 1 (TGFBR1) and 2 (TGFBR1),], extracellular matrix [cell adhesion molecule 3 (CADM3), chemokine (C-X-C motif) receptor 4 (CXCR4), heparanase (HSPE), and vinculin (VCL)], synthesis of glycoproteins [cathepsin S (CTSS) and oviductal glycoprotein 1 (OVGP1)], and cellular chaperone [Heat Shock 70kDa Protein 1A (HSPA1A)].

Statistical analyses

Prior to the statistical analyses, animals were evaluated according to the criteria we established in order to determine whether minimal premises were matched. Animals were removed from the experiment if: POF diameter on D0 was smaller than 8 mm, ovulation was detected at the D0 ultrasound examination or before (i.e. early ovulation), ovulation was detected at the D3 ultrasound examination (i.e., late ovulation), ovulation was not detected, and follicular or luteal cysts were detected at any moment during the experiment. According to these criteria, 13 animals of LF-LCL and 8 animals of SF-SCL that ovulated within 24–36 h of GnRH injection were used. In order to select the samples for the different laboratory analyses, animals in each group (LF-LCL and SF-SCL) were ranked according to the following ovarian and endocrine variables: maximum diameter of the POF and E2 concentration at D -1, CL area and P4 concentrations at D4. Then, ampulla and isthmus samples of the top-ranked animals in the LF-LCL group and the bottom ranked animals in the SF-SCL group were selected (RNAseq analyses: 3 animals per group; IHQ analyses: 5 animals per group; qPCR: 7 animals per group).

Data was tested for normality of residuals and homogeneity of variances. Ovarian and endocrine variables were analyzed for the main effect of group (LF-LCL vs. SF-SCL) by one-way ANOVA using the GLM procedure of SAS. The E2 and P4 concentration were analyzed for the main effect of group and time by repeated split-plot ANOVA using SAS PROC GLM. Transcript abundance was analyzed by two-way ANOVA, considering the main effects of group and region (isthmus and ampulla) and the interaction of group by region. All data will be shown as mean ± standard error of mean.

Results

Animal model

Forty one animals were synchronized in order to obtain the two experimental groups. Only 21 remain in the experiment (13 animals of LF-LCL and 8 animals of SF-SCL) after fulfilling all the premises required. As planned, hormonal manipulations successfully generated distinctly different groups of animals regarding both ovarian and endocrine variables. Specifically, on D-1, diameter of the POF in LF-LCL (15.70 ± 0.43 mm) was greater than in the SF-SCL group (11.31 ± 0.23 mm; $P < 0.01$). In agreement with these findings, E2 plasma concentrations were affected by time ($P < 0.01$) and group ($P = 0.02$), and were greater in the LF-LCL than in the SF-SCL cows in D-2, D-1 and D0 (Fig 2). Regarding the CL values at D4, a group effect was found in CL area but not in CL blood flow. At D4, CL of LF-LCL animals had an area of 1.39 ± 0.08 mm^2 and 43.75± 3.83% of blood flow. In comparison, SF-SCL animals achieved 1.02 ± 0.09 mm^2 of area ($P < 0.01$) and 36.25± 4.12% blood flow ($P > 0.1$). Plasma P4 concentration was also affected by time ($P < 0.01$) and group ($P = 0.03$) effects being greater for LF-LCL than SF-SCL group on day 4 (Fig 2).

Tissue responses to the endocrine changes elicited by the animal model are modulated by specific receptors. Thus, using 7 animals per group, abundance of transcripts of nuclear *ESR1*, *ESR2 and PGR* and membrane *PGRMC-2* were quantified in both oviduct regions.

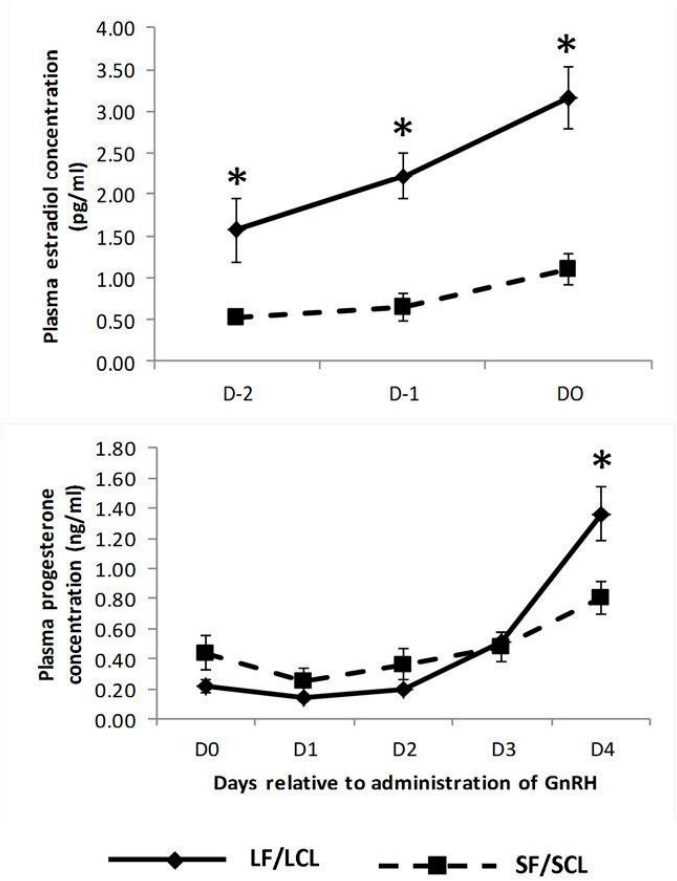

Fig 2. Plasma concentrations (mean ± SEM) of estradiol (top panel) and progesterone (bottom panel) of cows in the LF/LCL group (n = 13) and in the SF/SCL group (n = 8). Within a given Day, significantly different means (P < 0.05) were indicated by an asterisk (*). LF/LCL, large follicle-large CL; SF/SCL, small follicle-small CL.

doi:10.1371/journal.pone.0145321.g002

There was no region, treatment or interaction effect on the expression of *PGR* or *PGRMC-2* genes (Table 2). Using 5 animals per group, immunohistochemistry was performed using an ERa antibody and a PGR antibody that does not discriminate the PGR isoforms. The PGR immunostaining pattern was different between LF-LCL and SF-SCL animals (Fig 3; S1 Fig). Animals of the LF-LCL group showed similar strong immunostaining in the ampullar and isthmus LE, a weak staining in the SC, a mild staining on the ML, and no positive immunostaining in the SM (Table 3). In contrast, isthmus SF-SCL samples presented a mild immunostaining in LE, a weak staining in SC and ML, and no positive staining in the SM. However, SF-SCL ampullary samples had weak staining in SC and ML, and no staining in LE and SM (just one of five animals of the SF-SCL group showed moderate staining in the LE). *ESR1* expression was greater in the ampulla than in the isthmus (Fold Change: 1.65; $P<0.001$), but it was similar between treatments; no region or treatment effects were found for *ESR2* expression (Table 2).

Table 2. Relative Abundance of transcripts of different genes in the ampulla and isthmus of LF/LCL and SF/SCL Animals (n = 14).

Gene	LF/LCL		SF/SCL		*P* Value		
	Ampulla	Isthmus	Ampulla	Isthmus	Group	Region	Interaction
ANGPT2	0.225 ± 0.03	0.291 ± 0.092	0.230 ± 0.040	0.221 ± 0.069	0.61	0.87	0.77
ANGPT4	0.095 ± 0.016	0.238 ± 0.097	0.085 ± 0.017	0.221 ± 0.055	0.84	< 0.01	0.63
CADM3	0.496 ± 0.089	0.103 ± 0.055	0.257 ± 0.122	0.108 ± 0.027	0.96	0.45	0.57
C-MET	0.069 ± 0.007	0.083 ± 0.012	0.052 ± 0.016	0.064 ± 0.019	0.04	0.01	0.31
CTGF	0.192 ± 0.018	0.197± 0.104	0.164 ± 0.044	0.198 ± 0.048	0.58	0.41	0.83
CTSS	0.501 ± 0.061	0.305 ± 0.042	0.404 ± 0.074	0.456 ± 0.046	0.29	0.96	0.72
CXCR4	0.021 ± 0.000	0.016 ± 0.000	0.002 ± 0.000	0.001 ± 0.000	0.02	<0.001	0.28
EDN1	0.170 ± 0.013	0.211 ± 0.029	0.121 ± 0.008	0.444 ± 0.082	0.02	<0.001	0.72
ESR1	0.588 ± 0.057	0.326 ± 0.034	0.504 ± 0.040	0.335 ± 0.055	0.38	<0.001	0.48
ESR2	0.398 ± 0.07	0.294 ± 0.092	0.327 ± 0.076	0.22 ± 0.032	0.77	0.48	0.51
HPSE	0.338 ± 0.068	0.071 ± 0.050	0.256 ± 0.115	0.019 ± 0.003	0.03	<0.001	0.76
HSPA1A	0.290 ± 0.069	0.111 ± 0.036	0.367 ± 0.085	0.199 ± 0.128	0.88	0.01	0.96
OVGP1	0.118 ± 0.052	0.012 ± 0.010	0.233 ± 0.096	0.016 ± 0.010	0.62	<0.001	0.56
PCNA	0.949 ± 0.209	0.913 ± 0.174	0.622 ± 0.112	1.144 ± 0.144	0.30	0.13	0.33
PDGF	0.044 ± 0.003	0.032 ± 0.007	0.034 ± 0.007	0.028 ± 0.006	0.01	0.04	0.68
PGR	0.308 ± 0.030	0.311 ± 0.036	0.371 ± 0.064	0.317 ± 0.031	0.83	0.49	0.34
PGRMC2	0.479 ± 0.014	0.346 ± 0.078	0.450 ± 0.020	0.445 ± 0.043	0.26	0.24	0.46
RGS20	0.370 ± 0.101	0.220 ± 0.097	0.272 ± 0.077	0.291 ± 0.007	0.02	0.05	0.69
TGFB2	0.499 ± 0.060	0.520 ± 0.062	0.581 ± 0.032	0.331 ± 0.042	0.12	0.11	0.83
TGFB3	0.154 ± 0.02	0.572 ± 0.092	0.218 ± 0.046	0.36 ± 0.036	0.05	<0.001	0.98
TGFBR1	0.174 ± 0.052	0.291 ± 0.140	0.295 ± 0.107	0.181 ± 0.130	0.83	0.84	0.69
TGFBR2	0.163 ± 0.017	0.204 ± 0.104	0.071 ± 0.029	0.127 ± 0.044	0.60	0.01	0.66
VCL	0.086 ± 0.009	0.379 ± 0.060	0.016 ± 0.010	0.307 ± 0.042	0.03	0.01	0.12

Relative expression level normalized against Normalization factor for the most stable genes (GAPDH and PPIA) provided by geNorm.

doi:10.1371/journal.pone.0145321.t002

The immunostaining of the ERa showed also differences between groups and between regions (Table 3). There was a stronger immunostaining in the ampulla and isthmus in the LF-LCL group than the SF-SCL group (Fig 3; S2 Fig). Based on immunohistochemical data, greater abundance of PGR and ERa for the LF-LCL group indicates a greater availability of receptors and, possibly, sex steroids stimulated signaling, both in the ampulla and isthmus in this group of animals. Interestingly, protein staining intensities were not consistent with respective PGR and ESR1 transcript abundances.

RNA-Seq analyses

Ampulla RNAseq. The ampulla RNAseq produced a total of ~157 million reads with an average of 30 million reads for each sample. Three biological replicates were analyzed for each group with the reads ranging from 29–36 million per sample after filtering (S1 Table). After using HTSeq-count, approximately ~60% of the total reads uniquely mapped to the UMD 3.1 reference genome, excluding also reads that aligned ambiguously. There were approximately 10% of not-uniquely mapped reads, 15% non-specifically mapped reads, and 15% unmapped reads. Only the uniquely mapped reads were considered in the analysis. One sample of the LF-LCL group was discarded from the RNA-Seq analyses, due to inadequate library quality resulting in few reads. In order to categorize the genes with different level of expression, a multiphasic graph was obtained by plotting the log2 transformed baseMean values versus all

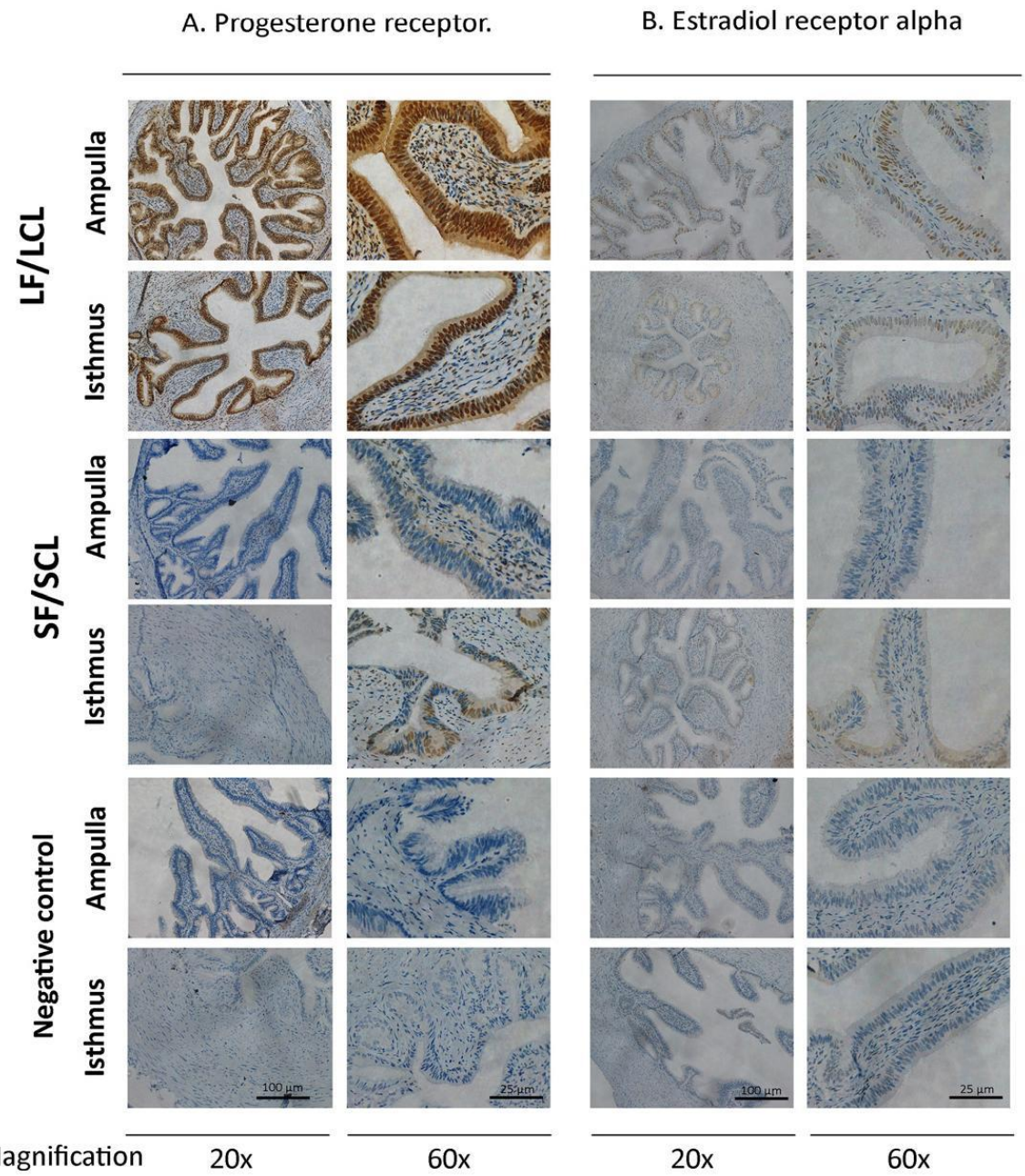

Fig 3. Localization of Progesterone receptor (PGR) and Estradiol receptor alpha (Er alpha) in the bovine oviduct by immunohistochemistry. Representative images of PGR and ER alpha immunohistochemical localization in the ampulla and the isthmus of LF/LCL and SF/SCL groups at Day 4 of the estrous cycle (n = 5 per group). Original magnification: 20x (scale bar: 100 µm) and 60x (scale bar: 25 µm). For an overview of PGR and ER alpha staining on samples of all animals see S1 and S2 Figs.

doi:10.1371/journal.pone.0145321.g003

Table 3. Subjective scores* of PGR staining in ampulla and isthmus on day 4 of the cycle of LF/LCL (n = 5) and SF/SCL (n = 5) animals.

Marked Protein	Region	Group	Mucous Membrane		Muscular Layer	Serous membrane
			Luminal epithelia	Stromal cells		
PGR	Ampulla	LF/LCL	+++	+	+	0
	Isthmus		+++	+	++	0
	Ampulla	SF/SCL	0	0	0	0
	Isthmus		++	+	+	0
ESR1	Ampulla	LF/LCL	++	++	+	0
	Isthmus		+++	+++	+	0
	Ampulla	SF/SCL	+	0	0	0
	Isthmus		++	+	0	0

* The staining intensity was evaluated using a four-point scoring scale: Strong (+++), mild (++), weak (+) or no staining (0).

doi:10.1371/journal.pone.0145321.t003

expressed genes from the *Bos taurus* genome. According to the phases in the graph, gene expression values were categorized into three groups: high (≥ 1000 reads normalized or base-Mean), medium (≥ 15 to 1000 baseMean), and low (< 15 baseMean) expression genes. There were 3,379 (25.6%) highly expressed genes, 10,456 (67.4%) medium expressed genes, and 1,107 genes (7%) with low expression. There were 2,123 (13.6%) and 2,162 (13.9%) highly expressed genes in SF-SCL and LF-LCL, and 449 (2.8%) and 485 (3.1%) lowly expressed genes in SF-SCL and LF-LCL, respectively. After applying the variance and minimal value of baseMean filtering, a total of 15,815 genes were included on the differential expression analysis (see MAplot on Fig 4A). A total of 692 out of the 15,815 analyzed genes showed differential expression, of which 325 and 367 were up-regulated in the ampulla of LF-LCL and SF-SCL samples, respectively. Differentially expressed genes, their respective Log2fold-changes and phenotype expression profiles averages are listed on the (S2 Table). Clustering analysis clearly separated the overall transcriptome signatures of the two groups indicating distinct tissue-specific characteristics of the expression profiles (Fig 5A). All reads sequences were deposited in the Sequence Read Archive (SRA) of the NCBI (http://www.ncbi.nlm.nih.gov/sra/; S3 Table), and an overview of this data has been deposited in NCBI's Gene Expression Omnibus (GEO) and is accessible through GEO Series accession number GSE65681.

Additionally, using an expanded number of individuals (n = 7 per group), we validated the differential expression data for 23 genes by qPCR (S4 Table). Validation showed agreement of the expression patterns of the RNA-seq results and the qPCR results.

Isthmus RNAseq. The isthmus RNAseq produced a total of ~451 million reads with an average of 75 million reads for each sample. Three biological replicates were analyzed for each group with the reads ranging from 63–80 million per sample after filtering (S1 Table). After using HTSeq-count, approximately ~60% of the total reads uniquely mapped to the UMD 3.1 reference genome and there were approximately 10% of not-uniquely mapped reads, 15% non-specifically mapped reads, and 15% unmapped reads. Only the uniquely mapped reads were considered in the analysis. As in the ampulla RNAseq, a multiphasic graph was obtained and gene expression values were categorized into three groups: high (≥ 1000 reads normalized or baseMean), medium (≥ 15 to 1000 baseMean), and low (< 15 baseMean) expressed genes. There were 6,212 (28%) highly expressed genes, 8,935 (35.8%) medium expressed genes and 9,759 genes (36.2%) with low expression. There were 2,059 (12.9%) and 413 (2.5%) highly expressed genes in SF-SCL and LF-LCL, and 10,268 (41.7%) and 11,700 (47.5) % lowly expressed genes in SF-SCL and LF-LCL, respectively.

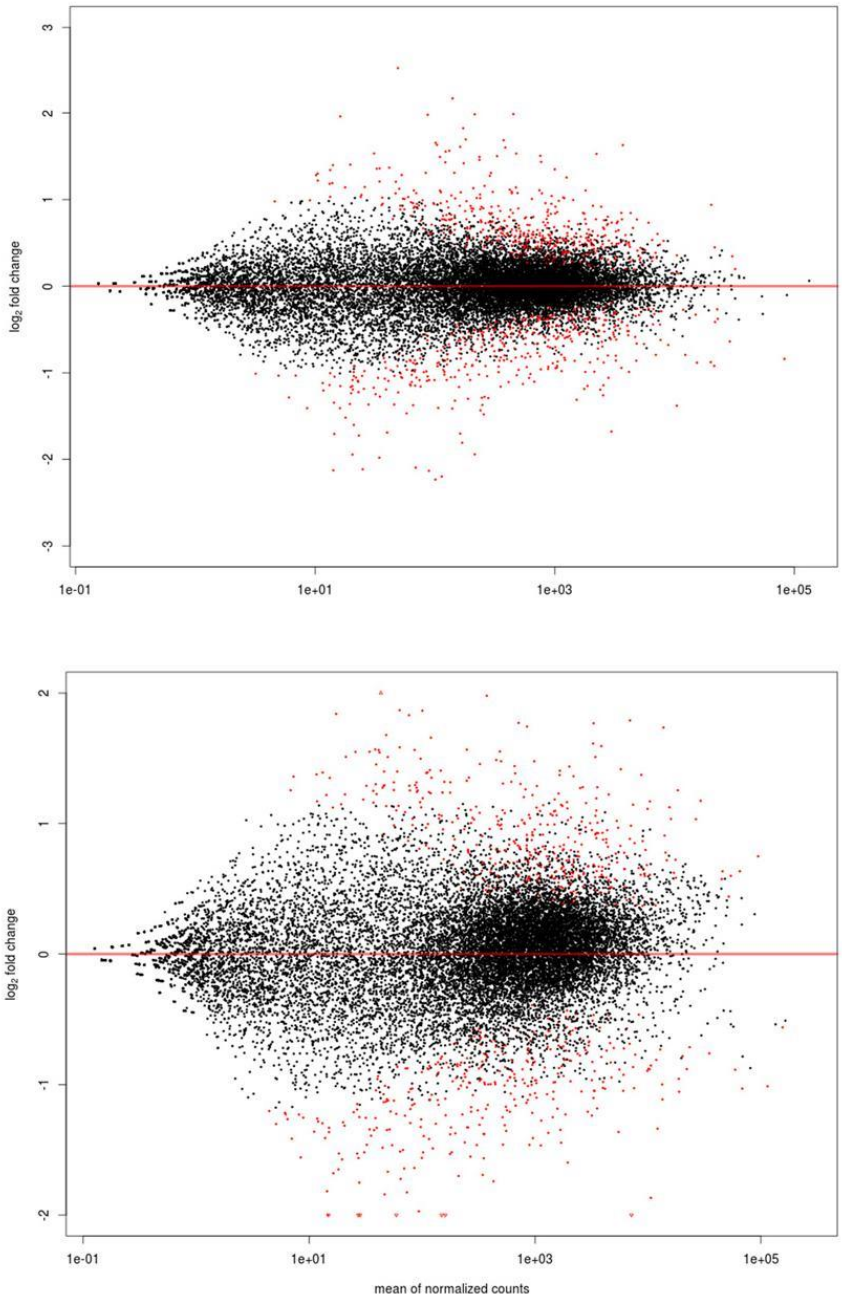

Fig 4. MA Plot showing ampulla (A; n = 5 samples) and isthmus (B; n = 6 samples) gene expression of LF/LCL and SF/SCL groups, in terms of the differentially expressed genes (p < 0.001).

doi:10.1371/journal.pone.0145321.g004

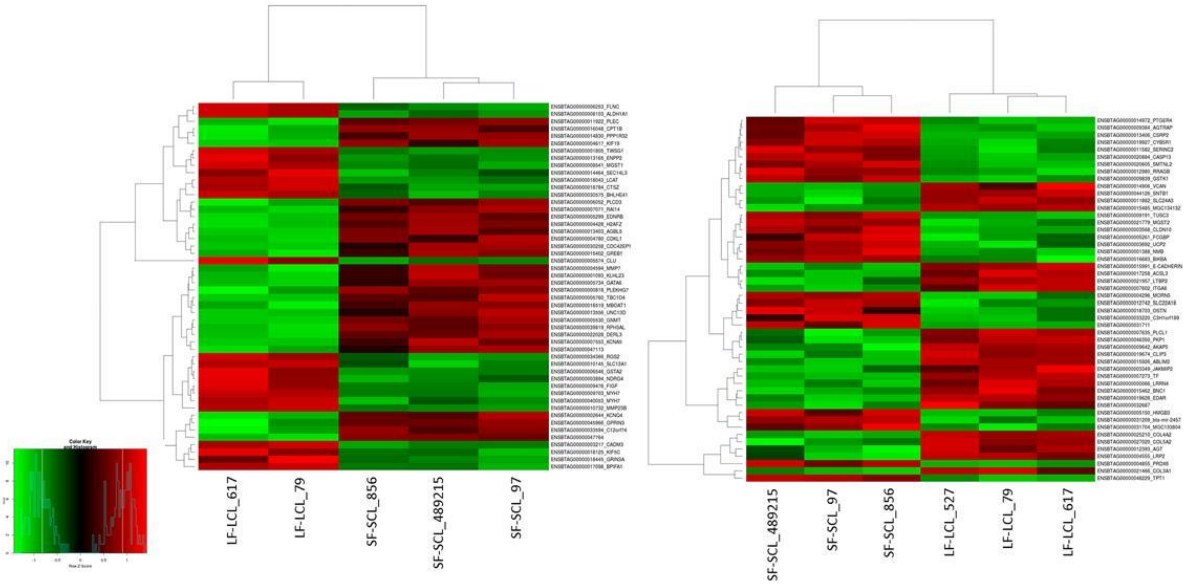

Fig 5. Heat map constructed by clustering of the 50 most differently expressed genes between LF/LCL and SF/SCL in the ampulla (n = 5) and the isthmus (n = 6). The colors in the map display the relative standing of the reads count data; GREEN indicates a count value that is lower than the mean value of the row while red indicates higher than the mean. The shades of the color indicate distance from each data point to the mean value of the row. Columns represent individual samples of LF/LCL and SF/SCL.

doi:10.1371/journal.pone.0145321.g005

After applying the variance and minimal value of baseMean filtering, a total of 15922 genes were included on the differential expression analysis (see MAplot on Fig 4B). A total of 590 out of the 15,922 analyzed genes showed differential expression, of which 274 and 316 were up-regulated in the isthmus of LF/LCL and SF/SCL samples, respectively. Differentially expressed genes, their respective Log2fold-changes and phenotype expression profiles averages are listed on the (S5 Table). Clustering analysis clearly separated the overall transcriptome signatures of the two groups indicating distinct tissue-specific characteristics of the expression profiles (Fig 5B). In addition, the reads sequences were deposited in the SRA (S3 Table), and the reads count was deposited in GEO under the same series accession number as that of the ampulla data. Validation of RNA-Seq data by qPCR was accomplished for 23 isthmus genes using an expanded number of animals (n = 7/group; S6 Table).

Functional enrichment analysis of RNA-Seq results

Using the ampulla RNAseq data, 43 GO terms were enriched on the LF-LCL samples (S7 Table), while only 29 were enriched on SF-SCL samples (p-adjusted < 0.1; S8 Table). Likewise, using the isthmus RNAseq data, 96 and 26 GO terms were enriched in LF-LCL and SF-SCL groups, respectively (S9 and S10 Tables).

The clustering of GO terms with at least three common genes is presented in Table 4. Using these criteria, terms associated with immune cell activation, vacuole and lysosome, homeostasis, cytoskeleton and extracellular matrix (ECM), chemokine signaling, plasma lipoprotein, and GTP binding were presented in the LF-LCL ampulla. In the SF-SCL ampulla, terms associated with cell development, differentiation and motility, and voltage-gated channel activity

Table 4. Group of the repeated GO terms in enriched processes. Using the gene enrichment data, similar GO terms were grouped when having 3 or more common genes.

Region and Group	Enriched process	Genes
Ampulla LF/ LCL	Immune cell activation	*BCL10*, *CD3E*, *CENPF*, *IL2RG*, *SASH3*
	Vacuole and lysosome	*ACP2*, *BCL10*, *GJA1*, *CTSS*, *PRDX6*, *C1orf85*, *FUCA1*, *CTSZ*, *GBA*
	Homeostasis	*MT3*, *GLRX5*, *PRDX6*, *NXN*, *NAB2*, *CAV1*, *SELT*, *PLN*, *SH3BGRL3*, *CD52*
	Cytoskeleton and extracellular matrix	*PFN1*, *MAPT*, *ARPC4*, *MYH7*, *PDLIM7*, *ACTB*, *PBXIP1*, *CTNNA1*, *ACTR2*, *CDC42SE1*, *ACTN1*, *S100A8*, *FGA*, *TWSG1*, *LOXL1*, *LAMA4*, Uncharacterized protein (ENSBTAG00000009703), *ELMO1*, *PLS3*, *CTNNA1*, *VCL*, *FIGF*, *MMP23B*, *LGALS1*, *SPOCK1*, *LCAT*, *LOXL1*, *ANGPTL1*
	Chemokine signaling	*VAV1*, *GNAI2*, *CLDN4*, *ACTB*, *CTNNA1*, *PLCG1*, *CXCR4*, *VCL*, *ACTN1*, *ELMO1*, *PAK1*, *GNG11*, *GNG10*, *CXCL10*, *CXCL14*
	Plasma lipoprotein	*LCAT*, *SAA3*, *SAA1*
	GTP binding	*GNAI2*, *RIT1*, *SEPT11*, *GEM*, *MRAS*, *RASEF*, Uncharacterized protein (ENSBTAG00000037510), *GIMAP7*, *GBP4*, *TUBA1B*, *RASL11B*
Ampulla SF/ SCL	Cell development, differentiation and motility	*PAX6*, *ABI2*, *EDNRB*, *IL16*, *EFNA5*, *KDR*, *TGFB2*, *EFNB1*, *GATA6*, *VEZF1*
	Voltage-gated channel activity	*KCNRG*, *KCTD1*,*KCNJ11*, *CACNB2*, *KCNQ4*, *KCNA5*, *KCNAB1*, *SLC4A4*, *SLC38A11*, *SCO2*, *LASP1*
	Ephrin receptor binding	*EFNB1*, *TIAM1*
	Adherens junction	*CTNNA2*, *ABI2*, *CXADR*, *LASP1*
Isthmus LF/ LCL	Cellular matrix	*H18*, *E-CADHERIN*, *CDH19*, *FN1*, *CCDC80*, *VCAN*, *BMP4*, *COL1A1*, *COL3A1*, *COL4A1*, *LUM*, *EPDR1*, *AGT*, *MGC142792*, *PI16*, *COLEC12*, *CHRNA1*, *MMP14*, *SV2A*, *LOX*, *ADAMTS2*, *ITGA11*, *DSG3*, *COL18A1*, *LAMC1*, *FBLN1*, *COL4A6*, *COL4A2*, *COL6A2*, *COL8A1*, *C1QTNF3*, *COL5A3*, *ASPN*, *ADAMTS4*, *IGF-I*, *SMOC2*, *MMP24*, *LTBP1*, *PCD*, *NGFR*, *ADAM23*
	Morphogenesis and cell proliferation	*MMP14*, *AGT*, *IGF-I*, *BMP4*, *ADAMTS2*,*LOX*, *HNF1A*, *COL1A1*, *NGFRCOL8A1*, *PDGFD*, *C-MET*, *BMI1*, *NGFR*, *F2R*, *IL1B*, *KCNMA1*, *E-CADHERIN*, *FOXL2*, *C-MET*
	Homeostasis	*F2R*, *SELV*, *HNF1A*, *CHRNA1*, *KCNMA1*, *TF*, *SV2A*, *IGF-I*, *CACNA1G*, *ITPR1*
	Ion transport	*CAPN11*, *LTBP2*, *EPDR1*, *LTBP1*, *NPNT*, *DSG3*, *MMP14*, *CDH19*, *MMP24*, *FKBP9*, *FKBP10*, *FBLN7*, *MYLK*, *E-CADHERIN*, *VCAN*, *ITPR1*, *FBLN1*, *CAPN1*, *PCDH18*, *KCNMA1*, *ACTN3*, *PLCB1*, *SMOC2*, *C1S*, *PLCL1*, *COLEC12*, *F2R*, *GRIN2D*, *P2RX3*, *ATP2B3*, *CACNA1G*, *CHRNA3*, *GABRA1*, *CHRNA1*, *CLCN4*, *CLIC4*, *GRIA3*, *KCNA4*, *TF*, *MOCOS*, *PLOD1*, *MGC142792*, *RGNEF*, *ADAMTS4*, *BNC1*, *ENPP1*, *BMI1*, *CLIC4*, *NMNAT1*, *TRIM9*, *JAZF1*, *PKLR*, *PPM1L*, *ADAM23*, *ADAMTS2*, *LOX*, *RORB*, *SLC12A2*
	Glycoprotein	*TFPI2*, *PLOD1*, *TF*, *ADAMTS4*, *LTBP2*, *KCNA4*, *PROCR*, *EPDR1*, *CHRNA3*, *GABRA1*, *GPM6A*, *PI16*, *SV2A*, *C7*, *FN1*, *LRRC8C*, *HYAL1*, *FKBP9*, *FKBP10*, *E-CADHERIN*, *VCAN*, *EDNRA*, *ASPN*, *COL3A1*, *C-MET*, *F2R*, *PCDH18*, *COL1A1*, *ACPP*, *CHRNA1*, *ADAMTS2*, *PTGDR*, *C1S*, *LOX*, *COLEC12*, *ANGPTL1*, *COL4A1*, *LUM*, *BMP4*, *MYOC*, *IL1B*, *CST9L*, *SRPX2*, *COL4A2*, *IGF-I*, *COL1A1*, *CHRNA3*, *KCNMA1*, *AGT*
Isthmus SF/ SCL	Protein kinase	*ROPN1*, *SPA17*, *ROPN1L*, *CABYR*
	Apoptosis	*TMBIM6*, *BNIPL*, *WDR92*, *CLU*, *TNS4*, *ITM2B*, *CASP8*, *CASP13*, *IFI6*
	Protein folding	*HSPA8*, *DNAJB1*, *HSPH1OSGEP*, *MME*, *PRDX6*, *RNF114*, *CBLC*
	Cellular metabolism	*GGT6*, *GSTK1*, *MGST1*, *MGST2*, *VNN1*, *BLVRA*, *NADSYN1*, *HS3ST5*, *SLC1A3*, *PCYOX1L*, *QSOX1*
	Antigen processing and presentation	*HSPA8*, *BOLA*, *HSPA1A*, *HSP90AA1*, *IFI30*, *HLA-DMB*, *FCGRT*, *AZGP1*
	Nucleotide biosynthetic process	*GUCY1B1*, *HPRT1*, *ATP5F1*, *ATP5S*, *ADSS*, Uncharacterized protein (ENSBTAG00000005217), *GUCY2C*, *NADSYN1*
	Lipid biosynthetic process	*ALG10*, *THG1L*, *TPST2*, *MBOAT7*, *HPRT1*, *MGST1*, Uncharacterized protein (Uncharacterized protein (ENSBTAG00000005217), *CEPT1*, *OAT*, *MGST2*, *GGT6*, *GSTK1*, *CKMT1*, *PIGW*, *B3GNT8*, *DDR1*, *MAPK13*, *HS3ST5*, *ACAA2*, *CPT1B*, *PAK1*, *LPCAT4*, *AS3MT*, *ACAA2*

doi:10.1371/journal.pone.0145321.t004

were found. In the LF-LCL isthmus samples, terms related with cellular matrix, morphogenesis and cell proliferation, homeostasis, ion transport, and glycoprotein were founded; while in the

SF-SCL isthmus samples, the enriched terms were protein kinase, apoptosis, protein folding, cellular metabolism, antigen processing and presentation, nucleotide biosynthetic process, and lipid biosynthetic process.

It is noteworthy that both regions in the LF-LCL group had enriched ECM and homeostasis GO terms. The ECM is composed of fibrous collagen and non-collagen proteins (glycoproteins and proteoglycans), which bind to proteins on cell surface promoting a variety of cellular responses including survival, proliferation, adhesion, and migration [49, 50]. In the present study, both oviduct regions of the LF-LCL group showed enrichment of the ECM pathways. This includes increased (P adjust < 0.05; log2 fold change ranging from -1.64 to 0.375) expression of ECM constituent genes such as collagens (*COL1A1*, *COL3A1*, *COL4A1*, *COL4A6*, *COL4A2*, *COL6A2*, *COL8A1*, *COL5A3*), versican (*VCAN*), actin beta (*ACTB*), actinin alpha 1 (*ACTN1*), integrin alpha 11 (*ITGA11*), fibronectin 1 (*FN1*), and vinculin (*VCL*). It also includes remodeling enzymes such as Matrix metalloproteinases (*MMP14*, *MMP24*), ADAM Metallopeptidase Domain 23 (*ADAM23*), ADAM metallopeptidase with thrombospondin type 1 motif 2 (*ADAMTS2*) and motif 4 (*ADAMTS4*), desmoglein 3 (*DSG3*), lysyl oxidase (*LOX*), profilin 1 (*PFN1*), and fibrinogen alpha chain (*FGA*). This suggests that in those animals an active process of ECM remodeling was occurring [49].

Homeostasis is the process by which cells maintain the optimal internal conditions to support their correct function. Both regions of the LF-LCL group have enriched expression of genes associated with homeostatic processes (P adjust < 0.05; log2 fold change ranging from -1.97 to 0.-7225). Enriched genes are involved in the control of important cell processes such as Redox systems {peroxiredoxin 6 (*PRDX6*), nucleoredoxin (*NXN*), selenoprotein V (*SELV*), and selenoprotein T (*SELT*)}, Ca and K transport {potassium large conductance calcium-activated channel subfamily M alpha member 1 (*KCNMA1*), calcium channel, voltage-dependent, T type, alpha 1G subunit (*CACNA1G*), and inositol 1,4,5-trisphosphate receptor, type 1 (*ITPR1*)}, iron binding, and transport {transferrin (*TF*)}. These findings could indicate that such homeostatic processes are more prevalent in animals manipulated to ovulate larger follicles.

Additionally, when comparing the two group's isthmus region, it is noteworthy that the LF-LCL isthmus is apparently signaling for cellular proliferation, while the SF-SCL isthmus tissue is signaling for apoptosis. In the LF-LCL animals, important proliferating genes were up-regulated {insulin-like growth factor 1 (*IGF1*) and bone morphogenetic protein 4 (*BMP4*)}, while in the SF/SCL isthmus, pro-apoptotic genes were up-regulated [caspase 8 (*CASP8*) and 13 (*CASP13*)].

Treatment and region effects on the expression of candidate genes

The effects of group and region on the expression of candidate genes were analyzed (Table 2) using 7 animals per group. Genes were selected from functional categories of interest. There was no interaction (Group * Region) effect on the expression of any of the 15 genes studied. CXCR4, HPSE, PDGF and RGS20 were more expressed in LF-LCL group and in the ampulla, while C-MET, TGFB3 and VCL were more expressed in the LF-LCL group and in the isthmus. EDN1 was more expressed in the SF-SCL group and in the isthmus.

OVGP1 and *HSP1A* were more expressed in the ampulla while *ANGPT4 and TGFBR2* were more expressed in the isthmus.

Finally, there was no region or treatment effect on the expression of genes involved in cell proliferation pathway (*CTGF*, *TGFB2*, *TGFBR1* and *PCNA*), one extracellular matrix gene (*CADM3*), one angiogenic gene (*ANGPT2*) and the *CTSS* gene.

Discussion

The oviduct provides the environment for oocyte transport, fertilization, and early embryonic development. Function of the oviduct is primarily regulated by periovulatory sex steroids

hormones [17]. Timing and magnitude of changes in sex steroids concentrations around ovulation are associated with reproductive tract receptivity to the embryo and, ultimately, fertility. However, information about the cellular and molecular needs of the oviductal tissue in the early post ovulation period is lacking. Thus, the hypothesis was that the oviductal transcriptome around D4 post-ovulation is regulated by the endocrine profile in such a way that it fulfills the needs of the early developing embryo. We aimed to determine the influence of different periovulatory endocrine milieus on the ampulla and isthmus transcriptome. Using a P4/E2 based protocol to synchronize ovulations, we manipulated Nelore cows to ovulate small (SF-SCL) or large (LF-LCL) follicles that resulted in different proestrus E2 and metestrus P4 concentrations. On D4, animals were slaughtered and oviduct was collected and studied for the effect of different periovulatory endocrine milieus on gene expression. Our study was the first to identify molecular pathways using RNAseq technology in oviductal samples on D4 and in response to distinct periovulatory endocrine profiles.

In this study, we showed clearly that the oviductal transcriptome is under sex-steroid control. However, an added step of complexity is the auto-regulatory effects of E2 and P4 on their receptors. Regulation was apparently both at the transcript and protein levels, which were not coupled. The results presented herein are in line with previous data showing that PGR and ERa expression can be up-regulated in response to an E2 stimulus, which is mediated by complex transcription and translation mechanism [51, 52]. Using an in vitro rat endometrial cell culture system, it was demonstrated that after an initial E2 stimulus, *PGR* mRNA accumulation was detected after 6 h and continued to accumulate until 18 h. Remarkably, this slow and gradual *PGR* transcription rate did not parallel binding of E2 to ER, which was maximized within 30 min [51]. Furthermore, results from in vivo experiments indicated that oviductal *ESR1* and *PGR* mRNA levels increased around estrus, but increases in abundance of ERa and PGR protein were only detected in the early luteal phase [11]. An integrated interpretation of the steroid / steroid receptor protein changes reported here is that there was a prominent P4 signaling to the oviduct of cows in the LF-LCL group. It is tempting to speculate that at least part of the transcriptome changes associated with the treatment groups were due to such differences in signaling.

It is important to remember that our experimental model cannot assess the possible effects of the presence of sperm or a developing embryo on the oviductal gene expression. Others have reported that these structures could modulate the gene expression of oviductal epithelial cells [5, 53]. Therefore, future studies should be performed to assess whether cows ovulating follicles of different sizes, respond differently to the stimuli caused by sperm cells and embryos.

To gain insight on the functional role of molecular and cellular changes induced by treatments in the oviductal tissues, we took a two-pronged approach. First, we employed transcriptomics and bioinformatics tools to define the pathways and processes most significantly affected between groups and regions. Second, we studied the expression of genes selected from the literature because of their known roles on oviduct function. Regarding the first approach, enrichment analysis successfully separated the two treatment groups in the context of particular oviduct regions. Among the many enriched processes and pathways detected, we will highlight ECM remodeling and cellular homeostasis because they were commonly enriched processes between isthmus and ampulla of LF-LCL animals, and cell proliferation and apoptosis because they were opposite processes when comparing the isthmus between groups.

The ECM interacts with cells in order to both provide mechanical support and molecular signals necessary for the regulation of many processes vital to the cell, such as adhesion and migration [54], proliferation [55], angiogenesis [49], among others. The ECM comprised of collagen fibers, viscous proteoglycans and adhesive extracellular proteins, which bind proteoglycans, collagen fibers and receptors in the cell surface [50, 56]. The ECM is under constant

remodeling, as cells constantly degrade and resynthesize the ECM components to promote rapid changes in the microenvironment [49]. All the ECM protein components are subject to degradation and modification, and there are two families of metalloproteinases, including matrix metalloproteinase (MMP) and a disintegrin and metalloproteinase with thrombospondin motifs (ADAMTS). Both are specialized in degrading the ECM [57, 58]. At the beginning of the remodeling process, there is an up-regulation in the expression of genes that code for both ECM constituents and ECM remodeling enzymes [57, 58]. In the present study, both oviduct regions of the LF-LCL showed enrichment in the expression of genes related to ECM remodeling pathways, including increased expression of matrix component genes (e.g., collagens) and remodeling enzymes (e.g., MMPs and ADAMs). Also, when the *HPSE* gene was evaluated by qPCR, it was more expressed in the LF-LCL groups. Matrix reorganization is closely associated with tissue morphogenesis and cell proliferation. Both of these processes are enriched in the LF-LCL isthmus based on the expression of *MMPs*, *ADAMS*, and *IGF1* for morphogenesis, and *BMP4*, *NGFR*, *BMI1*, and *C-MET* for cell proliferation. Regarding proliferation, it is noteworthy that remodeling uncouples a variety of growth factors linked to specific ECM proteins. For example, IGF1, FIGF, FGF, and VEGF are uncoupled from the ECM during tissue injury in order to promote healing [57, 59]. In addition to the potential of increasing available growth factors via increased remodeling, transcript abundance of *IGF1* and *FIGF* are both up-regulated in the LF-LCL ampulla and isthmus, respectively. In the oviduct, synthesis and secretion of these growth factors could result in increased availability in the lumen for stimulation of embryo growth and development [37]. Indeed, addition of these factors in vitro improved embryo production [60, 61].

We speculate that higher fertility associated with the LF-LCL cows could be at least partly explained by a favorable oviductal environment that results from a balanced array of growth factors. However, more studies must be conducted in order to establish if there is agreement between transcript and protein changes associate with the LF-LCL animals, and, if an active ECM remodeling process is going on, as indicated by transcript abundance changes.

The homeostatic processes enriched in the ampulla and isthmus of animals in the LF-LCL group include genes controlling cell-Redox systems (e.g., *PRDX6*, *NXN*, *SELV*, and *SELT*), Ca and K transport (*KCNMA*, *CACNA1G*, *ITPR1*), and iron binding and transport (*TF*). Proteins with antioxidant properties reduce cellular peroxides and protect cells from reactive oxygen species-mediated damage and death. For example, the overexpression of *PRDX6* gene in *HEPA1-6* cells was associated with resistance to peroxide-induced cell death [62]. Also, the presence of reactive oxygen species in vitro could decrease the fertilization and embryo development [63]. It is possible that a more adequate redox environment in the LF-LCL group prevents embryo cellular damage and cell death. Indeed, work from our group suggests that similar redox characteristics were associated with the uterine environment on D7, comparing LF-LCL and SF-SCL cows [64].

The net result of the up-regulation of ion transporter genes could be an increase in Ca^{2+} influx at the cell level. Ca^{2+} is a universal second messenger and is involved in many cellular processes including cell proliferation, migration, and secretion. It has been long known that the influx of external Ca^{2+} into the cell is needed to induce cell proliferation and cell cycle progression in mammalian cells [65]. These results are consistent with the effects expected for ECM remodeling mentioned above. Indeed, cellular process of apoptosis and proliferation are components of growth regulation in normal epithelia [66]. Here, we reported that cows in the LF-LCL showed increased abundance of genes related to proliferation, while, in contrast, genes related to apoptotic signaling were more abundant in tissues from SF-SCL group. Another important role of increased Ca^{2+} and K signaling is smooth muscle contraction and this may be important for embryo transport to the uterus on D4 after estrus.

One final aspect that deserves attention is oviductal secretions. In that regard, animals of the LF-LCL group showed up-regulation of TF. TF is a protein that binds iron for transport into the cells and also serves as a detoxifying agent, by sequestering metals from the medium. TF has been used in order to improve blastocyst yield of serum-free culture systems [67, 68] and has been directly associated with endometrial embryo nutrition because it functions as an iron transporter to the lumen and ultimately to the conceptus [69, 70].

In summary, our study identified, for the first time, a series of functional characteristics of the oviduct that are regulated by the periovulatory sex steroid milieu and that potentially affect early embryo development and, ultimately, fertility. Characteristics include tissue morphology changes (e.g., ECM remodeling), cellular changes (e.g., proliferation and apoptosis), and secretion changes (e.g., growth factors, ions, and metal transport). Future studies are warranted to investigate specific pathways in detail. In conclusion, differences in the periovulatory sex steroid milieu lead to different oviductal gene expression profiles that could modify the oviductal environment and affect embryo survival and development.

Supporting Information

S1 Fig. Localization of PGR in the bovine oviduct by immunohistochemistry: images of PGR immunohistochemical localization in the ampulla and the isthmus of LF/LCL and SF/SCL animals at Day 4 of the estrus cycle. In each column, ampulla and isthmus samples from individual animals of the LF-LCL and SF-SCL groups are shown. Original magnification 20x, Scale bar 100 μm (n = 5 per group).
(PDF)

S2 Fig. Localization of ERalpha in the bovine oviduct by immunohistochemistry: images of ERalpha immunohistochemical localization in the ampulla and the isthmus of LF/LCL and SF/SCL animals at Day 4 of the estrus cycle. In each column, ampulla and isthmus samples from individual animals of the LF-LCL and SF-SCL groups are shown. Original magnification 20x, Scale bar 100 μm (n = 5 per group).
(PDF)

S1 Table. N raw reads, N reads post filtering, Mapped reads, uniquely mapped reads and percentage of mapped reads obtained in the RNAseq of ampulla and isthmus samples.
(DOCX)

S2 Table. Differentially expressed genes in ampulla samples (n = 5; p-adjusted < 0.1), respective expression profiles and Log2fold-changes for both treatments, LF/LCL and SF/SCL.
(DOCX)

S3 Table. Bio-project, Bio-sample, Experiment and Run accession numbers of the Raw reads resulted from the RNAseq of ampulla and isthmus samples in the SRA data base.
(DOCX)

S4 Table. log2 Fold change and P value of ampulla gene expression in LF/LCL and SF/SCL animals. Validation of RNAseq gene expression data by qPCR. qPCR data was analyzed using the same RNAseq animals (n = 5) and using 7 animals for each group (n = 14).
(DOCX)

S5 Table. Differentially expressed genes in isthmus samples (n = 6; p-adjusted < 0.1). Respective expression profiles and Log2fold-changes for both treatments LF/LCL and

SF/SCL.
(DOCX)

S6 Table. log2 Fold change and P value of isthmus gene expression in LF/LCL and SF/SCL animals. Validation of RNAseq gene expression data by qPCR. qPCR data was analyzed using the same RNAseq animals (n = 6) and using 7 animals for each group (n = 14).
(DOCX)

S7 Table. Gene ontologies (GO category) of mRNA transcripts differentially expressed in day 4 Ampulla samples of the LF/LCL group. Gene ontology analysis is performed with DAVID tools (http://david.abcc.ncifcrf.gov/tools.jsp). The enrichment p-values are corrected by Benjamini's methods. GO categories are presented according to their biological process, cellular component and molecular function.
(DOCX)

S8 Table. Gene ontologies (GO category) of mRNA transcripts differentially expressed in day 4 Ampulla samples of the SF/SCL group. Gene ontology analysis is performed with DAVID tools (http://david.abcc.ncifcrf.gov/tools.jsp). The enrichment p-values are corrected by Benjamini's methods. GO categories are presented according to their biological process, cellular component and molecular function.
(DOCX)

S9 Table. Gene ontologies (GO category) of mRNA transcripts differentially expressed in day 4 Isthmus samples of the LF/LCL group. Gene ontology analysis is performed with DAVID tools (http://david.abcc.ncifcrf.gov/tools.jsp). The enrichment p-values are corrected by Benjamini's methods. GO categories are presented according to their biological process, cellular component and molecular function.
(DOCX)

S10 Table. Gene ontologies (GO category) of mRNA transcripts differentially expressed in day 4 Isthmus samples of the SF/SCL group. Gene ontology analysis is performed with DAVID tools (http://david.abcc.ncifcrf.gov/tools.jsp). The enrichment p-values are corrected by Benjamini's methods. GO categories are presented according to their biological process, cellular component and molecular function.
(DOCX)

Acknowledgments

The authors thank the Administration of the Pirassununga campus of the University of São Paulo for providing the animals and Ourofino Saúde Animal for providing the products for pharmacological manipulation of estrous cycle. We are also thankful to the staff of the FMVZ-USP and laboratory colleagues for animal handling and technical support.

Author Contributions

Conceived and designed the experiments: AMGD GP FSM MB. Performed the experiments: AMGD MS RFS GG LLC. Analyzed the data: AMGD SCSA LLC MB. Contributed reagents/materials/analysis tools: LLC RFS MB. Wrote the paper: AMGD GP VV MB.

References

1. BROWER L, ANDERSON E. Cytological Events Associated with the Secretory Process in the Rabbit Oviduct. BIOLOGY OF REPRODUCTION1969. p. 130–48. PMID: 4257488

2. Hunter RH. Have the Fallopian tubes a vital role in promoting fertility? Acta Obstet Gynecol Scand. 1998; 77(5):475–86. PMID: 9654166
3. Hunter RH. Components of oviduct physiology in eutherian mammals. Biol Rev Camb Philos Soc. 2012; 87(1):244–55. doi: 10.1111/j.1469-185X.2011.00196.x PMID: 21883867
4. Mondejar I, Acuna OS, Izquierdo-Rico MJ, Coy P, Aviles M. The Oviduct: Functional Genomic and Proteomic Approach. Reproduction in Domestic Animals. 2012; 47:22–9. doi: 10.1111/j.1439-0531.2012.02027.x PMID: 22681295
5. Maillo V, Gaora PO, Forde N, Besenfelder U, Havlicek V, Burns GW, et al. Oviduct-Embryo Interactions in Cattle: Two-Way Traffic or a One-Way Street? Biol Reprod. 2015; 92(6):144. doi: 10.1095/biolreprod.115.127969 PMID: 25926440
6. Hunter RHF, Flechon B, Flechon JE. DISTRIBUTION, MORPHOLOGY AND EPITHELIAL INTERACTIONS OF BOVINE SPERMATOZOA IN THE OVIDUCT BEFORE AND AFTER OVULATION—A SCANNING ELECTRON-MICROSCOPE STUDY. Tissue & Cell. 1991; 23(5):641–56.
7. Kolle S, Dubielzig S, Reese S, Wehrend A, Konig P, Kummer W. Ciliary Transport, Gamete Interaction, and Effects of the Early Embryo in the Oviduct: Ex Vivo Analyses Using a New Digital Videomicroscopic System in the Cow. Biology of Reproduction. 2009; 81(2):267–74. doi: 10.1095/biolreprod.108.073874 PMID: 19299315
8. Abe H. The mammalian oviductal epithelium: Regional variations in cytological and functional aspects of the oviductal secretory cells. Histology and Histopathology. 1996; 11(3):743–68. PMID: 8839764
9. Eriksen T, Terkelsen O, Hyttel P, Greve T. ULTRASTRUCTURAL FEATURES OF SECRETORY-CELLS IN THE BOVINE OVIDUCT EPITHELIUM. Anatomy and Embryology. 1994; 190(6):583–90. PMID: 7893011
10. Ayen E, Shahrooz R, Kazemie S. Histological and histomorphometrical changes of different regions of oviduct during follicular and lutealphases of estrus cycle in adult Azarbaijan buffalo. Iranian Journal of Veterinary Research: Shiraz University; 2012. p. 42–8.
11. Ulbrich SE, Kettler A, Einspanier R. Expression and localization of estrogen receptor alpha, estrogen receptor beta and progesterone receptor in the bovine oviduct in vivo and in vitro. Journal of Steroid Biochemistry and Molecular Biology. 2003; 84(2–3):279–89. PMID: 12711014
12. Wijayagunawardane MPB, Miyamoto A, Cerbito WA, Acosta TJ, Takagi M, Sato K. Local distributions of oviductal estradiol, progesterone, prostaglandins, oxytocin and endothelin-1 in the cyclic cow. Theriogenology. 1998; 49(3):607–18. PMID: 10732039
13. Aviles M, Gutierrez-Adan A, Coy P. Oviductal secretions: will they be key factors for the future ARTs? Molecular Human Reproduction. 2010; 16(12):896–906. doi: 10.1093/molehr/gaq056 PMID: 20584881
14. Li R, Whitworth K, Lai L, Wax D, Spate L, Murphy CN, et al. Concentration and composition of free amino acids and osmolalities of porcine oviductal and uterine fluid and their effects on development of porcine IVF embryos. Molecular Reproduction and Development. 2007; 74(9):1228–35. PMID: 17342727
15. Hugentobler SA, Sreenan JM, Humpherson PG, Leese HJ, Diskin MG, Morris DG. Effects of changes in the concentration of systemic progesterone on ions, amino acids and energy substrates in cattle oviduct and uterine fluid and blood. Reproduction Fertility and Development. 2010; 22(4):684–94.
16. Buhi WC, Alvarez IM, Kouba AJ. Secreted proteins of the oviduct. Cells Tissues Organs. 2000; 166(2):165–79. PMID: 10729726
17. Bauersachs S, Ulbrich SE, Gross K, Schmidt SEM, Meyer HHD, Einspanier R, et al. Gene expression profiling of bovine endometrium during the oestrous cycle: detection of molecular pathways involved in functional changes. Journal of Molecular Endocrinology. 2005; 34(3):889–908. PMID: 15956356
18. Binelli M, Hampton J, Buhi WC, Thatcher WW. Persistent dominant follicle alters pattern of oviductal secretory proteins from cows at estrus. Biology of Reproduction. 1999; 61(1):127–34. PMID: 10377040
19. Gandolfi F, Brevini TAL, Richardson L, Brown CR, Moor RM. CHARACTERIZATION OF PROTEINS SECRETED BY SHEEP OVIDUCT EPITHELIAL-CELLS AND THEIR FUNCTION IN EMBRYONIC-DEVELOPMENT. Development. 1989; 106(2):303-&. PMID: 2591316
20. Murray MK. EPITHELIAL LINING OF THE SHEEP AMPULLA OVIDUCT UNDERGOES PREGNANCY-ASSOCIATED MORPHOLOGICAL-CHANGES IN SECRETORY STATUS AND CELL HEIGHT. Biology of Reproduction. 1995; 53(3):653–63. PMID: 7578690
21. Cigankova V, Krajnicakova H, Kokardova M, Tomajkova E. Morphological changes in the ewe uterine tube (oviduct) epithelium during puerperium. Veterinarni Medicina. 1996; 41(11):339–46. PMID: 9001134
22. Bridges GA, Mussard ML, Burke CR, Day ML. Influence of the length of proestrus on fertility and endocrine function in female cattle. Animal Reproduction Science. 2010; 117(3–4):208–15. doi: 10.1016/j.anireprosci.2009.05.002 PMID: 19500921

23. Bridges GA, Mussard ML, Pate JL, Ott TL, Hansen TR, Day ML. Impact of preovulatory estradiol concentrations on conceptus development and uterine gene expression. Animal Reproduction Science. 2012; 133(1–2):16–26. doi: 10.1016/j.anireprosci.2012.06.013 PMID: 22789700

24. Peres RFG, Claro I Junior, Sa Filho OG, Nogueira GP, Vasconcelos JLM. Strategies to improve fertility in Bos indicus postpubertal heifers and nonlactating cows submitted to fixed-time artificial insemination. Theriogenology. 2009; 72(5):681–9. doi: 10.1016/j.theriogenology.2009.04.026 PMID: 19559472

25. Forde N, Beltman ME, Duffy GB, Duffy P, Mehta JP, O'Gaora P, et al. Changes in the Endometrial Transcriptome During the Bovine Estrous Cycle: Effect of Low Circulating Progesterone and Consequences for Conceptus Elongation. Biology of Reproduction. 2011; 84(2):266–78. doi: 10.1095/biolreprod.110.085910 PMID: 20881316

26. Forde N, Mehta JP, McGettigan PA, Mamo S, Bazer FW, Spencer TE, et al. Alterations in expression of endometrial genes coding for proteins secreted into the uterine lumen during conceptus elongation in cattle. Bmc Genomics. 2013; 14.

27. Shimizu T, Krebs S, Bauersachs S, Blum H, Wolf E, Miyamoto A. Actions and interactions of progesterone and estrogen on transcriptome profiles of the bovine endometrium. Physiological Genomics. 2010; 42A(4):290–300. doi: 10.1152/physiolgenomics.00107.2010 PMID: 20876846

28. Mesquita FS, Pugliesi G, Scolari SC, Franca MR, Ramos RS, Oliveira M, et al. Manipulation of the periovulatory sex steroidal milieu affects endometrial but not luteal gene expression in early diestrus Nelore cows. Theriogenology. 2014; 81(6):861–9. doi: 10.1016/j.theriogenology.2013.12.022 PMID: 24507960

29. Mesquita FS, Ramos RS, Pugliesi G, Andrade SC, Van Hoeck V, Langbeen A, et al. The Receptive Endometrial Transcriptomic Signature Indicates an Earlier Shift from Proliferation to Metabolism at Early Diestrus in the Cow. Biol Reprod. 2015; 93(2):52. doi: 10.1095/biolreprod.115.129031 PMID: 26178716

30. Araujo ER, Sponchiado M, Pugliesi G, Van Hoeck V, Mesquita FS, Membrive CM, et al. Spatio-specific regulation of endocrine-responsive gene transcription by periovulatory endocrine profiles in the bovine reproductive tract. Reprod Fertil Dev. 2014; 87(12).

31. Pugliesi G, Oliveria ML, Scolari SC, Lopes E, Pinaffi FV, Miagawa BT, et al. Corpus Luteum Development and Function after Supplementation of Long-Acting Progesterone During the Early Luteal Phase in Beef Cattle. Reproduction in Domestic Animals. 2014; 49(1):85–91. doi: 10.1111/rda.12231 PMID: 24001093

32. Kastelic JP, Pierson RA, Ginther OJ. ULTRASONIC MORPHOLOGY OF CORPORA-LUTEA AND CENTRAL LUTEAL CAVITIES DURING THE ESTROUS-CYCLE AND EARLY-PREGNANCY IN HEIFERS. Theriogenology. 1990; 34(3):487–98. PMID: 16726855

33. Garbarino EJ, Hernandez JA, Shearer JK, Risco CA, Thatcher WW. Effect of lameness on ovarian activity in postpartum Holstein cows. Journal of Dairy Science. 2004; 87(12):4123–31. PMID: 15545374

34. Siddiqui MAR, Gastal EL, Gastal MO, Almamun M, Beg MA, Ginther OJ. Relationship of vascular perfusion of the wall of the preovulatory follicle to in vitro fertilisation and embryo development in heifers. Reproduction. 2009; 137(4):689–97. doi: 10.1530/REP-08-0403 PMID: 19176313

35. Bauersachs S, Blum H, Mallok S, Wenigerkind H, Rief S, Prelle K, et al. Regulation of ipsilateral and contralateral bovine oviduct epithelial cell function in the postovulation period: a transcriptomics approach. Biol Reprod. 2003; 68(4):1170–7. PMID: 12606461

36. Zervomanolakis I, Ott H, Müller J, Seeber B, Friess S, Mattle V, et al. Uterine mechanisms of ipsilateral directed spermatozoa transport: Evidence for a contribution of the utero-ovarian countercurrent system. European Journal of Obstetrics & Gynecology and Reproductive Biology. 2009; 144:S45–S9.

37. Gabler C, Killian GJ, Einspanier R. Differential expression of extracellular matrix components in the bovine oviduct during the oestrous cycle. Reproduction. 2001; 122(1):121–30. PMID: 11425336

38. Cerny KL, Garrett E, Walton AJ, Anderson LH, Bridges PJ. A transcriptomal analysis of bovine oviductal epithelial cells collected during the follicular phase versus the luteal phase of the estrous cycle. Reprod Biol Endocrinol. 2015; 13:84. doi: 10.1186/s12958-015-0077-1 PMID: 26242217

39. Kim D, Pertea G, Trapnell C, Pimentel H, Kelley R, Salzberg SL. TopHat2: accurate alignment of transcriptomes in the presence of insertions, deletions and gene fusions. Genome Biol. 14. England2013. p. R36. doi: 10.1186/gb-2013-14-4-r36 PMID: 23618408

40. Langmead B, Salzberg SL. Fast gapped-read alignment with Bowtie 2. Nat Methods. 9. United States2012. p. 357–9.

41. Trapnell C, Roberts A, Goff L, Pertea G, Kim D, Kelley DR, et al. Differential gene and transcript expression analysis of RNA-seq experiments with TopHat and Cufflinks. Nat Protoc. 7. England2012. p. 562–78. doi: 10.1038/nprot.2012.016 PMID: 22383036

42. Li H, Handsaker B, Wysoker A, Fennell T, Ruan J, Homer N, et al. The Sequence Alignment/Map format and SAMtools. Bioinformatics. 25. England2009. p. 2078–9. doi: 10.1093/bioinformatics/btp352 PMID: 19505943

43. Anders S, Huber W. Differential expression analysis for sequence count data. Genome Biol. 11. England2010. p. R106. doi: 10.1186/gb-2010-11-10-r106 PMID: 20979621

44. Gentleman RC, Carey VJ, Bates DM, Bolstad B, Dettling M, Dudoit S, et al. Bioconductor: open software development for computational biology and bioinformatics. Genome Biol. 5. England2004. p. R80. PMID: 15461798

45. Benjamini Y, Hochberg Y. CONTROLLING THE FALSE DISCOVERY RATE—A PRACTICAL AND POWERFUL APPROACH TO MULTIPLE TESTING. Journal of the Royal Statistical Society Series B-Methodological. 1995; 57(1):289–300.

46. Dennis G, Sherman BT, Hosack DA, Yang J, Gao W, Lane HC, et al. DAVID: Database for annotation, visualization, and integrated discovery. Genome Biology. 2003; 4(9).

47. Smit A, Hubley R, Green P. RepeatMasker Open-3.0. http://www.repeatmasker.org1996-2010 [

48. Vandesompele J, De Preter K, Pattyn F, Poppe B, Van Roy N, De Paepe A, et al. Accurate normalization of real-time quantitative RT-PCR data by geometric averaging of multiple internal control genes. Genome Biology. 2002; 3(7).

49. Neve A, Cantatore FP, Maruotti N, Corrado A, Ribatti D. Extracellular Matrix Modulates Angiogenesis in Physiological and Pathological Conditions. BioMed Research International. 2014; 2014.

50. Batzios SP, Zafeiriou DI, Papakonstantinou E. Extracellular matrix components: An intricate network of possible biomarkers for lysosomal storage disorders? FEBS letters. 2013; 587(8):1258–67. doi: 10.1016/j.febslet.2013.02.035 PMID: 23454643

51. Lee Y, Gorski J. Estrogen-induced transcription of the progesterone receptor gene does not parallel estrogen receptor occupancy. Proceedings of the National Academy of Sciences. 1996; 93(26):15180–4.

52. Lee YJ, Gorski J. Estrogen receptor down-regulation is regulated noncooperatively by estrogen at the transcription level. Molecular and Cellular Endocrinology. 1998; 137(1):85–92. PMID: 9607732

53. Alminana C, Caballero I, Heath PR, Maleki-Dizaji S, Parrilla I, Cuello C, et al. The battle of the sexes starts in the oviduct: modulation of oviductal transcriptome by X and Y-bearing spermatozoa. BMC Genomics. 15. England2014. p. 293. doi: 10.1186/1471-2164-15-293 PMID: 24886317

54. Kutys ML, Doyle AD, Yamada KM. Regulation of cell adhesion and migration by cell-derived matrices. Exp Cell Res. 2013; 319(16):2434–9. doi: 10.1016/j.yexcr.2013.05.030 PMID: 23751565

55. Daley WP, Yamada KM. ECM-modulated cellular dynamics as a driving force for tissue morphogenesis. Current opinion in genetics & development. 2013; 23(4):408–14.

56. Cox TR, Erler JT. Remodeling and homeostasis of the extracellular matrix: implications for fibrotic diseases and cancer. Dis Model Mech. 4. England2011. p. 165–78. doi: 10.1242/dmm.004077 PMID: 21324931

57. Lu P, Takai K, Weaver VM, Werb Z. Extracellular matrix degradation and remodeling in development and disease. Cold Spring Harbor perspectives in biology. 2011; 3(12):a005058. doi: 10.1101/cshperspect.a005058 PMID: 21917992

58. Brown RD, Ambler SK, Mitchell MD, Long CS. The cardiac fibroblast: therapeutic target in myocardial remodeling and failure. Annu Rev Pharmacol Toxicol. 2005; 45:657–87. PMID: 15822192

59. Clemmons DR. Modifying IGF1 activity: an approach to treat endocrine disorders, atherosclerosis and cancer. Nat Rev Drug Discov. 6. England2007. p. 821–33. PMID: 17906644

60. Block J, Drost M, Monson R, Rutledge J, Rivera R, Paula-Lopes F, et al. Use of insulin-like growth factor-I during embryo culture and treatment of recipients with gonadotropin-releasing hormone to increase pregnancy rates following the transfer of in vitro-produced embryos to heat-stressed, lactating cows. Journal of animal science. 2003; 81(6):1590–602. PMID: 12817508

61. Ahumada CJ, Salvador I, Cebrian-Serrano A, Lopera R, Silvestre MA. Effect of supplementation of different growth factors in embryo culture medium with a small number of bovine embryos on in vitro embryo development and quality. Animal. 2013; 7(3):455–62. doi: 10.1017/S1751731112001991 PMID: 23121725

62. Walsh B, Pearl A, Suchy S, Tartaglio J, Visco K, Phelan SA. Overexpression of Prdx6 and resistance to peroxide-induced death in Hepa1-6 cells: Prdx suppression increases apoptosis. Redox Rep. 2009; 14(6):275–84. doi: 10.1179/135100009X12525712409652 PMID: 20003713

63. Takahashi M. Oxidative stress and redox regulation on in vitro development of mammalian embryos. J Reprod Dev. 58. Japan2012. p. 1–9. PMID: 22450278

64. Ramos RS, Oliveira ML, Izaguirry AP, Vargas LM, Soares MB, Mesquita FS, et al. The periovulatory endocrine milieu affects the uterine redox environment in beef cows. Reprod Biol Endocrinol. 2015; 13:39. doi: 10.1186/s12958-015-0036-x PMID: 25957795

65. Capiod T. The need for calcium channels in cell proliferation. Recent Pat Anticancer Drug Discov. 8. United Arab Emirates2013. p. 4–17. PMID: 22519598

66. Rotello RJ, Lieberman RC, Purchio AF, Gerschenson LE. Coordinated regulation of apoptosis and cell proliferation by transforming growth factor beta 1 in cultured uterine epithelial cells. Proceedings of the National Academy of Sciences. 1991; 88(8):3412–5.

67. George F, Daniaux C, Genicot G, Verhaeghe B, Lambert P, Donnay I. Set up of a serum-free culture system for bovine embryos: embryo development and quality before and after transient transfer. Theriogenology. 69. United States2008. p. 612–23. doi: 10.1016/j.theriogenology.2007.11.008 PMID: 18242668

68. Kurzawa R, Glabowski W, Baczkowski T, Brelik P. Evaluation of mouse preimplantation embryos exposed to oxidative stress cultured with insulin-like growth factor I and II, epidermal growth factor, insulin, transferrin and selenium. Reprod Biol. 2002; 2(2):143–62. PMID: 14666155

69. Vallet JL, Christenson RK, McGuire WJ. Association between uteroferrin, retinol-binding protein, and transferrin within the uterine and conceptus compartments during pregnancy in swine. Biol Reprod. 1996; 55(5):1172–8. PMID: 8902231

70. Vallet JL. Uteroferrin induces lipid peroxidation in endometrial and conceptus microsomal membranes and is inhibited by apotransferrin, retinol binding protein, and the uteroferrin-associated proteins. Biol Reprod. 1995; 53(6):1436–45. PMID: 8562701

APPENDIX B

Genomics Data 13 (2017) 27–29

Contents lists available at ScienceDirect

Genomics Data

journal homepage: www.elsevier.com/locate/gdata

Data in Brief

Oviductal transcriptional profiling of a bovine fertility model by next-generation sequencing

Angela Maria Gonella-Diaza[a], Sónia Cristina da Silva Andrade[b], Mariana Sponchiado[a], Guilherme Pugliesi[a], Fernando Silveira Mesquita[c], Veerle Van Hoeck[a], Ricardo de Francisco Strefezzi[d], Gustavo R. Gasparin[e], Luiz L. Coutinho[e], Mario Binelli[a,*]

[a] Faculdade de Medicina Veterinária e Zootecnia, Universidade de São Paulo, Pirassununga, São Paulo, Brazil
[b] Departamento de Genética e Biologia Evolutiva, IB-Universidade de São Paulo, Cidade Universitária, São Paulo, Brazil
[c] Faculdade de Medicina Veterinária, Universidade Federal do Pampa, Uruguaiana, Brazil
[d] Faculdade de Zootecnia e Engenharia de Alimentos, Universidade de São Paulo, Pirassununga, São Paulo, Brazil
[e] Laboratório de Biotecnologia Animal, Escola Superior de Agricultura Luiz de Queiroz, Universidade de São Paulo, Av Pádua Dias, 11, Piracicaba, SP, Brazil

ARTICLE INFO

Keywords:
RNAseq
Beef cattle
Ampulla
Isthmus
Sex steroids

ABSTRACT

In cattle, the oviduct plays a fundamental role in the reproductive process. Oviductal functions are controlled by the ovarian sex steroids: estradiol and progesterone. Here, we tested the hypothesis that the exposure to contrasting sex steroid milieus differentially impacts the oviductal transcriptional profile. We manipulated growth of the pre-ovulatory follicle to obtain cows that ovulated a larger (LF group) or a smaller (SF group) follicle. The LF group presented greater proestrus/estrus concentrations of estradiol and metaestrus concentrations of progesterone (Gonella-Diaza et al. 2015 [1], Mesquita et al. 2014 [2]). Also, the LF group was associated with greater fertility in timed-artificial insemination programs (Pugliesi et al. 2016 [3]). Cows were slaughtered on day 4 of the estrous cycle and total RNA was extracted from ampulla and isthmus fragments and analyzed by RNAseq. The resulting reads were mapped to the bovine genome (*Bos taurus* UMD 3.1, NCBI). The differential expression analyses revealed that 325 and 367 genes in ampulla and 274 and 316 genes in the isthmus were up-regulated and down-regulated in LF samples, respectively. To validate the RNAseq results, transcript abundance of 23 genes was assessed by qPCR and expression patterns were consistent between the two techniques. A functional enrichment analysis was performed using Database for Annotation, Visualization and Integrated Discovery (DAVID) software. Processes enriched in the LF group included tissue morphology changes (extracellular matrix remodeling), cellular changes (proliferation), and secretion changes (growth factors, ions and metal transporters). An overview of the gene expression data was deposited in the NCBI's Gene Expression Omnibus (GEO) and is accessible through the accession number GSE65681. In conclusion, differences in the peri-ovulatory sex steroid milieu modify the oviductal gene expression profiles. Such differences may be associated with the greater fertility of the LF cows. This dataset is useful for further investigations of the oviductal biology and the impact of sex-steroid on the female reproductive tract.

Specifications

Organism/cell line/tissue	*Bos taurus indicus*, Nelore Breed, oviducts ipsilateral to corpus luteum: ampulla and isthmus
Sex	Female
Sequencer or array type	Illumina HiSeq 2000 (ampulla samples) and Illumina HiSeq 2500 (isthmus samples).
Data format	Analyzed
Experimental factors	Cows were submitted to hormonal manipulation in order to ovulate large or small follicles, causing a different peri-ovulatory sex-steroid milieu.
Experimental features	Ampulla and isthmus samples were collected from cows submitted to endocrine manipulations resulting in the ovulation of smaller or larger follicles.
Consent	N/A

* Corresponding author at: Lab. De Fisiologia e Endocrinologia Molecular, Departamento de Reprodução Animal, CBRA Pirassununga, Universidade de São Paulo, Rua Duque de Caxias Norte, 255, Bairro, Jardim Elite, Pirassununga CEP: 13635-900, Brazil.
E-mail address: binelli@usp.br (M. Binelli).

http://dx.doi.org/10.1016/j.gdata.2017.06.004
Received 24 March 2017; Received in revised form 31 May 2017; Accepted 7 June 2017
Available online 15 June 2017

Sample source location	Experiment was performed in Pirassununga, Brazil, at a Campus of the University of São Paulo; Latitude - 21.953833; Longitude - 47.453143.

Direct link to deposited data

http://www.ncbi.nlm.nih.gov/geo/query/acc.cgi?acc=GSE65679

1. Experimental design, materials and methods

1.1. Animals, reproductive management and collection of samples

All animal procedures were approved by the Ethics and Animal Handling Committee of the Faculdade de Medicina Veterinária e Zootecnia — Universidade de São Paulo (CEUA-FMVZ/USP, N° 2287/2011). Animal and reproductive management was performed as described previously [1,2,4]. Non-lactating, multiparous, and cyclic Nelore cows were used in this study. Cows were pre-synchronized (day -27) by intramuscular (IM) injection of GnRH agonist (1 μg of buserelin acetate; Sincroforte, Ouro Fino, Cravinhos, Brazil) and, 7 days later (day -20) an injection of Prostaglandin F2 alpha analog (PGF; 0.5 mg of sodium cloprostenol; Sincrocio, Ouro Fino). On day -20, animals received a Heat detector patch (ESTROTECT, Rockway, Inc. Spring Valley, WI, USA). Animals showing estrus from D-20 to D-15 received an intravaginal progesterone releasing device (1 g; Sincrogest, Ouro Fino) and an IM injection of 2 mg estradiol benzoate (Sincrodiol, Ouro Fino) on D-10. Also, cows in the LF group received an IM injection of PGF. Progesterone devices were removed 8 days later and all animals received a PGF injection at removal and a second PGF injection 6 h later. The progesterone device removal occurred 42 or 30 h before the induction of ovulation in the LF and the SF groups, respectively. GnRH agonist was used to induce ovulation on day 0. Transrectal ultrasound exams were performed in all animals to evaluate growth and ovulation of the pre-ovulatory follicle (POF) and CL area and blood flow. Blood samples were collected from day -2 to day 4 in order to evaluate estradiol and progesterone concentrations by radioimmunoassay. On day 4, the reproductive tracts were collected and the oviduct ipsilateral to the ovary containing the CL was dissected. Samples of ampulla and isthmus were frozen in liquid nitrogen.

2. Animal ranking and selection for RNAseq

In order to be included in the study, animals must have complied with minimal premises that were established prior to the beginning of the study. Animals were excluded if: the preovulatoy follicle was smaller than 8 mm on day 0, ovulation was detected on day 0 or before (i.e. early ovulation) or after day 3 (i.e., late ovulation), ovulation was not detected, or follicular or luteal cysts were detected at any moment during the experiment. Thirteen animals of LF group and 8 animals of SF group matched the premises and were immediately submitted to the induction of ovulation by GnRH administration. Of all slaughtered animals, samples of six (three/group) were submitted to RNAseq analysis. RNAseq of the two regions was performed separately (n = 3 samples per group and per region). In order to select the animals for RNAseq analysis, animals were ranked according to the following variables: maximum diameter of the POF and estradiol concentration at D-1, and CL area and progesterone concentrations at D4. Samples of the top-ranked animals of the LF group and the bottom ranked animals of the SF group were used.

3. RNAseq and bioinformatics

Total RNA was extracted using a commercial kit (All Prep ® DNA/RNA/Protein Mini kit, No. 80004, Qiagen, São Paulo, São Paulo, Brazil)

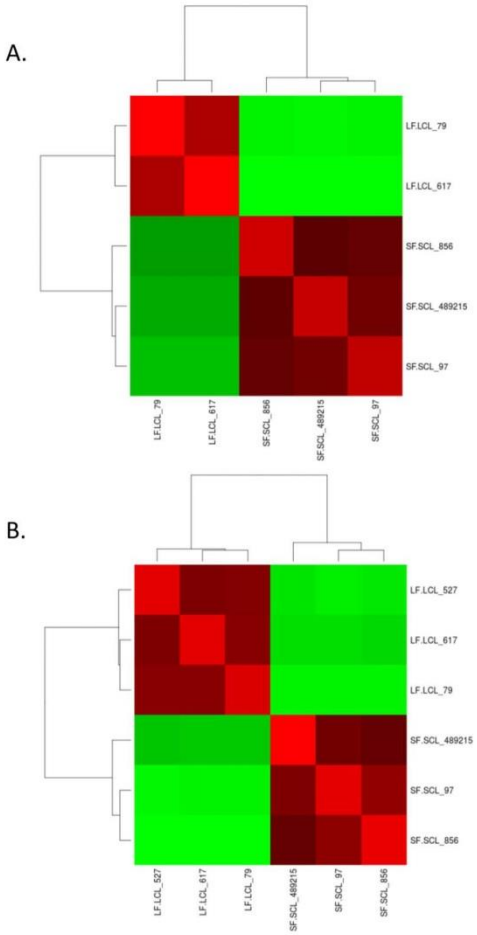

Fig. 1. Clustered heatmap showing the Euclidean distances between the ampulla (Panel A) and isthmus (Panel B) samples submitted to RNAseq, as calculated from the variance-stabilizing transformation of the count data. Each column represents one sample and shows the correlation to all samples with red for the lowest (0) distance and light green for the highest observed distance. Normalized count values were used.(For interpretation of the references to color in this figure legend, the reader is referred to the web version of this article.)

by following the manufacturer's instructions. Total RNA concentration and purity (260/280 and 260/230 nm ratios) was measured using the NanoVue spectrophotometer (GE Healthcare). RNA integrity was assessed using the Agilent Bioanalyzer (Agilent Technologies, Palo Alto, USA). Only samples with an RNA integrity number (RIN) ≥ 8.0 were used for RNAseq analysis. Libraries were generated using the TruSeq protocol for RNAlibraries (Illumina Technologies, San Diego, CA), with 1 μg of total RNA as input. After adapter ligation, end-repair steps, and cDNA synthesis, the cDNA libraries were purified and validated using the Bioanalyzer. Paired-end sequencing of 101 bp reads was performed using the Illumina HiSeq 2000 (ampulla samples) and Illumina HiSeq 2500 (isthmus samples) platforms. Using seqyClean v1.3.12. (https://bitbucket.org/izhbannikov/seqyclean/get/stable.zip) the quality filtering was performed. In order to generate the mapping file, accepted

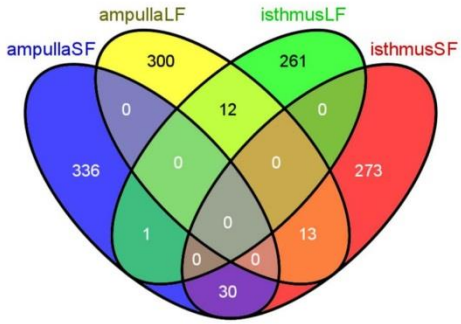

Fig. 2. Venn diagram of differentially expressed genes in ampulla and isthmus samples of LF and SF cows. This diagram shows that there are few common differentially expressed genes between regions and between treatments.

reads were mapped with Tophat v.2.0.8 [5] and Bowtie2 v2.1.0 [6] on the masked bovine genome assembly (*Bos taurus* UMD 3.1, NCBI). Then, the mapping file was sorted with SAMTools v 0.1.18 [7], and using the script from HTSeq-count v0.5.4p2 (http://www-huber.embl.de/users/anders/HTSeq/doc/count.html) the read counts were obtained. Differential expression analysis was performed with package DESEq v1.12.1 [8] from R/Bioconductor [9]. Clustering analysis revealed that gene expression of LF and SF groups differ significantly (Fig. 1). A Venn diagram was constructed using the list of differentially expressed genes (Fig. 2). This diagram shows that there are few common differentially expressed genes between regions. Finally, gene enrichment analysis was performed separately for each oviduct region, using the Database for Annotation, Visualization, and Integrated Discovery (DAVID) [10]. Processes enriched in the LF group included extracellular matrix remodeling, cell proliferation, and secretion. A detailed description of these results is available in Gonella et al. [1]. All reads sequences are available in the Sequence Read Archive (SRA) of the NCBI and an overview of the gene expression results is also available in NCBI's Gene Expression Omnibus (GEO) under the accession number GSE65681 (https://www.ncbi.nlm.nih.gov/geo/query/acc.cgi?acc=GSE65681).

4. RNAseq validation by qPCR

In order to validate the RNAseq results, the abundance of 23 transcripts was assessed by qPCR. Genes from different functional categories, relevant to oviductal biology, were analyzed (i.e. sex-steroid receptors, angiogenesis, cellular proliferation, extracellular matrix, and synthesis of glycoproteins). For that purpose 1 μg of total RNA was reverse transcribed using a commercial Kit (High Capacity cDNA Reverse Transcription Kit, Life Technologies). The qPCR was performed using the Step-One Plus apparatus (Life Technologies, Carlsbad, CA) and SYBR Green chemistry. Primers details are available in Gonella et al. [1]. Quantitative PCR products were purified and submitted to agarose gel electrophoresis and SANGER sequencing for identification of the PCR products, and identity of target transcripts was confirmed. Quantitative PCR expression data showed agreement with expression patterns obtained by RNAseq analysis, therefore validating global gene expression data [1].

References

[1] A.M. Gonella-Diaza, S.C. Andrade, M. Sponchiado, G. Pugliesi, F.S. Mesquita, V. Van Hoeck, et al., Size of the ovulatory follicle dictates spatial differences in the oviductal transcriptome in cattle, PLoS One 10 (12) (2015) e0145321.
[2] F.S. Mesquita, G. Pugliesi, S.C. Scolari, M.R. Franca, R.S. Ramos, M. Oliveira, et al., Manipulation of the periovulatory sex steroidal milieu affects endometrial but not luteal gene expression in early diestrus Nelore cows, Theriogenology 81 (6) (2014) 861–869.
[3] G. Pugliesi, F.B. Santos, E. Lopes, É. Nogueira, J.R. Maio, M. Binelli, Improved fertility in suckled beef cows ovulating large follicles or supplemented with long-acting progesterone after timed-AI, Theriogenology 85 (7) (2016) 1239–1248.
[4] F.S. Mesquita, R.S. Ramos, G. Pugliesi, S.C. Andrade, V. Van Hoeck, A. Langbeen, et al., The receptive endometrial transcriptomic signature indicates an earlier shift from proliferation to metabolism at early diestrus in the cow, Biol. Reprod. 93 (2) (2015) 52.
[5] D. Kim, G. Pertea, C. Trapnell, H. Pimentel, R. Kelley, S.L. Salzberg, TopHat2: accurate alignment of transcriptomes in the presence of insertions, deletions and gene fusions, Genome Biol. 14 (2013) R36 (England).
[6] B. Langmead, S.L. Salzberg, Fast gapped-read alignment with Bowtie 2, Nat Methods 9 (2012) 357–359 (United States).
[7] H. Li, B. Handsaker, A. Wysoker, T. Fennell, J. Ruan, N. Homer, et al., The sequence alignment/map format and SAMtools, Bioinformatics 25 (2009) 2078–2079 (England).
[8] S. Anders, W. Huber, Differential expression analysis for sequence count data, Genome Biol. 11 (2010) R106 (England).
[9] R.C. Gentleman, V.J. Carey, D.M. Bates, B. Bolstad, M. Dettling, S. Dudoit, et al., Bioconductor: open software development for computational biology and bioinformatics, Genome Biol. 5 (10) (2004).
[10] G. Dennis Jr., B.T. Sherman, D.A. Hosack, J. Yang, W. Gao, H.C. Lane, et al., DAVID: database for annotation, visualization, and integrated discovery, Genome Biol. 4 (5) (2003) (P3).

APPENDIX C

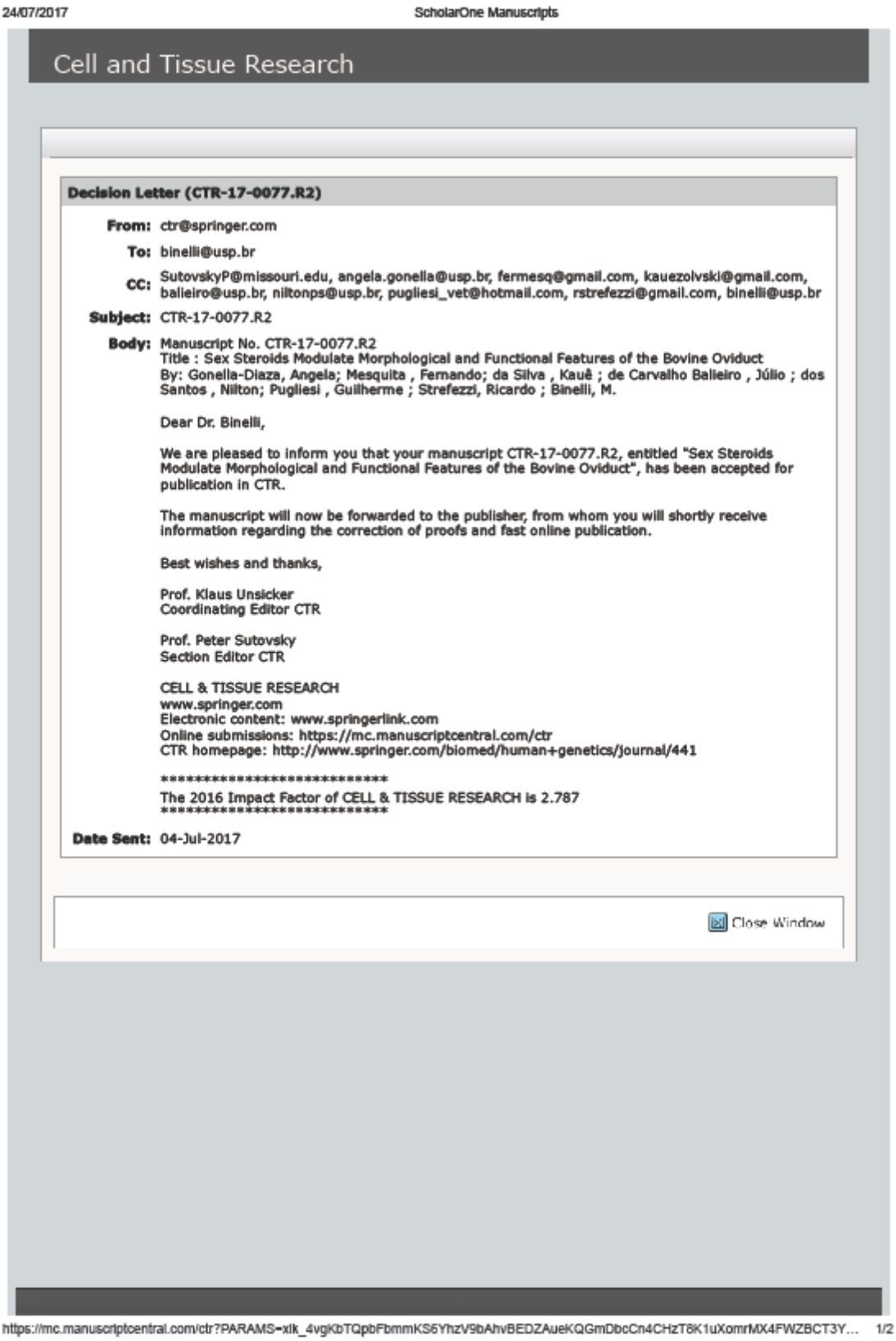

24/07/2017 ScholarOne Manuscripts

Cell and Tissue Research

Decision Letter (CTR-17-0077.R2)

From: ctr@springer.com

To: binelli@usp.br

CC: SutovskyP@missouri.edu, angela.gonella@usp.br, fermesq@gmail.com, kauezolvski@gmail.com, balieiro@usp.br, niltonps@usp.br, pugliesi_vet@hotmail.com, rstrefezzi@gmail.com, binelli@usp.br

Subject: CTR-17-0077.R2

Body: Manuscript No. CTR-17-0077.R2
Title : Sex Steroids Modulate Morphological and Functional Features of the Bovine Oviduct
By: Gonella-Diaza, Angela; Mesquita , Fernando; da Silva , Kauê ; de Carvalho Balieiro , Júlio ; dos Santos , Nilton; Pugliesi , Guilherme ; Strefezzi, Ricardo ; Binelli, M.

Dear Dr. Binelli,

We are pleased to inform you that your manuscript CTR-17-0077.R2, entitled "Sex Steroids Modulate Morphological and Functional Features of the Bovine Oviduct", has been accepted for publication in CTR.

The manuscript will now be forwarded to the publisher, from whom you will shortly receive information regarding the correction of proofs and fast online publication.

Best wishes and thanks,

Prof. Klaus Unsicker
Coordinating Editor CTR

Prof. Peter Sutovsky
Section Editor CTR

CELL & TISSUE RESEARCH
www.springer.com
Electronic content: www.springerlink.com
Online submissions: https://mc.manuscriptcentral.com/ctr
CTR homepage: http://www.springer.com/biomed/human+genetics/journal/441

****
The 2016 Impact Factor of CELL & TISSUE RESEARCH is 2.787
****

Date Sent: 04-Jul-2017

Close Window

https://mc.manuscriptcentral.com/ctr?PARAMS=xlk_4vgKbTQpbFbmmKS6YhzV9bAhvBEDZAueKQGmDbcCn4CHzT8K1uXomrMX4FWZBCT3Y... 1/2

APPENDIX D: Results of the human and bovine protein sequence alignment using the EMBOSS Pairwise Sequence Alignment Algorithm at the EMBL-EBI Web site (http://www.ebi.ac.uk/Tools/psa/emboss_needle/).

	Humane sequence ID	Bovine sequence ID	Identity	Similarity	Gaps
MMP1	NP_002412.1	NP_776537.1	397/472 (84.1%)	427/472 (90.5%)	6/472 (1.3%)
MMP2	NP_001121363.1	NP_777170.1	586/661 (88.7%)	600/661 (90.8%)	51/661 (7.7%)
MMP3	NP_002413.1	NP_001193566.1	396/477 (83.0%)	426/477 (89.3%)	0/477 (0.0%)
MMP8	NP_001291371.1	XP_015321916.1	335/470 (71.3%)	375/470 (79.8%)	26/470 (5.5%)
MMP9	NP_004985.2	NP_777169.1	572/712 (80.3%)	626/712 (87.9%)	5/712 (0.7%)
MMP10	NP_002416.1	Absent			
MMP13	NP_002418.1	NP_776814.1	423/471 (89.8%)	444/471 (94.3%)	0/471 (0.0%)
TIMP1	NP_003245.1	NP_776896.1	180/207 (87.0%)	191/207 (92.3%)	0/207 (0.0%)
TIMP2	NP_003246.1	NP_776897.2	202/220 (91.8%)	211/220 (95.9%)	0/220 (0.0%)
TIMP4	NP_003247.1	NP_001039336.1	202/224 (90.2%)	214/224 (95.5%)	0/224 (0.0%)

Source: Gonella-Diaza (2017).

Legend: The MMP10 bovine amino acid- sequence was not founded in the NCBI protein bank.

APPENDIX E: Results of the alignment of the bovine and human miRNAs sequences using the Pairwise Sequence Alignment algorithm of Clustal Omega v.1.2.3.

	SEQUENCE ALIGNMENT	IDENTITY	GAPS
bta-let-7b	1 UGAGGUAGUAGGUUGUGUGGUU 22	22/22 (100.0%)	0/22 (0.0%)
hsa-let-7b-5p	1 UGAGGUAGUAGGUUGUGUGGUU 22		
bta-miR-106a	1 AAAAGUGCUUACAGUGCAGGUA- 22	22/23 (95.7%)	1/23 (4.3%)
hsa-miR-106a-5p	1 AAAAGUGCUUACAGUGCAGGUAG 23		
bta-miR-106b	1 UAAAGUGCUGACAGUGCAGAU 21	21/21 (100.0%)	0/21 (0.0%)
hsa-miR-106b-5p	1 UAAAGUGCUGACAGUGCAGAU 21		
bta-miR-122	1 UGGAGUGUGACAAUGGUGUUUG 22	22/22 (100.0%)	0/22 (0.0%)
hsa-miR-122-5p	1 UGGAGUGUGACAAUGGUGUUUG 22		
bta-miR-125b	1 UCCCUGAGACCCUAACUUGUGA 22	22/22 (100.0%)	0/22 (0.0%)
hsa-miR-125b-5p	1 UCCCUGAGACCCUAACUUGUGA 22		

bta-miR-132	1 UAACAGUCUACAGCCAUGGUCG	22	22/22 (100.0%)	0/22 (0.0%)
hsa-miR-132-3p	1 UAACAGUCUACAGCCAUGGUCG	22		
bta-miR-138	1 AGCUGGUGUUGUGAAUCAGGCCG	23	23/23 (100.0%)	0/23 (0.0%)
hsa-miR-138-5p	1 AGCUGGUGUUGUGAAUCAGGCCG	23		
bta-miR-143	1 UGAGAUGAAGCACUGUAGCUCG	22	21/22 (95.5%)	1/22 (4.5%)
hsa-miR-143-3p	1 UGAGAUGAAGCACUGUAGCUC-	21		
bta-miR-17-3p	1 ACUGCAGUGAAGGCACUUGU--	20	20/22 (90.9%)	2/22 (9.1%)
hsa-miR-17-3p	1 ACUGCAGUGAAGGCACUUGUAG	22		
bta-miR-17-5p	1 CAAAGUGCUUACAGUGCAGGUAGU	24	23/24 (95.8%)	1/24 (4.2%)
hsa-miR-17-5p	1 CAAAGUGCUUACAGUGCAGGUAG-	23		
bta-miR-181b	1 AACAUUCAUUGCUGUCGGUGGGUU	24	23/24 (95.8%)	1/24 (4.2%)
hsa-miR-181b-5p	1 AACAUUCAUUGCUGUCGGUGGGU-	23		

bta-miR-181d	1 AACAUUCAUUGUUGUCGGUGGGU 23	23/23 (100.0%)	0/23 (0.0%)
hsa-miR-181d-5p	1 AACAUUCAUUGUUGUCGGUGGGU 23		
bta-miR-188	1 CAUCCCUUGCAUGGUGGAGGGU 22	21/22 (95.5%)	1/22 (4.5%)
hsa-miR-188-5p	1 CAUCCCUUGCAUGGUGGAGGG- 21		
bta-miR-192	1 CUGACCUAUGAAUUGACAGCCAG 23	21/23 (91.3%)	2/23 (8.7%)
hsa-miR-192-5p	1 CUGACCUAUGAAUUGACAGCC-- 21		
bta-miR-193a-5p	1 UGGGUCUUUGCGGGCGAGAUGA 22	22/22 (100.0%)	0/22 (0.0%)
hsa-miR-193a-5p	1 UGGGUCUUUGCGGGCGAGAUGA 22		
bta-miR-193b	1 AACUGGCCCACAAAGUCCCGCUUU 24	21/24 (87.5%)	2/24 (8.3%)
hsa-miR-193b-3p	1 AACUGGCCCUCAAAGUCCCGCU-- 22		
bta-miR-196b	1 UAGGUAGUUUCCUGUUGUUGGGA 23	22/23 (95.7%)	1/23 (4.3%)
hsa-miR-196b-5p	1 UAGGUAGUUUCCUGUUGUUGGG- 22		
bta-miR-199a-	1 ACAGUAGUCUGCACAUUGGUUA 22	22/22 (100.0%)	0/22 (0.0%)

hsa-miR-199a-3p	1 ACAGUAGUCUGCACAUUGGUUA 22			
bta-miR-200b	1 UAAUACUGCCUGGUAAUGAUG- 21		21/22 (95.5%)	1/22 (4.5%)
hsa-miR-200b-3p	1 UAAUACUGCCUGGUAAUGAUGA 22			
bta-miR-211	1 UUCCCUUUGUCAUCCUUUGCC- 21		20/22 (90.9%)	1/22 (4.5%)
hsa-miR-211-5p	1 UUCCCUUUGUCAUCCUUCGCCU 22			
bta-miR-219	1 AGAGUUGAGUCUGGACGUCCCG 22		22/22 (100.0%)	0/22 (0.0%)
hsa-miR-219a-1-3p	1 AGAGUUGAGUCUGGACGUCCCG 22			
bta-miR-30b-5p	1 UGUAAACAUCCUACACUCAGCU 22		22/22 (100.0%)	0/22 (0.0%)
hsa-miR-30b-5p	1 UGUAAACAUCCUACACUCAGCU 22			
bta-miR-30c	1 UGUAAACAUCCUACACUCUCAGC 23		23/23 (100.0%)	0/23 (0.0%)
hsa-miR-30c-5p	1 UGUAAACAUCCUACACUCUCAGC 23			
bta-miR-30d	1 UGUAAACAUCCCCGACUGGAAGCU 24		22/24 (91.7%)	2/24 (8.3%)
hsa-miR-30d-5p	1 UGUAAACAUCCCCGACUGGAAG-- 22			

bta-miR-339b	1 UCCCUGUCCUCCAGGAGCUC--- 20	20/23 (87.0%)	3/23 (13.0%)
hsa-miR-339-5p	1 UCCCUGUCCUCCAGGAGCUCACG 23		
bta-miR-345-5p	1 GCUGACUCCUAGUCCAGUGCU- 21	20/22 (90.9%)	1/22 (4.5%)
hsa-miR-345-5p	1 GCUGACUCCUAGUCCAGGGCUC 22		
bta-miR-375	1 UUUUGUUCGUUCGGCUCGCGUGA 23	22/23 (95.7%)	1/23 (4.3%)
hsa-miR-375	1 -UUUGUUCGUUCGGCUCGCGUGA 22		
bta-miR-378	1 ACUGGACUUGGAGUCAGAAGGC 22	22/22 (100.0%)	0/22 (0.0%)
hsa-miR-378a-3p	1 ACUGGACUUGGAGUCAGAAGGC 22		
bta-miR-383	1 AGAUCAGAAGGUGAUUGUGGCU 22	22/22 (100.0%)	0/22 (0.0%)
hsa-miR-383-5p	1 AGAUCAGAAGGUGAUUGUGGCU 22		
bta-miR-423-5p	1 UGAGGGGCAGAGAGCGAGACUUU 23	23/23 (100.0%)	0/23 (0.0%)
hsa-miR-423-5p	1 UGAGGGGCAGAGAGCGAGACUUU 23		
bta-miR-425-3p	1 AUCGGGAAUGUCGUGUCCGCCC 22	22/22 (100.0%)	0/22 (0.0%)

hsa-miR-425-3p	1 AUCGGGAAUGUCGUGUCCGCCC 22		
bta-miR-431	1 UGUCUUGCAGGCCGUCAUGCAGG 23	21/23 (91.3%)	2/23 (8.7%)
hsa-miR-431-5p	1 UGUCUUGCAGGCCGUCAUGCA-- 21		
bta-miR-432	1 UCUUGGAGUAGGUCAUUGGGUGG 23	23/23 (100.0%)	0/23 (0.0%)
hsa-miR-432-5p	1 UCUUGGAGUAGGUCAUUGGGUGG 23		
bta-miR-532	1 CAUGCCUUGAGUGUAGGACCGU 22	22/22 (100.0%)	0/22 (0.0%)
hsa-miR-532-5p	1 CAUGCCUUGAGUGUAGGACCGU 22		
bta-miR-631	1 AGACCUGGCUUAGACCUCAGC 21	19/21 (90.5%)	0/21 (0.0%)
hsa-miR-631	1 AGACCUGGCCCAGACCUCAGC 21		
bta-miR-654	1 UAUGUCUGCUGACCAUCACCUU 22	22/22 (100.0%)	0/22 (0.0%)
hsa-miR-654-3	1 UAUGUCUGCUGACCAUCACCUU 22		
bta-miR-671	1 AGGAAGCCCUGGAGGGGCUGGAG 23	23/23 (100.0%)	0/23 (0.0%)
hsa-miR-671-5p	1 AGGAAGCCCUGGAGGGGCUGGAG 23		

bta-miR-769	1 UGAGACCUCCGGGUUCUGAGCU	22	21/22 (95.5%)	0/22 (0.0%)
hsa-miR-769-5p	1 UGAGACCUCUGGGUUCUGAGCU	22		
bta-miR-92a	1 UAUUGCACUUGUCCCGGCCUGU	22	22/22 (100.0%)	0/22 (0.0%)
hsa-miR-92a-3	1 UAUUGCACUUGUCCCGGCCUGU	22		
bta-miR-92b	1 UAUUGCACUCGUCCCGGCCUCC	22	22/22 (100.0%)	0/22 (0.0%)
hsa-miR-92b-3p	1 UAUUGCACUCGUCCCGGCCUCC	22		
bta-miR-940	1 AAGGCUGGGCCCCCGCUCCGC	21	19/21 (90.5%)	0/21 (0.0%)
hsa-miR-940	1 AAGGCAGGGCCCCCGCUCCCC	21		
bta-miR-99a-5	1 AACCCGUAGAUCCGAUCUUGU-	21	21/22 (95.5%)	1/22 (4.5%)
hsa-miR-99a-5	1 AACCCGUAGAUCCGAUCUUGUG	22		

APPENDIX F. MicroRNAs detected (Cp≤ 37) in ampulla and isthmus from LF-LCL and SF-SCL cows.

microRNA	Cq Values		Cq Values
Detected only in Ampulla		Detected only in Isthmus	
let-7d	+++	miR-138	++
let-7e	+++	miR-145	++
let-7f	+++	miR-22-5p	+
let-7g	+++	miR-26a	++
miR-1	++	miR-28	++
miR-101	+++	miR-296-3p	++
miR-105b	++	miR-302b	+
miR-10b	+++	miR-409a	+
miR-129	++	miR-411c-5p	+
miR-133c	+	miR-421	+
miR-135a	+++	miR-425-3p	++
miR-135b	++	miR-425-5p	+
miR-136	++	miR-542-5p	++
miR-144	+	miR-582	+
miR-146a	+	miR-584	++
miR-149-3p	+++	miR-653	+
miR-149-5p	++	miR-877	++
miR-153	+		
miR-155	+		
miR-15a	+++	Not detected in	

miR-18a	++	ampulla or isthmus
miR-18b	+	miR-137
miR-190a	+	miR-139
miR-190b	++	miR-141
miR-200a	+++	miR-146b
miR-217	+	miR-147
miR-221	+++	miR-22-3p
miR-224	++	miR-23b-3p
miR-23a	+++	miR-26c
miR-27a-5p	+++	miR-380-5p
miR-27b	+++	miR-410
miR-29d-3p	+++	miR-423-3p
miR-301a	+	miR-592
miR-338	++	miR-628
miR-33a	++	miR-875
miR-340	+	miR-876
miR-34a	++	
miR-362-3p	++	
miR-365-3p	++	
miR-369-3p	+	
miR-369-5p	+	
miR-374a	++	
miR-374b	++	
miR-376b	+	
miR-376c	++	
miR-376d	+	
miR-376e	+	

miR-379	++
miR-380-3p	++
miR-382	++
miR-424-5p	+++
miR-448	+
miR-450a	+
miR-451	++
miR-454	+
miR-455-3p	+
miR-497	++
miR-505	++
miR-599	+
miR-670	+
miR-677	+++
miR-7	++
miR-708	++
miR-759	+
miR-9-3p	+
miR-9-5p	++
miR-98	++

	Cq	
microRNAs	Ampulla	Isthmus
Detected in booth, ampulla and isthmus		
let-7a-5p	+++	+
let-7b	+++	++
let-7c	+++	+
let-7i	+++	+
let-7a-3p	++	+
miR-100	+++	+

miR-103	+++	+
miR-105a	++	+
miR-106a	+++	+
miR-106b	+++	+
miR-107	++	+
miR-10a	+++	+
miR-122	++	++
miR-124a	++	++
miR-124b	++	++
miR-125a	+++	+
miR-125b	+++	++
miR-126-3p	+++	+
miR-126-5p	+++	+
miR-127	++	++
miR-128	++	+
miR-129-3p	++	++
miR-129-5p	++	++
miR-130a	++	+
miR-130b	+++	++
miR-132	++	++
miR-133a	++	++
miR-133b	+	+
miR-134	+	+
miR-140	++	+
miR-142-3p	++	+
miR-142-5p	++	+
miR-143	+++	++
miR-148a	+++	+
miR-148b	+++	+
miR-150	++	+
miR-151-3p	+++	++
miR-151-5p	+++	++
miR-152	++	++

miR-154a	+	+
miR-154b	++	++
miR-154c	++	+
miR-15b	++	+
miR-16a	+++	+
miR-16b	+++	+
miR-17-3p	++	+
miR-17-5p	++	++
miR-181a	++	+
miR-181b	++	++
miR-181c	++	+
miR-181d	+++	+
miR-182	+	+
miR-183	+	+
miR-184	+	+
miR-185	++	++
miR-186	+++	++
miR-187	++	++
miR-188	++	+
miR-191	+++	++
miR-192	++	++
miR-193a	+	+
miR-193a-3p	++	+
miR-193a-5p	++	++
miR-193b	++	++
miR-194	++	+
miR-195	+++	++
miR-196a	+	+
miR-196b	+	+
miR-197	++	++
miR-199a-3p	+++	+
miR-199a-5p	+++	+
miR-199b	+++	+

miR-199c	+++	+
miR-19a	+++	+
miR-19b	+++	+
miR-200b	+++	++
miR-200c	+++	+
miR-202	+	+
miR-204	++	+
miR-205	++	++
miR-206	+	++
miR-208a	+	+
miR-208b	+	+
miR-20a	+++	+
miR-20b	++	+
miR-21-3p	++	++
miR-21-5p	++	+
miR-210	+++	++
miR-211	++	++
miR-212	+	+
miR-214	+++	+++
miR-215	++	+
miR-216a	++	++
miR-216b	+	+
miR-218	++	+++
miR-219	++	+
miR-219-3p	++	++
miR-219-5p	+	+
miR-222	+++	++
miR-223	++	++
miR-23b-5p	++	+
miR-24	++	+++
miR-24-3p	+++	++
miR-25	+++	+
miR-26b	+++	+

miR-27a-3p	+	++
miR-296-5p	+++	++
miR-299	+	+
miR-29a	+++	+
miR-29b	+++	+
miR-29c	+++	+
miR-29d-5p	+++	++
miR-29e	++	+
miR-301b	+	+
miR-302a	+	+
miR-302c	+	+
miR-302d	+	+
miR-30a-5p	+++	++
miR-30b-3p	++	+
miR-30b-5p	+++	+
miR-30c	+++	++
miR-30d	+++	+
miR-30e-5p	+++	+
miR-30f	++	+
miR-31	+++	++
miR-32	+	+
miR-320a	+++	+++
miR-320b	++	++
miR-323	+++	+++
miR-324	++	+
miR-326	+++	+++
miR-328	++	++
miR-329a	+	+
miR-329b	+	++
miR-330	++	++
miR-331-3p	++	+++
miR-331-5p	++	+
miR-335	+	+

miR-339a	+++	++
miR-339b	+++	+++
miR-33b	++	+
miR-342	++	+
miR-345-3p	++	++
miR-345-5p	++	++
miR-346	++	++
miR-34b	+++	+
miR-34c	+++	+
miR-361	++	+
miR-362-5p	++	+
miR-363	+	+
miR-365-5p	+++	+++
miR-367	+	+
miR-370	++	++
miR-371	+	+
miR-375	+++	+
miR-376a	+	+
miR-377	+	+
miR-378	++	++
miR-378b	++	+
miR-378c	++	++
miR-381	++	+
miR-383	++	++
miR-409b	+	+
miR-411a	++	+
miR-411b	+	++
miR-411c-3p	+	+
miR-412	+	+
miR-423-5p	+++	++
miR-424-3p	++	+
miR-429	++	+
miR-431	++	++

miR-432	++	+
miR-433	++	+
miR-449a	+++	+
miR-449b	++	+
miR-449c	++	++
miR-449d	++	++
miR-450b	+	+
miR-452	++	++
miR-453	++	+
miR-455-5p	++	+
miR-483	++	++
miR-484	++	+
miR-485	+	+++
miR-486	++	++
miR-487a	++	++
miR-487b	++	+
miR-488	+	++
miR-489	+	+
miR-490	++	++
miR-491	++	++
miR-493	++	++
miR-494	+++	+++
miR-495	++	+
miR-496	+	+
miR-499	+	+
miR-500	++	+
miR-502a	++	++
miR-502b	++	++
miR-503-3p	++	+++
miR-503-5p	++	++
miR-504	++	+
miR-532	++	++
miR-539	+	+

miR-541	++	++
miR-543	+	+++
miR-544a	++	++
miR-544b	++	++
miR-545-3p	+	+
miR-545-5p	+	+
miR-551a	+	+
miR-551b	+	+
miR-562	+	+
miR-568	+	+
miR-574	+++	+++
miR-615	+++	+++
miR-631	+++	+++
miR-652	++	++
miR-654	++	++
miR-655	+	+
miR-656	+	+
miR-658	++	++
miR-660	++	++
miR-664	++	++
miR-664b	+++	+
miR-665	+++	++
miR-669	+++	+++
miR-671	++	+
miR-744	++	++
miR-758	+	+
miR-760-3p	++	++
miR-760-5p	++	++
miR-761	++	++
miR-763	++	++
miR-764	+	+
miR-767	++	++
miR-769	++	++

miR-873	+	++
miR-874	+++	++
miR-885	++	++
miR-92a	+++	++
miR-92b	+++	++
miR-93	+++	++
miR-935	++	+
miR-940	+++	+++
miR-95	+	+
miR-96	++	+
miR-99a-3p	++	+
miR-99a-5p	+++	+

Legend: + = when the Cq value is ≥ 30; ++ = when the Cq value is ranging from ≥ 25 to 30; +++ = when the Cq value in < 25.

APPENDIX G: KEGG pathways affected by putative targets of differentially expressed miRNAs in ampulla of LF-LCL animals.

KEGG pathway	*P*-value	Number of genes	Number of miRNAs
MicroRNAs in cancer	2.80E-47	84	6
Proteoglycans in cancer	9.69E-12	89	6
Adherens junction	1.66E-10	42	6
Prion diseases	1.95E-10	12	5
Cell cycle	3.30E-10	67	6
Lysine degradation	3.13E-08	23	6
Protein processing in endoplasmic reticulum	1.05E-07	79	6
Viral carcinogenesis	1.22E-07	89	6
Oocyte meiosis	2.71E-07	50	6
Endocytosis	2.74E-07	86	6
Hippo signaling pathway	2.74E-07	66	6
Fatty acid biosynthesis	7.92E-07	3	3
Ubiquitin mediated proteolysis	9.97E-07	65	6
p53 signaling pathway	9.85E-06	37	6
Thyroid hormone signaling pathway	1.29E-05	56	6
Bacterial invasion of epithelial cells	1.29E-05	38	6
TGF-beta signaling pathway	3.60E-05	37	6
Pathways in cancer	6.90E-05	146	6
FoxO signaling pathway	6.94E-05	61	6
Renal cell carcinoma	6.94E-05	32	6
Prostate cancer	6.94E-05	45	6
Colorectal cancer	0.00011935	30	6
Wnt signaling pathway	0.0001405	57	6
RNA transport	0.00014984	72	6
Pathogenic Escherichia coli infection	0.00027531	30	6
Shigellosis	0.00028654	32	6
Regulation of actin cytoskeleton	0.0002916	80	6
Hepatitis B	0.00032523	59	5

Chronic myeloid leukemia	0.00068067	35	5
Glioma	0.00068067	29	6
Spliceosome	0.00111253	56	6
Transcriptional misregulation in cancer	0.00219528	71	6
mTOR signaling pathway	0.00358483	29	6
Thyroid câncer	0.00416552	16	5
Focal adhesion	0.00569949	79	6
Huntington's disease	0.00569949	65	6
mRNA surveillance pathway	0.0070448	40	6
Estrogen signaling pathway	0.00980393	39	6
Signaling pathways regulating pluripotency of stem cells	0.01428907	54	6
Endometrial cancer	0.01484899	23	5
Axon guidance	0.01527135	45	6
Bladder câncer	0.01527135	20	6
HIF-1 signaling pathway	0.01536525	44	6
Insulin signaling pathway	0.01536525	55	6
RNA degradation	0.01605322	34	6
Pancreatic cancer	0.01947976	30	6
Glycosaminoglycan biosynthesis - keratan sulfate	0.01961431	6	5
Circadian rhythm	0.02455388	16	4
Non-small cell lung cancer	0.02611363	23	5
Notch signaling pathway	0.03073139	22	6
ERβ signaling pathway	0.03529214	36	6
Sphingolipid signaling pathway	0.03611942	48	6
Acute myeloid leukemia	0.03655298	23	6
Epstein-Barr virus infection	0.03683991	75	6
Valine, leucine and isoleucine biosynthesis	0.03789815	2	1
Small cell lung cancer	0.03899101	34	6
AMPK signaling pathway	0.04033011	51	6
N-Glycan biosynthesis	0.04353692	16	6
Central carbon metabolism in cancer	0.04353692	25	6

Choline metabolism in cancer	0.04353692	39	6
Salmonella infection	0.04388497	33	6

APPENDIX H: KEGG pathways affected by putative targets of differentially expressed miRNAs in ampulla of SF-SCL animals.

KEGG pathway	*P*-value	Number of genes	Number of miRNAs
Proteoglycans in cancer	2.48E-08	100	8
Adherens junction	2.48E-08	49	8
Oocyte meiosis	7.00E-08	62	8
Cell cycle	7.06E-08	70	8
Renal cell carcinoma	2.21E-07	42	7
Viral carcinogenesis	2.21E-07	92	8
Protein processing in endoplasmic reticulum	2.52E-07	88	8
TGF-beta signaling pathway	3.25E-07	43	8
Fatty acid biosynthesis	4.37E-07	7	7
Hippo signaling pathway	4.37E-07	74	8
Thyroid cancer	5.59E-06	21	7
Lysine degradation	1.30E-05	25	8
Endocytosis	1.70E-05	103	8
Ubiquitin mediated proteolysis	4.61E-05	71	7
Central carbon metabolism in cancer	4.61E-05	36	8
Pathways in cancer	0.00012729	168	8
Colorectal cancer	0.00013024	37	8
RNA transport	0.00014512	82	8
Prostate cancer	0.00019647	49	7
Epstein-Barr virus infection	0.00021849	98	8
FoxO signaling pathway	0.00024202	68	7
Focal adhesion	0.00038554	98	7
AMPK signaling pathway	0.0004008	65	8
Chronic myeloid leukemia	0.00045289	39	8
Estrogen signaling pathway	0.00049381	48	7
Hepatitis B	0.00055689	69	8
Fatty acid metabolism	0.00060462	19	7
Regulation of actin cytoskeleton	0.00060462	94	8

mRNA surveillance pathway	0.00067095	49	8
p53 signaling pathway	0.00082426	38	7
Glioma	0.00082426	33	7
Bacterial invasion of epithelial cells	0.00086915	40	8
Steroid biosynthesis	0.00151214	10	6
Endometrial cancer	0.00200936	28	8
Axon guidance	0.00480445	55	7
HIF-1 signaling pathway	0.00558432	51	7
Thyroid hormone signaling pathway	0.00576693	56	8
Gap junction	0.0065584	40	8
Sphingolipid signaling pathway	0.00694862	52	7
Signaling pathways regulating pluripotency of stem cells	0.00756192	60	8
Spliceosome	0.00900636	65	7
Small cell lung cancer	0.010632	42	8
RNA degradation	0.01176598	41	8
Transcriptional misregulation in cancer	0.01391867	77	8
Wnt signaling pathway	0.01434031	62	8
Insulin signaling pathway	0.01444955	64	7
mTOR signaling pathway	0.01501073	31	7
Circadian rhythm	0.01624494	17	7
Non-small cell lung cancer	0.01854159	28	7
Huntington's disease	0.01854159	76	8
Acute myeloid leukemia	0.01917572	29	8
cGMP-PKG signaling pathway	0.02137237	71	7
Pancreatic cancer	0.02137237	32	7
Mismatch repair	0.02530088	12	6
Pathogenic Escherichia coli infection	0.02972464	28	7
Terpenoid backbone biosynthesis	0.0300504	11	6
Adrenergic signaling in cardiomyocytes	0.03140281	55	7
B cell receptor signaling pathway	0.03140281	34	7
Neurotrophin signaling pathway	0.03140281	54	7
Progesterone-mediated oocyte maturation	0.03140281	41	7

Sulfur metabolism	0.03905265	5	3
HTLV-I infection	0.04544987	108	8
Biosynthesis of unsaturated fatty acids	0.04675666	10	6

APPENDIX I: KEGG pathways affected by putative targets of differentially expressed miRNAs in isthmus of LF-LCL animals.

KEGG pathway	*P*-value	Number of genes	Number of miRNAs
Proteoglycans in cancer	2.55E-14	107	10
Hippo signaling pathway	8.45E-13	86	10
Cell cycle	2.64E-09	78	9
Prion diseases	3.16E-09	17	10
Adherens junction	3.70E-08	46	9
ECM-receptor interaction	2.10E-07	36	10
Chronic myeloid leukemia	7.59E-07	46	9
TGF-beta signaling pathway	7.59E-07	45	10
Signaling pathways regulating pluripotency of stem cells	5.95E-06	74	9
Colorectal cancer	5.95E-06	40	9
Renal cell carcinoma	5.95E-06	43	10
Pathways in cancer	7.35E-06	181	10
Glioma	9.57E-06	38	10
Fatty acid biosynthesis	1.17E-05	6	7
Estrogen signaling pathway	1.97E-05	55	10
Viral carcinogenesis	2.31E-05	100	10
Protein processing in endoplasmic reticulum	2.99E-05	87	10
Endometrial cancer	6.86E-05	33	9
Spliceosome	6.86E-05	70	10
Pancreatic cancer	8.63E-05	40	9
Hepatitis B	8.79E-05	76	9
Axon guidance	0.00011798	60	9
Prostate cancer	0.00024676	52	9
Focal adhesion	0.00025857	104	10
Non-small cell lung cancer	0.00042449	33	10
AMPK signaling pathway	0.00058034	67	10
Neurotrophin signaling pathway	0.00061438	66	10

Endocytosis	0.00064392	97	10
Transcriptional misregulation in cancer	0.00076543	82	10
Thyroid câncer	0.000889	20	9
Insulin signaling pathway	0.000889	73	10
Wnt signaling pathway	0.00094893	68	9
mTOR signaling pathway	0.00106444	35	9
Oocyte meiosis	0.00106444	57	10
Central carbon metabolism in cancer	0.00115899	37	9
Bladder câncer	0.001415	25	10
Lysine degradation	0.00152802	24	8
mRNA surveillance pathway	0.00190569	50	10
Sphingolipid signaling pathway	0.00198327	59	10
HTLV-I infection	0.00376294	124	9
Pyrimidine metabolismo	0.00498159	52	9
FoxO signaling pathway	0.00537899	69	9
Thyroid hormone signaling pathway	0.00537899	62	10
Glycosaminoglycan biosynthesis - chondroitin sulfate / dermatan sulfate	0.00603949	9	7
Base excision repair	0.00696096	19	7
Dorso-ventral axis formation	0.00714302	18	9
Bacterial invasion of epithelial cells	0.0082611	39	9
Inositol phosphate metabolism	0.00871396	32	10
Ubiquitin mediated proteolysis	0.00974436	65	8
Other types of O-glycan biosynthesis	0.00982614	13	7
ERβ signaling pathway	0.0112445	47	10
HIF-1 signaling pathway	0.01299479	52	10
p53 signaling pathway	0.01299479	37	10
Notch signaling pathway	0.0173677	27	9

Selenocompound metabolism	0.02133165	11	5
Phosphatidylinositol signaling system	0.02317668	37	10
Acute myeloid leukemia	0.02834036	29	9
Melanoma	0.02915683	34	9
DNA replication	0.03002057	21	7
Prolactin signaling pathway	0.03132806	34	9
PI3K-Akt signaling pathway	0.03132806	144	10
Shigellosis	0.03217563	34	9
Small cell lung cancer	0.03217563	42	9
Influenza A	0.03217563	81	10
RNA degradation	0.03371873	41	9
Progesterone-mediated oocyte maturation	0.03552411	43	9
Regulation of actin cytoskeleton	0.03778761	91	9
RNA transport	0.03829968	74	10
Steroid biosynthesis	0.04868171	9	7
B cell receptor signaling pathway	0.04965595	35	10

APPENDIX J: KEGG pathways affected by putative targets of differentially expressed miRNAs in isthmus of SF-SCL animals.

KEGG pathway	*P*-value	Number of genes	Number of miRNAs
MicroRNAs in câncer	1.19E-80	120	18
Proteoglycans in câncer	8.66E-16	124	18
Adherens junction	8.66E-16	61	18
Protein processing in endoplasmic reticulum	2.33E-14	116	19
Pathways in câncer	1.52E-09	221	18
Hippo signaling pathway	6.20E-09	90	18
Colorectal câncer	2.54E-08	47	18
Cell cycle	4.03E-08	84	17
Chronic myeloid leucemia	1.91E-07	53	18
Thyroid câncer	2.09E-07	24	17
RNA transport	1.51E-06	106	19
Ubiquitin mediated proteolysis	2.24E-06	92	17
Prostate câncer	2.35E-06	61	17
Prion diseases	2.66E-06	16	14
TGF-beta signaling pathway	2.66E-06	50	15
Hepatitis B	5.50E-06	85	18
Lysine degradation	7.05E-06	29	16
Thyroid hormone signaling pathway	7.13E-06	76	18
Glioma	8.19E-06	42	16
Focal adhesion	8.19E-06	123	17
Bacterial invasion of epithelial cells	9.08E-06	49	17
p53 signaling pathway	1.27E-05	48	17
Bladder câncer	1.43E-05	31	17
Oocyte meiosis	1.49E-05	70	18
Non-small cell lung cancer	2.72E-05	39	17
Viral carcinogenesis	2.76E-05	122	19
Pancreatic câncer	3.17E-05	45	17
Neurotrophin signaling pathway	3.23E-05	77	18

Renal cell carcinoma	3.58E-05	46	15
Acute myeloid leukemia	8.04E-05	39	18
Endometrial cancer	8.32E-05	36	18
Estrogen signaling pathway	9.37E-05	59	17
Regulation of actin cytoskeleton	9.37E-05	115	18
ERβ signaling pathway	0.00012299	54	17
mRNA surveillance pathway	0.00012299	59	18
FoxO signaling pathway	0.00015387	82	17
RNA degradation	0.00018612	52	18
Small cell lung cancer	0.00019266	55	18
mTOR signaling pathway	0.00031476	41	16
Endocytosis	0.00042831	117	19
Transcriptional misregulation in cancer	0.00070808	99	18
Fatty acid biosynthesis	0.00092935	5	9
Circadian rhythm	0.00115261	23	13
Choline metabolism in cancer	0.00122811	61	17
Central carbon metabolism in cancer	0.00167933	42	16
Shigellosis	0.00167933	38	17
Long-term depression	0.00227881	33	14
Long-term potentiation	0.00340381	42	16
MAPK signaling pathway	0.00340381	131	19
Progesterone-mediated oocyte maturation	0.00593371	52	16
Fc gamma R-mediated phagocytosis	0.00593371	53	18
Signaling pathways regulating pluripotency of stem cells	0.00596478	74	17
Insulin signaling pathway	0.00655318	78	17
TNF signaling pathway	0.00814662	64	17
Wnt signaling pathway	0.00845271	75	18
Terpenoid backbone biosynthesis	0.01254286	14	11
ECM-receptor interaction	0.013774	37	16
Axon guidance	0.013774	62	18
N-Glycan biosynthesis	0.01688369	28	15
VEGF signaling pathway	0.02738629	36	17

AMPK signaling pathway	0.02738629	71	18
Pathogenic Escherichia coli infection	0.02738629	33	18
Spliceosome	0.02779416	68	17
Arrhythmogenic right ventricular cardiomyopathy (ARVC)	0.02805437	31	15
Salmonella infection	0.03270354	47	18
HIF-1 signaling pathway	0.03446125	59	16
Lysosome	0.03557055	63	18
Sphingolipid signaling pathway	0.03590709	63	17
Melanoma	0.04503496	38	16

APPENDIX K. Mean ± S.E.M. values of the concentration (µM) of amino acids and biogenic amines in oviductal fluid of cows of the LF-LCL and SF-SCL groups.

Code	Analyte	LF-LCL	SF-SCL	*P* Value
Ala	Alanine	30.929 ± 4.916	35.829 ± 4.516	0.253
Arg	Arginine	not detected	not detected	N/A
Asn	Asparagine	1.011 ± 0.176	1.037 ± 0.192	0.457
Asp	Aspartate	3.454 ± 0.635	4.771 ± 0.638	0.096
Cit	Citrulline	0.085 ± 0.055	0.313 ± 0.112	0.045
Gln	Glutamine	6.770 ± 1.710	6.937 ± 1.270	0.465
Glu	Glutamate	15.447 ± 2.891	28.514 ± 2.548	0.010
Gly	Glycine	224.671 ± 39.030	188.900 ± 42.359	0.279
His	Histidine	not detected	not detected	N/A
Ile	Isoleucine	not detected	not detected	N/A
Leu	Leucine	0.253 ± 0.183	0.317 ± 0.124	0.328
Lys	Lysine	not detected	not detected	N/A
Met	Methionine	not detected	not detected	N/A
Orn	Ornithine	not detected	not detected	N/A
Phe	Phenylalanine	0.019 ± 0.012	0.000 ± 0.000	0.090
Pro	Proline	0.701 ± 0.321	0.629 ± 0.200	0.430
Ser	Serine	2.759 ± 0.589	3.296 ± 0.695	0.283
Thr	Threonine	6.213 ± 2.718	4.119 ± 0.732	0.244
Trp	Tryptophan	not detected	not detected	N/A
Tyr	Tyrosine	not detected	not detected	N/A
Val	Valine	0.196 ± 0.196	0.030 ± 0.030	0.223
Ac-Orn	Acetylornithine	not detected	not detected	N/A
ADMA	Asymmetric dimethylarginine	0.023 ± 0.009	0.025 ± 0.009	0.434
alpha-AAA	alpha-Aminoadipic acid	0.047 ± 0.047	0.075 ± 0.075	0.390
c4-OH-Pro	cis-4-Hydroxyproline	not detected	not detected	N/A
Carnosine	Carnosine	0.050 ± 0.050	0.131 ± 0.078	0.121

Creatinine	Creatinine	2.021 ± 0.330	3.049 ± 0.373	0.040
DOPA	Dihydroxyphenylalanine	not detected	not detected	N/A
Dopamine	Dopamin	0.024 ± 0.004	0.022 ± 0.003	0.420
Histamine	Histamine	0.041 ± 0.041	0.058 ± 0.035	0.330
Kynurenine	Kynurenine	not detected	not detected	N/A
Met-SO	Methionine-Sulfoxide	not detected	not detected	N/A
Nitro-Tyr	Nitrotyrosine	not detected	not detected	N/A
PEA	Phenylethylamine	not detected	not detected	N/A
Putrescine	Putrescine	0.315 ± 0.080	0.367 ± 0.068	0.290
Sarcosine	Sarcosine	0.221 ± 0.153	0.301 ± 0.173	0.386
SDMA	Symmetric dimethylarginine	0.004 ± 0.001	0.005 ± 0.001	0.295
Serotonin	Serotonin	not detected	not detected	N/A
Spermidine	Spermidine	0.476 ± 0.082	0.623 ± 0.102	0.171
Spermine	Spermine	1.159 ± 0.157	1.456 ± 0.209	0.154
t4-OH-Pro	trans-4-Hydroxyproline	0.141±0.027	0.177 ± 0.066	0.343
Taurine	Taurine	6.153 ± 1.197	8.396 ± 1.039	0.030

APPENDIX L. Mean ± S.E.M. values of the concentration (µM) of acylcarnitines in oviductal fluid of cows of the LF-LCL and SF-SCL groups.

Code	Analyte	LF-LCL	SF-SCL	*P* Value
C0	Carnitine (free)	2.390 ± 0.276	2.694 ± 0.185	0.206
C2	Acetylcarnitine	0.903 ±0.118	1.153 ±0.102	0.104
C3	Propionylcarnitine	0.061 ±0.007	0.063 ±0.005	0.395
C3:1	Propenoylcarnitine	0.018 ±0.001	0.023 ±0.001	0.036
C3-OH	Hydroxypropionylcarnitine	0.010 ±0.000	0.010 ±0.001	0.363
C4	Butyrylcarnitine / Isobutyrylcarnitine	0.006 ±0.001	0.006 ±0.000	0.411
C4:1	Butenoylcarnitine	0.131 ±0.022	0.163 ±0.017	0.155
C4-OH (C3-DC)	Hydroxybutyrylcarnitine (Malonylcarnitine)	0.010 ±0.001	0.011 ±0.000	0.059
C5	Isovalerylcarnitine / 2-Methylbutyrylcarnitine / Valerylcarnitine	0.039 ±0.003	0.046 ±0.002	0.097
C5:1	Tiglylcarnitine / 3-Methyl-crotonylcarnitine	0.007 ±0.000	0.009 ±0.000	0.008
C5:1-DC	Glutaconylcarnitine / Mesaconylcarnitine	0.020 ±0.001	0.020 ±0.001	0.389
C5-DC (C6-OH)	Glutarylcarnitine (Hydroxyhexanoylcarnitine [= Hydroxycaproylcarnitine])	0.026 ±0.002	0.027 ±0.002	0.265
C5-M-	Methylglutarylcarnitine	0.023	0.025	0.150

DC		±0.001	±0.001	
C5-OH (C3-DC-M)	Hydroxyisovalerylcarnitine / Hydroxy-2-methylbutyryl / Hydroxyvalerylcarnitine (Methylmalonylcarnitine)	0.013 ±0.001	0.013 ±0.001	0.474
C6 (C4:1-DC)	Hexanoylcarnitine [= Caproylcarnitine] (Fumarylcarnitine)	0.028 ±0.001	0.030 ±0.002	0.154
C6:1	Hexenoylcarnitine	0.017 ±0.001	0.017 ±0.000	0.421
C7-DC	Pimelylcarnitine	0.007 ±0.000	0.007 ±0.001	0.380
C8	Octanoylcarnitine [= Caprylylcarnitine]	0.064 ±0.016	0.049 ±0.002	0.177
C9	Nonanoylcarnitine [= Pelargonylcarnitine]	0.012 ±0.001	0.011 ±0.000	0.126
C10	Decanoylcarnitine [= Caprylcarnitine]	0.036 ±0.002	0.037 ±0.001	0.291
C10:1	Decenoylcarnitine	0.038 ±0.001	0.034 ±0.002	0.186
C10:2	Decadienoylcarnitine	0.014 ±0.001	0.013 ±0.000	0.183
C12	Dodecanoylcarnitine [= Laurylcarnitine]	0.037 ±0.001	0.037 ±0.002	0.426
C12:1	Dodecenoylcarnitine	0.052 ±0.001	0.052 ±0.001	0.428
C12-DC	Dodecanedioylcarnitine	0.034 ±0.001	0.031 ±0.002	0.176
C14	Tetradecanoylcarnitine [= Myristylcarnitine]	0.010 ±0.001	0.010 ±0.001	0.351
C14:1	Tetradecenoylcarnitine [= Myristoleylcarnitine]	0.003 ±0.000	0.003 ±0.000	0.254

C14:1 -OH	Hydroxytetradecenoylcarnitine [= Hydroxymyristoleylcarnitine]	0.006 ±0.000	0.005 ±0.000	0.087
C14:2	Tetradecadienoylcarnitine	0.022 ±0.000	0.021 ±0.001	0.136
C14:2 -OH	Hydroxytetradecadienoylcarnitine	0.006 ±0.000	0.006±0.000	0.236
C16	Hexadecanoylcarnitine [= Palmitoylcarnitine]	0.005 ±0.000	0.005 ±0.000	0.255
C16:1	Hexadecenoylcarnitine [= Palmitoleylcarnitine]	0.005 ±0.000	0.004 ±0.000	0.306
C16:1 -OH	Hydroxyhexadecenoylcarnitine [= Hydroxypalmitoleylcarnitine]	0.009 ±0.000	0.009 ±0.000	0.200
C16:2	Hexadecadienoylcarnitine	0.004 ±0.000	0.004 ±0.000	0.279
C16:2 -OH	Hydroxyhexadecadienoylcarnitine	0.004 ±0.000	0.004 ±0.000	0.052
C16-OH	Hydroxyhexadecanolycarnitine [= Hydroxypalmitoylcarnitine]	0.007 ±0.000	0.008 ±0.000	0.007
C18	Octadecanoylcarnitine [= Stearylcarnitine]	0.005 ±0.000	0.003 ±0.000	0.035
C18:1	Octadecenoylcarnitine [= Oleylcarnitine]	0.010 ±0.000	0.009 ±0.001	0.105
C18:1 -OH	Hydroxyoctadecenoylcarnitine [= Hydroxyoleylcarnitine]	0.011 ±0.000	0.012 ±0.000	0.345
C18:2	Octadecadienoylcarnitine [= Linoleylcarnitine]	0.004 ±0.000	0.003 ±0.000	0.287

APPENDIX M. Mean ± S.E.M. values of the concentration (μM) of Phosphatidylcholines in oviductal fluid of cows of the LF-LCL and SF-SCL groups.

Code	Analyte	LF-LCL	SF-SCL	*P* Value
PC aa C24:0	Phosphatidylcholine with diacyl residue sum C24:0	0.012 ± 0.002	0.008 ± 0.001	0.044
PC aa C26:0	Phosphatidylcholine with diacyl residue sum C26:0	0.275 ± 0.003	0.276 ± 0.005	0.426
PC aa C28:1	Phosphatidylcholine with diacyl residue sum C28:1	0.004 ± 0.000	0.004 ± 0.000	0.068
PC aa C30:0	Phosphatidylcholine with diacyl residue sum C30:0	0.042 ± 0.002	0.044 ± 0.001	0.184
PC aa C30:2	Phosphatidylcholine with diacyl residue sum C30:2	0.001 ± 0.000	0.001 ± 0.000	0.328
PC aa C32:0	Phosphatidylcholine with diacyl residue sum C32:0	0.012 ± 0.004	0.012 ± 0.002	0.465
PC aa C32:1	Phosphatidylcholine with diacyl residue sum C32:1	0.004 ± 0.001	0.005 ± 0.001	0.223
PC aa C32:2	Phosphatidylcholine with diacyl residue sum C32:2	0.002 ± 0.001	0.003 ± 0.001	0.098
PC aa C32:3	Phosphatidylcholine with diacyl residue sum C32:3	0.001 ± 0.001	0.001 ± 0.001	0.425
PC aa	Phosphatidylcholine	0.070 ± 0.025	0.079 ± 0.017	0.388

C34:1	with diacyl residue sum C34:1			
PC aa C34:2	Phosphatidylcholine with diacyl residue sum C34:2	0.039 ± 0.020	0.021 ± 0.005	0.201
PC aa C34:3	Phosphatidylcholine with diacyl residue sum C34:3	0.003 ± 0.002	0.004 ± 0.001	0.387
PC aa C34:4	Phosphatidylcholine with diacyl residue sum C34:4	0.002 ± 0.001	0.002 ± 0.000	0.478
PC aa C36:0	Phosphatidylcholine with diacyl residue sum C36:0	0.112 ± 0.002	0.113 ± 0.002	0.403
PC aa C36:1	Phosphatidylcholine with diacyl residue sum C36:1	0.039 ± 0.013	0.047 ± 0.007	0.261
PC aa C36:2	Phosphatidylcholine with diacyl residue sum C36:2	0.049 ± 0.020	0.049 ± 0.011	0.493
PC aa C36:3	Phosphatidylcholine with diacyl residue sum C36:3	0.021 ± 0.009	0.020 ± 0.005	0.483
PC aa C36:4	Phosphatidylcholine with diacyl residue sum C36:4	0.022 ± 0.010	0.014 ± 0.003	0.254
PC aa C36:5	Phosphatidylcholine with diacyl residue sum C36:5	0.003 ± 0.001	0.002 ± 0.000	0.309
PC aa C36:6	Phosphatidylcholine with diacyl residue sum C36:6	0.002 ± 0.000	0.000 ± 0.000	0.022
PC aa	Phosphatidylcholine	0.008 ± 0.001	0.008 ± 0.000	0.410

C38:0	with diacyl residue sum C38:0			
PC aa C38:1	Phosphatidylcholine with diacyl residue sum C38:1	0.004 ± 0.001	0.002 ± 0.001	0.027
PC aa C38:3	Phosphatidylcholine with diacyl residue sum C38:3	0.011 ± 0.005	0.010 ± 0.002	0.467
PC aa C38:4	Phosphatidylcholine with diacyl residue sum C38:4	0.020 ± 0.008	0.019 ± 0.003	0.479
PC aa C38:5	Phosphatidylcholine with diacyl residue sum C38:5	0.010 ± 0.005	0.012 ± 0.002	0.349
PC aa C38:6	Phosphatidylcholine with diacyl residue sum C38:6	0.006 ± 0.003	0.005 ± 0.001	0.362
PC aa C40:1	Phosphatidylcholine with diacyl residue sum C40:1	0.104 ± 0.003	0.104 ± 0.002	0.468
PC aa C40:2	Phosphatidylcholine with diacyl residue sum C40:2	0.004 ± 0.001	0.003 ± 0.000	0.010
PC aa C40:3	Phosphatidylcholine with diacyl residue sum C40:3	0.001 ± 0.000	0.001 ± 0.000	0.265
PC aa C40:4	Phosphatidylcholine with diacyl residue sum C40:4	0.005 ± 0.001	0.004 ± 0.001	0.384
PC aa C40:5	Phosphatidylcholine with diacyl residue sum C40:5	0.001 ± 0.001	0.000 ± 0.000	0.178
PC aa	Phosphatidylcholine	0.092 ± 0.002	0.095 ± 0.002	0.118

C40:6	with diacyl residue sum C40:6			
PC aa C42:0	Phosphatidylcholine with diacyl residue sum C42:0	0.013 ± 0.001	0.013 ± 0.001	0.493
PC aa C42:1	Phosphatidylcholine with diacyl residue sum C42:1	0.002 ± 0.001	0.003 ± 0.000	0.194
PC aa C42:2	Phosphatidylcholine with diacyl residue sum C42:2	0.028 ± 0.001	0.026 ± 0.001	0.199
PC aa C42:4	Phosphatidylcholine with diacyl residue sum C42:4	0.002 ± 0.000	0.003 ± 0.000	0.258
PC aa C42:5	Phosphatidylcholine with diacyl residue sum C42:5	0.004 ± 0.001	0.003 ± 0.001	0.138
PC aa C42:6	Phosphatidylcholine with diacyl residue sum C42:6	0.027 ± 0.003	0.029 ± 0.002	0.260
PC ae C30:0	Phosphatidylcholine with acyl-alkyl residue sum C30:0	0.025 ± 0.001	0.024 ± 0.001	0.319
PC ae C30:1	Phosphatidylcholine with acyl-alkyl residue sum C30:1	not detected	not detected	N/A
PC ae C30:2	Phosphatidylcholine with acyl-alkyl residue sum C30:2	0.100 ± 0.002	0.104 ± 0.002	0.053
PC ae C32:1	Phosphatidylcholine with acyl-alkyl residue sum C32:1	0.001 ± 0.000	0.002 ± 0.000	0.181
PC ae	Phosphatidylcholine	0.004 ± 0.000	0.004 ± 0.001	0.436

C32:2	with acyl-alkyl residue sum C32:2			
PC ae C34:0	Phosphatidylcholine with acyl-alkyl residue sum C34:0	0.005 ± 0.001	0.005 ± 0.001	0.462
PC ae C34:1	Phosphatidylcholine with acyl-alkyl residue sum C34:1	0.007 ± 0.002	0.008 ± 0.001	0.147
PC ae C34:2	Phosphatidylcholine with acyl-alkyl residue sum C34:2	0.003 ± 0.001	0.002 ± 0.001	0.228
PC ae C34:3	Phosphatidylcholine with acyl-alkyl residue sum C34:3	0.002 ± 0.001	0.002 ± 0.001	0.143
PC ae C36:0	Phosphatidylcholine with acyl-alkyl residue sum C36:0	0.042 ± 0.001	0.047 ± 0.002	0.007
PC ae C36:1	Phosphatidylcholine with acyl-alkyl residue sum C36:1	0.012 ± 0.003	0.014 ± 0.002	0.271
PC ae C36:2	Phosphatidylcholine with acyl-alkyl residue sum C36:2	0.012 ± 0.001	0.013 ± 0.001	0.379
PC ae C36:3	Phosphatidylcholine with acyl-alkyl residue sum C36:3	0.002 ± 0.001	0.001 ± 0.000	0.110
PC ae C36:4	Phosphatidylcholine with acyl-alkyl residue sum C36:4	0.010 ± 0.001	0.007 ± 0.000	0.008
PC ae C36:5	Phosphatidylcholine with acyl-alkyl residue sum C36:5	0.003 ± 0.001	0.004 ± 0.001	0.275
PC ae	Phosphatidylcholine	0.028 ± 0.001	0.028 ± 0.001	0.478

C38:0	with acyl-alkyl residue sum C38:0			
PC ae C38:1	Phosphatidylcholine with acyl-alkyl residue sum C38:1	0.002 ± 0.001	0.002 ± 0.001	0.419
PC ae C38:2	Phosphatidylcholine with acyl-alkyl residue sum C38:2	0.002 ± 0.001	0.002 ± 0.001	0.330
PC ae C38:3	Phosphatidylcholine with acyl-alkyl residue sum C38:3	0.002 ± 0.001	0.002 ± 0.000	0.308
PC ae C38:4	Phosphatidylcholine with acyl-alkyl residue sum C38:4	0.006 ± 0.001	0.006 ± 0.000	0.352
PC ae C38:5	Phosphatidylcholine with acyl-alkyl residue sum C38:5	0.003 ± 0.001	0.003 ± 0.000	0.481
PC ae C38:6	Phosphatidylcholine with acyl-alkyl residue sum C38:6	0.000 ± 0.000	0.000 ± 0.000	0.397
PC ae C40:1	Phosphatidylcholine with acyl-alkyl residue sum C40:1	0.004 ± 0.000	0.004 ± 0.000	0.406
PC ae C40:2	Phosphatidylcholine with acyl-alkyl residue sum C40:2	0.001 ± 0.000	0.002 ± 0.000	0.088
PC ae C40:3	Phosphatidylcholine with acyl-alkyl residue sum C40:3	0.002 ± 0.001	0.001 ± 0.000	0.142
PC ae C40:4	Phosphatidylcholine with acyl-alkyl residue sum C40:4	0.017 ± 0.001	0.017 ± 0.001	0.390
PC ae	Phosphatidylcholine	0.001 ± 0.001	0.001 ± 0.000	0.482

C40:5	with acyl-alkyl residue sum C40:5			
PC ae C40:6	Phosphatidylcholine with acyl-alkyl residue sum C40:6	0.002 ± 0.001	0.002 ± 0.000	0.428
PC ae C42:0	Phosphatidylcholine with acyl-alkyl residue sum C42:0	0.238 ± 0.003	0.245 ± 0.003	0.051
PC ae C42:1	Phosphatidylcholine with acyl-alkyl residue sum C42:1	0.019 ± 0.001	0.017 ± 0.001	0.149
PC ae C42:2	Phosphatidylcholine with acyl-alkyl residue sum C42:2	0.003 ± 0.000	0.003 ± 0.000	0.169
PC ae C42:3	Phosphatidylcholine with acyl-alkyl residue sum C42:3	0.002 ± 0.000	0.001 ± 0.000	0.068
PC ae C42:4	Phosphatidylcholine with acyl-alkyl residue sum C42:4	not detected	not detected	N/A
PC ae C42:5	Phosphatidylcholine with acyl-alkyl residue sum C42:5	0.360 ± 0.005	0.361 ± 0.004	0.479
PC ae C44:3	Phosphatidylcholine with acyl-alkyl residue sum C44:3	0.011 ± 0.001	0.009 ± 0.001	0.040
PC ae C44:4	Phosphatidylcholine with acyl-alkyl residue sum C44:4	0.031 ± 0.001	0.030 ± 0.001	0.130
PC ae C44:5	Phosphatidylcholine with acyl-alkyl residue sum C44:5	0.016 ± 0.001	0.016 ± 0.001	0.330
PC ae	Phosphatidylcholine	0.006 ± 0.000	0.007 ± 0.001	0.175

C44:6	with acyl-alkyl residue sum C44:6

APPENDIX N. Mean ± S.E.M. values of the concentration (µM) of lysophosphatidylcholines in oviductal fluid of cows of the LF-LCL and SF-SCL groups.

Code	Analyte	LF-LCL	SF-SCL	*P* Value
lysoPC a C14:0	Lysophosphatidylcholine with acyl residue C14:0	4.091 ± 0.045	4.083 ± 0.045	0.448
lysoPC a C16:0	Lysophosphatidylcholine with acyl residue C16:0	0.034 ± 0.004	0.023 ± 0.003	0.055
lysoPC a C16:1	Lysophosphatidylcholine with acyl residue C16:1	0.026 ± 0.002	0.028 ± 0.003	0.302
lysoPC a C17:0	Lysophosphatidylcholine with acyl residue C17:0	0.006 ± 0.001	0.006 ± 0.001	0.362
lysoPC a C18:0	Lysophosphatidylcholine with acyl residue C18:0	0.086 ± 0.006	0.077 ± 0.004	0.170
lysoPC a C18:1	Lysophosphatidylcholine with acyl residue C18:1	0.018 ± 0.003	0.020 ± 0.001	0.278
lysoPC a C18:2	Lysophosphatidylcholine with acyl residue C18:2	0.020 ± 0.003	0.017 ± 0.002	0.072
lysoPC a C20:3	Lysophosphatidylcholine with acyl residue C20:3	0.032 ± 0.002	0.031 ± 0.001	0.302
lysoPC a C20:4	Lysophosphatidylcholine with acyl residue C20:4	0.005 ± 0.001	0.005 ± 0.001	0.419
lysoPC a C24:0	Lysophosphatidylcholine with acyl residue C24:0	0.242 ± 0.006	0.245 ± 0.007	0.370
lysoPC a C26:0	Lysophosphatidylcholine with acyl residue C26:0	0.010 ± 0.001	0.009 ± 0.000	0.151
lysoPC a C26:1	Lysophosphatidylcholine with acyl residue C26:1	0.005 ± 0.001	0.006 ± 0.001	0.342
lysoPC a C28:0	Lysophosphatidylcholine with acyl residue C28:0	0.042 ± 0.003	0.038 ± 0.002	0.188

lysoPC a C28:1	Lysophosphatidylcholine with acyl residue C28:1	0.007 ± 0.001	0.007 ± 0.001	0.446

APPENDIX O. Mean ± S.E.M. values of the concentration (µM) of sphingomyelins in oviductal fluid of cows of the LF-LCL and SF-SCL groups.

Code	Analyte	LF-LCL	SF-SCL	*P* Value
SM (OH) C14:1	Hydroxysphingomyelin with acyl residue sum C14:1	not detected	not detected	N/A
SM (OH) C16:1	Hydroxysphingomyelin with acyl residue sum C16:1	0.005 ± 0.002	0.007 ± 0.001	0.218
SM (OH) C22:1	Hydroxysphingomyelin with acyl residue sum C22:1	0.008 ± 0.003	0.008 ± 0.001	0.500
SM (OH) C22:2	Hydroxysphingomyelin with acyl residue sum C22:2	0.004 ± 0.001	0.003 ± 0.001	0.129
SM (OH) C24:1	Hydroxysphingomyelin with acyl residue sum C24:1	0.003 ± 0.001	0.002 ± 0.000	0.084
SM C16:0	Sphingomyelin with acyl residue sum C16:0	0.099 ± 0.032	0.134 ± 0.022	0.176
SM C16:1	Sphingomyelin with acyl residue sum C16:1	0.003 ± 0.001	0.003 ± 0.000	0.439
SM C18:0	Sphingomyelin with acyl residue sum C18:0	0.017 ± 0.005	0.023 ± 0.003	0.170
SM C18:1	Sphingomyelin with acyl residue sum C18:1	0.003 ± 0.001	0.002 ± 0.001	0.292
SM C20:2	Sphingomyelin with acyl residue sum C20:2	0.001 ± 0.000	0.001 ± 0.000	0.366
SM C22:3	Sphingomyelin with acyl residue sum C22:3	0.000 ± 0.000	0.001 ± 0.000	0.038
SM C24:0	Sphingomyelin with acyl residue sum C24:0	0.035 ± 0.011	0.055 ± 0.011	0.089
SM C24:1	Sphingomyelin with acyl residue sum C24:1	0.027 ± 0.008	0.033 ± 0.007	0.309

SM C26:0	Sphingomyelin with acyl residue sum C26:0	0.002 ± 0.001	0.002 ± 0.000	0.449
SM C26:1	Sphingomyelin with acyl residue sum C26:1	0.001 ± 0.000	0.002 ± 0.000	0.204

APPENDIX P. Mean ± S.E.M. values of the concentration (µM) of Prostaglandins and related compounds in oviductal fluid of cows of the LF-LCL and SF-SCL groups.

Code	Analyte	LF-LCL	SF-SCL	*P* Value
12S-HETE	12(S)-hydroxy-5Z,8Z,10E,14Z-eicosatetraenoic acid	0.952 ± 0.075	1.011 ± 0.085	0.237
13S-HODE	13(S)-hydroxy-9Z,11E-octadecadienoic acid	not detected	not detected	N/A
14(15)-EpETE	(±)14(15)-epoxy-5Z,8Z,11Z,17Z-eicosatetraenoic acid	not detected	not detected	N/A
15-deoxy PGJ2	15-deoxy-delta(12,14)-prostaglandin J2	0.276 ± 0.191	0.162 ± 0.107	0.301
15S-HETE	15(S)-hydroxy-5Z,8Z,11Z,13E-eicosatetraenoic acid	0.032 ± 0.032	0.000 ± 0.000	0.178
6-keto-PGF1a	6-keto-Prostaglandin F1alpha	not detected	not detected	N/A
8-iso PGF2a	8-iso-Prostaglandin F2alpha	not detected	not detected	N/A
9S-HODE	(±)9-hydroxy-10E,12Z-octadecadienoic acid	0.174 ± 0.112	0.035 ± 0.035	0.158
AA	Arachidonic acid	74.729 ± 28.497	111.686 ± 13.454	0.100
DHA	Docosahexaenoic acid	17.986 ± 6.924	20.929 ± 5.688	0.365
LTB4	Leukotriene B4	not detected	not detected	N/A
LTD4	Leukotriene D4	0.023 ± 0.015	0.005 ± 0.005	0.164
PGD2	Prostaglandin D2	0.207 ± 0.134	0.243 ± 0.157	0.415
PGE2	Prostaglandin E2	0.742 ± 0.189	0.794 ± 0.154	0.369
PGF2a	Prostaglandin F2alpha	1.412 ±	1.930 ±	0.091

tetranor PGE-M	Prostaglandin E2 metabolite	0.140 not detected	0.275 not detected	N/A
TXB2	Thromboxane B2	0.109 ± 0.054	0.222 ± 0.120	0.227